

**Exploring Mucoadhesive and Toxicological
Characteristics of Novel Water-Soluble Polymers
Synthesised by Modifying Linear
Polyethyleneimine with Various Anhydrides**

Manfei Fu

**Thesis submitted in partial fulfilment of the requirement for the
degree of Doctor of Philosophy**

School of Pharmacy

March 2024

Declaration of Original Authorship

The work described in this thesis was performed in the Department of Pharmacy of the University of Reading, United Kingdom between September 2019 and September 2023. I confirm that this is my own work and the use of all material from other sources has been properly and fully acknowledged.

Manfei Fu

Date: 27/02/2024

Acknowledgements

This thesis marks an end of a long and challenging but memorable and rewarding journey. Though I felt anxious, confused, self-doubting on this journey, now I am proud to say that I have become a better version of myself. I deeply believe that I could not get my doctorate without the support of my supervisors, my parents and my friends.

I would like to express my heartfelt gratitude to my supervisors Professor Vitaliy V. Khutoryanskiy and Professor Adrian C. Williams for providing me an opportunity to pursue a PhD degree and an excellent scientific research platform. Their invaluable guidance and recommendation, patience, encouragement support me to complete my PhD studies. They taught me pursuit of truth instead of perfection, which inspires me throughout my life.

My eternal thanks go to my father Jiapo Fu and my mother Xianzhen Fu for their unwavering support. Their love and encouragement have been the strongest back up to me.

I would like to thank the people who have helped me with various research work: Dr. Ellen Hackl, Dr. Pedro Rivas-Ruiz, Dr. Daulet Kaldybekov, Dr. Raymond Lau, Mr. Nicholas Spencer, Professor Rebecca Green, Dr. Abhishek Sharma, Dr. Sanna Auer, Professor Frantisek Hartl and other wonderful people that I cannot afford to express all their names. And thanks to University of Reading for technical support and assistance in the work.

Thank you to my research collaborators Professor Sergey K. Filippov, Dr. Silvia Amadesi and Dr. Roman V. Moiseev for your meticulous work. It has been a pleasure working with all of you.

To my research group: Dr. Jamila Al Mahrooqi, Dr. Sam Aspinall, Dr. Roman V. Moiseev, Dr. Sayyed Ibrahim Shah, Dr. Fhataheya Buang, Dr. Sitthiphong Soradech, Claudia Aguguo, Myrale Habel, Shiva Vanukuru, and Yuehuai Xiong. I am grateful to all your help and friendship.

Manfei Fu
February 2024

Abstract

Linear polyethyleneimine (L-PEI) has been extensively used in various fields, such as pharmaceutical formulations, gene delivery, and water treatment. Though L-PEI is considered as a potential gene delivery vector or as a pharmaceutical excipient, the applications of L-PEI are limited as L-PEI displays relatively high toxicity and low biocompatibility. The secondary amine groups within L-PEI can interact with cell membranes and the extracellular matrix, and these interactions are predominantly electrostatically driven. Herein, we selected succinic anhydride, phthalic anhydride, methacrylic anhydride, crotonic anhydride and maleic anhydride to modify L-PEI to improve functionality and lower its toxicity. Firstly, L-PEI was prepared by fully hydrolyzing commercially available poly(2-ethyl-2-oxazoline) (PEOZ, 50 kDa) and then reacted with different anhydrides. The obtained succinylated L-PEI, phthaylated L-PEI, methacrylated L-PEI, crotonylated L-PEI and maleylated L-PEI were fully characterized using $^1\text{H-NMR}$ and FTIR spectroscopies, turbidity-pH measurements and electrophoretic mobility. The resultant polymers (succinylated L-PEI, phthaylated L-PEI and maleylated L-PEI) were the polyampholytes which each have an isoelectric point (pH_{IEP}), and two cationic polyelectrolytes methacrylated L-PEI, crotonylated L-PEI according to their structures. Water-soluble polymers generally exhibit mucoadhesive activity, interacting with mucin via electrostatic effects or hydrogen bonding or/and formation of interpenetrating layer between polymers and mucus gel. Mucoadhesion of polymers can provide significant opportunities when designing pharmaceutical formulations, such as tablets, films, patches and gels. However, the mucoadhesive properties of polyampholytes are rarely reported in the literature. This work thus explored the factors affecting the mucoadhesive properties of both synthetic and natural polyampholytes. Turbidimetric titrations and isothermal titration calorimetry (ITC) were conducted to investigate the interactions between polyampholytes and porcine gastric mucin in solutions. Both synthetic and natural polyampholyte demonstrated more pronounced interactions with mucin at $\text{pH} < \text{pH}_{\text{IEP}}$ than at $\text{pH} \geq \text{pH}_{\text{IEP}}$, where the polyampholytes are positively charged and mucin remains negatively charged. Electrostatic effects are predominantly responsible for their mucoadhesion whilst hydrogen bonding and hydrophobic effects have synergistic effects. A system of polyampholyte and fluorescein isothiocyanate (FITC) coated tablets were used to assess adhesion to porcine gastric mucosa at different pHs in essentially “static” systems. In addition, to reflecting fluid dynamics encountered on clinical application, the polyampholytes were labelled

fluorescently and prepared in solutions to determine their retention using a fluorescence microscopy-based flow-through assay. These *ex vivo* assays confirmed that the polyampholytes exhibited superior mucoadhesive properties at $\text{pH} < \text{pH}_{\text{IEP}}$. All these studies demonstrated solution pH and pH_{IEP} of polyampholytes are primary factors affect mucoadhesive properties of polyampholytes, and hydrogen bonding, hydrophobic effects, water transport, capillary forces, penetration also contribute to mucoadhesion. To test the generalisability of these findings, the retention of methacrylated L-PEI, crotonylated L-PEI, maleylated L-PEI and succinylated L-PEI on bovine palpebral conjunctiva at physiological pH ($\text{pH}=7.4$) was assessed using a fluorescence microscopy-based flow-through assay. Methacrylated-L-PEI and crotonylated L-PEI exhibited strong mucoadhesive properties at pH 7.4, due to the formation of covalent bonding between unsaturated C=C moieties within these synthetic cationic polyelectrolytes and mucin thiol groups. Conversely, maleylated L-PEI and succinylated L-PEI were poorly-mucoadhesive since physiological pH was above their isoelectric point, leading to electrostatic repulsion between the polyampholytes and mucin. In addition, the contribution of amine groups within these polyelectrolytes to adhesion are minimal at $\text{pH}=7.4$, where these polyelectrolytes are either non-charged or negatively charged. Toxicological evaluation and irritation studies of the modified L-PEI derivatives were undertaken. *In vivo* assays with planaria and the 3-(4,5-dimethylthiazol-2-yl)-2,5-diphenyl-2H-tetrazolium bromide (MTT) cell viability assay, and slug mucosa irritation assay suggested anhydride modified L-PEIs alleviated the adverse toxicity effects seen for the parent L-PEI.

In summary, modification of L-PEI with organic anhydrides enhanced mucoadhesive properties and biocompatibility of L-PEI, and reduced its toxicity, displaying great potential of modified L-PEI derivates as novel water-soluble functional excipients for mucoadhesive delivery systems.

List of conferences and presentations

1. Pharmacy PhD Showcase 2020, University of Reading, 4th July 2020 - Oral (3 minutes).
2. Pharmacy PhD Showcase 2021, University of Reading, 16th April 2021 - Oral (5 minutes).
3. Pharmacy PhD Showcase 2022, University of Reading, 31st March 2022 - Oral (15 minutes).
4. The 13th APS PharmSci Conference, Belfast, Northern Ireland, UK, 7-9th September 2022 - Poster.
5. The 6th London Polymer Group meeting, University College, London, UK, 27th April 2023 - Poster.
6. The 4th Virtual European Polymer Conference, 12-13th June 2023 - Oral (30 minutes)

List of publications from this thesis

1. Manfei Fu, Sergey K. Filippov, Adrian C. Williams, Vitaliy V. Khutoryanskiy. On the mucoadhesive properties of synthetic and natural polyampholytes. *Journal of Colloid and Interface Science* 659 (2024) 849–858.
<https://doi.org/10.1016/j.jcis.2023.12.176> **Published (Chapter 2)**
2. Manfei Fu, Roman V. Moiseev, Silvia Amadesi, Adrian C. Williams, Vitaliy V. Khutoryanskiy*. Exploring Mucoadhesive and Toxicological Characteristics Following Modification of Linear Polyethyleneimine with Various Anhydrides.
Revised (Chapter 3)

List of publications not from this thesis

1. Fhataheya Buang, Manfei Fu, Afroditi Chatzifragkou, Mohd Cairul Iqbal Mohd Amin, Vitaliy V. Khutoryanskiy. Hydroxyethyl cellulose functionalised with maleimide groups as a new excipient with enhanced mucoadhesive properties, *International Journal of Pharmaceutics*, Volume 642, 2023, 123113, ISSN 0378-5173.
<https://doi.org/10.1016/j.ijpharm.2023.123113>.

List of chapters

Chapter 1: Literature Review: Applications of Commercially Available Water-Soluble Polymers in Pharmaceutical Formulations

A detailed review systemically discusses applications of water-soluble polymers in pharmaceutical formulations. Specifically, this chapter summarises commercial products composed of polymers and reviews extensive literature on the topic related to the thesis.

Chapter 2: On the mucoadhesive properties of synthetic and natural polyampholytes

The paper from this chapter was accepted and published in the Journal of Colloid and Interface Science in 2024. This chapter clarifies the relationship between solution pH, isoelectric point (pH_{IEP}) and mucoadhesive properties of polyampholytes. This chapter demonstrates that both synthetic and natural polyampholytes displayed mucoadhesive properties at $pH < pH_{IEP}$.

Chapter 3: Exploring Mucoadhesive and Toxicological Characteristics Following Modification of Linear Polyethyleneimine with Various Anhydrides

In this chapter, linear polyethyleneimine (L-PEI) was modified with various organic anhydrides to enhance its functionality and reduce its toxicity. This chapter describes the synthesis, characterisation, retention studies and toxicity evaluations of anhydride modified L-PEI derivatives.

Chapter 4: Concluding remarks and future work

This chapter summarises and critically discusses the key findings in the thesis and proposes a plan of future work.

Table of Contents

Exploring Mucoadhesive and Toxicological Characteristics of Novel Water-Soluble Polymers Synthesised by Modifying Linear Polyethyleneimine with Various Anhydrides

School of Pharmacy	i
Acknowledgements	ii
Abstract	iii
List of conferences and presentations	v
List of publications from this thesis	vi
List of publications not from this thesis	vi
List of chapters	vii
Table of Contents	viii
List of Abbreviations	xiv
List of Tables	xix
List of Figures	xx
List of Schemes	xxv
Chapter 1.....	1
Chapter 1. Applications of Commercially Available Water-Soluble Polymers in Pharmaceutical Formulations	2
1.1 Introduction	2
1.2 Physicochemical properties of water-soluble polymers	9

1.3	Pharmaceutical applications	18
1.3.1	Oral administration.....	18
1.3.1.1	Tableting.....	19
1.3.1.2	Solutions for oral and other routes	20
1.3.2	Controlled release systems	21
1.3.3	Rheology modifiers	26
1.3.4	Mucoadhesive and mucus-penetrating systems	28
1.3.5	Solid drug dispersions	32
1.3.6	Injectable formulations.....	35
1.3.7	PEGylation	40
1.3.8	Micellar polymers.....	46
1.3.9	Drug conjugation.....	48
1.4	Linear Poly (ethylene imine).....	50
1.5	Reference.....	54
Chapter 2	76

Chapter 2.	On the mucoadhesive properties of synthetic and natural polyampholytes	77
	Abstract	77
2.1	Introduction	78
2.2	Materials and methods.....	80
2.2.1	Materials.....	80
2.2.2	Synthesis of succinylated L-PEI and phthaylated L-PEI	80
2.2.3	Characterization of succinylated L-PEI and phthaylated L-PEI	80

2.2.3.1	¹ H-nuclear magnetic resonance spectroscopy (¹ H-NMR).....	81
2.2.3.2	Fourier transform infrared (FTIR) spectroscopy	81
2.2.3.3	Turbidity measurements	81
2.2.3.4	Electrophoretic mobility measurements	81
2.2.4	Mucin interaction studies	81
2.2.5	Isothermal titration calorimetry (ITC).....	82
2.2.6	<i>Ex vivo</i> gastric mucoadhesive studies	82
2.2.6.1	Mucoadhesive studies of tablets on porcine gastric mucosa.....	82
2.2.6.2	Retention studies on porcine gastric mucosa	83
2.2.7	Statistical analysis	84
2.3	Results and discussion.....	84
2.3.1	Synthesis and characterization of succinylated L-PEI and phthaylated L-PEI.....	84
2.3.2	Mucin interaction studies	86
2.3.3	<i>Ex vivo</i> gastric mucoadhesion studies	89
2.4	Conclusion.....	95
2.5	References	95
2.6	Supporting Information	100
	Appendix I. ¹ H-NMR spectra of PEOZ and L-PEI recorded in methanol-d4.....	103
	Appendix II. FTIR spectra of PEOZ and L-PEI.....	103
	Appendix III. ¹ H-NMR spectra of L-PEI recorded in methanol-d4; succinylated L-PEI and phthaylated L-PEI recorded in D ₂ O.....	104
	Appendix IV. FTIR spectra of L-PEI, succinylated L-PEI and phthaylated L-PEI.....	105

Appendix V. Representative fluorescence images showing retention of FITC labelled phthaylated L-PEI after irrigation with different volumes of SGF under different pH at a flow rate of 0.43mL/min, FITC-dextran as negative control. Scale bar = 2 mm.	105
Appendix VI. Representative fluorescence images showing retention of FITC labelled BSA after irrigation with different volumes of SGF under different pH at a flow rate of 0.43mL/min, FITC-dextran as negative control. Scale bar = 2 mm...	106
Appendix VII. Ratio of polymers to mucin for turbidimetric titration curve (g/g).	106
Appendix VIII. Retention study of FITC-labelled polyampholytes under different pHs at 5 min and 60 min.	107
Chapter 3.....	109

Chapter 3. Exploring Mucoadhesive and Toxicological Characteristics Following Modification of Linear Polyethyleneimine with Various Anhydrides 110

Abstract	110
3.1 Introduction	112
3.2 Materials and methods.....	112
3.2.1 Materials.....	112
3.2.2 Synthesis of linear polyethyleneimine (L-PEI)	113
3.2.3 Synthesis of methacrylated L-PEI, crotonylated L-PEI, maleylated L-PEI and succinylated L-PEI	113
3.2.4 Characterization of methacrylated L-PEI, crotonylated L-PEI, maleylated L-PEI and succinylated L-PEI	114
3.2.4.1 ¹ H-nuclear magnetic resonance spectroscopy (¹ H-NMR).....	114
3.2.4.2 Fourier transform infrared (FTIR) spectroscopy	114

3.2.4.3	Turbidity measurements	114
3.2.4.4	Electrophoretic mobility measurements	115
3.2.5	<i>Ex Vivo</i> mucoadhesion studies	115
3.2.5.1	Preparation of simulated tear fluid	115
3.2.5.2	Preparation of fluorescently labelled polymers.....	115
3.2.5.3	Retention studies on ocular tissues.....	115
3.2.6	Slug mucosal irritation assay.....	116
3.2.7	Toxicology.....	117
3.2.7.1	Acute toxicity assay.....	117
3.2.7.2	Planarian toxicity fluorescent assay	117
3.2.7.3	Cell viability	118
3.2.7.3.1	Cell culture and treatment.....	118
3.2.7.3.2	MTT assay	118
3.2.7.4	Measurement of cell death	119
3.2.8	Statistical analysis	119
3.3	Results and discussion.....	120
3.3.1	Synthesis and characterization of methacrylated L-PEI, crotonylated L-PEI, maleylated L-PEI and succinylated L-PEI	120
3.3.2	<i>Ex Vivo</i> mucoadhesion studies of methacrylated L-PEI, crotonylated L-PEI, maleylated L-PEI and succinylated L-PEI	124
3.3.3	Slug mucosal irritation test.....	126
3.3.4	Toxicological tests in live planaria.....	128
3.4	Conclusion.....	132
3.5	References	133

3.6	Supporting Information	138
	Appendix IX. ¹ H-NMR spectra of PEOZ and L-PEI recorded in methanol-d4.	138
	Appendix X. FTIR spectra of PEOZ and L-PEI.	139
	Appendix XI. FTIR spectra of methacrylated L-PEI, crotonylated L-PEI, maleylated L-PEI and succinylated L-PEI.....	139
	Appendix XII. Fluorescence spectra of FITC labelled methacrylated L-PEI, crotonylated L-PEI, maleylated L-PEI and succinylated L-PEI at 1mg/mL.....	140
	Appendix XIII. Exemplar images of <i>ex vivo</i> bovine palpebral conjunctiva with applied FITC-dextran, FITC-methacrylated L-PEI, FITC-crotonylated L-PEI, FITC-maleylated L-PEI and FITC-succinylated L-PEI. Scale bars are 1 mm.....	140
	Appendix XIV. Acute toxicity assay was conducted after 48h exposure of planaria to 1 mg/mL methacrylated L-PEI, crotonylated L-PEI, maleylated L-PEI, succinylated L-EPI, APW and 24h exposure of planaria to 0.1 mg/mL b-PEI. ‘A’ denotes live planaria whereas ‘D’ denotes dead planaria.....	141
	Appendix XV. FTIR absorption bands from methacrylated L-PEI, crotonylated L-PEI, maleylated L-PEI and succinylated L-PEI.	141
	Chapter 4. Concluding remarks and future work.....	142
	Chapter 4. Concluding remarks and future work.....	143
4.1	General discussion and conclusion.....	143
4.2	Future work	147
4.3	Reference.....	149

List of Abbreviations

¹ H-NMR	proton nuclear magnetic resonance
ALL	acute lymphoblastic leukemia
ANOVA	analysis of variance
APW	artificial pond water
ASD	amorphous solid dispersion
AuNP	Au nanoparticle
b-PEI	branched polyethyleneimine
BAC	benzalkonium chloride
BAC	benzalkonium chloride
BPM	4-bromophenyl maleimide
BSA	bovine serum albumin
BSM	bovine submaxillary glands
C _{12h}	12 hour mean plasma concentration
CAC	aggregation concertation
CaCl ₂	calcium chloride
CM-Dex	carboxymethyl dextran
C _{max}	maximum plasma concentration
CMC	critical micelle concentration
CMC	carboxymethyl cellulose
CMLBG	carboxymethyl locust bean gum
CMT	critical micelle temperature
COVID-19	coronavirus disease of 2019
CP	clobetasol 17-propionate
CPT	camptothecin
CROP	cationic ring-opening polymerization
D ₂ O	deuterium oxide
Da	Dalton
DAPI	6-diamidino-2-phenylindole
DDC	N, N'-dicyclohexyl carbodiimide
DI	deionized water
DIPEC	drug-interpolyelectrolyte complex
DLS	dynamic light scattering

DMI	dimethyl isosorbide
DMSO	dimethyl sulfoxide
DMSO-d6	deuterated dimethyl sulfoxide
DNA	deoxyribonucleic acid
DOX	doxorubicin
DP	degrees of polymerization
DPBS	Dulbecco's phosphate buffered saline
DPC	drug-polyelectrolyte complex
DS	degree of substitution
ECL	electrochemiluminescence
EDC	1-ethyl-3-(3-dimethylamino-propyl) carbodiimide
EDTA	ethylenediaminetetraacetic acid
EDTA	trypsin-EDTA solution
EtOH	ethanol
F-12	Ham's F-12 nutrient mixture
FBS	fetal bovine serum
FITC	fluorescein isothiocyanate
FITC-dextran	fluorescein isothiocyanate-dextran
FTIR	Fourier transformed infrared spectroscopy
FVIII	factor VIII
G-CSF	granulocyte colony-stimulating factor
GEJ	gastroesophageal junction
GI tract	gastrointestinal tract
GQDs	graphene quantum dots
GTP	group transfer polymerization
GTP	group transfer polymerization
H ₂ SO ₄	sulfuric acid
HA	hyaluronic acid
HA-Q	hyaluronic acid-quercetin
HACHI	half-acetylated chitosan derivative
hATTR	hereditary transthyretin amyloidosis
HBSS	Hanks' Balanced Salt Solution
HCl	hydrochloric acid

HEC	hydroxyethyl cellulose
HPC	hydroxypropyl cellulose
HPMC	hydroxypropyl methylcellulose
HPMCAS	hydroxypropyl methylcellulose acetate succinate
I_0	initial fluorescence intensity
$I_{\text{background}}$	background fluorescence of the tissue
IBP	ibuprofen
IM	intramuscular injection
IND	indomethacin
I_t	fluorescence images of the mucosal tissue
ITC	isothermal titration calorimetry
IV	intravenous injection
KBr	potassium bromide
KCl	potassium chloride
kDa	kilo Dalton
KI	potassium iodide
KNO_3	potassium nitrate
L-PEI	linear polyethylene imine
LCST	lower critical solution temperature
LD_{50}	50% hemolysis of red blood cells
LGS	Lennox-Gastaut syndrome
MC	methylcellulose
MeOD-d4	deuterated methanol
MgCl_2	magnesium chloride
MgSO_4	magnesium sulfate
MNZ	metronidazole
MP%	amount of mucus produced
mPEG	methoxy-PEG
MPS	mononuclear phagocyte system
MTT	thiazolyl blue tetrazolium bromide
MTT	3-(4, 5-Dimethyl-2-thiazolyl)-2, 5-diphenyl-2H-tetrazolium bromide
M_v	viscosity-average molecular weight

MW	molecular weight
MWCO	molecular weight cut off
Nab TM	nanoparticle albumin-bound
NaCl	sodium chloride
NaFI	sodium fluorescein
NaOH	sodium hydroxide
NCA-ROP	N-carboxyanhydride ring-opening polymerization
NHS	N-hydroxy succinimide
OLP	oral lichen planus
PAA-Hb	poly (acrylic acid)-met-hemoglobin
PA	phthalic anhydride
PAA	poly (acrylic acid)
PAA-Hb	poly (acrylic acid)-met-hemoglobin
PBS	phosphate-buffered saline
PDMAEMA	poly (2-dimethylaminoethyl methacrylate)
PEG	polyethylene glycol
PEG-Mal	maleimide-functionalised PEGylated
PEI	polyethylene imine
PEO	polyethylene oxide
PEO-PPO-PEO	poly (ethylene oxide)-poly (propylene oxide)-poly (ethylene oxide)
PEOZ	poly(2-ethyl-2-oxazoline)
PGM	mucin from porcine stomach (type II)
PHEA	poly (2-hydroxyethyl acrylate)
pH _{IEP}	isoelectric point
PI	propidium iodide
pK _a	acid dissociation constant
PMA	poly (methacrylate)
PMAA	poly (methacryl amide)
PMAA	poly (methacrylic acid)
PMOZ	poly(2-methyl-2-oxazoline)
PiPOZ	poly(2-isopropyl-2-oxazoline)
PnPOZ	poly(2-propyl-2-oxazoline)

POx	poly (2-oxazoline)
PPI	poly (propylene imine)
PSA	prostate-specific antigen
PVA	poly (vinyl alcohol)
PVAc	polyvinyl acetate
PVP	poly (vinylpyrrolidone)
PVPVA	poly (vinylpyrrolidone-co-vinyl acetate)
RNA	ribonucleic acid
RTV	ritonavir
S100	Eudragit [®] S100
SA	succinic anhydride
SC	subcutaneous injections
SD	solid dispersion
SD	standard deviation
SMIT	slug mucosal irritation test
sodium CMC	sodium carboxymethyl cellulose
STF	simulated tear fluid
$t_{1/2}$	half-life
TEA	triethylamine
T_g	glass transition temperature
TPV	Telaprevir
UCST	upper critical solution temperature
α -PLL	α -poly-L-lysine
ϵ -PLL	ϵ -poly-L-lysine
η	intrinsic viscosity
η^*	complex viscosity
η_{rel}	relative viscosity
ΔH	enthalpy

List of Tables

Table 1.1-1. Classification of common water-soluble polymers.....	4
Table 1.3-1 Examples of commercially available solid dispersion. Reproduced from Ref. ²⁶⁸ by permission of Oxford University Press.	33
Table 1.3-2. Advantages and disadvantages for intravenous, intramuscular and subcutis injections.	37
Table 1.3-3 FDA approved PEGylated formulations.	42
Table 2.3-1. Characteristics of polyampholytes	86
Table 4.1-1. p _H ^I _{EP} values of succinylated L-PEI, maleylated L-PEI and phthaylated L-PEI determined by turbidimetric technique and electrophoretic mobility measurement.....	144

List of Figures

- Figure 1.2-1. Effect of pH on aqueous solubility for amphoteric polymers. 10
- Figure 1.2-2. Phase diagram demonstrating LCST and UCST of polymers in aqueous solution. Modified from Bansal et al.¹⁹⁵ 12
- Figure 1.2-3. Schematic illustration of the transition behaviour of LCST and UCST thermo-responsive polymers; the red line represents the macroscopic phase transition. The left panel shows the behaviour of LCST polymers and the right panel shows the behaviour of UCST polymers. Reproduced from Nasserri et al.¹⁹⁶ by permission of Elsevier Science Ltd., UK. 13
- Figure 1.2-4. The solution complex viscosity (η^*) at high concentration (~250mg/mL) of BSA solution (left axis) and the relative viscosity (η_{rel}) at low concentration (~40mg/mL) of BSA solution (right axis) as a function of solution pH. Reproduced from Yadav et al.¹⁹⁷ by permission of Springer Nature. 14
- Figure 1.2-5. Illustration of power-type correlation between weight average molar mass and intrinsic viscosity of fibroin in lithium bromide. Reproduced from Pawcenis et al.²⁰⁰ by permission of The Royal Society of Chemistry..... 15
- Figure 1.2-6. The structure of intra-polymer chelate (a) and inter-polymer chelate (b). R=coordinating atom or group; M=metal ion. 17
- Figure 1.2-7. Common structure of polymer-metal complexes (a) carboxylic type complexes; (b) acrylamide type complexes; (c) maleylglycine type complexes and (d) amine type complexes. Reproduced by Rivas et al.²¹² by permission of Elsevier Science Ltd., UK. 18
- Figure 1.3-1. The swelling properties of pure PMM (-■- and tablet A), PMM combined with 10% (w/w) MgCl₂ (-□- and tablet B), PMM combined with 10% (w/w) HPMC (-▲- and tablet C) and PMM combined with 10% (w/w) MgCl₂ and HPMC (-◇- and tablet D). Reproduced by Cilurzo et al.²³⁵ by permission of Elsevier Science Ltd., UK. 23

Figure 1.3-2. Reticular-erosive lichen planus before (a) and after (b) treatment with prepared Clobetasol 17-Propionate (CP) mucoadhesive extended-release tablet. Reproduced by Cilurzo et al. ²³⁵ by permission of Elsevier Science Ltd., UK.....	24
Figure 1.3-3. Illustration of viscosity is increased by solvent molecules penetrating into void spaces of polymer chains.....	27
Figure 1.3-4. Schematic structures of mucosal tissue.	29
Figure 1.3-5. A typical temperature-composition phase diagram for an ASD. Reproduced from Zhang et al. ²⁶⁹ by permission of Elsevier Science Ltd., UK.	34
Figure 1.3-6. The site of different injection administrations within skin. Modified from Frost, Gregory I. ²⁷⁷	36
Figure 1.3-7. Method for the activation of PEG molecules (a) Cyanuric chloride method; (b) a variation on the cyanuric chloride method; (c ¹) PEG–succinimidyl succinate method; (c ²) substitution of the succinate residue by glutarate; (c ³) substitution of the aliphatic ester in c ¹ by an amide bond; (d) imidazolyl formate method; (e) and (f) variations using phenylcarbonates of PEG; (g) succinimidyl carbonates of PEG and (h) succinimidyl active ester of PEG. Modified from Harris and Chess ²⁸⁵ by permission of Springer Nature.	40
Figure 1.3-8. Relevance of PEG shape on protein surface coverage or enzyme active site access. The higher steric hindrance of branched PEGs ensures more complete protein shielding and makes difficult the access to recognition or active site cleft. Reproduced from Pasut and Veronese ²⁹⁵ by permission of Elsevier Science Ltd., UK.	44
Figure 1.3-9. Types of FDA approved PEGylated drugs. P/D, the molar ratio of PEG to drug. Reproduced from Gao et al. ²⁸⁸ by permission of John Wiley & Sons Ltd., UK.....	45
Figure 1.3-10. (a) Structure of Pluronic [®] , and (b) Pluronic [®] grid (color code: physical state of copolymers under ambient conditions: green = liquid; red = paste; orange = flake). Reproduced from Pitto-Barry and Barry ²⁹⁹ by permission of The Royal Society of Chemistry.	46

Figure 1.3-11. The mechanism of cloud point reduction by salting-out. Reproduced from An et al. ³⁰⁶ by permission of Springer Nature.....	47
Figure 2.3-1. Effect of pH on solution turbidity (a) and electrophoretic mobility (b) of 1mg/mL succinylated L-PEI, phthaylated L-PEI and BSA aqueous solution.	85
Figure 2.3-2. Turbidimetric titration curves of 1 mg/mL porcine gastric mucin with 1 mg/mL succinylated L-PEI (a), phthaylated L-PEI (b) and BSA (c) in aqueous solution; turbidimetric titration curves of 1 mg/mL porcine gastric mucin with 1 mg/mL succinylated L-PEI (d), phthaylated L-PEI (e) and BSA (f) in urea solution; effect of the pH on the interaction between polyampholytes and mucin using isothermal titration calorimetry: 1 mg/mL PGM was titrated with 1 mg/mL succinylated L-PEI at pH 2.50 and pH 7.00 (g), 1 mg/mL PGM was titrated with 1 mg/mL phthaylated L-PEI at pH 3.00 and pH 10.00 (h) and 1 mg/mL PGM was titrated with 1 mg/mL BSA at pH 2.50 and pH 7.00 (i). Mean average \pm standard deviation, n=3.	87
Figure 2.3-3. Illustration of tensile test methodology (a); effect of pH on peak force of detachment (b) and work of adhesion (c) of model tablets coated with succinylated L-PEI, phthaylated L-PEI and BSA on porcine gastric mucosa at $37\pm 0.1^\circ\text{C}$. Mean \pm standard deviation, n=20. The statistically significant differences are represented as: **** p < 0.0001; ns: no significance.	90
Figure 2.3-4. Effect of pH on mucosal retention of 1 mg/mL FITC-succinylated L-PEI (a), FITC-phthaylated L-PEI (b), FITC-BSA (c) and FITC-dextran (d) on porcine gastric mucosa washed with different volumes of SGF (0.43 mL/min) for 60 min and FITC-dextran as negative control at $37\pm 0.1^\circ\text{C}$; exemplar fluorescence images (e) with retention of FITC labelled succinylated L-PEI and FITC-dextran after irrigation with different volumes of SGF under different pH at a flow rate of 0.43mL/min; FITC-dextran was used as negative control. Scale bars are 2 mm. Mean \pm standard deviation, n=3. The statistically significant differences are represented as: *** p<0.001; ** p < 0.01; * p < 0.05; ns: no significance.....	93

Figure 3.3-1. ¹ H NMR spectra of methacrylated L-PEI, crotonylated L-PEI, maleylated L-PEI and succinylated L-PEI recorded in D ₂ O.	121
Figure 3.3-2. Effect of pH on solution turbidity (a) and electrophoretic mobility (b) of 1 mg/mL methacrylated L-PEI, crotonylated L-PEI, maleylated L-PEI and succinylated L-PEI aqueous solutions.....	123
Figure 3.3-3. Retention of FITC-methacrylated L-PEI, FITC-crotonylated L-PEI, FITC-maleylated L-PEI, FITC-succinylated L-PEI and FITC-dextran on bovine palpebral conjunctiva when washed with STF (0.1 mL/min) for 30 min at 34.5±0.1°C. Mean ± standard deviation, n=3. The statistically significant differences are represented as: ** p < 0.01; * p < 0.05; ns – no significance.	125
Figure 3.3-4. Exemplar images of slugs following 60 min of exposure to controls and test solutions using a slug mucosal irritation test (a); and mucus production in contact with 1% BAC in PBS, PBS, methacrylated L-PEI, crotonylated L-PEI, maleylated L-PEI, succinylated L-PEI and branched PEI (b). Data is given as mean ± standard deviation (n = 5). Statistically significant differences were represented as: **** – p < 0.0001; ns – no significance..	127
Figure 3.3-5. (a) Exemplar fluorescent images of individual planaria exposed to 1 mg/mL methacrylated-, crotonylated-, maleylated- and succinylated L-PEI with APW used as a negative control and 0.1 mg/mL b-PEI as a positive control. Note that fluorescent images could not be obtained after 24 h and 48 h exposure to b-PEI as these conditions resulted in partial disintegration of the worms. Scale bar is 2 mm. (b) Mean fluorescence intensity values of planaria exposed to 1 mg/mL methacrylated-, crotonylated-, maleylated- and succinylated L-PEI with APW as negative control and 0.1 mg/mL b-PEI as positive control, calculated from the analysis of images. Mean ± standard deviation, n=5. The statistically significant differences are represented as: ** p < 0.01; ns: no significance.....	129
Figure 3.3-6. Viability of A549 cells determined after treatment with solutions of methacrylated L-PEI, crotonylated L-PEI, maleylated L-PEI and	

succinylated L-PEI for 24 h using MTT assay. Cells treated with complete medium 1% FBS were used as a negative control and cells exposed to 0.5 mg/mL b-PEI were used as a positive control. Data are expressed as % of external control, cells untreated, left in complete medium 10% FBS. Values are shown as means \pm SD (n = 6 replicated per treatment). Statistically significant differences are represented as: * p < 0.05; ** p < 0.01; ns: *** p < 0.001; **** p < 0.0001. 130

Figure 3.3-7. Mortality of A549 cells evaluated after treatment with methacrylated L-PEI and crotonylated L-PEI at 0.5 mg/mL and 1.0 mg/mL for 24 h, with untreated cells in 1% FBS as the negative control (a); representative DAPI (left) and PI (right) staining images of methacrylated L-PEI and crotonylated L-PEI at 0.5 mg/mL and 1.0 mg/mL with cells cultured in 1% FBS as a negative control and cells exposed in 0.5 mg mg/mL b-PEI as a positive control, scale bar is 100 nm (b). Cell mortality % is expressed as values are expressed as means \pm SD (n = 3). Statistically significant differences are represented as: * p < 0.05. 131

List of Schemes

Scheme 1.4-1. Basic hydrolysis of L-PEI start with parent POx.	50
Scheme 1.4-2. Acidic hydrolysis of L-PEI start with parent POx.	51
Scheme 1.4-3. Illustrative examples of modification of L-PEI with a) Michael addition, b) carboxylic acid, c) acetylation and d) nucleophilic substitution.	52
Scheme 2.3-1. Synthesis of succinylated and phthaylated L-PEI from PEOZ.	84
Scheme 3.3-1. L-PEI was obtained by acidic hydrolysis of PEOZ and subsequently modified with methacrylic anhydride, crotonic anhydride, maleic anhydride and succinic anhydride, respectively.....	121

Chapter 1.

Applications of Commercially Available Water-Soluble Polymers in Pharmaceutical Formulations

(QUAD system contribution of Manfei Fu: 80% of conception and design, 100% of data collection, 90% of data analysis and conclusions, and 100% of manuscript preparation).

Chapter 1. Applications of Commercially Available Water-Soluble Polymers in Pharmaceutical Formulations

(QUAD system contribution of Manfei Fu: 80% of conception and design, 100% of data collection, 90% of data analysis and conclusions, and 100% of manuscript preparation).

By Manfei Fu^a, Adrian C. Williams^a, Vitaliy V. Khutoryanskiy^{*a,b}

^a School of Pharmacy, University of Reading, Whiteknights, Post Office Box 224, Reading RG6 6AD, United Kingdom

^b Physicochemical, Ex Vivo and Invertebrate Tests and Analysis Centre (PEVITAC, www.pevitac.co.uk), University of Reading, Whiteknights, Reading, RG6 6DX, UK

*Correspondence author: v.khutoryanskiy@reading.ac.uk
Reading School of Pharmacy, University of Reading,
Whiteknights, PO Box 224, Reading RG6 6AD, United Kingdom

1.1 Introduction

Water-soluble polymers are typically composed of hydrophilic repeating units, allowing them to interact with water and form stable solutions. The water solubility of these polymers is generally attributed to the presence of -OH, -COOH or -NH₂ groups within the polymers to form hydrogen bonds with water. Water-soluble polymers can also form complexes with drugs via hydrogen bonding, electrostatic interactions and Van der Waals force or can physically mix with drugs.

Over recent decades, novel drug candidates have tended to be increasingly hydrophobic to support more specific target engagements with fewer off target interactions and so tend to have poor aqueous solubility and consequent bioavailability. To mitigate these issues, polymeric excipients have been used to explore novel drug delivery system. Initially, polymers were employed as formulation excipients¹, stabilizers² and carriers for controlled release systems³. More recently, polymers have been explored in various functional pharmaceutical formulations, such as nano drug delivery platforms⁴, mucoadhesive drug delivery⁵, conjugation with biomacromolecules⁶, tissue engineering⁷, antimicrobial agents⁸ and gene delivery⁹.

Since being reviewed over 50 year ago¹⁰, novel polymeric systems and their applications have been developed. Here, we classify common water-soluble polymers according to their

structure as cationic, anionic and amphoteric polymers; their origins, structure and example applications are summarised in Table 1-1.

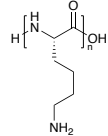
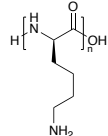
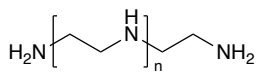
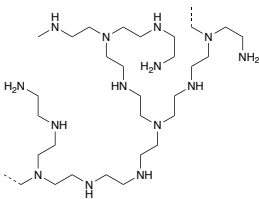
Cationic polymers are macromolecules containing positive charges in the polymer backbone and/or the pendant chains, usually through protonation of primary, secondary or tertiary amine groups. On the basis of origin, cationic polymers can be classed as natural materials such as chitosan and ϵ -poly-lysine (ϵ -PLL), or synthetic such as α -poly-lysine (α -PLL), polyethylene imine (PEI) or poly (2-dimethylaminoethyl methacrylate) (PDMAEMA).

Anionic polymers are macromolecules containing negative charges in their backbone and/or pendant chains, generally through -COOH, -SO₃H and -PO₃H₂ groups. Again, anionic polymers may be natural materials such as alginate, hyaluronic acid (HA), carboxymethyl cellulose (CMC), semi-natural such as guar gum, or synthetic with examples including polycarbophil, polyacrylic acid (PAA) and carboxymethyl dextran (CM-Dex).

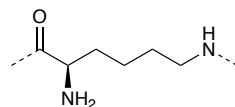
Amphoteric polymers are defined as macromolecules containing both positive and negative charges in their backbone and/or pendant chains, as so can include primary, secondary or tertiary amine groups and -COOH, -SO₃H or -PO₃H₂ groups. Natural amphoteric polymers include albumins, phosphatidylcholine (PC) and gelatin, with synthetic examples being as poly (methacryl amide) (PMAA) and poly (methacrylate) (PMA).

Non-ionic polymers carry neither positive or negative charges in their backbone and/or pendant chains. On the basis of origin, natural non-ionic polymers include the cellulose derivatives methylcellulose (MC), hydroxypropyl methylcellulose (HPMC), hydroxypropyl cellulose (HPC) and hydroxyethyl cellulose (HEC) whereas the synthetic materials include poly (vinyl pyrrolidone) (PVP), poly (ethylene glycol) (PEG), poly (vinyl alcohol) (PVA) and poly (2-oxazoline) (POx).

Table 1.1-1. Classification of common water-soluble polymers

Type of polyelectrolytes	Classification	Exemplar polymers	Structures	Origins	Pharmaceutical applications
		α -Poly-L-lysine (α -PL)	 <p>α-PLL</p>  <p>α-PDL</p>	Synthesized from L-lysine and D-lysine ¹¹ , or produced by N-carboxyanhydride ring-opening polymerization (NCA-ROP). ¹²	coating (enhancing cell adhesion) ¹³ , biocatalyst ¹⁴ , α -Poly-L-lysine-enzymes conjugates ¹⁵ , gene therapy ¹⁶
Cationic polyelectrolytes	<i>Synthetic polymers</i>	Linear PEI	 <p>Linear PEI</p>	Linear PEI (L-PEI) is obtained via acidic hydrolysis of poly (2-ethyl-2-oxazoline). ¹⁷	gene delivery ¹⁹ , hydrogel ²⁰ , chemotherapy ^{8,21} , controlled release system ²² , antimicrobial agents ²³ , magnetic resonance imaging ²⁴ , tissue engineering ²⁵ , drug delivery carrier ^{26,27} , mucoadhesion ^{5,28} , vaccine adjuvants ^{18,29} , biological labels ⁹ , enzyme biocatalyst ³⁰
		Polyethyleneimine (PEI)	 <p>Branched PEI</p>	Branched PEI (b-PEI) is obtained through cationic polymerization of aziridine and contains primary, secondary, and tertiary amino groups. ¹⁸	

ϵ -Poly-L-lysine
(ϵ -PL)

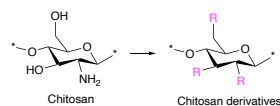


Produced by *Streptomyces albulus* NBRC14147 as a secondary metabolite.³¹

biocatalyst¹⁴, antimicrobial emulsifier³², drug carriers^{33,34} antibacterial agent³⁵

Natural polymers

Chitosan and its derivatives



R=quaternary ammonium, guanidine, alkyl, carboxyalkyl, hydroxyalkyl, aminoalkyl, amino acids and peptides

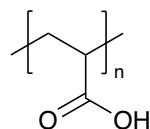
Produced by basic hydrolysis of chitin³⁶ which can be obtained from the exoskeleton of insects and crustaceans, such as shrimp, lobsters, and crabs³⁷.

antibacterial agent³⁸, wound dressing^{7,39-41}, dental application^{42,43}, biosensor⁴⁴,theranostic⁴⁵, drug delivery^{46,47}, mucoadhesion⁴⁸⁻⁵¹, gene delivery⁵², hemostatic agent⁵³, hyperthermia treatment⁵⁴, bone engineering^{55,56}

Anionic polyelectrolytes

Synthetic polymers

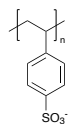
Polyacrylic acid (PAA)



Produced from acrylic acid monomer.⁵⁷

wound healing⁵⁸, nano platforms⁵⁹, drug delivery^{60,61}, antibacterial agent⁶², bone engineering^{63,64}, adhesion⁶⁵, coating⁶⁶, artificial tears⁶⁷, biosensor⁶⁸, theranostic^{45,69}

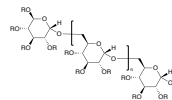
Polystyrene sulfonate



Produced by sulfonation of polystyrene.

hyperkalemia treatment⁷⁰

Dextran sulfonate



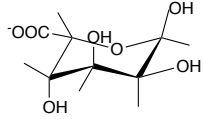
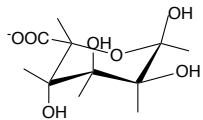
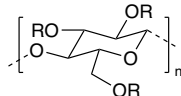
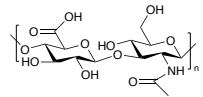

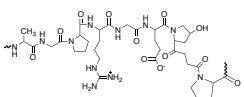
Produced by sulfation of selected dextran fractions.

clinical model of colitis⁷¹

R=H or SO₃Na

Amphoteric polyelectrolytes

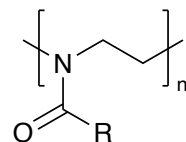
Natural polymers

		<p>The component monosaccharides of alginate:</p>  <p>D-mannuronate</p>  <p>L-guluronate</p>	<p>Obtained from brown seaweed.⁷²</p>	<p>enteric delivery vehicles⁷³, wound healing^{74,75}, magnetic resonance imaging⁷⁶, drug delivery²⁶, controlled release system⁷⁷, protein delivery⁷⁸, cell culture⁷⁹, blood vessels⁷², bone regeneration^{80,81}</p>
		<p>Cellulose ethers: carboxymethyl cellulose (CMC)</p> 	<p>Produced by alkylation-etherification process.⁸²</p>	<p>drug delivery⁸³, wound dressing⁸⁴, tissue engineering⁸⁵, bone engineering⁸⁶, auxiliary agent⁸⁷, biosensors⁸⁸, 3D printing⁸⁹</p>
		<p>Hyaluronic acid (HA)</p> 	<p>Distributed in the extracellular matrix and the joint liquid of mammals.</p>	<p>wound dressing⁹⁰, wound healing⁷⁵</p>
		<p>Albumins</p> 	<p>Synthesized in the liver.⁹¹</p>	<p>drug carrier⁹², polymer-conjugates⁹³, targeted drug delivery⁹⁴, stealth effect⁹⁵, imaging agent⁹⁶, plasma substitutes⁹⁷</p>
		<p>Gelatin</p> 	<p>Obtained from animal skins, boiled and crushed bones and the connective muscle tissues of cows and pigs.</p>	<p>mucoadhesive delivery system⁹⁸, gene delivery⁹⁹, microneedles¹⁰⁰, tissue engineering¹⁰¹, capluse¹⁰²</p>

**Non-ionic
polymers**

Synthetic polymers

Poly
(2-oxazoline)s
(POx)

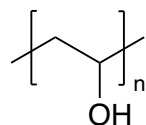


R = H, alkyl, aryl

Produced by cationic ring-opening
polymerization (CROP) of 2-
oxazolines.¹⁰³

conjugation¹⁰⁴, drug carrier¹⁰⁵,
pharmaceutical excipient¹⁰⁶, gene
delivery¹⁰⁷, antimicrobial agent¹⁰⁸,
magnetic resonance imaging (MRI)
contrast agents¹⁰⁹, hydrogel¹¹⁰,
micelles^{111,112}

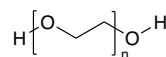
Polyvinyl
alcohol (PVA)



Synthesized by polymerization of vinyl
acetate to polyvinyl acetate (PVAc)
which is then hydrolysed to get
PVA.^{10,113}

drug delivery¹¹⁴, contact lens¹¹⁵, tissue
engineering¹¹⁶, adhesion barrier¹¹⁷,
coating⁵⁸, eye drop¹, bone
engineering¹¹⁸, embolic agent¹¹⁹

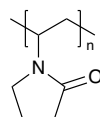
Poly (ethylene
glycol)
(PEG)



Produced by ring-opening
polymerization of ethylene oxide¹²⁰

drug delivery^{121,122}, anticancer
agents¹²³⁻¹²⁵, PEG-protein
conjugates^{6,126,127}, theranostic¹²⁸,
gene delivery¹²⁹, cell culture¹³⁰
tissue engineering^{131,132}

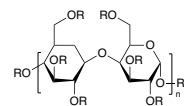
Poly (vinyl
pyrrolidone)
(PVP)



Produced by polymerization of vinyl
pyrrolidone.¹³³

pharmaceutical excipients¹³⁴⁻¹³⁶:
binder, film, solubilizer, disintegrant,
thickener, coating; drug carrier¹³⁷,
bone engineering¹³⁸, drug conjugate¹³⁹,
dialysis membrane¹⁴⁰, tissue
engineering¹⁴¹

Hydroxypropyl
methylcellulose
(HPMC)

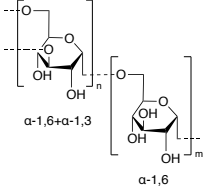
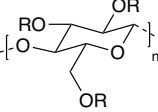
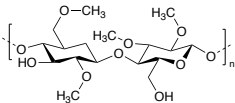
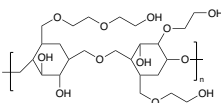


R=H, CH₃ or
CH₂CH(OH)CH₃

Produced by reacting alkali cellulose
with propylene oxide and methyl
chloride.¹⁴²

pharmaceutical excipients:
binder¹⁴³, tablet coating¹⁴⁴, film-
forming agent¹⁴⁵, eye drop¹⁴⁶,
controlled release system¹⁴⁷,

Natural polymers

Dextran	 <p>α-1,6+α-1,3 α-1,6</p>	Obtained from sucrose by lactic-acid bacteria.	ocular inserts ¹⁴⁸ , polymer matrix ¹⁴² , mucoadhesive ^{149,150} MRI applications ¹⁵¹ , nano platform ¹⁵² , gene delivery ¹⁵³ , hydrogel ¹⁵⁴ , insulin delivery ¹⁵⁵ , spinal cord injury ¹⁵⁶ , tissue engineering ¹⁵⁷
Hydroxypropyl cellulose (HPC)	 <p>R=H or CH₂CH(OH)CH₃</p>	Produced by treating cellulose with alkali and propylene oxide. ¹⁵⁸	pharmaceutical excipients ¹⁵⁹⁻¹⁶¹ , DNA separation ¹⁶² , hydrogels ¹⁶³ , artificial tears ¹⁶⁴ , nanoparticles ¹⁶⁵
Methyl cellulose (MC)		Produced by etherification of cellulose.	pharmaceutical excipients ^{2,166,167} , artificial tear ¹⁶⁸ , constipation treatment ¹⁶⁶ , cell culture ¹⁶⁹ , mucoadhesive ¹⁷⁰
Hydroxyethyl cellulose (HEC)		Produced by etherification of alkali cellulose with ethylene oxide produces HEC. ¹⁷¹	cryogel ¹⁷² , hydrogel ¹⁷³ , film ¹⁷⁴ , tissue engineering ¹⁷⁵ , bone engineering ¹⁷⁶ , surfactant ¹⁷⁷ , drug delivery system ¹⁷⁸ , protein and DNA separation ^{179,180}

1.2 Physicochemical properties of water-soluble polymers

Water-soluble polymers possessing cationic and/or anionic functional groups are susceptible to ionization in aqueous solution, providing polyelectrolyte properties depending on their pK_a under acidic or basic conditions. Thus, the effect of pH on solubility of water-soluble polymers is considerable; for example, chitosan dissolves in aqueous solution at $pH < 6$.¹⁸¹ In acidic conditions, the amino group of chitosan is partially protonated leading to electrostatic repulsion between positively charged polysaccharide chains, with the subsequent extension of the polymer chains allowing diffusion of water then solvation of the macromolecules.

PDMAEMA is a weak cationic polyelectrolyte with a pK_a at 7.4; the amine groups in the pendant chain of PDMAEMA are protonated when $pH < pK_a$ and are deprotonated when $pH > pK_a$. It thus follows that the dimethylamino groups in PDMAEMA are partially protonated under normal physiological conditions (pH 7.4). PDMAEMA forms a strong polyelectrolyte via introduction of cationic functional groups that selectively quaternize with alkyl halides through group transfer polymerization (GTP).¹⁸²

Conversely for anionic polymers, due to deprotonation of carboxylic groups, sulfonic acids, phosphonic acids or boronic acids under basic conditions, they form anionic polyelectrolytes, again resulting in electrostatic repulsion between negatively charged polymer chains leading to extension of the chains allowing diffusion of water into macromolecules. Due to the protonation of these functional groups under acidic condition, coiling of uncharged polymer chains leads to weak solvation of the polymers. The pK_a of CM-Dex is reported to be 6.1, when $pH > pK_a$, the diffusion rate of protein (lysozyme) through a CM-Dex pH-sensitive hydrogel membrane was greater than when $pH < pK_a$ and was attributed to electrostatic repulsion of the polymer chains to facilitate penetration of lysozyme through CM-Dex hydrogel due to deprotonation of $-COOH$ at $pH > pK_a$.¹⁸³ A similar trend was observed for a CMC hydrogel whose swelling ability was enhanced when $pH > pK_a$.¹⁸⁴

Amphoteric polymers possess unique physicochemical properties, such as an isoelectric point (pH_{IEP}), which is characterized as the pH at which the net charge of macromolecules is zero. When solution pH is at or near pH_{IEP} of amphoteric polymers, due to the electrostatic interactions between polyampholytes carrying both positive and negative charges, intra- and inter-molecular chain aggregation often results in macroscopic phase separation which is a pronounced property of proteins.¹⁸⁵ When solution pH is beyond the pH_{IEP} of amphoteric polymers, cationic and anionic functional groups are protonated or deprotonated, leading to

enhancement of solubility in aqueous solutions (Figure 1.2-1). For example, we have explored the aqueous solubility of synthetic succinylated and phthaylated L-PEI which exhibited a notable turbidity increase at $\text{pH}=\text{pH}_{\text{IEP}}$ and a decrease of solution turbidity when pH was below or above the pH_{IEP} .¹⁸⁶

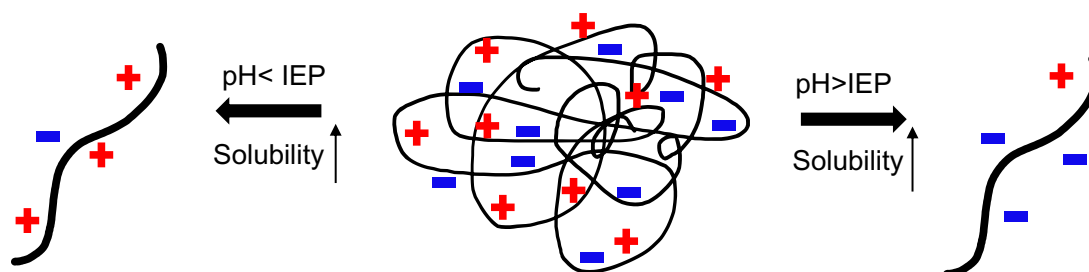


Figure 1.2-1. Effect of pH on aqueous solubility for amphoteric polymers.

Clearly the chemical composition of polymers affects their aqueous solubility with, for example, O or N atoms in a polymer backbone able to supply lone pair electrons to form hydrogen bonds with water, or indeed with polymers containing hydrophilic side groups, e.g., -OH or -NH₂.¹⁸⁷

Non-ionic water-soluble polymers (e.g. PEG, PVP and PVA) contain polar and non-polar groups. When the polymer dissolves in water, the polar groups form hydrogen bonds with water molecules and break the structure or assembly of the water molecules: PEG, PVP and poly (acrylamide) are known to be strong breakers of water structure. However, non-polar materials tend to aggregate in the presence of water molecules through the hydrophobic effect. Thus, the solubility of non-ionic polymers in aqueous solution is a result of these two opposing interactions, hydrogen bonding and hydrophobic effects.

Beyond the macromolecular structure, the aqueous solubility of water-soluble polymers is highly dependent on the structure of the repeating unit, especially the hydrophobic-hydrophilic balance.¹⁸⁸ For example, PVA is water soluble, while its nearest homologs which contains different numbers of methylene group in the backbone are insoluble in water. For example, poly (methacrylamide) differs from PAA through the presence of a methyl group but is insoluble in water or polar solvent (e.g. dimethylsulfoxide).

Polymer aqueous solubility is also affected by molecular weight; Ueberreiter et al. showed that the aqueous solubility of polymers decreases with increasing molecular weight.¹⁸⁹ Atactic poly (propylene oxide) of low molecular weight is water-soluble whereas high-molecular weight materials are insoluble in water.¹⁸⁸ The degree of crystallization within polymers also affects their aqueous solubility. Chitosan is a semi-crystalline

polysaccharide with intra- and inter-macromolecular hydrogen bonds generating crystalline domains which limit its solubility in aqueous solution unless $\text{pH} < 6$. Disruption of chitosan crystallinity enables expansion of its aqueous solubility window, and can be achieved by re-acetylation of chitosan, increasing the $\text{p}K_a$ of half-acetylated chitosan derivative (HACHI) up to $\text{pH} = 7.4$ or through physical strategies including addition of urea or guanidine hydrochloride to disrupt intra- and inter-macromolecular hydrogen bonds, reducing crystallinity of HACHI which becomes soluble over a broader pH range.¹⁸¹ Cellulose behaves similarly to chitosan in terms of crystallinity with methylcellulose (MC), an etherification derivative from cellulose having enhanced solubility in aqueous solution due to the methyl group disrupting the crystallinity of cellulose.

The effect of increasing temperature on the water solubility of polymers is generally expected to increase solubility due to hydrogen bond breaking. Dissolution is an endothermic reaction¹⁹⁰ and, since some semi-crystalline and crystalline polymers have lower free energy comparing to amorphous polymers, water solubility of polymers is often defined alongside a dissolution temperature. Chantani et al. reported that linear PEI (L-PEI), as a semi-crystalline polymer, only dissolves at elevated temperatures, leading to melting of polymer crystallites which then dissolves in water over 60°C .¹⁹¹ The cloud point is the temperature at which transparent solutions undergo phase separation, and is related to the molecular weight of the polymer. Lin et al. reported the cloud point of 20kDa, 50kDa and 500kDa poly (ethyl oxazoline) was 63.5 , 63 and 61°C , respectively.¹⁹²

The lower critical solution temperature (LCST) is the temperature below which the components of a mixture are miscible (soluble-insoluble transition), attributed to heat inducing fracture of hydrogen bonds between water molecules and polymer chains (Figure 1.2-2). At LCST, the increasing of entropy that assigned with the disordered arrangement of water molecules is greater than enthalpy induced by formation of hydrogen bonds between water molecules and polymer chains, and so LCST is regulated by entropy of the system. Examples of LCST polymers include poly (N-isopropyl acrylamide), poly (N,N-diethylacrylamide), poly(N-vinylalkyl amide), poly (N-vinylcaprolactam), phosphazene derivatives and PDMAEMA. Though the LCST of PDMAEMA is 40 - 50°C , it can be tuned by introducing quaternization of the tertiary amine groups.¹⁹³ Upper critical solution temperature (UCST) is the temperature above which the components of mixture are miscible (insoluble-soluble transition), and is related to breaking of intra- and inter-electrostatic interactions between polymer chains and deconstruction of hydrogen bonding between

polymer chains (Figure 1.2-2); UCST is thus governed by the enthalpy of the system.¹⁹⁴ Examples of UCST polymers include poly (acrylamide-co-acrylonitrile), poly (N-acryloyl glycinamide) and poly (sulfobetaine). Poly (sulfobetaine) displays UCST behaviour by electrostatic interaction in aqueous solution due to the existence of charged ammonium and sulfonate groups and so the UCST is mainly altered via the concentration of salt.¹⁹⁵

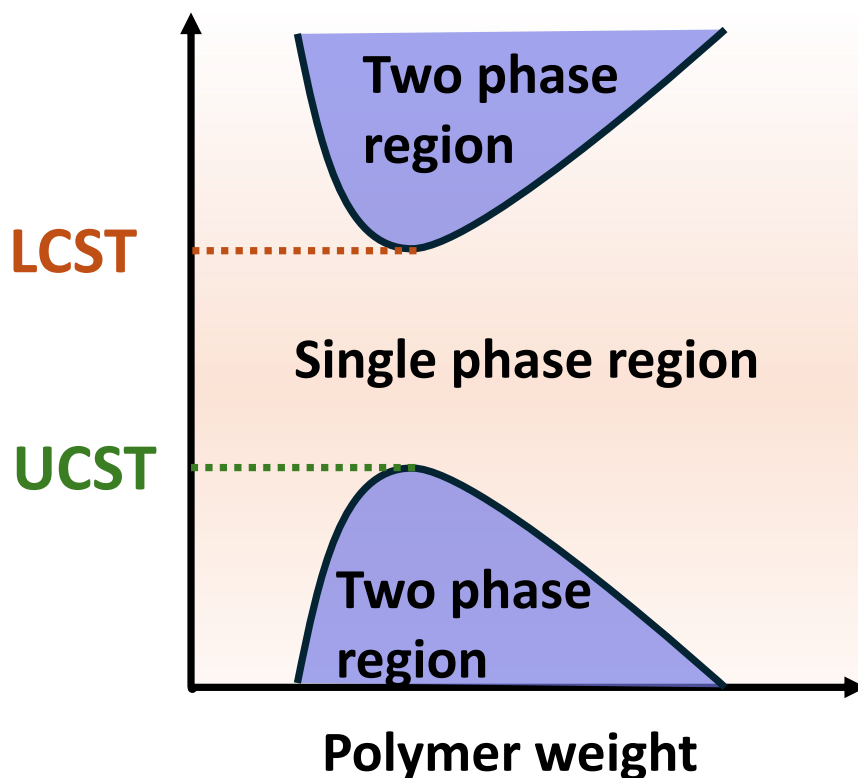


Figure 1.2-2. Phase diagram demonstrating LCST and UCST of polymers in aqueous solution. Modified from Bansal et al.¹⁹⁵.

Thermo-sensitive polymers exhibit expansion of polymer chains or a collapsed globule conformation depending on LCST or UCST with increasing temperature, as illustrated in Figure 1.2-3. Increasing the temperature for LCST polymers induces a coil to globule transition and then a reversible collapse or aggregation of the polymer chains leading to a decrease in polymer aqueous solubility. In contrast, UCST polymers show the reverse profile with the polymer chains extending as temperature increases due to fracture of hydrogen bonds between polymer chains, resulting in enhancement of polymer aqueous solubility.

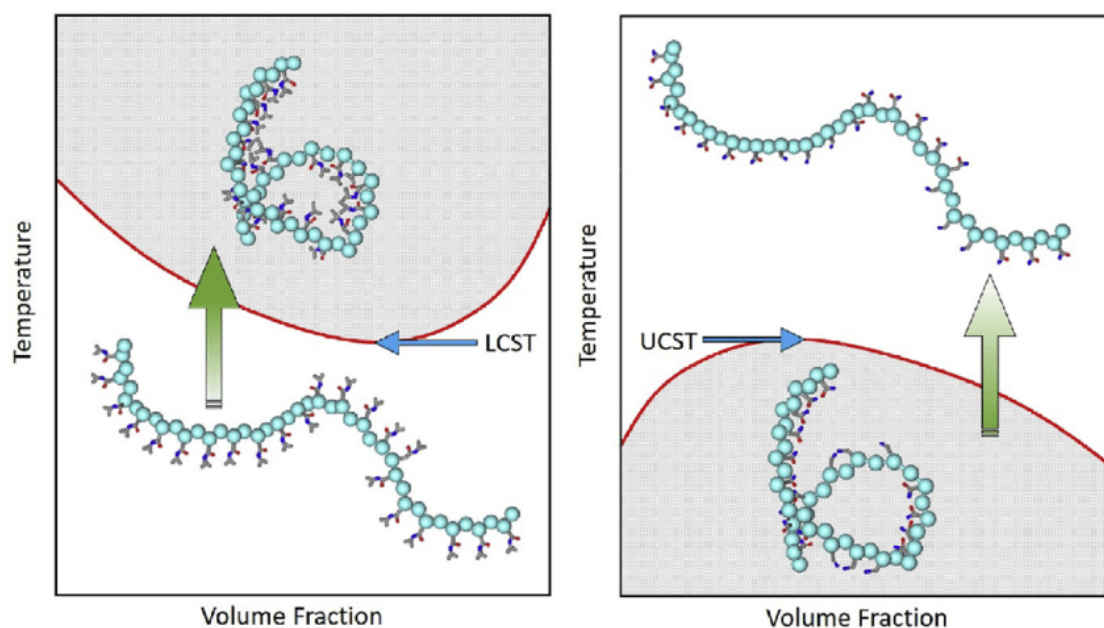


Figure 1.2-3. Schematic illustration of the transition behaviour of LCST and UCST thermo-responsive polymers; the red line represents the macroscopic phase transition. The left panel shows the behaviour of LCST polymers and the right panel shows the behaviour of UCST polymers. Reproduced from Nasseri et al.¹⁹⁶ by permission of Elsevier Science Ltd., UK.

Viscosity is a measure of the resistance of a fluid to flow and essentially describes the internal friction of the fluid. Viscosity increases in the presence of high concentrations of solutes owing to intermolecular attractive interaction. Yadav and co-workers investigated the different viscosity behaviour of bovine serum albumin (BSA) at low ($\sim 40\text{mg/mL}$) or high concentrations ($\sim 250\text{mg/mL}$)¹⁹⁷ and showed that viscosity of the low concentration solution was governed by the net charge on the molecules, with electroviscous effects playing a predominant role. The minimum of viscosity was at pH_{IEP} ($\text{pH}=4.95$) where net charge of BSA was zero and an increase in viscosity was observed when pH was beyond pH_{IEP} as molecules were charged (Figure 1.2-4). In contrast, at high concentration ($\sim 250\text{mg/mL}$), maximum of viscosity was measured at pH_{IEP} and decrease when pH was above or below pH_{IEP} . This was attributed to short-range attractive interactions dominating at pH_{IEP} promoting self-association of BSA molecules, whereas the net molecular charge beyond the pH_{IEP} caused repulsion between the molecules and hence a lower viscosity.

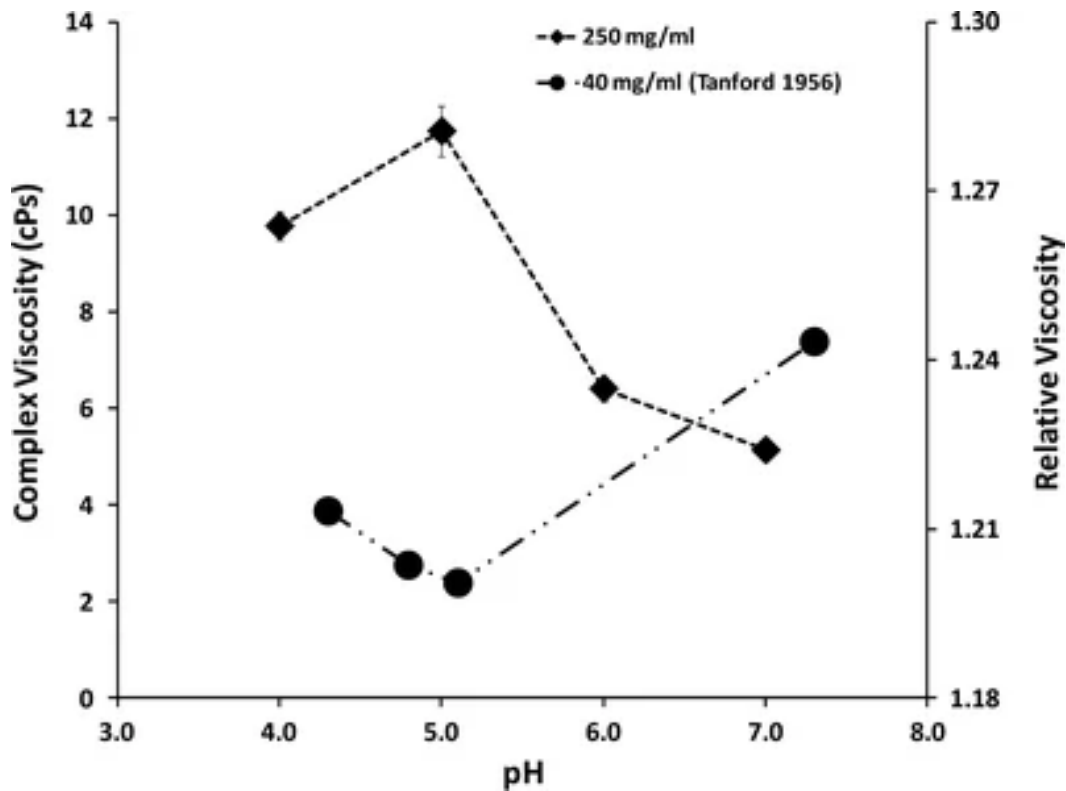


Figure 1.2-4. The solution complex viscosity (η^*) at high concentration ($\sim 250\text{mg/mL}$) of BSA solution (left axis) and the relative viscosity (η_{rel}) at low concentration ($\sim 40\text{mg/mL}$) of BSA solution (right axis) as a function of solution pH. Reproduced from Yadav et al.¹⁹⁷ by permission of Springer Nature.

Though drug aqueous solubility is not related to solution viscosity, the dissolution rate of a drug decreases with increasing viscosity. According to Nernst-Brunner equation:

$$\frac{dM}{dt} = \frac{S \cdot D}{\delta} \cdot (c_s - c_t) \quad (1)$$

where dM is amount of polymer which dissolves in the time interval dt , S is the area for polymer contacting with solvent; D is the diffusion coefficient of the drug within the liquid unstirred boundary layer, δ is the thickness of this layer; c_s is solubility of polymer in water and c_t is concentration of polymer in water.¹⁹⁸ An increase in viscosity results in decreasing the dissolution rate by decreasing D and increasing δ .

The Stokes-Einstein equation relates the diffusion coefficient (D) of spherical particles in a fluid with the viscosity of that fluid:

$$D = \frac{\kappa_B T}{6\pi\eta r} \quad (2)$$

where κ_B is the Boltzmann constant, T is the absolute temperature, η is the dynamic viscosity of the fluid, r is the radius of the spherical particle. The diffusion coefficient decreases with an increase of particle radius or dynamic viscosity of fluid. The equation is used to predict the behaviour of particles in fluid.

The Mark-Houwink equation describes the relationship between intrinsic viscosity and molecular weight of a polymer:

$$[\eta]=K \cdot M_v^a \quad (3)$$

where $[\eta]$ is the intrinsic viscosity, M_v the viscosity-average molecular weight, and K and a are the constants for a given solute–solvent system.¹⁹⁹ In essence, the intrinsic viscosity increases with an increase of polymer molecular weight. Figure 1.2-5 displays relationship between molecular weight and intrinsic viscosity of fibroin.²⁰⁰

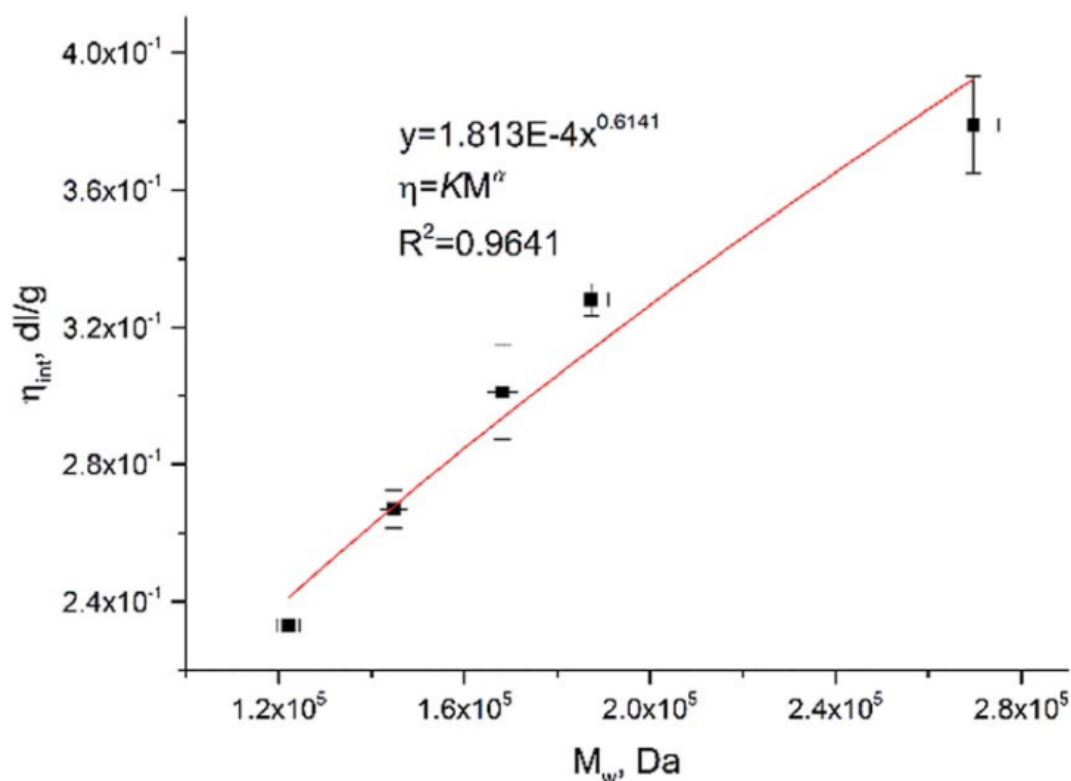


Figure 1.2-5. Illustration of power-type correlation between weight average molar mass and intrinsic viscosity of fibroin in lithium bromide. Reproduced from Pawcenis et al.²⁰⁰ by permission of The Royal Society of Chemistry.

Solvents for polymers can be classified as “good“ solvents when they exhibit strong interactions between the polymer and solvent and weak interactions between polymer chains while “poor” solvents exhibit weak interactions between the polymer and solvent.¹⁹⁹ θ of a solvent is defined as, when polymers are placed in a solvent, if the interactions between polymer chains are equal to interactions between polymer and solvent, and the polymer chains thus behave in random walk or ideal chain model. Constant a is indicative of the quality of solvent, such as $a=0.5$ is suitable for θ solvent, $0.5 < a < 0.8$ is adopted for mostly flexible polymers, $a=0.8$ is typical for good solvents, $a > 0.8$ is applied for semi-flexible polymers and $a=2.0$ is applied for highly rigid polymers. With macromolecules, intrinsic

viscosity tends to decrease with increasing temperature due to a decrease in the hydrodynamic radius of the macromolecule. An increase in temperature also enhances mobility of polymer chains leading to reduction of intermolecular cohesion and friction and hence reduced viscosity.

Water-soluble polymer-surfactant systems are widely used for pharmaceutical applications.²⁰¹ The interaction of an ionic surfactant with a polymer is characterized by the critical interaction of the surfactant, also termed the critical aggregation concentration (CAC), and follows similar principles to micelle formation²⁰². When surfactant concentration is lower than the CAC, no significant interaction between surfactant and polymer is observed. When at CAC, the onset of interactions between the surfactant and polymer is seen as the surfactant starts binding to the polymer. The aggregates dramatically increase as the concentration of surfactant increases, followed by a plateau stage where further increases results in free surfactant. Ultimately, the surfactant activity reaches its critical micelle concentration (CMC), forming free micelles.^{202,203} Non-ionic surfactants usually show weak interactions with polymers as micelles tend to remain in their original stabilized state.^{203,204} Anionic surfactants generally exhibit greater interaction with water-soluble polymers than cationic surfactants. Chavanpatil et al. employed the anionic surfactant Aerosol OT™ (AOT) with the water-soluble polymer alginate as a novel polymer-surfactant nanoparticle platform for controlled release of water-soluble drugs.²⁰⁵ Due to the predominantly electrostatic interaction of the anionic matrix and basic drug, higher drug encapsulation efficiency was reported and sustained drug release over 15 days.

Water-soluble polymers and metal ions are able to form polymeric metal complexes and have been applied in various fields²⁰⁶, such as catalysis²⁰⁷, conductive²⁰⁸ or photoconductive²⁰⁹ materials, biomaterials²¹⁰ and as precursors of a nanoplatfrom²¹¹.

Two types of polymer chelates have been described (Figure 1.2-6), intra- and interchain which commonly contains four or six coordinate bound site, the former type displaying relatively high chemical and thermal stability.²¹² Generally, metal ions bind ‘acidic’ groups within one polymer chain and ‘basic’ groups within another polymer chain to form an inter-polymer chelate.

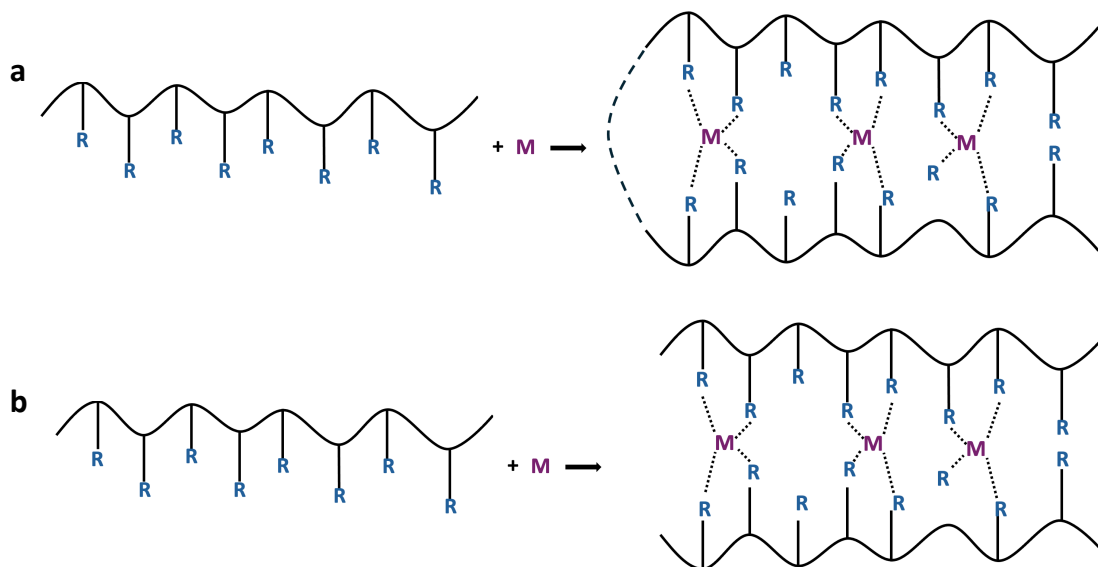


Figure 1.2-6. The structure of intra-polymer chelate (a) and inter-polymer chelate (b). R=coordinating atom or group; M=metal ion.

Electrostatic forces and coordination bonds are predominantly responsible for interactions between water-soluble polymers and metal ions. Weak interactions, for example when metal ions are trapped in the polymer phase, are also involved. There are three general theories of counterion binding, namely territorial binding, site binding and hydrophobic binding (adsorption), which have been adapted to explain the electrostatic interactions between polymers and metal ions. Territorial binding is primarily long-range electrostatic interactions where counterions move along the axis of the polymer chain to polyions and condense on the polymer surface becoming fixed by the polymer ligands. Site binding occurs when counterions interact with charged groups of polyions at short-range. Hydrophobic binding is seen for organic counterions showing stronger binding than inorganic ions due to the hydrocarbon nature of the polymer chains.²¹² Figure 1.2-7 shows the structure of general polymer-metal complex.

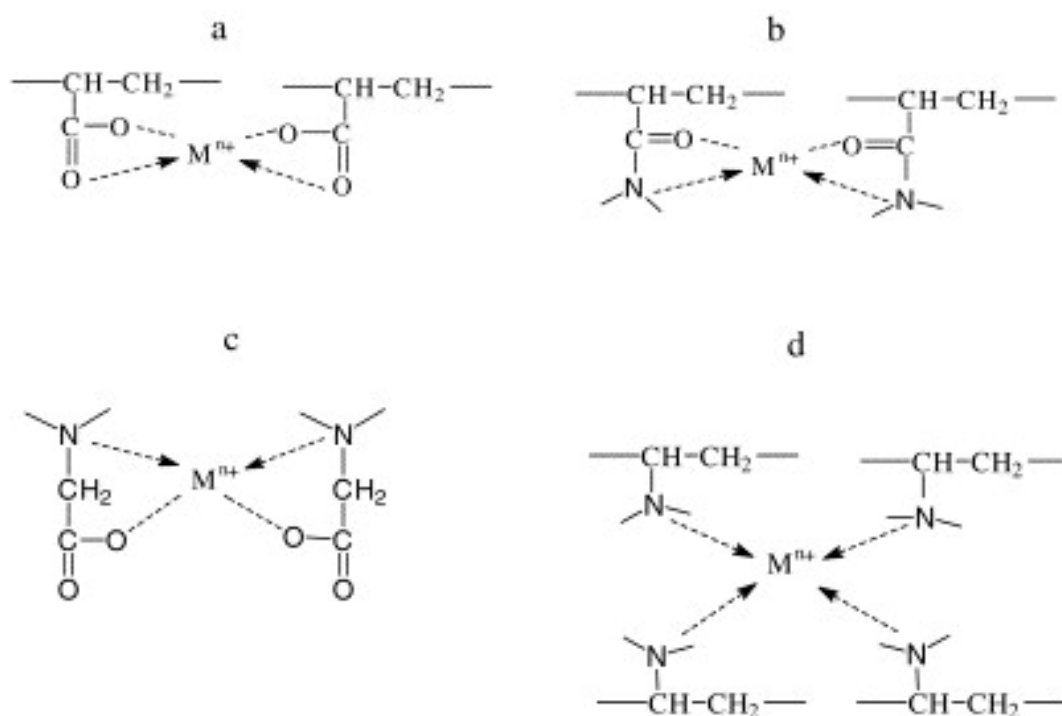


Figure 1.2-7. Common structure of polymer-metal complexes (a) carboxylic type complexes; (b) acrylamide type complexes; (c) maleylglycine type complexes and (d) amine type complexes. Reproduced by Rivas et al.²¹² by permission of Elsevier Science Ltd., UK.

Poly(acrylic acid) (PAA) has shown relatively high chelating efficiency with Cr(VI) and Pb(II) for 75% and 99%, respectively.²¹³ When pH=4.5, due to electrostatic interactions with carboxylic groups, the PAA globule shrank leading to metal ion coordination with 2-4 carboxyl groups. Conversely, at high pH values, PAA extends due to electrostatic repulsion with the charged carboxylate groups.²¹⁴ Complexes are formed through the free electron pair of the nitrogen atom of amino groups. The stability of the complex depends on pH; the amino groups are protonated at low pH resulting in weak affinity for metal ions and low stability of the complex. As pH increases, the complex shown greater affinity and stability.²¹⁵ Due to abundant amine groups in poly(ethylene imine) (PEI), PEI and its derivatives are well known to binding metal ions.²¹⁴ Linear and branched PEI were reported to possess chelating ability, specifically under basic conditions when the amine groups are more readily chelated with metal ions²¹⁶.

1.3 Pharmaceutical applications

1.3.1 Oral administration

Oral drug delivery is the most extensively used administration route due to its relatively high patient compliance, non-invasiveness and cost-effectiveness. There are multiple types of oral formulation, including tablets, capsules and solutions. Water-soluble polymers are

excipients being widely used in pharmaceutical formulations, for example PEG 3350 is used in mini tablets Desitin[®] and also in the constipation formulation MiraLax[®] or polyvinyl alcohol (PVA) in a tablet coating used in Wellbutrin XL and Aplenzin. Examples of the various uses of water-soluble polymers in pharmaceutical systems are described below.

1.3.1.1 Tableting

Binders provide cohesion for powder blends for dry or wet granulation, prior to compaction to form tablets.^{217,218} Various water-soluble polymers are employed as binders, including hydroxyethyl cellulose (HEC), hydroxypropyl cellulose (HPC), hydroxypropyl methylcellulose (HPMC), sodium carboxymethyl cellulose (sodium CMC), poly(vinylpyrrolidone) (PVP), gelatin, starch and polysaccharides. Solutions of PVP are widely used as a binder for granulation or can be added as a powder to a mix and granulated *in situ* by the addition of a liquid.²¹⁸ The addition of binder tends to influence the hardness of the resultant tablets with increasing binder typically increasing tablet hardness and reducing their friability. Some binders possess thermoplastic characteristic and plastic flow behaviour; Joneja et al. reported that the thermoplastic properties of HPC absorbed compression energy giving greater tablet hardness when compared with methylcellulose (MC), povidone and starch.²¹⁷ Different grades of water-soluble polymers are generally available from manufacturers and which possess differing properties. For example, HPC is available with different degrees of polymerization (DP) which affects the viscosity of HPC solutions. Low viscosity HPC is a useful binder in immediate drug release system, while medium- or high viscosity HPC is employed as a matrix for controlled release systems as it retards drug release from the matrix.²¹⁸ Diluent materials such as cellulose, dextrin and starch are also employed in tablets to bulk a low dose tablet and water-soluble polymers may thus act concurrently as a binder and diluent (filler).

Disintegrants are often added to immediate release tablet formulations to ensure that the tablet breaks into smaller fragments to increase surface area for dissolution, leading to more rapid drug absorption.²¹⁹ It is favorable when fast drug release is required, such as tranquillizers, anesthetic and pain treatment²²⁰; disintegrants are generally classified as disintegrants or superdisintegrants. Ordinary disintegrants include corn starch, microcrystalline cellulose, low-substituted HPC, guar gum, alginate.²¹⁹ Common superdisintegrants include sodium starch, glycolate, croscarmellose sodium and crospovidone.²²¹ The considerable swellability of some superdisintegrants is attributed to the existence of carboxylate group within sodium starch glycolate and croscarmellose sodium.²²²

Swelling is generally recognized as the prime mechanism for disintegration,²¹⁹ when disintegrant particles contact the dissolution medium, the particles absorb liquid and expand leading to break up of the tablets. Other factors also impact the disintegration of tables. For example, highly porous tablets can impede disintegration due to lack of swelling force, whereas low porosity hinders the penetration of dissolution medium and extends disintegration time.²²³ It is thus essential to prepare tablets with optimal porosity for rapid drug release.

Lubricants are also commonly added to tablet formulations to aid in the tableting process by improving powder flow, reducing friction between the tablet surface and the die and to prevent adhesion of the tablet to the punch. Magnesium stearate is the most commonly used lubricant in tablet formulations although other materials are also employed; 6% PEG 8000 was co-micronized with sodium citrate or calcium ascorbate as a lubricant and generated a lubricating film due to the low friction coefficient of PEG 8000.

1.3.1.2 Solutions for oral and other routes

Oral solutions are also widely used for drug administration, typically for rapid therapeutic onset since the drug is dissolved and hence a dissolution step prior to absorption is not required. Oral solutions are particularly beneficial for patients who unable to swallow tablets or capsules, especially pediatric and elderly patients. Driven by the solubility of the drug, oral solutions can be aqueous-based, organic-based or aqueous/organic mixed. The challenge of developing oral solutions based on organic solvents is minimize the volume of organic solvent to achieve the desired solubility. Common organic solvents include ethanol, propylene glycol, medium-chain triglycerides, D- α -tocopheryl polyethylene glycol-100 succinate (TPGS) and PEGs. Though the accurate volume of solvent is rarely reported, the maximum amount of solvent used in pediatric formulations is up to 100% medium-chain triglyceride, 55% propylene glycol (the higher percentages are contraindicated in children younger than 4 years of age), 17% PEG400 and 42% ethanol.²²⁴

PEGs are available with various molecular weight (MW), manufactured by varying the time of polymerization process, with average molecular weights 200 Da to 8000 Da. When MW<600Da, PEGs are typically liquid at room temperature, MW at 600-1000 Da are soft semisolids and MW over 1000 Da PEG are waxy solids. PEG has notable water solubility and biocompatibility, is non-toxic and has low immunogenicity. PEGs use in pharmaceutical formulation, foods and cosmetics was approved by the FDA in 1990. For example, PEG 400 has been used as a solubilizer in the oral solution of Agenerase[®] for treating HIV-1 infection.

Amprenavir, a protease inhibitor, is dissolved at a 15mg/mL in a solvent system consisting of 17% PEG 400, 55% propylene glycol, 12% TPGS and other inactive ingredients.²²⁵ However, amprenavir was shown to be 14% less bioavailable administered from liquid Agenerase[®] when compared to Agenerase[®] capsules.

PEG 3350 hydrates in the lumen of the intestine to increase stool volume which then triggers colon motility to enhance transition of softened stools and defecation process.²²⁶ Thus, PEG3350 is traditionally used as a bowel cleansing agent for colonoscopy. For instance, MoviPrep[®] is a 2 liters PEG bowel cleansing liquid agent used before colonoscopy, barium enema X-ray examination or other intestinal operations. GoLYTELY[®] is an osmotic laxative with 227.1g PEG 3350, supplied as a powder and reconstituted with water as an oral solution before use, exerting similar effects to MoviPrep[®] in adults. GaviLyte[™]-H oral solution is a combination of osmotic laxative and stimulant laxative indicated for cleansing of the colon in a preparation for colonoscopy in adults. Recently, Wiener et al. reported a Phase II study for a new sports drink-like flavored PEG and sulfate solution (FPSS, SUFLAVE[®], Braintree Laboratories, Inc.) for bowel cleansing in preparation of colonoscopy which was approved by FDA in June 2023.²²⁷ FPSS provided a similar efficacy to a commonly used but not FDA approved PEG and sports drink bowel preparation (PEG-SD) without bisacodyl (a harsh stimulant laxative) and the cleansing efficacy of FPSS was reportedly over 90%, comparable with other FDA approved bowel preparations. PEG 3550 is also as an effective treatment for treating constipation. A novel and convenient aqueous solution concentrate (ASC) of PEG 3350, which required an appropriate dilution volume (4-8 ounces) before ingestion, was evaluated in a clinical study to assess safety and tolerability in patients who were struggling with functional constipation.²²⁸ A 14 days treatment and 1 month follow-up assessment demonstrated the ACS PEG 3350 showed identical efficacy and comparable safety and tolerability with a powder formulation of PEG 3350.

Other water-soluble polymers are also employed in oral solution dosage forms, such as HEC in Hemangeol[™] oral solution (FDA approved in 2014) for systemic therapy of proliferating infantile hemangioma and poloxamer 188 in Prexxartan[™] as an angiotensin-converting enzyme inhibitor for treating hypertension.²²⁹

1.3.2 Controlled release systems

Water-soluble polymers are increasingly used in controlled drug release systems. Dissolution of drug particles, diffusion of the drug through a hydrated matrix and erosion of an outer hydrated polymer layer are mechanisms described for controlled release systems.²³⁰

When tablets are exposed to a dissolution medium, the polymer can form a 'gel-layer' surrounding the tablet matrix that keeps the core of the tablet dry during this initial stage. As water penetrates into matrix with time, the gel-layer expands and generates a diffusion barrier to drug release.²³¹ The rigidity of polymer chain is decreased since the outer layer is fully hydrated, leading to disentanglement of polymer chains and erosion of matrix.²³² For example, high viscosity HPMC and HPC are common water-soluble polymers applied for controlled release system.²¹⁸

Tonglairoum et al. synthesised PVP nanogels using a surfactant-free emulsion polymerisation technique as a scaffold for maleimide monomers, forming maleimide-PVP (Mal-PVP) nanogels, which displayed considerable mucoadhesive properties on conjunctival mucosa and potential as a drug carrier for sustained drug release due to the swellability of the hydrophilic nanogel.²³³ The *in vitro* release from Mal-PVP nanogels loaded with fluorescein sodium as a model compound showed first-order release kinetics. Approximately 45% fluorescein sodium was released in the first 4 hours, and another 40% fluorescein sodium was released within 24h, showing an initial burst and then sustained drug release. Moustafine et al. reported that a drug-polyelectrolyte complex (DPC) composed of positive charged Eudragit[®] EPO and indomethacin (IND), coated with the conventional enteric coating material Eudragit[®] S100 (S100) which is negatively charged, formed a pH controlled drug-interpolyelectrolyte complex (DIPEC) for colon-targeting sustained release.³ The IND release profiles showed that DIPEC tablets did not release in the gastric environment (pH =1.2) due to S100 forming an extra transparent hydrophobic layer to hinder IND diffusion from the swollen DIPEC matrix. Subsequently, IND started to release as pH rose to 5.8 since the formed layer appeared turbid and was fully released within 7h. Eudragit[®] L30 D-55 is an anionic copolymer composed of carboxylic group and ester group at a ratio of 1:1. Due to the carboxylic group, Eudragit[®] L30 D-55 is insoluble in acidic medium such as gastric fluid while it is soluble at pH \geq 5.5 such as in intestinal fluid. Chauhan and Nutalapati employed Eudragit[®] L30 D-55 as an enteric coating for preparing multilayer omeprazole tablets in US patent 2009/0280173 A1.²³⁴

A novel clobetasol 17-propionate (CP) mucoadhesive extended-release tablet for treatment of oral lichen planus (OLP) was prepared by Cilurzo et al.²³⁵ A low swellability tablet formulation was designed using 24 μ g CP with HPMC, MgCl₂ and a non-swellable mucoadhesive polymer PMM to achieve a sustained release profile over 6 h. PMM was obtained by adding 10% (w/w) NaOH aqueous solution to 15% (w/w) Eudragit[®] S100 aqueous suspension, until complete salification, then lyophilized powder was milled with

0.25mm ring sieves. Upon contact with water, rapid hydration and a slight increase of size for tablet A, made from pure PMM, was observed within 10 min, before erosion with accompanying weight loss and complete dissolution of the tablet in 90 min. Though notable swelling was not observed in tablet B (PMM with 10% magnesium chloride), weight again decreased with time but to a lesser extent than for the pure PMM tablet. With the addition of 10% HPMC (tablet C), an increase in weight and diameter of the tablet was observed. The presence of both HPMC and MgCl₂ resulted in minimal weight loss over 90 min (Figure 1.3-1).

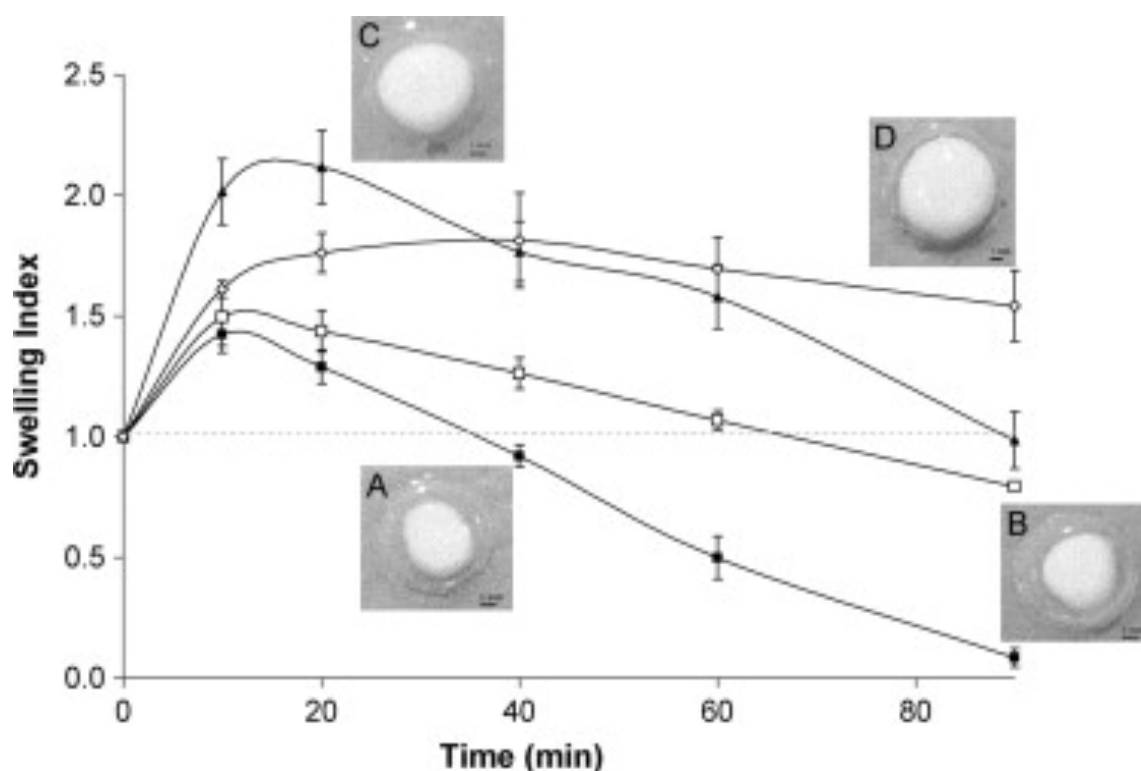


Figure 1.3-1. The swelling properties of pure PMM (■- and tablet A), PMM combined with 10% (w/w) MgCl₂ (□- and tablet B), PMM combined with 10% (w/w) HPMC (-▲- and tablet C) and PMM combined with 10% (w/w) MgCl₂ and HPMC (-◇- and tablet D). Reproduced by Cilurzo et al.²³⁵ by permission of Elsevier Science Ltd., UK.

Moreover, measurement of tablet erosion rate suggested that the formulation combining 10 % (w/w) HPMC and MgCl₂ controlled hydration/erosion and the release profile of PMM with minimal effects on mucoadhesion. A double-blind, controlled clinical study was performed to determine the efficacy of the tablets for treating OLP (Figure 1.3-2).

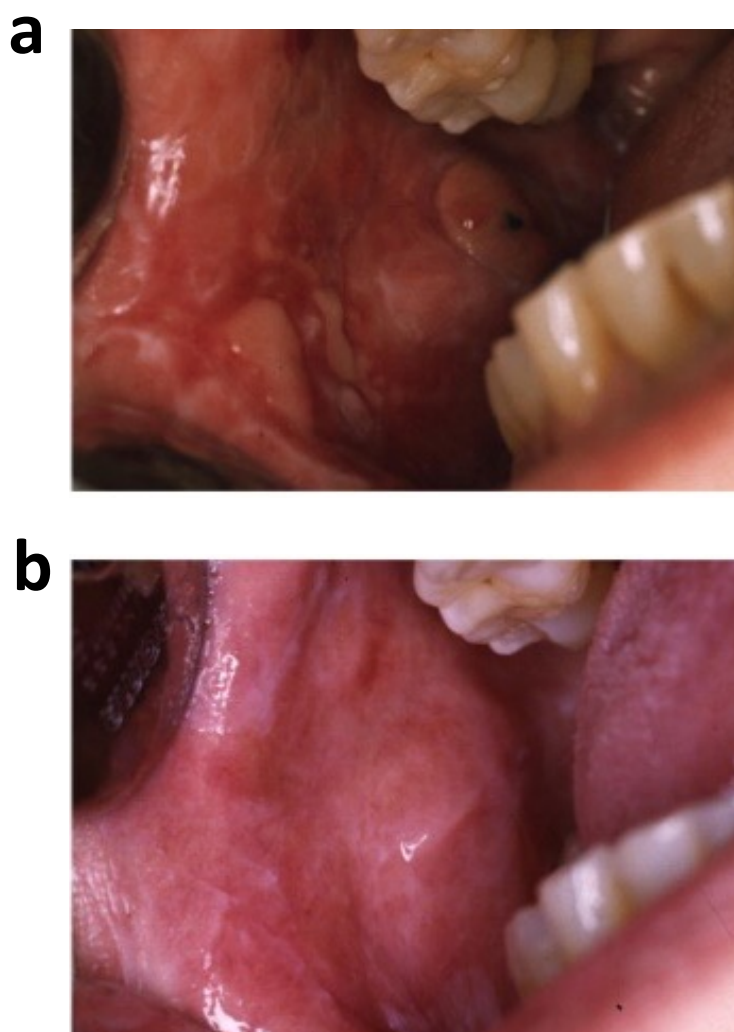


Figure 1.3-2. Reticular-erosive lichen planus before (a) and after (b) treatment with prepared Clobetasol 17-Propionate (CP) mucoadhesive extended-release tablet. Reproduced by Cilurzo et al.²³⁵ by permission of Elsevier Science Ltd., UK.

The study employed three groups of patients ($n=16$) administered the novel CP tablets (group CP-T) three times per day for 4 weeks, placebo tablets (group CP-P) or commercial CP ointment for cutaneous application ($123 \mu\text{g}/\text{application}$) extemporaneous mixed with OrabaseTM (group CP-O). 13/16 patients in group CP-T who suffered from OLP recovered (oral pain and ulceration disappeared) after 4 weeks study and 11/16 patients in group CP-O recovered. The symptoms of patients in group CP-P worsened as expected and no adverse effects were observed in group CP-T, however, a transient acute hyperaemic candidosis ($n = 2$) and taste alteration ($n = 4$) were reported in group CP-O.

In US Patent 11,576,865 B2, sustained release formulations of ruxolitinib employed HPMC to control the release profile for treating Janus kinase associated diseases such as myeloproliferative disorders.²³⁶ Clinical studies demonstrated that the relationship between the mean maximum plasma concentration (C_{max}) and the 12 hour mean plasma concentration

(C_{12h}) of ruxolitinib is 2 to 7, and a half-life ($t_{1/2}$) approximately from 3.5 -11 h. Thus, a sustained release formulation with HPMC to supply a constant and therapeutically effective plasma drug levels with administration once daily, also minimize potentially harmful spikes in plasma drug concentrations which are assigned with immediate release dosage form, is desirable. The bioavailability was determined as 65%-110% from the sustained release formulation compared to 75%-95% for the immediate release dosage form containing the same content of ruxolitinib.

Coating is an important process for protecting drugs from light, moisture and oxidation, enhancing drug stability, masking taste and odour and effectively controlling drug release profiles. There are three approaches for tablets coating, including sugar coating, press coating and film coating. Film coating uses polymeric solutions and other components, such as pigments and plasticizer which are sprayed on to a rotating tablet bed with hot air is passed through the bed to evaporate the solvent, leaving an intact and thin film to cover the tablet surface.²³⁷

The selection of polymers for a film coating depends on the drug release site or drug release rate. For example, HPMC, PVP and EC are commonly employed non-enteric coating materials, whereas cellulose acetate phthalate, polyvinyl acetate phthalate and sodium alginate are enteric materials. Due to its high glass transition (T_g), EC (133.4°C) was selected to coat propranolol hydrochloride-loaded pellets in a dry powder coating process to achieve an extended-release profile.²³⁸ EC dry powder coated pellets displayed poorer film formation comparing to an aqueous colloidal EC dispersion coated pellets, attributed to the larger size of micronized EC, the non-spherical shape of the EC powder and the high T_g of EC. A curing step was introduced at 80°C for 24h to improve coalescence of the EC coated pellets, resulting in an extended release profile comparing to uncured pellets.²³⁸

Enteric coatings are generally applied to resist release of active pharmaceutical ingredients (API) in acidic gastric milieu for drugs such as aspirin which may cause gastric irritation, or to preserve APIs stability when they are exposed to acidic gastric fluid, including omeprazole and pancreatin. Polysaccharides such as guar gum, chitosan, sodium alginate and dextran are biodegradable by colonic enzymes and have been developed as tablet coatings for colon targeted drug delivery.²³⁹

Sa et al. coated two immediate release drugs ibuprofen (IBP) and metronidazole (MNZ) with carboxymethyl locust bean gum (CMLBG) which is able to resist pancreatic enzymes in the upper gastrointestinal tract (GI tract) while it is degraded by enzymes secreted from colonic microflora.²⁴⁰ This device kept the integrity of tablets in the upper GI tract but

induced a rapid and completed drug release in the colon as the CMLBG coating degraded by colonic enzymes²⁴¹, though some studies showed that rat caecal fluid induced faster drug release²⁴². The strength of the formed gel layer, following hydration, increased with increasing of coat weight which retarded penetration of water through the gel layer leading to a decrease in swelling. In a higher pH solution, lower swelling decreased entanglement of polymer chains with decreasing erosion, resulting in a slower release period.

In US Patent 2,897,122 Millar et al. developed enteric materials for oral dosage forms.²⁴³ In this patent, the molecular weight of polyvinyl acetate phthalate was from 25 kDa to 40 kDa aligned with the degree of polymerization from 600 to 800. Polyvinyl acetate phthalate was relatively insoluble at pH<3.5 (e.g. stomach fluid) with increasing solubility observed up to pH=6 and was readily soluble in simulated intestinal fluids containing pancreatin at pH 7-7.5 and completely soluble in 9-95% ethyl alcohol solution. Tablets were coated 6-8 layers of 30% (w/v) polyvinyl acetate phthalate dissolved in 95% ethanol using a standard rotating coating pan. Disintegrating tests showed that coated tablets retained integrity in simulated gastric fluid (pH =1.5) over 3 hours while tablets disintegrated in simulated intestinal juice (pH=7.5) within 20 min. Cook et al. prepared an enteric alginate microcapsule by a fluid-bed drying technique coated with chitosan using electrostatic interactions between the carboxyl group within alginate and amine group within chitosan for enteric delivery of probiotic bacteria.⁷³ At pH<2, less of the ionic of alginate chitosan dissociated from chitosan, and a similar effect was observed when pH>7 where chitosan is less charged. Thus, chitosan provided protection when the microcapsule transited through the stomach (pH 2-5) and release occurred when the microcapsule entered the intestine. The mucoadhesive properties of chitosan and alginate also extended release in the intestinal. Thus, chitosan coated alginate microcapsules contain mucoadhesive and controlled release activity as a promising drug delivery vehicle.

1.3.3 Rheology modifiers

Rheology modifiers are important components in pharmaceutical formulations and generally increase viscosity and control shear thinning or thickening, resulting in desired viscosity and greater stability.

A thickener is commonly used to increase viscosity of liquid pharmaceutical formulations with minimum effects to other properties. When a thickener dissolves or is dispersed in a liquid medium, it appears as a solution, suspension or gel due to the formation of weakly cohesive colloidal structures. Thickeners increase viscosity via the formation of

hydrogen bonds between coiled and/or swollen macromolecules, and surrounding solvent molecules (Figure 1.3-3).

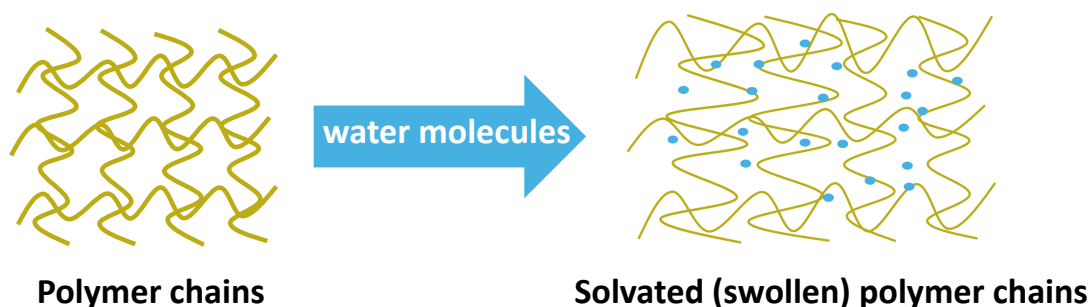


Figure 1.3-3. Illustration of viscosity is increased by solvent molecules penetrating into void spaces of polymer chains.

Hydrocolloids include plant-derived hydrocolloids such as alginates, guar gum, starch and cellulose, fermented products such as xanthan gum, dextran and gellan gum, semi-synthetic hydrocolloids including cellulose ethers (MC, HPC, HEC), amidated pectin, modified starch and propylene glycol alginate, and animal derived hydrocolloids including caseinates, gelatin and chitosan.

Xanthan gum is water soluble with high viscosity even at low concentrations due to hydrogen bonding since xanthan gum is abundant in hydroxyl and carboxyl group and has a high molecular mass.²⁴⁴ The rheological properties, pseudoplasticity and stability in acidic or alkane conditions of xanthan gum allow it to be used as a thickener, gelling agent and stabilizer in pharmaceutical formulations.²⁴⁵ Xanthan gum is prone to form a gel under alkaline conditions (pH >10) when surrounded with divalent cations, while it forms gel under acid or neutral pH in the presence of aluminium, iron or other trivalent cations. High concentration monovalent metal salts may hinder gelling of xanthan gum. Guan and Yu et al. prepared chitosan/xanthan gum based (HPMC-co-2-acrylamido-2-methylpropane sulfonic acid) hydrogels as a controlled release system for a *Pueraria lobatae* extract solid dispersion (SD) via a free radical polymerization technique.²⁴⁶ A pH-independent drug release profile was reported for hydrogels with 63% (pH 1.2) and 49% (pH 7.4) *Pueraria lobatae* released after 48h, respectively, with predominantly Fickian diffusion. Xanthan gum also displayed excellent antioxidant activity, due to the presence of hydroxyl, reducing sugar, pyruvate and *o*-acetylation, and other antioxidant components which alleviate oxidative stress.²⁴⁶

Carbopols[®], as a weakly cross-linked derivative of poly (acrylic acid), shows *in situ* sol-gel transformations depending on pH and is commercially used as pharmaceutical excipients. However, its susceptibility to interact with cationic drugs limits some applications of

Carbopols[®]. Non-ionic polymers have thus been investigated for *in situ* gelling systems as the effects from complexation with ionic drugs on gelation are negligible. Pluronic[®] is transparent and shows temperature-triggered *in situ* gelling properties and so has been selected for ocular formulations. Al Khateb and co-workers investigated the use of Pluronic F127 and Pluronic F68 as excipients to formulate *in situ* polymeric gelling systems for ocular drug delivery.²⁴⁷ Gelation at physiological temperature was only observed for 20% wt% Pluronic F127, whereas the addition of Pluronic F68 to Pluronic F127 increased gelation temperature above physiological conditions. *In vivo* and *in vitro* drug retention studies revealed 20 wt% Pluronic F127 showed better performance compared to other formulations with the addition of Pluronic F68. A slug mucosa irritation assay and bovine corneal erosion studies demonstrated all formulations were not irritant to slugs and ocular tissues. Thus, 20 wt% Pluronic F127 solutions provide an attractive approach for ocular administration by *in situ* gelling at physiological temperature with minimum irritation.

The efficacy of a once daily *in situ* forming metronidazole (MTZ) vaginal gel for treatment of bacterial vaginosis was studied in Phase II and Phase III trials.²⁴⁸ Treatment group A received *in situ* MTZ vaginal gel for 5 days, while group B administered a conventional MTZ vaginal gel. Administration in group A was provided as a bottle of 100 mL aqueous solution composing of 0.8% MTZ, 20% Pluronic F-127, 10% Pluronic F-68, and 0.01% benzalkonium chloride. The prepared *in situ* forming gel possessed temperature sensitive properties. It remained as an aqueous solution at room temperature, while sol-gel transition was induced and spontaneously solidify into gels when it was exposed to vaginal mucosa at body temperature (37°C).

1.3.4 Mucoadhesive and mucus-penetrating systems

Mucosal membranes play a crucial role in protecting epithelial cells via forming a fully hydrated viscoelastic gel layer referred as mucus. Lubrication is essential physiological function of mucosal surface, additionally gas exchange, protection are also its significant properties. Mucin (0.5-40 MDa) is a primary functional component of mucus and comprises a glycoprotein backbone which constitute approximately 12-17% of mucin weight; and primarily oligosaccharide-based grafted chains cover around 63% glycoprotein backbone composing of N-acetylgalactosamine, N-acetylglucosamine, galactose, fucose and N-acetylneuramic acid (sialic acid) (Figure 1.3-4).^{250,356} Mucins generally carry a negative charge since the presence of carboxylate groups (sialic acid) and ester sulfates at the terminus of some sugar units ($pK_a=1.0-2.6$).³⁵⁶

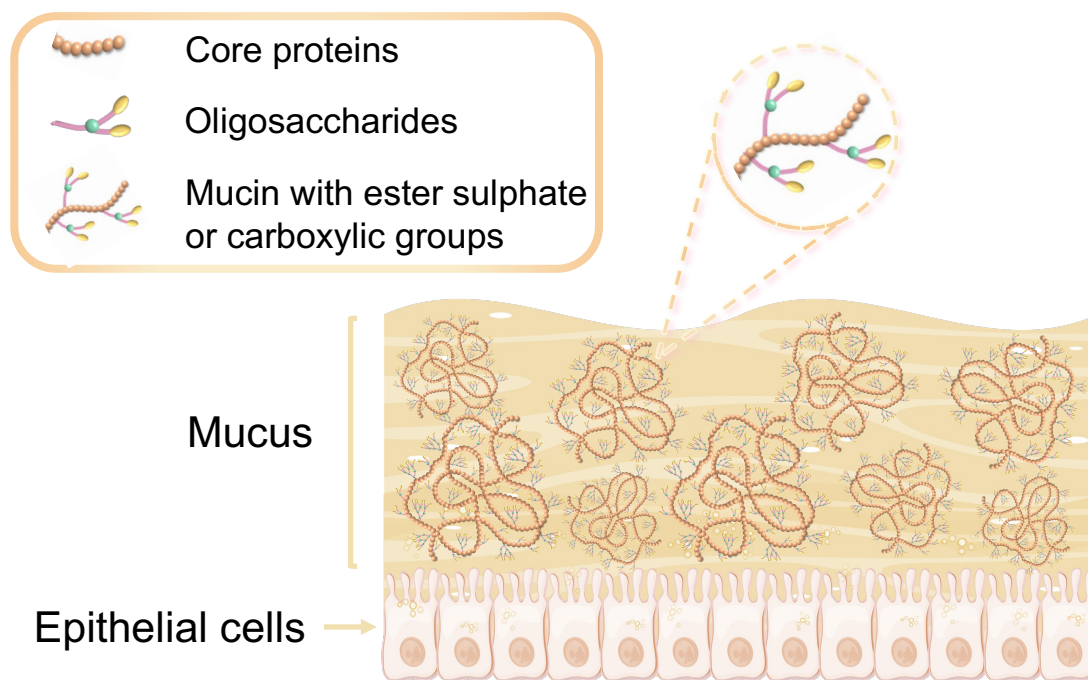


Figure 1.3-4. Schematic structures of mucosal tissue.

Mucosal administration is an approach for local or systemic pharmaceutical treatments, targeting drug release at mucosa, while systemic administration aims for drug absorption via mucosa.²⁴⁹ Mucoadhesion is defined as the ability of materials adhere to biological mucosal tissue.²⁵⁰ Generally, water-soluble polymers such as chitosan, PAA, PEG, HPMC, HEC and sodium alginate, exhibit mucoadhesive properties due to interactions with mucin via electrostatic effects or hydrogen bonding or hydrophobic effect or/and interpenetration of polymers into mucus gel.²⁵¹

Grabovac et al. reported mucoadhesion improved with increasing molecular weight of polymers.²⁵² Albarkah et al. supported this finding that a small molecular weight of PAA (2 kDa) and PEG (10 kDa) did not display specific interactions with mucin.²⁵³ It is broadly accepted that polymers require $MW > 100$ kDa to exhibit significant bioadhesive behaviour. For example, PEG (400 kDa) has stronger mucoadhesive properties than PEG (200 kDa), PAA (450 kDa) and poly (methacrylic acid) (PMAA) (100 kDa) exhibit notable interaction with mucin²⁵³. The greater mucoadhesive properties with increasing polymer chain length simply reflects that functional groups within the polymer are able to interact with mucin. Flexible polymer chains enable significant interpenetration and entanglement with mucosal layer to improve mucoadhesive ability of polymers. The flexibility of polymer chains is associated with crosslinking and hydration of the polymer, lowering the mobility of polymer chains. Clearly polymer concentration also affects mucoadhesion with concentrations around

1-2.5 wt% displaying notable mucoadhesive properties. Insufficient and unstable interaction occur for polymers at low concentrations, resulting in poor mucoadhesion.

Environmental factors also impact mucoadhesion that function groups are ionized when exposed in acidic or basic medium, this provides an approach to tailor mucoadhesive properties of polymers. For example, chitosan shows strong mucoadhesion in neutral or alkaline media. Similarly, at acidic pH's, the carboxylic group within PAA is presumed to form hydrogen bonds with hydroxyl group or/and carboxyl group within mucin, whereas PAA is ionized at neutral or basic pH that lowers its ability to form hydrogen bond, weakening its mucoadhesive activity.²⁵⁴ European Patent 3,173,067 A1 disclosed a novel mucoadhesive buccal *in situ* gel formulation for treatment of oral candidiasis or aphtha.²⁵⁵ This dosage form comprised nystatin, a corticosteroid agent and at least one local anesthetic, covering most of the oral cavity through spraying into mouth after which the formulation gelled at body temperature and adhered to the buccal mucosa due to the presence of mucoadhesive polymers. 0.1%-0.5% Carbopol 934 as a water-soluble cross-linked PAA was applied in an *in situ* gel to impart mucoadhesive properties for adhering to buccal mucosa. The bioadhesive activity between mucin and Carbopol 934 could be attributed to the synergetic effects of formation of hydrogen bonding, hydrophobic effect and van der Waals forces. Additionally, the gelation and swelling abilities of Carbopol 934 increases physically interpenetration or machinal interlocking with mucosal surface, enhancing its mucoadhesive ability to mucosa. Drug release occurred through matrix diffusion and by matrix erosion, realizing rapid release of lidocaine and hydrocortisone in the first hours and then sustained release.²⁵⁵ Ways et al. modified chitosan with four non-ionized water-soluble polymers, including PEG, poly (2-hydroxyethyl acrylate) (PHEA), PEOZ and PVP, to form nanoparticles with sodium tripolyphosphate via an ionic gelation method.²⁵⁶ The obtained nanoparticles contained mucus-inert surfaces and stealth properties. When comparing with unmodified chitosan nanoparticles, the resultant nanoparticles showed greater aqueous solubility in the range of physiological pH (pH=3-10), improved diffusivity in bovine submaxillary glands (BSM) solution and deeper penetrated into sheep nasal mucosa. Among these chitosan derivatives, chitosan modified with PVP exhibited superior diffusivity in BSM solution and into mucosal tissue. Thus, PVP was identified as a potential polymer to facilitate mucus penetration and inspired a novel approach to optimise mucus penetration of nanoparticles by modifying chitosan with other non-ionized polymers.

Despite HEC is known for poor mucoadhesive properties, Buang et al. enhanced mucoadhesive activity of HEC by modifying it with 4-bromophenyl maleimide (BPM) at

different molar ratios [HEC]:[BPM] = [1]:[1] (HECMAL_{low}), [1]:[2] (HECMAL_{medium}) and [1]:[3] (HECMAL_{high}), introducing maleimide groups to interact with thiol groups within mucin to form covalent bonds via a Michael addition reaction.²⁵⁷ The mucoadhesion of the obtained HEC was determined by model tablets coated with maleimide-functionalised HEC. The maleimide-functionalised HEC demonstrated excellent mucoadhesive properties compared to the parent HEC with higher concentration of maleimide groups achieving greater mucoadhesive properties. HECMAL is a promising excipient for pharmaceutical formulations applied for transmucosal drug delivery system.

Complex natural substances provide an innovative approach to treat cough and are considered as medical devices (according to EU Directive 93/42/EC). The substances supply a topical physical barrier to protect the oropharynx with a mucoadhesive film instead of suppressing cough via interaction with specific receptors. A novel polysaccharide-resin-saponins-honey-based medical device was formulated to treat post-viral acute cough. Mucilage polysaccharides display mucoadhesive and hydrophilic properties leading to formation of a polysaccharide layer on the upper respiratory tract mucosa. The complex comprises polysaccharide, various sugar and uronic acid units which are non-pharmacological, non-immunological, and have no metabolic mechanism of action. An *in vivo* study suggested polysaccharide extracted from plants (*Adhatoda vasica*, *Withania somnifera* and *Glycyrrhiza glabra*) significantly alleviated cough.²⁵⁸ A randomized and single-blinded clinical study was performed to evaluate efficacy and tolerability of a pediatric polysaccharide-resin-honey based cough syrup (PRH syrup) compared to Carbocysteine syrup (Mucolit, CTS Ltd, Israel).²⁵⁹ Carbocysteine is a mucolytic drug to reduce mucus viscosity in the respiratory tract by deconstruction of disulfide bonds for macromolecules, widely used for treating pediatric acute cough.²⁶⁰ In the study conducted for 4 consecutive days, children of treatment group A received PRH syrup (Grintuss[®], Aboca S.p.A. Italy), while group B were administered Carbocysteine syrup. Though the study indicated both PRH syrup and Carbocysteine syrup were effective cough remedy and well tolerated in children over 2 years old, PRH syrup was reported to provide a more rapid and superior remission of cough symptoms for both nocturnal and daytime from first night therapy to 4 consecutive days treatment.

Buccal mucosa is a suitable administration route for delivering mucoadhesive drugs due to its facile access and a wide area mucosa for applying tablets, patches or films. Moreover, drugs administered through the buccal route are absorbed via the internal jugular vein which bypasses the first pass effect and avoids drug degradation in gastric and intestinal fluids. WO

Patent 2011/070125 A1 disclosed the preparation of an extended release mucoadhesive buccal tablet (AMBT) containing 50 mg acyclovir with 20% milk concentrate protein selective as the mucoadhesive components.²⁶¹ This formulation produced a rapid release of acyclovir in first 30 min and subsequently sustained release for 36h to treat the herpes simplex virus. Adhesion times were measured and showed that the maximum adhesion period of AMBT 50 mg was 18h and minimum period was 14h suggesting the adhesive ability of AMBT 50mg is comparable with a once-daily formulation. Treatment with AMBT 50mg was equivalent to placebo for side effects (diarrhoea, headache and/or site irritation) and hematology and biochemistry parameters were consistent during administration, demonstrating high tolerability of AMBT 50 mg.

1.3.5 Solid drug dispersions

Solid dispersions (SD) were first proposed by Sekiguchi and Obi in 1960s²⁶². Chiou and Riegelman have defined solid dispersions as the dispersion of one or more active ingredients in an inert carrier or matrix at solid state prepared by the melting (fusion), solvent, or melting-solvent method.²⁶³ Nowadays, the approach is generally directed at poorly water-soluble drugs dispersed in a hydrophilic matrix to enhance aqueous solubility and bioavailability. According to the composition of a SD, they can be classified into four generations: The first generation SDs were prepared with a crystalline carrier such as sugar, urea and organic acid. Though this formed crystalline SDs, accomplishing thermodynamically stability, they failed to achieve fast release of drugs compared to later generations. The second generation SDs used amorphous polymers, including PEG²⁶⁴, PVP²⁶⁵ and HEC. The third generation SDs were composed of self-emulsifying carriers or with the addition of a surfactant to increase bioavailability and prevent crystallization of drugs, for example, with Poloxamers²⁶⁶ and Tween 80 as carriers. The fourth generation SDs, also called controlled release SDs, use swellable polymers such as HPMC²⁶⁷, PEO and Eudragit RL, RS and were introduced as carriers to provide controlled drug release, prolonging the half-life of the drug and reducing dosing frequency. Table 1.3-1 lists exemplar SD products on the market based on a water-soluble polymeric matrix.²⁶⁸

Table 1.3-1 Examples of commercially available solid dispersion. Reproduced from Ref.²⁶⁸ by permission of Oxford University Press.

Brand name	Drug	Carrier	Manufacturer
Gris-PEG [®]	Griseofulvin	PEG6000	Pedinol Pharmacal Inc.
Cesamet [®]	Nabilone	PVP	Valeant Pharmaceuticals
Kaletra [®]	Lopinavir, Ritonavir	PVPVA	Abbott
Sporanox [®]	Itraconazole	HPMC	Janssen Pharmaceutica
Intelence [®]	Etravirin	HPMC	Tibotec
Certican [®]	Everolimus	HPMC	Novartis
Isoptin SR-E [®]	Verapamil	HPC/HPMC	Abbott
Nivadil [®]	Nivaldipine	HPMC	Fujisawa Pharmaceutical Co., Ltd
Prograf [®]	Tacrolimus	HPMC	Fujisawa Pharmaceutical Co., Ltd; developed by Sankyo
Rezulin [®]	Troglitazone	PVP	Manufactured by Parke-Davis division of Warner-Lambert

The preparation of SD uses solvent methods, melting methods, melt extrusion methods and other approaches²⁶⁹ such as co-grinding, microwave techniques and 3D printing. The solvent methods traditionally dissolve drug and carrier in suitable solvents then remove solvent via methods such as solvent evaporation, spray drying, lyophilization, gel entrapment and electrospinning. Melting methods take a mix of drugs and carriers and heat to molten status followed by solidifying at room temperature to crush and sieve, including dropping method, melt agglomeration method; detailed manufacturing strategies for preparing SD were reported by Bhujbal et al.²⁷⁰ and Zhang et al.²⁶⁹. The appropriate polymer and drug loading is crucial to physical stability of SDs since immiscibility of the polymeric carrier and drug may induce phase separation and crystallization.²⁷¹ An ideal amorphous solid dispersion (ASD) is thermodynamically stable at its storage temperature when drugs disperse in amorphous polymeric matrix.

Figure 1.3-5 indicates phase separation appears spontaneously below the phase separation curve, as for position between phase separation curve and solubility curve,

destabilization may be attributed to local fluctuations of drug and polymer contents.²⁶⁹

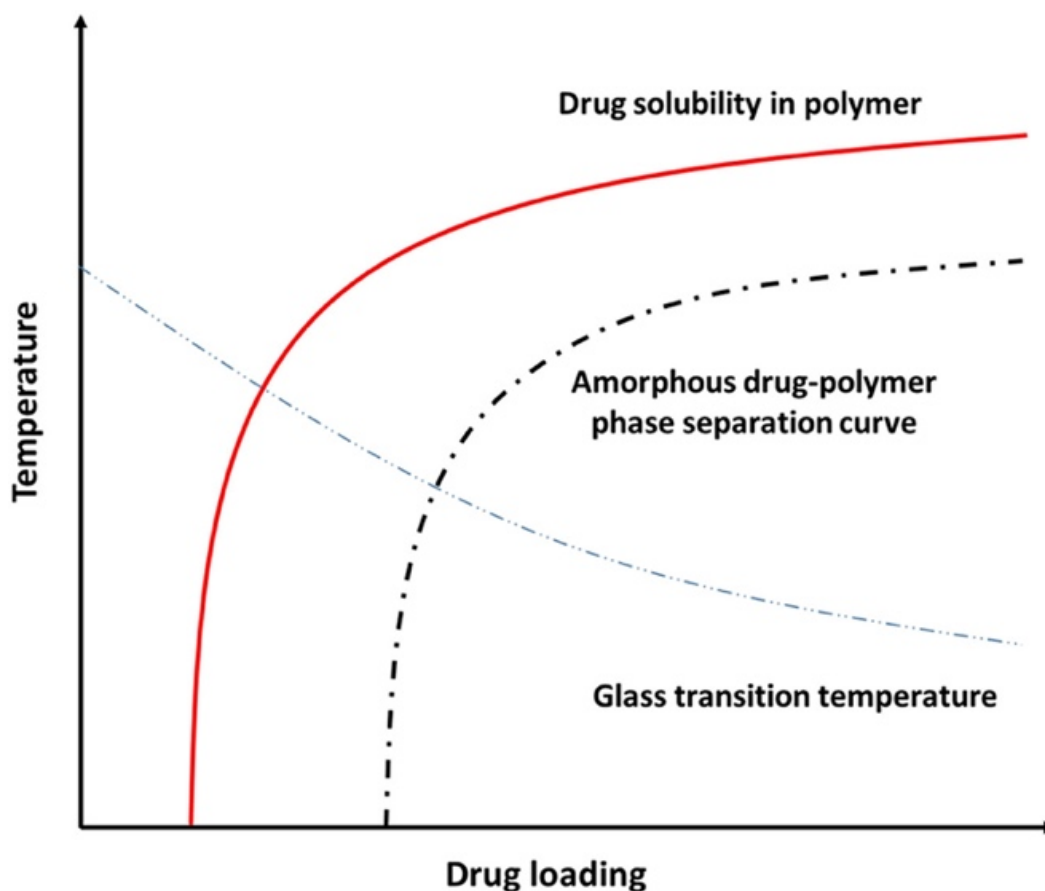


Figure 1.3-5. A typical temperature-composition phase diagram for an ASD. Reproduced from Zhang et al.²⁶⁹ by permission of Elsevier Science Ltd., UK.

Investigations of phase separation in SDs are required when selecting appropriate polymers as a matrix. Qian et al. claimed the single T_g is not an accurate indication to assess homogeneity of amorphous solid dispersions.²⁷² Though HPMC, hydroxypropyl methylcellulose acetate succinate (HPMCAS) and poly(vinylpyrrolidone-co-vinyl acetate) (PVPVA) have similar T_g , Li and Taylor found differences between their miscibility with Telaprevir (TPV).²⁷³ Phase separation was observed when HPMC and PVPVA was loaded at over 10% TPV, whereas phase separation started with HPMCAS at TPV loadings over 30%.

The polymeric additive possesses high T_g to decrease molecular mobility and so inhibits drug recrystallization. Conversely, ASDs convert from stable glass status to a supercooled liquid phase if the temperature is above T_g with the increasing molecular mobility leading to phase separation or drug recrystallization via the ‘plasticization’ effect.²⁷⁴

Polymer-drug interactions including hydrogen bonding, electrostatic interaction and van der Waals force also contribute to stability of ASDs. Shan et al. produced SDs of haloperidol

with poly(2-oxazoline)s (POx) and PVP, where the ability to inhibit crystallinity of haloperidol was in the order of: PVP > poly(2-propyl-2-oxazoline) (PnPOZ) = poly(2-ethyl-2-oxazoline) (PEOZ) > poly(2-methyl-2-oxazoline) (PMOZ).²⁶⁵ These results were explained by formation of hydrogen bonds between PVP with haloperidol and strong hydrophilicity of PVP. When SDs were exposed to moisture, the molecular mobility increased with plasticization of SDs.

SD formulation improves dissolution of poorly water-soluble drugs by increasing wettability and reducing drug particles size and agglomeration.²⁶⁸ Further, Yang et al. reported drug loading was related to drug release from ASD by evaluating release profiles of ritonavir (RTV) ASDs formulation with PVPVA as the polymeric matrix. Rapid and complete drug release was observed due to the formation of discrete drug-rich droplets when drug loading was less than 30%. In contrast, 30% drug loading generated partial release, while no drug release was shown at drug loading over 30%. These findings were attributed to the formation of a continuous drug-rich phase at the ASD matrix-solvent interface interfering with drug release.²⁷⁵ The mechanisms of drug release from SDs with water-soluble polymeric matrices was thoroughly discussed by Craig.²⁷⁶ Two main mechanisms operate via carrier controlled release or drug controlled release, the proportions of which depend on the aqueous solubility of the drug in concentrated solutions of the carrier.²⁷⁶

Due to lyotropic liquid crystalline behaviour of xanthan gum in aqueous solutions, it is generally used as a suspending agent in pediatric oral suspension, such as xanthan gum is used in oral suspension Purixan™ (Rare Disease Therapeutics, Inc.) to treat acute lymphoblastic leukemia (ALL), employed in Noxafil® (Merck) as an antifungal which was approved in 2006 and applied in Onfi® to treat anti-seizure only with Lennox-Gastaut syndrome (LGS).

1.3.6 Injectable formulations

Injection formulations are widely used via intradermal, intravenous, intramuscular and subcutaneous routes (Figure 1.3-6).

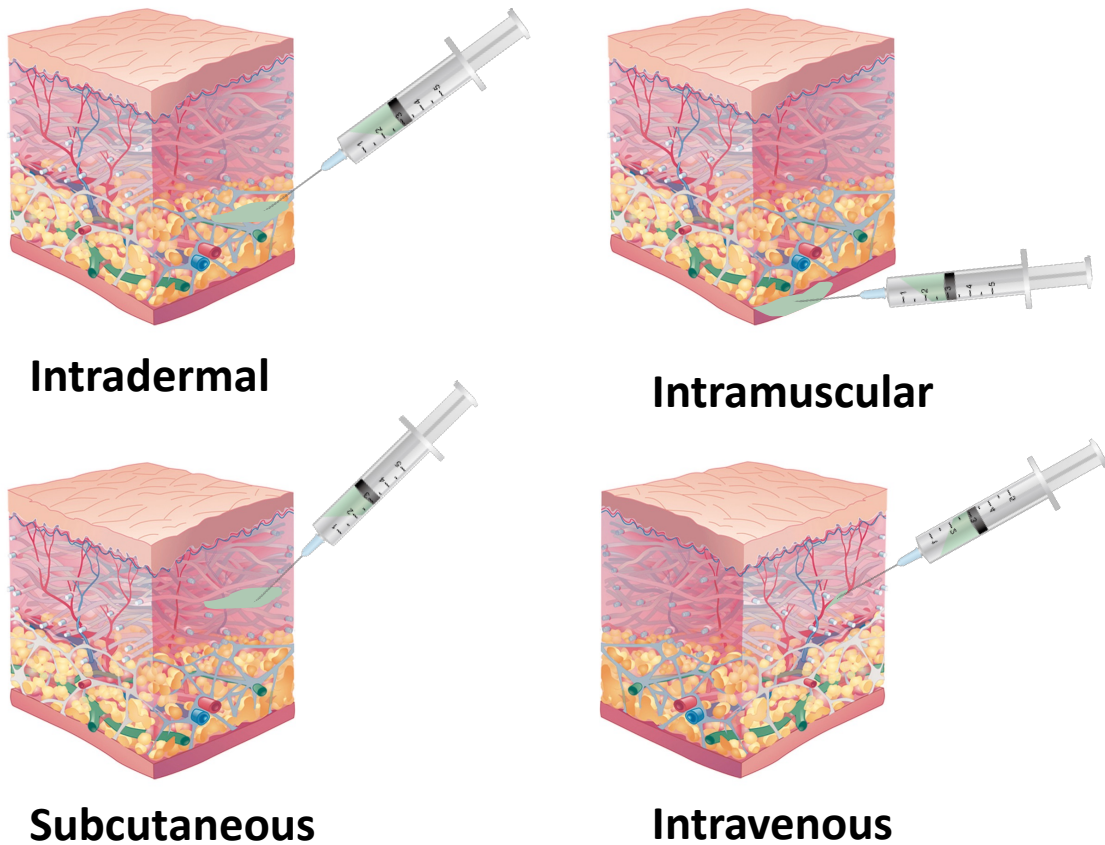


Figure 1.3-6. The site of different injection administrations within skin. Modified from Frost, Gregory I.²⁷⁷

Intravenous injection (IV) is an invasive administration route to apply medicine directly into veins, while intramuscular injection (IM) delivers medicine into a specific muscle, and subcutaneous injections (SC) are widely used for administering insulin, growth hormone and epinephrine. Table 1.3-2. Advantages and disadvantages for intravenous, intramuscular and subcutis injections. demonstrates the advantages and disadvantages for different injection routes.

Table 1.3-2. Advantages and disadvantages for intravenous, intramuscular and subcutis injections.

Injection routes	Intravenous	Intramuscular	Subcutaneous	
Advantages	<ul style="list-style-type: none"> • Complete bioavailability • Avoid first pass effect • Rapid absorption, suitable for treating dehydration, nutrient deficiencies, and other emergency conditions 	<ul style="list-style-type: none"> • Administration for vaccines, vitamins and analgesic • Highly vascularized muscle tissue • Rapid absorption • Avoid veins damages • Avoid first pass effect 	<ul style="list-style-type: none"> • Self-administered by patients • Cost efficacy • High safety • Numerous available injection sites • High patient compliance 	
	<ul style="list-style-type: none"> • Precise control of dose and administration rate • Minimum volume restriction 			
		<ul style="list-style-type: none"> • Risk of systemic infection • Low patient compliance • Professional administration required 	<ul style="list-style-type: none"> • Cause irritation, pain and swelling for injection sites • Cause erratic absorption of drugs • Possibility of improper deposition of drug 	<ul style="list-style-type: none"> • Volume constraint (< 2 mL) • Retention of drug at injection site cause local adverse
	Disadvantages	<ul style="list-style-type: none"> • Sterile conduction required • Costly expense • Preparation and injection are time consuming 	<ul style="list-style-type: none"> • Professional administration required • Volume constraint (2-5 mL) 	<ul style="list-style-type: none"> • Slow absorption, not suitable for emergency • Only available for non-irritant drugs

Excipients form the major components of pharmaceutical formulations to achieve desired functions, such as increasing bulk, aiding manufacturing, improving stability and aqueous solubility, enhancing efficacy and safety, imparting targetability and modifying pharmacokinetic and pharmacodynamic profiles. Targeted drug delivery systems are attractive deliver drug specifically to the target site. For example, nanoparticle-based

formulations aim to deliver chemotherapeutic drugs to targeted areas of tumours and control release profiles at the target site via injection.

Albumin is a non-toxic, biocompatible and biodegradable water-soluble polymer used as a pharmaceutical carrier. Albumin can extend drug circulation half-life due to its large size (around 66.4 kDa) which precludes glomerular filtration. Albumin in tumour tissue since tumour cells trap albumin as their nutrients source to promote cell proliferation, hence albumin has been used to prepare nanoparticles carrying anti-tumour agents. Protein-based nanoparticles are commonly fabricated by techniques including desolvation, nanoparticle albumin-bound (Nab™) technology and self-assembly.²⁷⁸ Abraxane® is a commercial nanoparticle dosage form of paclitaxel with the stabilizing agent albumin, and was the first product based on protein-nanotechnology for treating breast cancer, approved by FDA in 2005. The nanoparticles are prepared by Nab™ technology to encapsule paclitaxel in 130 nm particles. Briefly, hydrophobic paclitaxel is dissolved in organic solvent and emulsified with albumin before homogenization to control particle size, accompanied with the formation of disulfide bonds.²⁷⁹ Abraxane® improves the aqueous solubility of hydrophobic paclitaxel by introducing albumin and alleviates toxicity and anaphylactoid hypersensitivity reactions induced by cremophor EL as a solubilizer in the traditional paclitaxel formulation (Taxol®). Nab-paclitaxel (Phase II) is a type of albumin bound nanoparticles for treating metastatic breast cancer loading 49% higher content of paclitaxel due to the presence of albumin. Another albumin bound nanoparticle, Nab-paclitaxel/Rituximab-coated Nanoparticle AR160 for treating relapsed or refractory B-Cell non-Hodgkin lymphoma was developed at the Mayo Clinic (completed Phase I trial) recently.

Parenteral dosage forms are required to be isotonic with human plasma to avoid damage to tissues; dextrose, glycerin and mannitol are commonly used tonicity adjusting agents. 4.8% w/v ascorbate (sodium/acid) in Vibramycin®, 0.66% w/v bisulfite sodium in Amikin™ and 0.1% metabisulfite potassium in Vasoxyl® as antioxidant are used to minimize oxidation reactions, while antimicrobial agents are used to eliminate micro-organisms in products such as 0.5% w/v phenol in Calcimar®, 0.315% meta-cresol in Humalog® or 0.02% w/v benzalkonium chloride in Celestone® Soluspan®. Ethylenediaminetetraacetic acid (EDTA) is a popular chelating agent able to bind metal ions via four carboxylate and two amine groups and is used as 0.11% w/v disodium EDTA to chelate in the Calcijex® injection formulation. Buffers are added to adjust and stabilize pH until close to physiological pH, which also optimizes drug stability and aqueous solubility. Citrates are common buffers that play a dual role as a chelating agent.

The solubilizing agent is a significant component to enhance aqueous solubility of poorly water-soluble drugs at a desired concentration. Solubilizers are broadly classified as surfactants that increase dissolution through reducing surface tension of drugs and include the commercially available Tween 20, Tween 80 and Pluronic®; and co-solvents, defined as a combination of two different solvents, exert synergetic effects to dissolve drugs with materials such as PEG 300, PEG400, ethanol (EtOH) and glycerin commonly used. Organic solvent or surfactant used in injectable formulations are associated with latent precipitation, pain, inflammation and hemolysis. Prediction of intravenous compatibility *in vitro* measures total volume percent of solvent in whole blood that induces 50% hemolysis of red blood cells (LD₅₀). Values for common solvents were: 39.5% dimethyl isosorbide (DMI) > 37.0% DMA > 30.0% PEG 400 > 21.2% EtOH > 5.7% propylene glycol > 5.1% DMSO.²⁸⁰ The maximum content of organic solvent and surfactant used in commercially intravenous bolus injection is up to 68% propylene glycol (phenobarbitol), 50% PEG 300 (methocarbamil), 20% ethanol (paricalcitol), 15% glycerin (dihydroergotamine), and 9% PEG 400 (lorazepam).²⁸¹ For intravenous bolus injection route, content of the organic solvent and surfactant is up to 25% Tween 80 (docetaxel), 15% glycerin (dihydroergotamine), 10% Cremophor EL (paclitaxel), 13% ethanol (docetaxel), and 6% propylene glycol (melphalan). Intramuscular administration route has greater tolerable capacity than intravenous injections for up to 100% organic solvents or surfactant, though the threshold of each injection site is usually restricted to 5 mL. However, due to the limited volume of the subcutis injection route, a few organic solvents or surfactant such as 15% glycerin (dihydroergotamine), 7% polyoxyethylated fatty acid (phtyonadione, vitamin K1) and 6% ethanol with 1-2 mL are added to formulations.²⁸¹

Among organic cosolvents, PEG 300 and PEG 400 are generally considered as the safest organic cosolvents and are broadly applied in pharmaceutical formulations due to their aqueous solubility, biocompatibility and safety. For example, VePesid® is an antineoplastic medication used to treat small cell lung cancer in an injectable dosage form with 65% PEG 300 as solubilizer, Methocarbamol is a skeletal muscle relaxant administered via intramuscular, intravenous bolus or intravenous infusion with 50% PEG 300 as solubilizer, Lorazepam as an anxiolytic and sedative is administrated intramuscularly or by intravenous bolus injection at 2mg/mL using 18% PEG 400.

Beyond PEG 300 and PEG 400 which are popular solubilizers in medications, other PEGs at different molecular weight also employed such as 5% PEG 600 used in Persantine® (antiplatelet) for intravenous injection, 2.95% PEG 3000 in Depo-Medrol® which is an anti-inflammatory glucocorticoid for intramuscular intra-articular soft tissue or intralesional

injection and PEG 4000 (30 mg/mL) in Invega® Sustenna® (atypical antipsychotic) for intramuscular injection. Pluronic® is an extensively used surfactant in injectable medications, approved by the FDA at a maximum potency per unit dose up to 6mg poloxamer 188 for intravenous injection and 0.2% (w/v) for intramuscular injection accompanying with maximum daily exposure (4 mg) for intramuscular use.²⁸² Orencia® has the highest concentration of poloxamer 188 at 8 mg/mL for subcutaneous use.²⁸³

1.3.7 PEGylation

PEGylation was proposed by Abuchowski and Davis et al. in 1970s so that proteins conjugate with PEG forming covalent bonds²⁸⁴; to reduce protein immunogenicity, methoxy-PEG (mPEG) is usually attached to an end functional group of a protein. Protein and peptide drugs are promising therapeutic agents, however their degradation by proteolytic enzymes, short circulating half-life, generation of neutralizing antibodies, rapid kidney clearance and low aqueous solubility restricted their applications. These drawbacks are overcome via conjugation with PEG, achieving greater aqueous solubility, prolonged half-life *in vivo*, lower kidney clearance rate and less proteolytic destruction to improve pharmacokinetic profiles of protein and peptide drugs. Function groups such as active carbonate, active ester, aldehyde, or tresylate are used to obtain active PEG derivatives (Figure 1.3-7).²⁸⁵

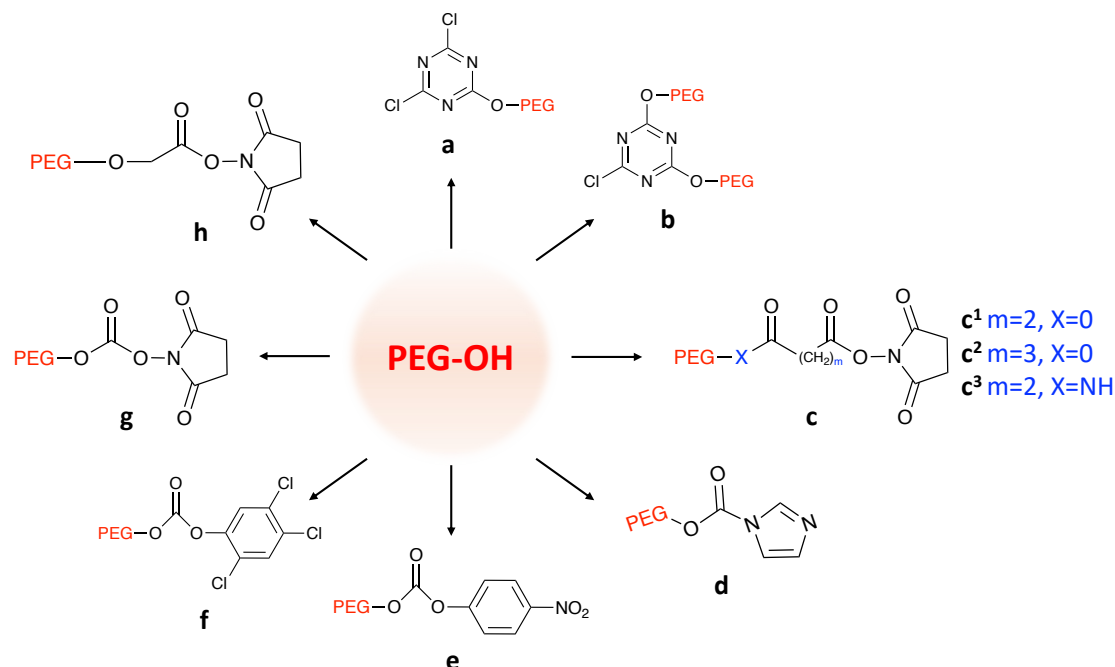


Figure 1.3-7. Method for the activation of PEG molecules (a) Cyanuric chloride method; (b) a variation on the cyanuric chloride method; (c¹) PEG–succinimidyl succinate method; (c²) substitution of the succinate residue by glutarate; (c³) substitution of the aliphatic ester in c¹ by an amide bond; (d) imidazolyl formate method; (e) and (f) variations using phenylcarbonates of PEG; (g) succinimidyl carbonates of PEG and (h) succinimidyl active ester of PEG. Modified from Harris and Chess²⁸⁵ by permission of Springer Nature.

To date, there are thirty-eight FDA approved PEGylated drugs; twenty-eight PEGylated formulations are based on therapeutic proteins, five PEGylated therapeutics are associated with small molecules drug and five PEGylated systems are related to nanoparticle-based drug delivery system (Table 1.3-3).

In addition to direct conjugation to therapeutic molecules, PEGylation of nanoparticles-based drug delivery systems aims to extend their half-life and provide stealth properties against the mononuclear phagocyte system (MPS). Due to the ‘stealth’ effect of PEG, PEGylated liposomes have been employed in formulating chemotherapeutics; the first PEGylated liposome Doxil[®] (doxorubicin·HCl liposome) was approved by FDA in 1995 achieving extension of circulation time. And another PEGylated liposome Onivyde[™] (chemotherapeutic irinotecan) was approved by FDA in 2015. Due to the stealth effect of PEG, the presence of PEG on the surface of a liposome prolongs circulation time and lessens uptake into the mononuclear phagocyte system.²⁸⁶

Small 23 to 25 nucleotide double stranded RNAs, which can divided into single strands to complement with target messenger RNA (mRNA) leading to gene silencing, are referred as small interfering RNA (siRNA).²⁸⁷ Onpattro[®] (Patisiran) is the first siRNA therapy formulated in PEGylated lipid nanoparticles to treat polyneuropathy caused by hereditary transthyretin amyloidosis (hATTR) which was approved by FDA in 2018. PEGylated lipid nanoparticles were employed to delivery mRNA-based COVID-19 vaccines including Comirnaty[™] (Pfizer, approved by FDA in 2022) and Spikevax[™] (Moderna, approved by FDA in 2023).²⁸⁸

Table 1.3-3 FDA approved PEGylated formulations.

	Type	Trade name
PEGylated Growth factors	granulocyte colony-stimulating factor (G-CSF)	Neulasta [®] , Stimufend [®] , Rolvedon [™] , Fulphila [™] , Ziextenzo [™] , Nyvepria [™] , Fylnetra [™] , Udenyca [™]
	erythropoietin	Mircera [™]
PEGylated Enzymes	adenosine deaminase	Adagen [™] , Revcovi [™]
	L-asparaginase	Oncaspar [™] , Asparlas [™]
	α -Galactosidase A	Elfabrio [®]
	phenylalanine ammonia-lyase	Palynziq [™]
	uricase	Krystexxa [®]
PEGs interferons		Sylatron [™] , Plegridy [™] , Besremi [™] , Pegintron [™] , Pegasya [™] ,
PEGylated Proteins		Adynovate [®] , Rebinyn [®] , Jivi [™] , Esperoct [™]
PEGylated Antibody		Cimzia [™]
PEGylated Human growth hormone		Skytrofa [™] , Somavert [™]
PEGylated Small molecules		Movantik [™] , Empaveli [™] , Syfovre [™] , Omontys [™] , Macugen [™]
PEGylated Nanoparticles		Doxil [®] , Onpattro [®] , Onivyde [™] , Comirnaty [™] , Spikevax [™]

The first generation PEGylation generally refers to PEG conjugates with enzymes, Adagen[™] (1990) was the first approved PEGylated therapeutic and Oncaspar[™] was approved by FDA in 1994 and was feasible since proteins contain abundant lysine to allow conjugation. However, due to multiple PEGylated sites in each protein, PEG isomers were obtained with different molecular masses with low reproducibility and generated antigenicity

to the drugs. Additionally, first generation methods generally employed linear PEG with molecular weight ≤ 12 kDa, which formed unstable bonds leading to degradation of PEG-drug conjugate during production and injection.²⁸⁹

The second generation PEGylation provided site-specific conjugation of PEG accompanied with utilization of high molecular weight PEGs (MW>5000 g/mol)²⁹⁰. The first mono-PEGylated drug, Pegintron™, was approved by the FDA in 2001, which mitigated deactivation and immunogenicity of the former conjugates and extended circulation half-life. These conjugates showed uniform structure and increased pharmacokinetics, for example, Neulasta® (PEGfilgrastim) is prepared by PEG (20 kDa) attaching on the α -amino group of the N-terminus of filgrastim, decreasing renal clearance due to the formation of larger molecules consequently increasing half-life from 3.5h to 15-80h.²⁹¹ Another development in second generation PEGylation was the introduction of branched PEG with molecular masses up to 80 kDa. Monfardini and co-workers reported the 'Y' shape branched PEG exhibited remarkable shielding effects on protein surfaces (Figure 1.3-8), increasing the activity of the PEG conjugates and effectivity protecting PEG conjugates from proteolytic enzymes and antibodies.²⁹² This effect may be attributed to steric effects hampering PEG reaching enzyme active site clefts or other biological active sites. Pegasys™ is a representative branched-PEGylated drug that was approved by the FDA in 2002 with interferon alfa-2a modified with PEG (40 kDa), achieving sustained release and reducing renal clearance due to conjugation increasing hydrodynamic size. On the basis of this property, versatile marketed products have been produced such as Somavert™ which increases half-life from 20 min to 72h²⁹³ and Krystexxa® with half-life increases from <24 h to 2 weeks. Skytrofa™ approved by the FDA in 2021 introduced a four-arm branched PEG attaching to the human growth hormone via a cleavable TransCon linker to release human growth hormone via injection.²⁹⁴

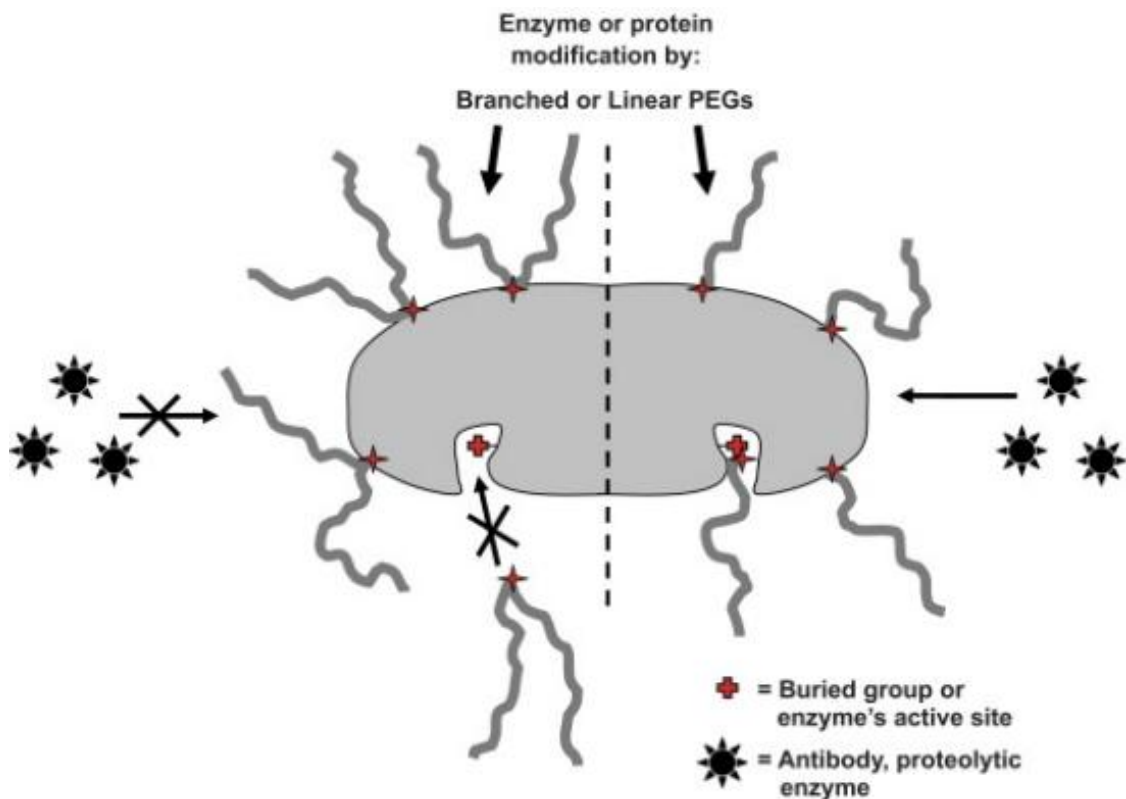


Figure 1.3-8. Relevance of PEG shape on protein surface coverage or enzyme active site access. The higher steric hindrance of branched PEGs ensures more complete protein shielding and makes difficult the access to recognition or active site cleft. Reproduced from Pasut and Veronese²⁹⁵ by permission of Elsevier Science Ltd., UK.

PEGylation is also used to modulate drug-receptor binding affinity. For example, Mircera™ (2007) is a PEGylated epoetin-beta product showing slower association and faster dissociation rate from its corresponding receptor accompanied with an enhanced half-life that allows less frequency dosage administration compared to the free drug. Adynovate® (2015) is one of the first four PEGylated anti-hemophilic agents possessing all the physiological functions of free factor VIII (FVIII, an essential blood-clotting protein) with a less binding affinity to low-density lipoprotein receptor-related protein clearance receptor, leading to extension of circulation time and decreasing clearance rate.²⁹⁶

The different types of PEGylated drugs approved by FDA are illustrated in Figure 1.3-9.

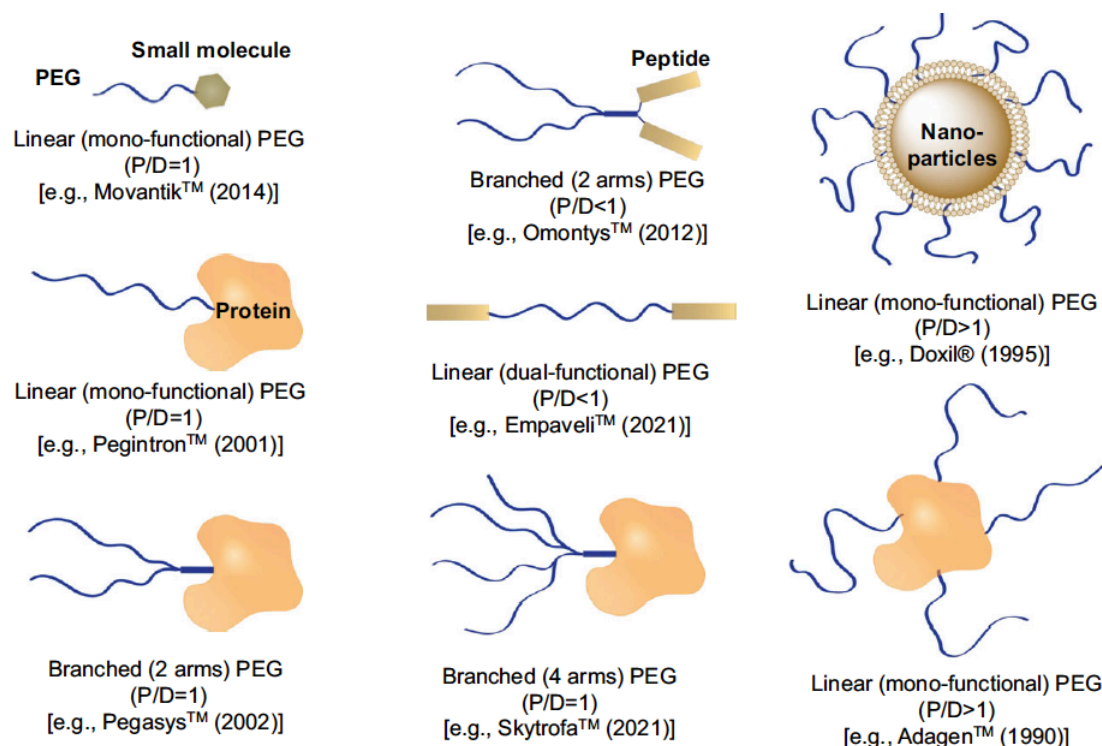


Figure 1.3-9. Types of FDA approved PEGylated drugs. P/D, the molar ratio of PEG to drug. Reproduced from Gao et al.²⁸⁸ by permission of John Wiley & Sons Ltd., UK.

Kaldybekov et al. produced maleimide-functionalised PEGylated (PEG-Mal), PEGylated and conventional liposomes using thin film hydration and a sonication method for urinary bladder drug delivery.²⁹⁷ The size of the liposomes was 90 ± 1 nm with a PDI < 0.23, illustrating the homogeneity of the prepared liposomes and narrow size distribution. The zeta potential of the vesicles was ≤ -30 mV indicating superior colloidal stability and propensity to form unilamellar vesicles because of the electrostatic repulsion between vesicles. It was noted that the entrapment ability of liposomes increased with greater zeta potential.²⁹⁸ The maleimide function group was introduced to enhance mucoadhesion of the PEGylated liposomes via covalent bonding between maleimide groups and thiol groups within the bladder mucosal surface. However, PEGylated liposomes provided greater penetration ability than PEG-Mal and conventional liposomes since the stealth properties of PEG reduced interaction with biological tissues promoting diffusivity of PEGylated liposomes through the mucosal tissue. In contrast, the PEG-Mal liposomes formed covalent bonds retarding penetration of these liposomes. NaFI was used as a model drug to assess the release profile from the liposomes; conventional liposomes showed a rapid release in 2h, while PEGylated and PEG-Mal liposomes demonstrated prolonged release over 4 and 8 h, respectively which was attributed to the presence of PEG. PEG-Mal liposomes maintained an efficient drug concentration during a long period following intravesical administration.

1.3.8 Micellar polymers

A representative amphiphilic ABA triblock polymer composed of hydrophilic and hydrophobic moieties is poly(ethylene oxide)-poly(propylene oxide)-poly(ethylene oxide) (PEO-PPO-PEO) (Figure 1.3-10), with hydrophilic poly(ethylene oxide) as the end blocks and hydrophobic poly(propylene oxide) as the middle block, commercially available as Pluronic[®] (manufacturer BASF) or poloxamers. BASF introduced a specific notation system for Pluronic[®], starting with L (liquid), P (paste), F (flake) to signify the morphology of polymers followed by one or two numbers indicating the molecular weight (1/300) of the PPO block and the last number referring to 1/10 molecular weight of PEO block (Figure 1.3-10). For example, P84 and P85 are both pastes containing the same percentage of PPO moieties, while consisting of 40% PEO for P84 and 50% PEO for P85.²⁹⁹

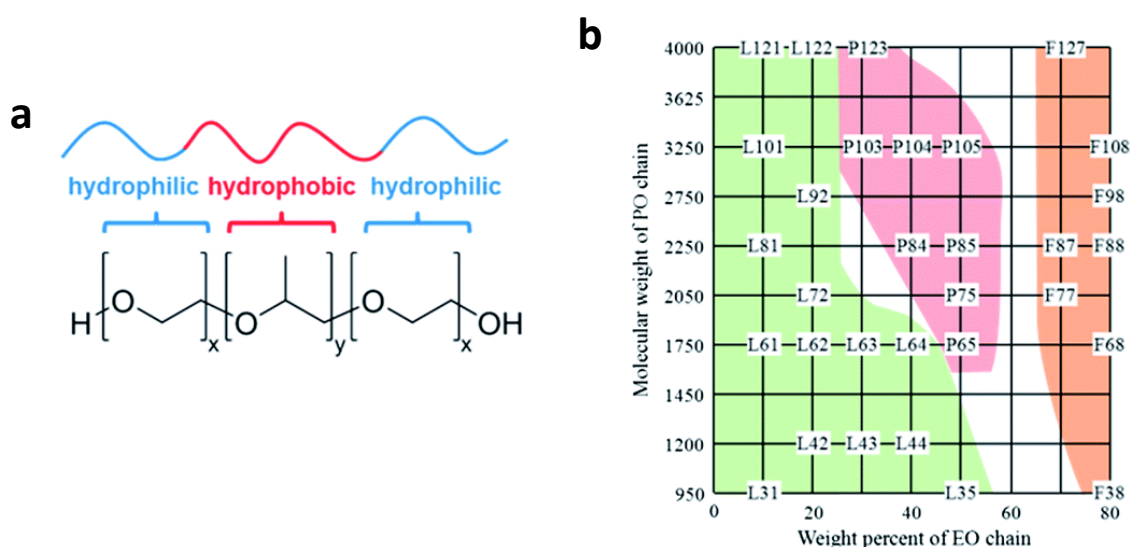


Figure 1.3-10. (a) Structure of Pluronic[®], and (b) Pluronic[®] grid (color code: physical state of copolymers under ambient conditions: green = liquid; red = paste; orange = flake). Reproduced from Pitto-Barry and Barry²⁹⁹ by permission of The Royal Society of Chemistry.

Due to the various ratio of PPO/PEO and molecular weights, Pluronic[®] provides different amphiphilic materials. Self-assembly micellization of Pluronic[®] forms core-shell micelles with the core comprised of hydrophobic PPO enclosed an outer shell consisting of hydrated hydrophilic PEO above the critical micelle concentration (CMC) or critical micelle temperature (CMT) in aqueous solution.³⁰⁰ The micellization of Pluronic[®] in aqueous solution exhibits concentration or temperature-dependent behaviour and the content of PPO block dominates the micellization. The CMC and CMT decrease two orders of magnitude with increasing temperature 20°C.³⁰⁰ The CMC and CMT decrease with an increasing of PPO portion in block polymers or molecular weight, while CMT is significantly influenced by

molecular weight. Thus, with 30% (L64, P65, F68), 40% (P84, P85, F88) and 60% (P104, F108) PO segments, the CMC and CMT decreased with an increase content of PO moieties.³⁰¹ At lower polymer concentration, polymer chains are distributed throughout solution and play the role of a surfactant to absorb at air-water or aqueous-organic solvent interfaces as individual coils due to insufficient chains to form micelles³⁰², whereas increasing polymer concentration results in the formation of thermodynamically stable micelle systems.

Due to the application of salts in pharmaceutical formulations, such as NaCl as an osmotic regulator, phosphate is commonly used to produce buffer solutions and carbonate is used to mitigate acid reflux, the effects of salts on micellization of Pluronic[®] was extensively explored.^{303,304} The formation of hydrogen bonding between ether bonds within PEO block and water results in the dissolution of Pluronic[®] in water. With an increase of temperature, the aqueous solubility is decreased due to breakage of hydrogen bonding. With ascending temperature, collapse of the PEO corona followed by dehydration of the corona to shield the dense PPO core is observed resulting in phase separation of the micellar solution at a defined temperature, termed the cloud point.³⁰⁵ Ohashi and co-workers explored the effects of inorganic salts on cloud point for P85 and showed that increasing addition of salts led to a linear decrease of cloud point in the order $\text{NaHPO}_4 > \text{NaH}_2\text{PO}_4 > \text{NaCl} > \text{NaBr}$, fitting the Hofmeister series. This effect may be attributed to hydration of the PEO corona is weakened by adding inorganic salts, such as Na^+ , K^+ , Cl^- , Br^- , and SO_4^{2-} , since salts facilitate self-hydration of water through hydrogen bonding (Figure 1.3-11). In contrast, Mg^{2+} , Al^{3+} , ClO_4^- , SCN^- and I^- enhance hydration of these copolymers to increase cloud point.

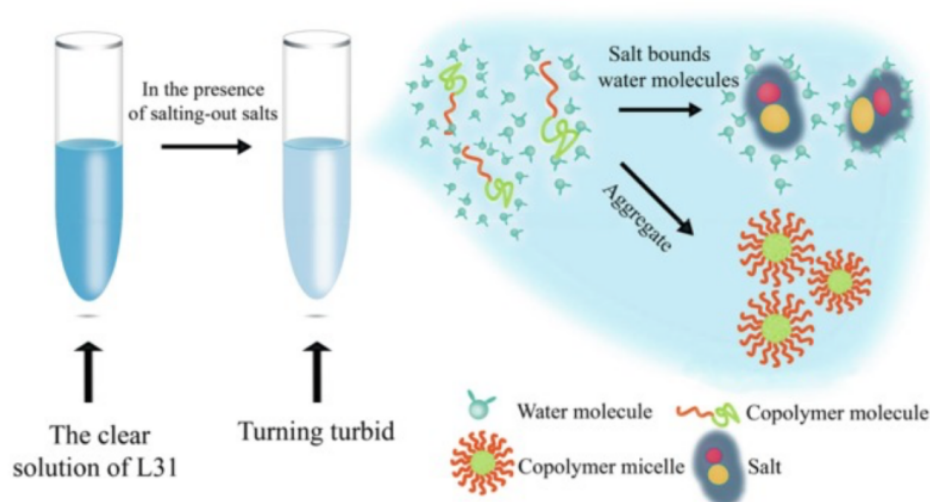


Figure 1.3-11. The mechanism of cloud point reduction by salting-out. Reproduced from An et al.³⁰⁶ by permission of Springer Nature.

Further, salts with cloud point decreasing effects also decrease CMC and CMT of Pluronic[®].^{300,307} MgCl₂ and CaCl₂ decreased CMC of P105 approximately two orders of magnitude while NaCl decreased CMC by approximately one order of magnitude.³⁰⁸ The effects of KCl, KNO₃, KBr and KI on CMC for F108 was investigated via UV-visible spectroscopy.³⁰⁹ The presence of the salts decreased CMC to 3.25-3.55 × 10⁻⁴ M from 4.42 × 10⁻⁴ M when salts were not added.

Pluronic F-68 (poloxamer 188) and F-127 (poloxamer 407) are FDA approved materials among the Pluronic[®] series and widely used in pharmaceutical formulation. On the basis of the average EO units and PO units, the block length of Pluronic F-68 and F-127 are approximately 76-29-76 and 100-65-100, respectively.²⁹⁹ Due to the presence of hydrophobic moieties promoting micellization of Pluronic[®], the CMC of F127 (0.039 mg/mL) is lower than F68 (4.204 mg/mL). Doxorubicin (DOX) is an extensively used anticancer agent and was formulated with Pluronic L61 and Pluronic F127 to form a mixed micellar system (SP1049C) to treat oesophagus adenocarcinoma and gastroesophageal junction (GEJ) and studied in clinical trials.^{310,311} This first Pluronic[®]-based micellar formulation exhibited notable antitumor ability comparing to conventional DOX formulation at Phase I and II clinical trials. Supratek Pharma Inc. conducted a clinical Phase III trial of SP1049C for treatment of metastatic adenocarcinoma of the upper GI tract which was approved by FDA.

1.3.9 Drug conjugation

Water-soluble polymers are widely used to form complexes with small molecules to enhance their solubility in aqueous solutions. Water-soluble polymers-drug conjugations have been synthesised since 1960s³¹²; conjugation was intended to enhance the aqueous solubility of hydrophobic drugs and, due to the increase of molecular weight, circulation time is prolonged, improving drug bioavailability and half-life of drugs.³¹³ PEG was reported as transport platform for camptothecin (CPT) to enhance its solubility in aqueous solution (2 mg/mL), compared with free CPT (0.025 mg/mL). The results showed a higher concentration of CPT in circulation and accumulated more CPT in solid tumors achieving significantly antitumor activity.³¹⁴ The formation of polymer-drug conjugates is generally via electrostatic bonding, such as ion-to-ion, ion-to-dipole, dipole-to-dipole bonds, also sometimes van der Waals force and hydrogen bonding are involved for forming complexes.³¹⁵ Rao et al. synthesized a hyaluronic acid-quercetin (HA-Q) conjugate for wound healing that exhibited higher water solubility and promoted growth and migration of skin fibroblast cells.³¹⁶ The hydroxyl group of quercetin was conjugated to the carboxylic group of hyaluronic acid via

1-ethyl-3-(3-dimethylamino-propyl) carbodiimide (EDC) coupling. The conjugate improved the antioxidant properties of quercetin.

Proteins, peptides, enzymes and nucleic acid as biomacromolecules are potential candidates in biopharmaceuticals, however, the drawbacks include short *in vivo* half-lives, instability and degradation under harsh gastrointestinal condition and poor aqueous solubility.³¹⁷ Conjugation of water-soluble polymers and biomacromolecules benefit from the synergistic properties of both compositions since polymers provide protection of their activation and structure.³¹⁸ The bioconjugate generally increases aqueous solubility, stability and *in vivo* circulation time. Thilakarathne et al. reported a poly (acrylic acid)-met-hemoglobin (PAA-Hb) conjugate via covalent conjugation of carboxyl group of PAA and amino group of Hb.³¹⁹ The conjugate retained the bioactivity and structure of Hb, prolonged *in vivo* half-life and improved storage stability at room temperature, compared to unmodified Hb.

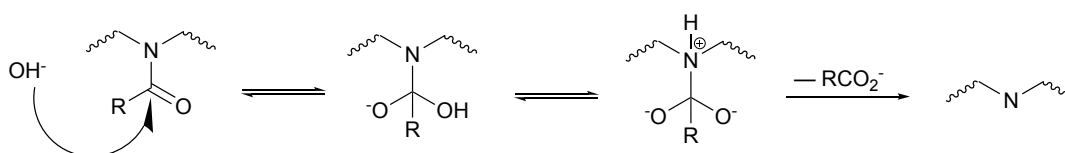
1.4 Linear Poly (ethylene imine)

Linear poly (ethylene imine) (L-PEI) is a synthetic, non-biodegradable, cationic polyelectrolyte comprising two carbon aliphatic (-CH₂CH₂-) spacer groups and an amine group in the repeating units. L-PEI contains all secondary amine groups, whereas branched poly (ethylene imine) (b-PEI) contains primary, secondary and tertiary amine groups. b-PEI is generally synthesised via ring-opening polymerization of aziridine, while L-PEI is prepared by hydrolysis of POx under acidic or basic condition.^{320,321}

Due to the commercial availability from large-scale production and superior water solubility of PMOZ and PEOZ, the preparation of L-PEI commonly derives from PMOZ or PEOZ.

a) Basic hydrolysis

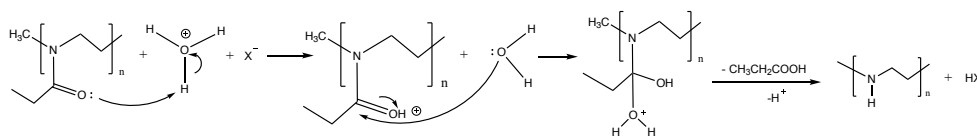
The initial method for preparation of L-PEI from POx by hydrolysis was under basic condition.^{322,323} The reaction follows second order kinetics with rate = $k^2[\text{amide}][\text{OH}^-]$.³²⁰ The OH⁻ attacks the carbonyl group to form tetrahedral intermediates, the nitrogen is protonated followed by an irreversible release of the carboxylate (Scheme 1.4-1). However, there is an unintended consequence of basic hydrolysis of L-PEI with the partial degradation of the backbone evidenced by SEC.³²⁴



Scheme 1.4-1. Basic hydrolysis of L-PEI start with parent POx.

b) Acidic hydrolysis

Acidic hydrolysis is considered as a preferred strategy to prepare L-PEI since the protonated (partially) hydrolyzed copolymer displays aqueous solubility. Kim firstly proposed hydrolysis of PMOZ, PEOZ and PnPOZ using HCl aqueous solutions.³²⁵ Since hydrolysis is conducted in an excess volume of HCl, it follows pseudo-first order kinetics.³²⁰ Under acidic condition, the carbonyl group is protonated and subsequently attacked by water as a nucleophile to form a tetrahedral intermediate. The tetrahedral intermediate is rapidly converted into the amine group, releasing the corresponding acid such as acetic acid from PMOZ or propionic acid from PEOZ (Scheme 1.4-2).



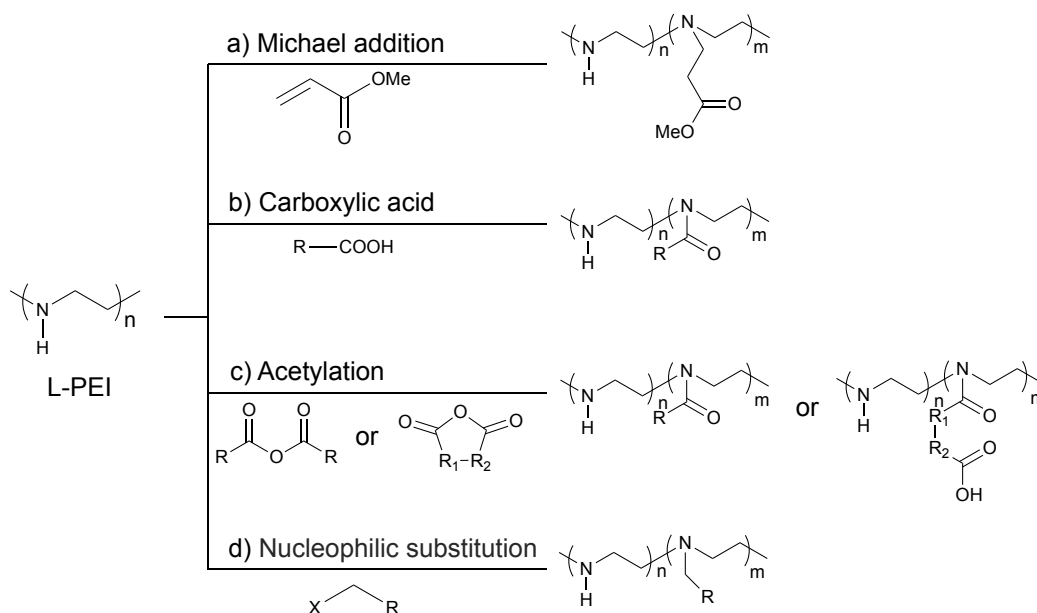
Scheme 1.4-2. Acidic hydrolysis of L-PEI start with parent POx.

Due to the differences in structure, b-PEI as an amorphous polymer is readily soluble in aqueous solution, whereas L-PEI is semi-crystalline and an increase of chain mobility and melting of polymer crystallites only occurs above 60°C, resulting in dissolution in water to a hydrated state.¹⁹¹ L-PEI is employed in diverse fields, such as gene delivery³²⁶, for hydrogels²⁰, controlled release systems²², water treatment³²⁷ and PEI-conjugates³²⁸. Soradech et al. provided a novel approach to prepare cross-linked or initiator free L-PEI cryogels by freezing and subsequent thawing of its aqueous solutions. These physical cross-linked L-PEI cryogels exhibited properties suited to biomedical and pharmaceutical applications.³²⁹

PEI is an extensively used polymer vector for gene therapy since it was first suggested by Boussif et al. in 1995.³³⁰ PEI possesses a "proton sponge" effect under a wide range of pHs, attributed to protonation of every third nitrogen atom. PEI has a high cationic charge density to electrostatically interact with DNA to form complexes with DNA.³³¹ Elzes et al. designed novel gene delivery agents composed of PEI and poly (propylene imine) (PPI). This linear random copolymer displayed superior serum tolerance and impressive transfection efficiency at a 1:1 ratio of PEI and PPI and a DP=500. This system was reported to be a promising agent for *in vitro* transfection of plasmid DNA without cytotoxicity.³³² Casper et al. provided a comprehensive analysis of clinical trials of PEI formulations from 2005 to 2023, but noted that there are only 9 formulations of PEI derivatives and nucleic acid encoded transgenes being evaluated in clinical trials.³³³

Due to electrostatic interactions between PEI and cell membranes, and the extracellular matrix, the cytotoxicity of PEI limits its applications.³²⁸ The introduction of novel functionalities for L-PEI significantly broadens its potential applications. L-PEI contains abundant secondary amine groups which can act as a nucleophile in order to prepare diverse (co)polymers. Generally, partially functionalized L-PEI exhibits polyelectrolyte properties of L-PEI and favorable properties from the introduced pendant chains. Common modification strategies of L-PEI are demonstrated in

Scheme 1.4-3.



Scheme 1.4-3. Illustrative examples of modification of L-PEI with a) Michael addition, b) carboxylic acid, c) acetylation and d) nucleophilic substitution.

a) Modification via Michael addition

The secondary amine groups within L-PEI allows nucleophilic attack of the β -carbon of α , β -unsaturated carbonyl compounds (e.g. acrylates, acrylamides, or maleimides), thus introducing ester side chain functionality³³⁴ and is the most common approach for gene delivery or formation of DNA complexes. Liu et al. reported conjugation of methyl acrylate to L-PEI whilst tuning the degree of substitution between 0-1; side chain terminated with a hydrolyzed or amidated methyl ester group enhanced cell transfection efficiency.³³⁵

b) Modification with carboxylic acids

The coupling of L-PEI to a carboxylic acid in the presence of a coupling agent (e.g. 1-ethyl-3-(3-dimethylaminopropyl) carbodiimide (EDC), N, N'-dicyclohexyl carbodiimide (DCC)) or using a combination of additives e.g. N-hydroxy succinimide (NHS) imparts functional side chains into L-PEI to broaden its applicability. The carboxylic acid is activated by the coupling agent, which is subsequently attacked by the secondary amine groups within L-PEI, which act as nucleophile, to form an amide group. Limiti et al. designed a high drug loading and sustained release nanogel platform by conjugating hyaluronic acid (HA) and L-PEI to release doxorubicin (DOX).³³⁶ HA is widely used for intracellular delivery to target tumor cells since it shows affinity to CD44, a HA receptor highly expressed in tumor.³³⁷ The introduction of HA reduced the toxicity of L-PEI and enhanced targeting ability of the HA-PEI nano platform, suggesting the possibility of L-PEI in targeted drug delivery systems. A prospective electrochemiluminescence (ECL) immunosensor composed of Au

nanoparticle/graphene quantum dots-poly(ether imide)-graphene oxide (AuNP/GQDs-PEI-GO) to detect cancer biomarkers was reported by Yang et al.³³⁸ In this study, GO was covalently bonded to L-PEI to enhance water solubility and stability of the L-PEI/GO composite membrane. Consequently, the GQDs (graphene quantum dots) and AuNP (Au nanoparticle) were modified on the membrane via formation of amide bond and electrostatic interaction, separately. The novel ECL sensor provided a broad linear response range for prostate-specific antigen (PSA) detection from 0.001 ng/mL to 100 ng/mL with a detection limit of 0.44 pg/mL.

Additionally, N-succinimidyl-4-pentenate has been coupled with L-PEI to introduce double bonds in the side chain, providing access to thiol-ene photoaddition reactions.^{339,340}

c) Modification via acetylation

The addition of an acetyl group into L-PEI via acetylation with different compounds, including organic anhydrides, proteins and nucleic acids has been demonstrated.

Acylation of L-PEI with different anhydrides in the presence of a base, that also act as a catalyst, is an effective alternative to prepare well-defined POx, avoiding chain transfer reactions. Sedlacek and co-workers prepared well-defined high molecular weight PMOZ through L-PEI acylation with acetic anhydride.³⁴¹ Shan et al. developed this strategy to synthesise PMOZ, PnPOZ and PiPOZ via acylation with L-PEI and acetic, butyric and isobutyric anhydrides, respectively.²⁶⁵

Besides linear anhydrides, partially acetylation of L-PEI with cyclic anhydrides (e.g. succinic anhydrides, phthalic anhydrides and maleic anhydrides) is a promising strategy to prepare polyampholytes with enhanced mucoadhesive properties compared to L-PEI at $\text{pH} < \text{pH}_{\text{IEP}}$.¹⁸⁶ The superior mucoadhesive properties of succinylated L-PEI and phthalylated L-PEI were predominantly driven by electrostatic interactions between protonated amine group within the polyampholytes and carboxyl groups within mucin.

d) Modification via nucleophilic substitution

The secondary amine groups within L-PEI allow nucleophilic attack of electrophilic carbon in the presence of a base, for example the reaction with carboxylic acid described above. Another typical nucleophilic substitution of L-PEI is alkylation with an alkyl halogenide in the presence of a base.³²⁰

L-PEI has also attracted attention for mucoadhesive delivery systems (e.g. nasal⁵ and buccal³⁴² drug delivery) as the secondary amine group within L-PEI can combine with negatively charged mucin via electrostatic interactions. The mucoadhesive properties of L-PEI are extensively explored in the following chapters.

1.5 Reference

- (1) Jóhannsdóttir, S.; Jansook, P.; Stefánsson, E.; Loftsson, T. Development of a cyclodextrin-based aqueous cyclosporin A eye drop formulations. *International journal of pharmaceutics* **2015**, *493* (1-2), 86.
- (2) Kedzior, S. A.; Dubé, M. A.; Cranston, E. D. Cellulose Nanocrystals and Methyl Cellulose as Costabilizers for Nanocomposite Latexes with Double Morphology. *ACS Sustainable Chemistry & Engineering* **2017**, *5* (11), 10509.
- (3) Moustafine, R. I.; Sitenkov, A. Y.; Bukhovets, A. V.; Nasibullin, S. F.; Appeltans, B.; Kabanova, T. V.; Khutoryanskiy, V. V.; Van den Mooter, G. Indomethacin-containing interpolyelectrolyte complexes based on Eudragit® E PO/S 100 copolymers as a novel drug delivery system. *International Journal of Pharmaceutics* **2017**, *524* (1), 121.
- (4) Koczur, K. M.; Mourdikoudis, S.; Polavarapu, L.; Skrabalak, S. E. Polyvinylpyrrolidone (PVP) in nanoparticle synthesis. *Dalton transactions* **2015**, *44* (41), 17883.
- (5) Shan, X.; Aspinall, S.; Kaldybekov, D. B.; Buang, F.; Williams, A. C.; Khutoryanskiy, V. V. Synthesis and Evaluation of Methacrylated Poly(2-ethyl-2-oxazoline) as a Mucoadhesive Polymer for Nasal Drug Delivery. *ACS Applied Polymer Materials* **2021**, *3* (11), 5882.
- (6) Kozma, G. T.; Shimizu, T.; Ishida, T.; Szebeni, J. Anti-PEG antibodies: Properties, formation, testing and role in adverse immune reactions to PEGylated nano-biopharmaceuticals. *Advanced Drug Delivery Reviews* **2020**, *154-155*, 163.
- (7) Borges-Vilches, J.; Unalan, I.; Aguayo, C. R.; Fernández, K.; Boccaccini, A. R. Multifunctional Chitosan Scaffold Platforms Loaded with Natural Polyphenolic Extracts for Wound Dressing Applications. *Biomacromolecules* **2023**.
- (8) Shirakura, T.; Ray, A.; Kopelman, R. Polyethylenimine incorporation into hydrogel nanomatrices for enhancing nanoparticle-assisted chemotherapy. *RSC advances* **2016**, *6* (53), 48016.
- (9) Hayek, A.; Ercelen, S.; Zhang, X.; Bolze, F.; Nicoud, J.-F.; Schaub, E.; Baldeck, P. L.; Mély, Y. Conjugation of a New Two-Photon Fluorophore to Poly(ethylenimine) for Gene Delivery Imaging. *Bioconjugate Chemistry* **2007**, *18* (3), 844.
- (10) Kadajji, V. G.; Betageri, G. V. Water Soluble Polymers for Pharmaceutical Applications. *Polymers* **2011**, *3* (4), 1972.
- (11) Patil, N. A.; Kandasubramanian, B. Functionalized polylysine biomaterials for advanced medical applications: A review. *European Polymer Journal* **2021**, *146*, 110248.
- (12) Pranantyo, D.; Xu, L. Q.; Hou, Z.; Kang, E.-T.; Chan-Park, M. B. Increasing bacterial affinity and cytocompatibility with four-arm star glycopolymers and antimicrobial α -polylysine. *Polymer Chemistry* **2017**, *8* (21), 3364.
- (13) Mazia, D.; Schatten, G.; Sale, W. Adhesion of cells to surfaces coated with polylysine. Applications to electron microscopy. *J Cell Biol* **1975**, *66* (1), 198.
- (14) Sun, H.; Wu, H.; Teng, Q.; Liu, Y.; Wang, H.; Wang, Z.-G. Enzyme-Mimicking Materials from Designed Self-Assembly of Lysine-Rich Peptides and G-Quadruplex DNA/Hemin DNAzyme: Charge Effect of the Key Residues on the Catalytic Functions. *Biomacromolecules* **2022**, *23* (8), 3469.
- (15) Grotzky, A.; Manaka, Y.; Kojima, T.; Walde, P. Preparation of Catalytically Active, Covalent α -Polylysine–Enzyme Conjugates via UV/Vis-Quantifiable Bis-aryl Hydrazone Bond Formation. *Biomacromolecules* **2011**, *12* (1), 134.

- (16) Mann, A.; Richa, R.; Ganguli, M. DNA condensation by poly-L-lysine at the single molecule level: role of DNA concentration and polymer length. *Journal of Controlled Release* **2008**, *125* (3), 252.
- (17) Mees, M. A.; Hoogenboom, R. Full and partial hydrolysis of poly (2-oxazoline) s and the subsequent post-polymerization modification of the resulting polyethylenimine (co) polymers. *Polymer Chemistry* **2018**, *9* (40), 4968.
- (18) Shen, C.; Li, J.; Zhang, Y.; Li, Y.; Shen, G.; Zhu, J.; Tao, J. Polyethylenimine-based micro/nanoparticles as vaccine adjuvants. *International Journal of Nanomedicine* **2017**, *12* (null), 5443.
- (19) Lei, Y.; Rahim, M.; Ng, Q.; Segura, T. Hyaluronic acid and fibrin hydrogels with concentrated DNA/PEI polyplexes for local gene delivery. *Journal of controlled release* **2011**, *153* (3), 255.
- (20) Yin, Y.; Li, X.; Ma, H.; Zhang, J.; Yu, D.; Zhao, R.; Yu, S.; Nie, G.; Wang, H. In Situ Transforming RNA Nanovaccines from Polyethylenimine Functionalized Graphene Oxide Hydrogel for Durable Cancer Immunotherapy. *Nano Letters* **2021**, *21* (5), 2224.
- (21) Li, J.; Yu, X.; Shi, X.; Shen, M. Cancer nanomedicine based on polyethylenimine-mediated multifunctional nanosystems. *Progress in Materials Science* **2022**, *124*, 100871.
- (22) Lu, Y.; Wu, F.; Duan, W.; Mu, X.; Fang, S.; Lu, N.; Zhou, X.; Kong, W. Engineering a “PEG-g-PEI/DNA nanoparticle-in- PLGA microsphere” hybrid controlled release system to enhance immunogenicity of DNA vaccine. *Materials Science and Engineering: C* **2020**, *106*, 110294.
- (23) Beyth, N.; Houry-Haddad, Y.; Baraness-Hadar, L.; Yudovin-Farber, I.; Domb, A. J.; Weiss, E. I. Surface antimicrobial activity and biocompatibility of incorporated polyethylenimine nanoparticles. *Biomaterials* **2008**, *29* (31), 4157.
- (24) Sun, W.; Zhang, J.; Zhang, C.; Wang, P.; Peng, C.; Shen, M.; Shi, X. Construction of Hybrid Alginate Nanogels Loaded with Manganese Oxide Nanoparticles for Enhanced Tumor Magnetic Resonance Imaging. *ACS Macro Letters* **2018**, *7* (2), 137.
- (25) Rahman, M.; Peng, X.-L.; Zhao, X.-H.; Gong, H.-L.; Sun, X.-D.; Wu, Q.; Wei, D.-X. 3D bioactive cell-free-scaffolds for in-vitro/in-vivo capture and directed osteoinduction of stem cells for bone tissue regeneration. *Bioactive Materials* **2021**, *6* (11), 4083.
- (26) Wu, S.-Y.; Debele, T. A.; Kao, Y.-C.; Tsai, H.-C. Synthesis and Characterization of Dual-Sensitive Fluorescent Nanogels for Enhancing Drug Delivery and Tracking Intracellular Drug Delivery. *International Journal of Molecular Sciences* **2017**, *18* (5), 1090.
- (27) Wang, J.; Li, S.; Chen, T.; Xian, W.; Zhang, H.; Wu, L.; Zhu, W.; Zeng, Q. Nanoscale cationic micelles of amphiphilic copolymers based on star-shaped PLGA and PEI cross-linked PEG for protein delivery application. *Journal of Materials Science: Materials in Medicine* **2019**, *30* (8), 93.
- (28) Tiyaboonchai, W.; Rodleang, I.; Ounaron, A. Mucoadhesive polyethylenimine–dextran sulfate nanoparticles containing Punica granatum peel extract as a novel sustained-release antimicrobial. *Pharmaceutical Development and Technology* **2015**, *20* (4), 426.
- (29) Cho, H.-J.; Han, S.-E.; Im, S.; Lee, Y.; Kim, Y. B.; Chun, T.; Oh, Y.-K. Maltosylated polyethylenimine-based triple nanocomplexes of human papillomavirus 16L1 protein and DNA as a vaccine co-delivery system. *Biomaterials* **2011**, *32* (20), 4621.
- (30) Virgen-Ortíz, J. J.; dos Santos, J. C. S.; Berenguer-Murcia, Á.; Barbosa, O.; Rodrigues, R. C.; Fernandez-Lafuente, R. Polyethylenimine: a very useful ionic polymer in the design of immobilized enzyme biocatalysts. *Journal of Materials Chemistry B* **2017**, *5* (36), 7461.

- (31) Shima, S.; Sakai, H. Polylysine produced by *Streptomyces*. *Agricultural and Biological Chemistry* **1977**, *41* (9), 1807.
- (32) Li, C.; Liu, F.; Gong, Y.; Wang, Y.; Xu, H.; Yuan, F.; Gao, Y. Investigation into the Maillard reaction between ϵ -polylysine and dextran in subcritical water and evaluation of the functional properties of the conjugates. *LWT - Food Science and Technology* **2014**, *57* (2), 612.
- (33) Wu, Q.-X.; Wang, Z.-D.; Zheng, M.-F.; Su, T.; Wang, X.-H.; Guan, Y.-X.; Chen, Y. Development of metformin hydrochloride loaded dissolving tablets with novel carboxymethylcellulose/poly-L-lysine/TPP complex. *International Journal of Biological Macromolecules* **2020**, *155*, 411.
- (34) Chen, S.; Huang, S.; Li, Y.; Zhou, C. Recent advances in epsilon-poly-L-lysine and L-lysine-based dendrimer synthesis, modification, and biomedical applications. *Frontiers in Chemistry* **2021**, *9*, 659304.
- (35) Wang, L.; Zhang, C.; Zhang, J.; Rao, Z.; Xu, X.; Mao, Z.; Chen, X. Epsilon-poly-L-lysine: recent advances in biomanufacturing and applications. *Frontiers in Bioengineering and Biotechnology* **2021**, *9*, 748976.
- (36) Manna, S.; Seth, A.; Gupta, P.; Nandi, G.; Dutta, R.; Jana, S.; Jana, S. Chitosan Derivatives as Carriers for Drug Delivery and Biomedical Applications. *ACS Biomaterials Science & Engineering* **2023**, *9* (5), 2181.
- (37) Sahariah, P.; Másson, M. Antimicrobial Chitosan and Chitosan Derivatives: A Review of the Structure–Activity Relationship. *Biomacromolecules* **2017**, *18* (11), 3846.
- (38) Inta, O.; Yoksan, R.; Limtrakul, J. Hydrophobically modified chitosan: A bio-based material for antimicrobial active film. *Materials Science and Engineering: C* **2014**, *42*, 569.
- (39) Ong, S.-Y.; Wu, J.; Moochhala, S. M.; Tan, M.-H.; Lu, J. Development of a chitosan-based wound dressing with improved hemostatic and antimicrobial properties. *Biomaterials* **2008**, *29* (32), 4323.
- (40) Stawski, D.; Sahariah, P.; Hjálmarsdóttir, M.; Wojciechowska, D.; Puchalski, M.; Másson, M. N, N, N-trimethyl chitosan as an efficient antibacterial agent for polypropylene and polylactide nonwovens. *The Journal of The Textile Institute* **2017**, *108* (6), 1041.
- (41) Chen, Z.; Yao, J.; Zhao, J.; Wang, S. Injectable wound dressing based on carboxymethyl chitosan triple-network hydrogel for effective wound antibacterial and hemostasis. *International Journal of Biological Macromolecules* **2023**, *225*, 1235.
- (42) Ji, Q. X.; Lü, R.; Zhang, W. Q.; Deng, J.; Chen, X. G. In vitro evaluation of the biomedical properties of chitosan and quaternized chitosan for dental applications. *Carbohydrate research* **2009**, *344* (11), 1297.
- (43) Fakhri, E.; Eslami, H.; Maroufi, P.; Pakdel, F.; Taghizadeh, S.; Ganbarov, K.; Yousefi, M.; Tanomand, A.; Yousefi, B.; Mahmoudi, S. et al. Chitosan biomaterials application in dentistry. *International Journal of Biological Macromolecules* **2020**, *162*, 956.
- (44) Mukherjee, M. D.; Solanki, P. R.; Sumana, G.; Manaka, T.; Iwamoto, M.; Malhotra, B. D. Thiol modified chitosan self-assembled monolayer platform for nucleic acid biosensor. *Applied biochemistry and biotechnology* **2014**, *174*, 1201.
- (45) Feng, B.; Hong, R. Y.; Wu, Y. J.; Liu, G. H.; Zhong, L. H.; Zheng, Y.; Ding, J. M.; Wei, D. G. Synthesis of monodisperse magnetite nanoparticles via chitosan–poly(acrylic acid) template and their application in MRI. *Journal of Alloys and Compounds* **2009**, *473* (1), 356.

- (46) Yeh, T.-H.; Hsu, L.-W.; Tseng, M. T.; Lee, P.-L.; Sonjae, K.; Ho, Y.-C.; Sung, H.-W. Mechanism and consequence of chitosan-mediated reversible epithelial tight junction opening. *Biomaterials* **2011**, *32* (26), 6164.
- (47) Smith, J.; Wood, E.; Dornish, M. Effect of chitosan on epithelial cell tight junctions. *Pharmaceutical research* **2004**, *21*, 43.
- (48) Chatelet, C.; Damour, O.; Domard, A. Influence of the degree of acetylation on some biological properties of chitosan films. *Biomaterials* **2001**, *22* (3), 261.
- (49) M. Ways, T. M.; Lau, W. M.; Khutoryanskiy, V. V. Chitosan and its derivatives for application in mucoadhesive drug delivery systems. *Polymers* **2018**, *10* (3), 267.
- (50) Abilova, G. K.; Kaldybekov, D. B.; Irmukhametova, G. S.; Kazybayeva, D. S.; Iskakbayeva, Z. A.; Kudaibergenov, S. E.; Khutoryanskiy, V. V. Chitosan/poly (2-ethyl-2-oxazoline) films with ciprofloxacin for application in vaginal drug delivery. *Materials* **2020**, *13* (7), 1709.
- (51) Sogias, I. A.; Williams, A. C.; Khutoryanskiy, V. V. Chitosan-based mucoadhesive tablets for oral delivery of ibuprofen. *International journal of pharmaceutics* **2012**, *436* (1-2), 602.
- (52) Kwak, S.-Y.; Lew, T. T. S.; Sweeney, C. J.; Koman, V. B.; Wong, M. H.; Bohmert-Tatarev, K.; Snell, K. D.; Seo, J. S.; Chua, N.-H.; Strano, M. S. Chloroplast-selective gene delivery and expression in planta using chitosan-complexed single-walled carbon nanotube carriers. *Nature nanotechnology* **2019**, *14* (5), 447.
- (53) Apryatina, K.; Koryagin, A.; Smirnova, O.; Smirnova, L. Hemostatic compositions based on chitosan complexes with calcium ions. *Pharmaceutical chemistry journal* **2021**, *54*, 1269.
- (54) Linh, P.; Chien, N.; Dung, D.; Nam, P.; Hoa, D.; Anh, N.; Hong, L.; Phuc, N.; Phong, P. Biocompatible nanoclusters of O-carboxymethyl chitosan-coated Fe₃O₄ nanoparticles: synthesis, characterization and magnetic heating efficiency. *Journal of materials science* **2018**, *53*, 8887.
- (55) Tao, F.; Cheng, Y.; Shi, X.; Zheng, H.; Du, Y.; Xiang, W.; Deng, H. Applications of chitin and chitosan nanofibers in bone regenerative engineering. *Carbohydrate polymers* **2020**, *230*, 115658.
- (56) LogithKumar, R.; KeshavNarayan, A.; Dhivya, S.; Chawla, A.; Saravanan, S.; Selvamurugan, N. A review of chitosan and its derivatives in bone tissue engineering. *Carbohydrate polymers* **2016**, *151*, 172.
- (57) Arkaban, H.; Barani, M.; Akbarizadeh, M. R.; Pal Singh Chauhan, N.; Jadoun, S.; Dehghani Soltani, M.; Zarrintaj, P. Polyacrylic Acid Nanoplatfoms: Antimicrobial, Tissue Engineering, and Cancer Theranostic Applications. *Polymers* **2022**, *14* (6), 1259.
- (58) Deng, X.; Gould, M.; Ali, M. A. A review of current advancements for wound healing: Biomaterial applications and medical devices. *Journal of Biomedical Materials Research Part B: Applied Biomaterials* **2022**, *110* (11), 2542.
- (59) Melinda Molnar, R.; Bodnar, M.; Hartmann, J. F.; Borbely, J. Preparation and characterization of poly(acrylic acid)-based nanoparticles. *Colloid and Polymer Science* **2009**, *287* (6), 739.
- (60) Liu, L.; Yao, W.; Rao, Y.; Lu, X.; Gao, J. pH-Responsive carriers for oral drug delivery: challenges and opportunities of current platforms. *Drug Delivery* **2017**, *24* (1), 569.
- (61) de la Torre, P. M.; Torrado, G.; Torrado, S. Poly (acrylic acid) chitosan interpolymer complexes for stomach controlled antibiotic delivery. *Journal of Biomedical Materials Research Part B: Applied Biomaterials: An Official Journal of The Society for Biomaterials, The Japanese Society for Biomaterials, and The Australian Society for Biomaterials and the Korean Society for Biomaterials* **2005**, *72* (1), 191.

- (62) Gratzl, G.; Paulik, C.; Hild, S.; Guggenbichler, J. P.; Lackner, M. Antimicrobial activity of poly (acrylic acid) block copolymers. *Materials Science and Engineering: C* **2014**, *38*, 94.
- (63) Ghaffari-Bohlouli, P.; Zahedi, P.; Shahrousvand, M. Enhanced osteogenesis using poly (l-lactide-co-d, l-lactide)/poly (acrylic acid) nanofibrous scaffolds in presence of dexamethasone-loaded molecularly imprinted polymer nanoparticles. *International journal of biological macromolecules* **2020**, *165*, 2363.
- (64) Cheng, Y.; Hu, Y.; Xu, M.; Qin, M.; Lan, W.; Huang, D.; Wei, Y.; Chen, W. High strength polyvinyl alcohol/polyacrylic acid (PVA/PAA) hydrogel fabricated by Cold-Drawn method for cartilage tissue substitutes. *Journal of Biomaterials Science, Polymer Edition* **2020**, *31* (14), 1836.
- (65) Li, X.; Wang, Z.; Li, W.; Sun, J. Superstrong water-based supramolecular adhesives derived from poly (vinyl alcohol)/poly (acrylic acid) complexes. *ACS Materials Letters* **2021**, *3* (6), 875.
- (66) Xiong, L.; Yang, T.; Yang, Y.; Xu, C.; Li, F. Long-term in vivo biodistribution imaging and toxicity of polyacrylic acid-coated upconversion nanophosphors. *Biomaterials* **2010**, *31* (27), 7078.
- (67) Swilem, A. E.; Elshazly, A. H. M.; Hamed, A. A.; Hegazy, E.-S. A.; Abd El-Rehim, H. A. Nanoscale poly(acrylic acid)-based hydrogels prepared via a green single-step approach for application as low-viscosity biomimetic fluid tears. *Materials Science and Engineering: C* **2020**, *110*, 110726.
- (68) Akkhat, P.; Mekboonsonglarp, W.; Kiatkamjornwong, S.; Hoven, V. P. Surface-grafted poly (acrylic acid) brushes as a precursor layer for biosensing applications: Effect of graft density and swellability on the detection efficiency. *Langmuir* **2012**, *28* (11), 5302.
- (69) Chen, Y.; Nan, J.; Lu, Y.; Wang, C.; Chu, F.; Gu, Z. Hybrid Fe₃O₄-poly (acrylic acid) nanogels for theranostic cancer treatment. *Journal of biomedical nanotechnology* **2015**, *11* (5), 771.
- (70) Lepage, L.; Dufour, A.-C.; Doiron, J.; Handfield, K.; Desforges, K.; Bell, R.; Vallee, M.; Savoie, M.; Perreault, S.; Laurin, L.-P. Randomized clinical trial of sodium polystyrene sulfonate for the treatment of mild hyperkalemia in CKD. *Clinical journal of the American Society of Nephrology: CJASN* **2015**, *10* (12), 2136.
- (71) Yan, Y.; Kolachala, V.; Dalmasso, G.; Nguyen, H.; Laroui, H.; Sitaraman, S. V.; Merlin, D. Temporal and spatial analysis of clinical and molecular parameters in dextran sodium sulfate induced colitis. *PloS one* **2009**, *4* (6), e6073.
- (72) Lee, K. Y.; Mooney, D. J. Alginate: properties and biomedical applications. *Prog Polym Sci* **2012**, *37* (1), 106.
- (73) Cook, M. T.; Tzortzis, G.; Charalampopoulos, D.; Khutoryanskiy, V. V. Production and Evaluation of Dry Alginate-Chitosan Microcapsules as an Enteric Delivery Vehicle for Probiotic Bacteria. *Biomacromolecules* **2011**, *12* (7), 2834.
- (74) Saraiva, M. M.; Campelo, M. d. S.; Camara Neto, J. F.; Lima, A. B. N.; Silva, G. d. A.; Dias, A. T. d. F. F.; Ricardo, N. M. P. S.; Kaplan, D. L.; Ribeiro, M. E. N. P. Alginate/polyvinyl alcohol films for wound healing: Advantages and challenges. *Journal of Biomedical Materials Research Part B: Applied Biomaterials* **2023**, *111* (1), 220.
- (75) Catanzano, O.; D'Esposito, V.; Acierno, S.; Ambrosio, M. R.; De Caro, C.; Avagliano, C.; Russo, P.; Russo, R.; Miro, A.; Ungaro, F. et al. Alginate-hyaluronan composite hydrogels accelerate wound healing process. *Carbohydrate Polymers* **2015**, *131*, 407.

- (76) Sun, W.; Yang, J.; Zhu, J.; Zhou, Y.; Li, J.; Zhu, X.; Shen, M.; Zhang, G.; Shi, X. Immobilization of iron oxide nanoparticles within alginate nanogels for enhanced MR imaging applications. *Biomaterials Science* **2016**, *4* (10), 1422.
- (77) Leonard, M.; De Boissesson, M. R.; Hubert, P.; Dalencon, F.; Dellacherie, E. Hydrophobically modified alginate hydrogels as protein carriers with specific controlled release properties. *Journal of controlled release* **2004**, *98* (3), 395.
- (78) Gombotz, W. R.; Wee, S. F. Protein release from alginate matrices. *Advanced drug delivery reviews* **2012**, *64*, 194.
- (79) Rowley, J. A.; Madlambayan, G.; Mooney, D. J. Alginate hydrogels as synthetic extracellular matrix materials. *Biomaterials* **1999**, *20* (1), 45.
- (80) Park, D.-J.; Choi, B.-H.; Zhu, S.-J.; Huh, J.-Y.; Kim, B.-Y.; Lee, S.-H. Injectable bone using chitosan-alginate gel/mesenchymal stem cells/BMP-2 composites. *Journal of Cranio-Maxillofacial Surgery* **2005**, *33* (1), 50.
- (81) Lin, H. R.; Yeh, Y. J. Porous alginate/hydroxyapatite composite scaffolds for bone tissue engineering: preparation, characterization, and in vitro studies. *Journal of Biomedical Materials Research Part B: Applied Biomaterials: An Official Journal of The Society for Biomaterials, The Japanese Society for Biomaterials, and The Australian Society for Biomaterials and the Korean Society for Biomaterials* **2004**, *71* (1), 52.
- (82) Rahman, M. S.; Hasan, M. S.; Nitai, A. S.; Nam, S.; Karmakar, A. K.; Ahsan, M. S.; Shiddiky, M. J. A.; Ahmed, M. B. Recent Developments of Carboxymethyl Cellulose. *Polymers* **2021**, *13* (8), 1345.
- (83) Maver, U.; Khanari, K.; Žižek, M.; Gradišnik, L.; Repnik, K.; Potočnik, U.; Finšgar, M. Carboxymethyl cellulose/diclofenac bioactive coatings on AISI 316LVM for controlled drug delivery, and improved osteogenic potential. *Carbohydrate polymers* **2020**, *230*, 115612.
- (84) Sadeghi, S.; Nourmohammadi, J.; Ghaee, A.; Soleimani, N. Carboxymethyl cellulose-human hair keratin hydrogel with controlled clindamycin release as antibacterial wound dressing. *International Journal of Biological Macromolecules* **2020**, *147*, 1239.
- (85) Verma, N.; Pramanik, K.; Singh, A. K.; Biswas, A. Design of magnesium oxide nanoparticle incorporated carboxy methyl cellulose/poly vinyl alcohol composite film with novel composition for skin tissue engineering. *Materials Technology* **2022**, *37* (8), 706.
- (86) Sharmila, G.; Muthukumar, C.; Kirthika, S.; Keerthana, S.; Kumar, N. M.; Jeyanthi, J. Fabrication and characterization of Spinacia oleracea extract incorporated alginate/carboxymethyl cellulose microporous scaffold for bone tissue engineering. *International journal of biological macromolecules* **2020**, *156*, 430.
- (87) Schmidts, T.; Dobler, D.; Schlupp, P.; Nissing, C.; Garn, H.; Runkel, F. Development of multiple W/O/W emulsions as dermal carrier system for oligonucleotides: Effect of additives on emulsion stability. *International Journal of Pharmaceutics* **2010**, *398* (1-2), 107.
- (88) Fu, J.; Pang, Z.; Yang, J.; Huang, F.; Cai, Y.; Wei, Q. Fabrication of polyaniline/carboxymethyl cellulose/cellulose nanofibrous mats and their biosensing application. *Applied Surface Science* **2015**, *349*, 35.
- (89) Habib, A.; Sathish, V.; Mallik, S.; Khoda, B. 3D printability of alginate-carboxymethyl cellulose hydrogel. *Materials* **2018**, *11* (3), 454.
- (90) Eskandarinia, A.; Kefayat, A.; Gharakhloo, M.; Agheb, M.; Khodabakhshi, D.; Khorshidi, M.; Sheikmoradi, V.; Rafienia, M.; Salehi, H. A propolis enriched polyurethane-hyaluronic acid nanofibrous wound dressing with remarkable antibacterial and wound healing activities. *International Journal of Biological Macromolecules* **2020**, *149*, 467.

- (91) Kratz, F. Albumin as a drug carrier: Design of prodrugs, drug conjugates and nanoparticles. *Journal of Controlled Release* **2008**, *132* (3), 171.
- (92) Dosio, F.; Brusa, P.; Crosasso, P.; Arpicco, S.; Cattel, L. Preparation, characterization and properties in vitro and in vivo of a paclitaxel–albumin conjugate. *Journal of controlled release* **1997**, *47* (3), 293.
- (93) Jiang, Y.; Stenzel, M. Drug delivery vehicles based on albumin–polymer conjugates. *Macromolecular bioscience* **2016**, *16* (6), 791.
- (94) Xu, L.; He, X.-Y.; Liu, B.-Y.; Xu, C.; Ai, S.-L.; Zhuo, R.-X.; Cheng, S.-X. Aptamer-functionalized albumin-based nanoparticles for targeted drug delivery. *Colloids and Surfaces B: Biointerfaces* **2018**, *171*, 24.
- (95) Fujita, T.; Nishikawa, M.; Ohtsubo, Y.; Ohno, J.; Takakura, Y.; Sezaki, H.; Hashida, M. Control of in vivo fate of albumin derivatives utilizing combined chemical modification. *Journal of Drug Targeting* **1994**, *2* (2), 157.
- (96) Sleep, D. Albumin and its application in drug delivery. *Expert opinion on drug delivery* **2015**, *12* (5), 793.
- (97) Mendez, C. M.; McClain, C. J.; Marsano, L. S. Albumin Therapy in Clinical Practice. *Nutrition in Clinical Practice* **2005**, *20* (3), 314.
- (98) Ahmady, A.; Samah, N. H. A. A review: Gelatine as a bioadhesive material for medical and pharmaceutical applications. *International Journal of Pharmaceutics* **2021**, *608*, 121037.
- (99) Madkhali, O.; Mekhail, G.; Wettig, S. D. Modified gelatin nanoparticles for gene delivery. *International Journal of Pharmaceutics* **2019**, *554*, 224.
- (100) Zhu, J.; Zhou, X.; Kim, H. J.; Qu, M.; Jiang, X.; Lee, K.; Ren, L.; Wu, Q.; Wang, C.; Zhu, X. Gelatin methacryloyl microneedle patches for minimally invasive extraction of skin interstitial fluid. *Small* **2020**, *16* (16), 1905910.
- (101) Aldana, A. A.; Abraham, G. A. Current advances in electrospun gelatin-based scaffolds for tissue engineering applications. *International journal of pharmaceutics* **2017**, *523* (2), 441.
- (102) Zhang, N.; Liu, H.; Yu, L.; Liu, X.; Zhang, L.; Chen, L.; Shanks, R. Developing gelatin–starch blends for use as capsule materials. *Carbohydrate polymers* **2013**, *92* (1), 455.
- (103) Penczek, S.; Cypryk, M.; Duda, A.; Kubisa, P.; Słomkowski, S. Living ring-opening polymerizations of heterocyclic monomers. *Progress in Polymer Science* **2007**, *32* (2), 247.
- (104) Tong, J.; Luxenhofer, R.; Yi, X.; Jordan, R.; Kabanov, A. V. Protein Modification with Amphiphilic Block Copoly(2-oxazoline)s as a New Platform for Enhanced Cellular Delivery. *Molecular Pharmaceutics* **2010**, *7* (4), 984.
- (105) Hwang, D.; Ramsey, J. D.; Makita, N.; Sachse, C.; Jordan, R.; Sokolsky-Papkov, M.; Kabanov, A. V. Novel poly(2-oxazoline) block copolymer with aromatic heterocyclic side chains as a drug delivery platform. *Journal of Controlled Release* **2019**, *307*, 261.
- (106) Claeys, B.; Vervaeck, A.; Vervaet, C.; Remon, J. P.; Hoogenboom, R.; De Geest, B. G. Poly(2-ethyl-2-oxazoline) as Matrix Excipient for Drug Formulation by Hot Melt Extrusion and Injection Molding. *Macromolecular Rapid Communications* **2012**, *33* (19), 1701.
- (107) Gaspar, V. M.; Gonçalves, C.; de Melo-Diogo, D.; Costa, E. C.; Queiroz, J. A.; Pichon, C.; Sousa, F.; Correia, I. J. Poly(2-ethyl-2-oxazoline)–PLA-g–PEI amphiphilic triblock micelles for co-delivery of minicircle DNA and chemotherapeutics. *Journal of Controlled Release* **2014**, *189*, 90.
- (108) Waschinski, C. J.; Tiller, J. C. Poly (oxazoline) s with telechelic antimicrobial functions. *Biomacromolecules* **2005**, *6* (1), 235.

- (109) Kaberov, L. I.; Verbraeken, B.; Riabtseva, A.; Brus, J.; Radulescu, A.; Talmon, Y.; Stepanek, P.; Hoogenboom, R.; Filippov, S. K. Fluorophilic–Lipophilic–Hydrophilic Poly(2-oxazoline) Block Copolymers as MRI Contrast Agents: From Synthesis to Self-Assembly. *Macromolecules* **2018**, *51* (15), 6047.
- (110) You, Y.; Kobayashi, K.; Colak, B.; Luo, P.; Cozens, E.; Fields, L.; Suzuki, K.; Gautrot, J. Engineered cell-degradable poly(2-alkyl-2-oxazoline) hydrogel for epicardial placement of mesenchymal stem cells for myocardial repair. *Biomaterials* **2021**, *269*, 120356.
- (111) Luxenhofer, R.; Schulz, A.; Roques, C.; Li, S.; Bronich, T. K.; Batrakova, E. V.; Jordan, R.; Kabanov, A. V. Doubly amphiphilic poly(2-oxazoline)s as high-capacity delivery systems for hydrophobic drugs. *Biomaterials* **2010**, *31* (18), 4972.
- (112) Salgarella, A. R.; Zahoranová, A.; Šrámková, P.; Majerčíková, M.; Pavlova, E.; Luxenhofer, R.; Kronek, J.; Lacík, I.; Ricotti, L. Investigation of drug release modulation from poly(2-oxazoline) micelles through ultrasound. *Scientific Reports* **2018**, *8* (1), 9893.
- (113) Baker, M. I.; Walsh, S. P.; Schwartz, Z.; Boyan, B. D. A review of polyvinyl alcohol and its uses in cartilage and orthopedic applications. *Journal of Biomedical Materials Research Part B: Applied Biomaterials* **2012**, *100B* (5), 1451.
- (114) Kayal, S.; Ramanujan, R. Doxorubicin loaded PVA coated iron oxide nanoparticles for targeted drug delivery. *Materials Science and Engineering: C* **2010**, *30* (3), 484.
- (115) Musgrave, C. S. A.; Fang, F. Contact lens materials: a materials science perspective. *Materials* **2019**, *12* (2), 261.
- (116) Kumar, A.; Han, S. S. PVA-based hydrogels for tissue engineering: A review. *International journal of polymeric materials and polymeric biomaterials* **2017**, *66* (4), 159.
- (117) Lang, R. A.; Grüntzig, P. M.; Weisgerber, C.; Weis, C.; Odermatt, E. K.; Kirschner, M. H. Polyvinyl alcohol gel prevents abdominal adhesion formation in a rabbit model. *Fertility and Sterility* **2007**, *88* (4, Supplement), 1180.
- (118) Kobayashi, M.; Chang, Y.-S.; Oka, M. A two year in vivo study of polyvinyl alcohol-hydrogel (PVA-H) artificial meniscus. *Biomaterials* **2005**, *26* (16), 3243.
- (119) Das, R.; Champaneria, R.; Daniels, J. P.; Belli, A.-M. Comparison of embolic agents used in uterine artery embolisation: a systematic review and meta-analysis. *Cardiovascular and interventional radiology* **2014**, *37*, 1179.
- (120) Herzberger, J.; Niederer, K.; Pohlit, H.; Seiwert, J.; Worm, M.; Wurm, F. R.; Frey, H. Polymerization of Ethylene Oxide, Propylene Oxide, and Other Alkylene Oxides: Synthesis, Novel Polymer Architectures, and Bioconjugation. *Chemical Reviews* **2016**, *116* (4), 2170.
- (121) Grossen, P.; Witzigmann, D.; Sieber, S.; Huwyler, J. PEG-PCL-based nanomedicines: A biodegradable drug delivery system and its application. *Journal of Controlled Release* **2017**, *260*, 46.
- (122) Wang, R.; Xiao, R.; Zeng, Z.; Xu, L.; Wang, J. Application of poly(ethylene glycol)–distearoylphosphatidylethanolamine (PEG-DSPE) block copolymers and their derivatives as nanomaterials in drug delivery. *International Journal of Nanomedicine* **2012**, *7* (null), 4185.
- (123) Pasut, G.; Veronese, F. M. PEG conjugates in clinical development or use as anticancer agents: an overview. *Advanced drug delivery reviews* **2009**, *61* (13), 1177.
- (124) Wang, Z.; Ye, Q.; Yu, S.; Akhavan, B. Poly Ethylene Glycol (PEG)-Based Hydrogels for Drug Delivery in Cancer Therapy: A Comprehensive Review. *Advanced Healthcare Materials* **2023**, *12* (18), 2300105.
- (125) Pacheco, C.; Baião, A.; Ding, T.; Cui, W.; Sarmiento, B. Recent advances in long-acting drug delivery systems for anticancer drug. *Advanced Drug Delivery Reviews* **2023**, *194*, 114724.

- (126) Abuchowski, A.; Kazo, G.; Verhoest Jr, C.; Van Es, T.; Kafkewitz, D.; Nucci, M.; Viau, A.; Davis, F. F. Cancer therapy with chemically modified enzymes. I. Antitumor properties of polyethylene glycol-asparaginase conjugates. *Cancer biochemistry biophysics* **1984**, *7* (2), 175.
- (127) Herman, S.; Hoofman, G.; Schacht, E. Poly (ethylene glycol) with reactive endgroups: I. Modification of proteins. *Journal of bioactive and compatible polymers* **1995**, *10* (2), 145.
- (128) Huang, P.; Lin, J.; Li, W.; Rong, P.; Wang, Z.; Wang, S.; Wang, X.; Sun, X.; Aronova, M.; Niu, G. Biodegradable gold nanovesicles with an ultrastrong plasmonic coupling effect for photoacoustic imaging and photothermal therapy. *Angewandte Chemie* **2013**, *125* (52), 14208.
- (129) Endres, T.; Zheng, M.; Kılıç, A. e.; Turowska, A.; Beck-Broichsitter, M.; Renz, H.; Merkel, O. M.; Kissel, T. Amphiphilic biodegradable PEG-PCL-PEI triblock copolymers for FRET-capable in vitro and in vivo delivery of siRNA and quantum dots. *Molecular pharmaceutics* **2014**, *11* (4), 1273.
- (130) Gould, S. T.; Matherly, E. E.; Smith, J. N.; Heistad, D. D.; Anseth, K. S. The role of valvular endothelial cell paracrine signaling and matrix elasticity on valvular interstitial cell activation. *Biomaterials* **2014**, *35* (11), 3596.
- (131) Frith, J. E.; Menzies, D. J.; Cameron, A. R.; Ghosh, P.; Whitehead, D. L.; Gronthos, S.; Zannettino, A. C.; Cooper-White, J. J. Effects of bound versus soluble pentosan polysulphate in PEG/HA-based hydrogels tailored for intervertebral disc regeneration. *Biomaterials* **2014**, *35* (4), 1150.
- (132) Hoffman, M. D.; Van Hove, A. H.; Benoit, D. S. W. Degradable hydrogels for spatiotemporal control of mesenchymal stem cells localized at decellularized bone allografts. *Acta Biomaterialia* **2014**, *10* (8), 3431.
- (133) Haaf, F.; Sanner, A.; Straub, F. Polymers of N-vinylpyrrolidone: synthesis, characterization and uses. *Polymer Journal* **1985**, *17* (1), 143.
- (134) Kornblum, S. S.; Stoopak, S. B. A New Tablet Disintegrating Agent: Cross-Linked Polyvinylpyrrolidone. *Journal of Pharmaceutical Sciences* **1973**, *62* (1), 43.
- (135) Yang, M.; Xie, S.; Li, Q.; Wang, Y.; Chang, X.; Shan, L.; Sun, L.; Huang, X.; Gao, C. Effects of polyvinylpyrrolidone both as a binder and pore-former on the release of sparingly water-soluble topiramate from ethylcellulose coated pellets. *International Journal of Pharmaceutics* **2014**, *465* (1), 187.
- (136) Luo, Y.; Hong, Y.; Shen, L.; Wu, F.; Lin, X. Multifunctional Role of Polyvinylpyrrolidone in Pharmaceutical Formulations. *AAPS PharmSciTech* **2021**, *22* (1), 34.
- (137) Kodaira, H.; Tsutsumi, Y.; Yoshioka, Y.; Kamada, H.; Kaneda, Y.; Yamamoto, Y.; Tsunoda, S.-i.; Okamoto, T.; Mukai, Y.; Shibata, H. et al. The targeting of anionized polyvinylpyrrolidone to the renal system. *Biomaterials* **2004**, *25* (18), 4309.
- (138) Choubar, E. G.; Nasirtabrizi, M. H.; Salimi, F.; Sohrabi-gilani, N.; Sadeghianamryan, A. Fabrication and in vitro characterization of novel co-electrospun polycaprolactone/collagen/polyvinylpyrrolidone nanofibrous scaffolds for bone tissue engineering applications. *Journal of Materials Research* **2022**, *37* (23), 4140.
- (139) D'Souza, A. J. M.; Schowen, R. L.; Topp, E. M. Erratum to "Polyvinylpyrrolidone–drug conjugate: synthesis and release mechanism" [Journal of Controlled Release 94 (2004) 91–100]. *Journal of Controlled Release* **2004**, *97* (2), 385.
- (140) Bowry, S. K.; Ronco, C. Surface Topography and Surface Elemental Composition Analysis of Helixone®, a New High-Flux Polysulfone Dialysis Membrane. *The International Journal of Artificial Organs* **2001**, *24* (11), 757.

- (141) Doustdar, F.; Ghorbani, M. ZIF-8 enriched electrospun ethyl cellulose/polyvinylpyrrolidone scaffolds: The key role of polyvinylpyrrolidone molecular weight. *Carbohydrate Polymers* **2022**, *291*, 119620.
- (142) Tundisi, L. L.; Mostaçõ, G. B.; Carricondo, P. C.; Petri, D. F. S. Hydroxypropyl methylcellulose: Physicochemical properties and ocular drug delivery formulations. *European Journal of Pharmaceutical Sciences* **2021**, *159*, 105736.
- (143) Dugar, R. P.; Dave, R. H. To study the effects of solvent and relative humidity on rheological and thermal properties of microcrystalline cellulose granules using hydroxypropyl methylcellulose as binder. *International Journal of Pharmaceutical Sciences and Research* **2014**, *5* (9), 3616.
- (144) Rujvipat, S.; Bodmeier, R. Modified release from hydroxypropyl methylcellulose compression-coated tablets. *International Journal of Pharmaceutics* **2010**, *402* (1), 72.
- (145) Ding, C.; Zhang, M.; Li, G. Preparation and characterization of collagen/hydroxypropyl methylcellulose (HPMC) blend film. *Carbohydrate Polymers* **2015**, *119*, 194.
- (146) Liu, D.; Wu, Q.; Chen, W.; Lin, H.; Zhu, Y.; Liu, Y.; Liang, H.; Zhu, F. A novel FK506 loaded nanomicelles consisting of amino-terminated poly(ethylene glycol)-block-poly(D,L)-lactic acid and hydroxypropyl methylcellulose for ocular drug delivery. *International Journal of Pharmaceutics* **2019**, *562*, 1.
- (147) Siepmann, J.; Peppas, N. A. Modeling of drug release from delivery systems based on hydroxypropyl methylcellulose (HPMC). *Advanced Drug Delivery Reviews* **2012**, *64*, 163.
- (148) Morrison, P. W.; Khutoryanskiy, V. V. Advances in ophthalmic drug delivery. *Therapeutic Delivery* **2014**, *5* (12), 1297.
- (149) Boateng, J.; Popescu, A. Composite bi-layered erodible films for potential ocular drug delivery. *Colloids and Surfaces B: Biointerfaces* **2016**, *145*, 353.
- (150) Silva, M. M.; Calado, R.; Marto, J.; Bettencourt, A.; Almeida, A. J.; Gonçalves, L. M. Chitosan nanoparticles as a mucoadhesive drug delivery system for ocular administration. *Marine drugs* **2017**, *15* (12), 370.
- (151) Hong, R.; Feng, B.; Chen, L.; Liu, G.; Li, H.; Zheng, Y.; Wei, D. Synthesis, characterization and MRI application of dextran-coated Fe₃O₄ magnetic nanoparticles. *Biochemical Engineering Journal* **2008**, *42* (3), 290.
- (152) Chen, F.; Huang, G.; Huang, H. Preparation and application of dextran and its derivatives as carriers. *International journal of biological macromolecules* **2020**, *145*, 827.
- (153) Chen, Z.; Krishnamachary, B.; Penet, M.-F.; Bhujwalla, Z. M. Acid-degradable dextran as an image guided siRNA carrier for COX-2 downregulation. *Theranostics* **2018**, *8* (1), 1.
- (154) Maia, J.; Evangelista, M. B.; Gil, H.; Ferreira, L. Dextran-based materials for biomedical applications. *Res Signpost* **2014**, *37661*, 31.
- (155) Alibolandi, M.; Alabdollah, F.; Sadeghi, F.; Mohammadi, M.; Abnous, K.; Ramezani, M.; Hadizadeh, F. Dextran-b-poly (lactide-co-glycolide) polymersome for oral delivery of insulin: In vitro and in vivo evaluation. *Journal of Controlled Release* **2016**, *227*, 58.
- (156) Fehlings, M. G.; Tator, C. H.; Linden, R. D. The effect of nimodipine and dextran on axonal function and blood flow following experimental spinal cord injury. *Journal of neurosurgery* **1989**, *71* (3), 403.
- (157) Lévesque, S. G.; Lim, R. M.; Shoichet, M. S. Macroporous interconnected dextran scaffolds of controlled porosity for tissue-engineering applications. *Biomaterials* **2005**, *26* (35), 7436.

- (158) Lavanya, D.; Kulkarni, P.; Dixit, M.; Raavi, P. K.; Krishna, L. N. V. Sources of cellulose and their applications—A review. *International Journal of Drug Formulation and Research* **2011**, *2* (6), 19.
- (159) Tanaka, A.; Furubayashi, T.; Tomisaki, M.; Kawakami, M.; Kimura, S.; Inoue, D.; Kusamori, K.; Katsumi, H.; Sakane, T.; Yamamoto, A. Nasal drug absorption from powder formulations: The effect of three types of hydroxypropyl cellulose (HPC). *European Journal of Pharmaceutical Sciences* **2017**, *96*, 284.
- (160) Desai, D.; Rinaldi, F.; Kothari, S.; Paruchuri, S.; Li, D.; Lai, M.; Fung, S.; Both, D. Effect of hydroxypropyl cellulose (HPC) on dissolution rate of hydrochlorothiazide tablets. *International Journal of Pharmaceutics* **2006**, *308* (1), 40.
- (161) Takeuchi, Y.; Umemura, K.; Tahara, K.; Takeuchi, H. Formulation design of hydroxypropyl cellulose films for use as orally disintegrating dosage forms. *Journal of Drug Delivery Science and Technology* **2018**, *46*, 93.
- (162) Sanders, J. C.; Breadmore, M. C.; Kwok, Y. C.; Horsman, K. M.; Landers, J. P. Hydroxypropyl cellulose as an adsorptive coating sieving matrix for DNA separations: artificial neural network optimization for microchip analysis. *Analytical chemistry* **2003**, *75* (4), 986.
- (163) Wach, R. A.; Mitomo, H.; Yoshii, F.; Kume, T. Hydrogel of Radiation-Induced Cross-Linked Hydroxypropylcellulose. *Macromolecular Materials and Engineering* **2002**, *287* (4), 285.
- (164) El-Newehy, M. H.; El-Naggar, M. E.; Alotaiby, S.; El-Hamshary, H.; Moydeen, M.; Al-Deyab, S. Green electrospinning of hydroxypropyl cellulose nanofibres for drug delivery applications. *Journal of nanoscience and nanotechnology* **2018**, *18* (2), 805.
- (165) Bielska, D.; Karczewska, A.; Kamiński, K.; Kiełkiewicz, I.; Lachowicz, T.; Szczubiałka, K.; Nowakowska, M. Self-organized thermo-responsive hydroxypropyl cellulose nanoparticles for curcumin delivery. *European Polymer Journal* **2013**, *49* (9), 2485.
- (166) Nasatto, P. L.; Pignon, F.; Silveira, J. L. M.; Duarte, M. E. R.; Nosedá, M. D.; Rinaudo, M. Methylcellulose, a Cellulose Derivative with Original Physical Properties and Extended Applications. *Polymers* **2015**, *7* (5), 777.
- (167) Wan, L. S.; Prasad, K. P. Effect of microcrystalline cellulose and cross-linked sodium carboxymethylcellulose on the properties of tablets with methylcellulose as a binder. *International journal of pharmaceutics* **1988**, *41* (1-2), 159.
- (168) Lin, C.-P.; BOEHNKE, M. Influences of methylcellulose on corneal epithelial wound healing. *Journal of Ocular Pharmacology and Therapeutics* **1999**, *15* (1), 59.
- (169) Freedman, V. H.; Shin, S.-i. Cellular tumorigenicity in nude mice: correlation with cell growth in semi-solid medium. *Cell* **1974**, *3* (4), 355.
- (170) Bonetti, L.; Caprioglio, A.; Bono, N.; Candiani, G.; Altomare, L. Mucoadhesive chitosan–methylcellulose oral patches for the treatment of local mouth bacterial infections. *Biomaterials Science* **2023**, *11* (8), 2699.
- (171) Noreen, A.; Zia, K. M.; Tabasum, S.; Khalid, S.; Shareef, R. A review on grafting of hydroxyethylcellulose for versatile applications. *International Journal of Biological Macromolecules* **2020**, *150*, 289.
- (172) Petrov, P.; Mokreva, P.; Kostov, I.; Uzunova, V.; Tzoneva, R. Novel electrically conducting 2-hydroxyethylcellulose/polyaniline nanocomposite cryogels: Synthesis and application in tissue engineering. *Carbohydrate Polymers* **2016**, *140*, 349.
- (173) Chang, C.; Zhang, L. Cellulose-based hydrogels: Present status and application prospects. *Carbohydrate polymers* **2011**, *84* (1), 40.

- (174) Chu, M.; Feng, N.; An, H.; You, G.; Mo, C.; Zhong, H.; Pan, L.; Hu, D. Design and validation of antibacterial and pH response of cationic guar gum film by combining hydroxyethyl cellulose and red cabbage pigment. *International Journal of Biological Macromolecules* **2020**, *162*, 1311.
- (175) Zulkifli, F. H.; Hussain, F. S. J.; Zeyohannes, S. S.; Rasad, M. S. B. A.; Yusuff, M. M. A facile synthesis method of hydroxyethyl cellulose-silver nanoparticle scaffolds for skin tissue engineering applications. *Materials Science and Engineering: C* **2017**, *79*, 151.
- (176) Chahal, S.; Hussain, F. S. J.; Kumar, A.; Rasad, M. S. B. A.; Yusoff, M. M. Fabrication, characterization and in vitro biocompatibility of electrospun hydroxyethyl cellulose/poly (vinyl) alcohol nanofibrous composite biomaterial for bone tissue engineering. *Chemical Engineering Science* **2016**, *144*, 17.
- (177) Huang, X.; Liu, H.; Shang, S.; Rao, X.; Song, J. Preparation and characterization of polymeric surfactants based on epoxidized soybean oil grafted hydroxyethyl cellulose. *Journal of agricultural and food chemistry* **2015**, *63* (41), 9062.
- (178) Hsieh, M.-F.; Van Cuong, N.; Chen, C.-H.; Chen, Y. T.; Yeh, J.-M. Nano-sized micelles of block copolymers of methoxy poly (ethylene glycol)-poly (ϵ -caprolactone)-graft-2-hydroxyethyl cellulose for doxorubicin delivery. *Journal of Nanoscience and Nanotechnology* **2008**, *8* (5), 2362.
- (179) Yang, R.; Shi, R.; Peng, S.; Zhou, D.; Liu, H.; Wang, Y. Cationized hydroxyethylcellulose as a novel, adsorbed coating for basic protein separation by capillary electrophoresis. *Electrophoresis* **2008**, *29* (7), 1460.
- (180) Peng, S.; Shi, R.; Yang, R.; Zhou, D.; Wang, Y. Hydroxyethylcellulose-graft-poly (N, N-dimethylacrylamide) copolymer as a multifunctional separation medium for CE. *Electrophoresis* **2008**, *29* (21), 4351.
- (181) Sogias, I. A.; Khutoryanskiy, V. V.; Williams, A. C. Exploring the Factors Affecting the Solubility of Chitosan in Water. *Macromolecular Chemistry and Physics* **2010**, *211* (4), 426.
- (182) Bütün, V.; Armes, S. P.; Billingham, N. C. Selective Quaternization of 2-(Dimethylamino)ethyl Methacrylate Residues in Tertiary Amine Methacrylate Diblock Copolymers. *Macromolecules* **2001**, *34* (5), 1148.
- (183) Zhang, R.; Tang, M.; Bowyer, A.; Eisenthal, R.; Hubble, J. A novel pH- and ionic-strength-sensitive carboxy methyl dextran hydrogel. *Biomaterials* **2005**, *26* (22), 4677.
- (184) Akar, E.; Altınışık, A.; Seki, Y. Preparation of pH- and ionic-strength responsive biodegradable fumaric acid crosslinked carboxymethyl cellulose. *Carbohydrate Polymers* **2012**, *90* (4), 1634.
- (185) Malamud, D.; Drysdale, J. W. Isoelectric points of proteins: a table. *Analytical biochemistry* **1978**, *86* (2), 620.
- (186) Fu, M.; Filippov, S. K.; Williams, A. C.; Khutoryanskiy, V. V. On the mucoadhesive properties of synthetic and natural polyampholytes. *Journal of Colloid and Interface Science* **2024**, *659*, 849.
- (187) Glass, J. E. Water-soluble polymers. *Kirk-Othmer Encyclopedia of Chemical Technology* **2000**.
- (188) Bekturov, E. A.; Khamzamalina, R. E. Solution Properties of Water-Soluble Nonionic Polymers. *Journal of Macromolecular Science-Reviews in Macromolecular Chemistry and Physics* **1987**, *27* (2), 253.
- (189) Ueberreiter, K. The solution process. *Diffusion in polymers* **1968**, 219.

- (190) Long, G. L.; Hill, J. W.; Petrucci, R. H. *General Chemistry: An Integrated Approach*; Prentice Hall, 1999.
- (191) Chatani, Y.; Tadokoro, H.; Saegusa, T.; Ikeda, H. Structural studies of poly (ethylenimine). 1. Structures of two hydrates of poly (ethylenimine): sesquihydrate and dihydrate. *Macromolecules* **1981**, *14* (2), 315.
- (192) Lin, P.; Clash, C.; Pearce, E. M.; Kwei, T.; Aponte, M. Solubility and miscibility of poly (ethyl oxazoline). *Journal of Polymer Science Part B: Polymer Physics* **1988**, *26* (3), 603.
- (193) Manouras, T.; Koufakis, E.; Anastasiadis, S. H.; Vamvakaki, M. A facile route towards PDMAEMA homopolymer amphiphiles. *Soft Matter* **2017**, *13* (20), 3777.
- (194) Zhao, J.; Burke, N. A. D.; Stöver, H. D. H. Preparation and study of multi-responsive polyampholyte copolymers of N-(3-aminopropyl)methacrylamide hydrochloride and acrylic acid. *RSC Advances* **2016**, *6* (47), 41522.
- (195) Bansal, K.; Upadhyay, P.; Saraogi, G.; Rosling, A.; Rosenholm, J. Advances in thermo-responsive polymers exhibiting upper critical solution temperature (UCST). *eXPRESS Polymer Letters* **2019**, *13* (11).
- (196) Nasser, R.; Deutschman, C. P.; Han, L.; Pope, M. A.; Tam, K. C. Cellulose nanocrystals in smart and stimuli-responsive materials: a review. *Materials Today Advances* **2020**, *5*, 100055.
- (197) Yadav, S.; Shire, S. J.; Kalonia, D. S. Viscosity Analysis of High Concentration Bovine Serum Albumin Aqueous Solutions. *Pharmaceutical Research* **2011**, *28* (8), 1973.
- (198) Siepmann, J.; Siepmann, F. Mathematical modeling of drug dissolution. *International Journal of Pharmaceutics* **2013**, *453* (1), 12.
- (199) Kasaai, M. R. Calculation of Mark–Houwink–Sakurada (MHS) equation viscometric constants for chitosan in any solvent–temperature system using experimental reported viscometric constants data. *Carbohydrate Polymers* **2007**, *68* (3), 477.
- (200) Pawcenis, D.; Syrek, M.; Aksamit-Koperska, M. A.; Łojewski, T.; Łojewska, J. Mark–Houwink–Sakurada coefficients determination for molar mass of silk fibroin from viscometric results. SEC-MALLS approach. *RSC Advances* **2016**, *6* (44), 38071.
- (201) La Mesa, C. Polymer–surfactant and protein–surfactant interactions. *Journal of Colloid and Interface Science* **2005**, *286* (1), 148.
- (202) Mészáros, R.; Varga, I.; Gilányi, T. Effect of Polymer Molecular Weight on the Polymer/Surfactant Interaction. *The Journal of Physical Chemistry B* **2005**, *109* (28), 13538.
- (203) Holmberg, K.; Jönsson, B.; Kronberg, B.; Lindman, B. *Polymers in aqueous solution*. Wiley-Blackwell **2002**.
- (204) Kamenka, N.; Kaplun, A.; Talmon, Y.; Zana, R. Interactions between polysoaps and surfactants in aqueous solutions. *Langmuir* **1994**, *10* (9), 2960.
- (205) Chavanpatil, M. D.; Khair, A.; Patil, Y.; Handa, H.; Mao, G.; Panyam, J. Polymer-surfactant nanoparticles for sustained release of water-soluble drugs. *Journal of Pharmaceutical Sciences* **2007**, *96* (12), 3379.
- (206) Tsuchida, E.; Nishide, H., Berlin, Heidelberg, 1977; p 1.
- (207) Maier, A. S.; Thomas, C.; Kränzlein, M.; Pehl, T. M.; Rieger, B. Macromolecular Ruthenium–Ruthenium Complexes for Photocatalytic CO₂ Conversion: From Catalytic Lewis Pair Polymerization to Well-Defined Poly(vinyl bipyridine)–Metal Complexes. *Macromolecules* **2022**, *55* (16), 7039.
- (208) Nguyen, M. T.; Jones, R. A.; Holliday, B. J. Understanding the Effect of Metal Centers on Charge Transport and Delocalization in Conducting Metallopolymers. *Macromolecules* **2017**, *50* (3), 872.

- (209) Zhang, J.; Li, J.; Huo, M.; Li, N.; Zhou, J.; Li, T.; Jiang, J. Photochromic Inorganic/Organic Thermoplastic Elastomers. *Macromolecular Rapid Communications* **2017**, *38* (16), 1700210.
- (210) Barbosa, H. F. G.; Attjioui, M.; Ferreira, A. P. G.; Moerschbacher, B. M.; Cavalheiro, É. T. G. New series of metal complexes by amphiphilic biopolymeric Schiff bases from modified chitosans: Preparation, characterization and effect of molecular weight on its biological applications. *International Journal of Biological Macromolecules* **2020**, *145*, 417.
- (211) Callari, M.; Aldrich-Wright, J. R.; de Souza, P. L.; Stenzel, M. H. Polymers with platinum drugs and other macromolecular metal complexes for cancer treatment. *Progress in Polymer Science* **2014**, *39* (9), 1614.
- (212) Rivas, B. L.; Pereira, E. D.; Moreno-Villoslada, I. Water-soluble polymer–metal ion interactions. *Progress in Polymer Science* **2003**, *28* (2), 173.
- (213) Vetriselvi, V.; Jaya Santhi, R. Redox polymer as an adsorbent for the removal of chromium (VI) and lead (II) from the tannery effluents. *Water Resources and Industry* **2015**, *10*, 39.
- (214) Dzhardimalieva, G. I.; Uflyand, I. E. Design Strategies of Metal Complexes Based on Chelating Polymer Ligands and Their Application in Nanomaterials Science. *Journal of Inorganic and Organometallic Polymers and Materials* **2018**, *28* (4), 1305.
- (215) Rivas, B. L.; Geckeler, K. E. In *Polymer Synthesis Oxidation Processes*; Springer Berlin Heidelberg: Berlin, Heidelberg, 1992, DOI:10.1007/3-540-55090-9_6 10.1007/3-540-55090-9_6.
- (216) Guo, X.; Wang, C.-F.; Fang, Y.; Chen, L.; Chen, S. Fast synthesis of versatile nanocrystal-embedded hydrogels toward the sensing of heavy metal ions and organoamines. *Journal of Materials Chemistry* **2011**, *21* (4), 1124.
- (217) Joneja, S. K.; Harcum, W. W.; Skinner, G. W.; Barnum, P. E.; Guo, J.-H. Investigating the Fundamental Effects of Binders on Pharmaceutical Tablet Performance. *Drug Development and Industrial Pharmacy* **1999**, *25* (10), 1129.
- (218) Guo, J.-H.; Skinner, G. W.; Harcum, W. W.; Barnum, P. E. Pharmaceutical applications of naturally occurring water-soluble polymers. *Pharmaceutical Science & Technology Today* **1998**, *1* (6), 254.
- (219) Desai, P. M.; Liew, C. V.; Heng, P. W. S. Review of Disintegrants and the Disintegration Phenomena. *Journal of Pharmaceutical Sciences* **2016**, *105* (9), 2545.
- (220) Quodbach, J.; Kleinebudde, P. Performance of tablet disintegrants: impact of storage conditions and relative tablet density. *Pharmaceutical Development and Technology* **2015**, *20* (6), 762.
- (221) Bisharat, L.; AlKhatib, H. S.; Muhaisen, S.; Quodbach, J.; Blaibleh, A.; Cespi, M.; Berardi, A. The influence of ethanol on superdisintegrants and on tablets disintegration. *European Journal of Pharmaceutical Sciences* **2019**, *129*, 140.
- (222) Debotton, N.; Dahan, A. Applications of Polymers as Pharmaceutical Excipients in Solid Oral Dosage Forms. *Medicinal Research Reviews* **2017**, *37* (1), 52.
- (223) Pahwa, R.; Gupta, N. Superdisintegrants in the development of orally disintegrating tablets: a review. *International journal of pharmaceutical sciences and research* **2011**, *2* (11), 2767.
- (224) Strickley, R. G. Solubilizing excipients in oral and injectable formulations. *Pharmaceutical research* **2004**, *21*, 201.
- (225) Strickley, R. G.; Iwata, Q.; Wu, S.; Dahl, T. C. Pediatric drugs—a review of commercially available oral formulations. *Journal of Pharmaceutical Sciences* **2008**, *97* (5), 1731.

- (226) Cinca, R.; Chera, D.; Gruss, H.-J.; Halphen, M. Randomised clinical trial: macrogol/PEG 3350+electrolytes versus prucalopride in the treatment of chronic constipation - a comparison in a controlled environment. *Alimentary Pharmacology & Therapeutics* **2013**, *37* (9), 876.
- (227) Wiener, G.; Winkle, P.; McGowan, J. D.; Cleveland, M. v.; Di Palma, J. A. A Phase 2 evaluation of a new flavored peg and sulfate solution compared to an over-the-counter laxative, peg and sports drink bowel preparation combination. *BMC Gastroenterology* **2023**, *23* (1), 433.
- (228) McGraw, T. Safety of polyethylene glycol 3350 solution in chronic constipation: randomized, placebo-controlled trial. *Clinical and Experimental Gastroenterology* **2016**, *9* (null), 173.
- (229) Strickley, R. G. Pediatric Oral Formulations: An Updated Review of Commercially Available Pediatric Oral Formulations Since 2007. *Journal of Pharmaceutical Sciences* **2019**, *108* (4), 1335.
- (230) Tagami, T.; Nagata, N.; Hayashi, N.; Ogawa, E.; Fukushige, K.; Sakai, N.; Ozeki, T. Defined drug release from 3D-printed composite tablets consisting of drug-loaded polyvinylalcohol and a water-soluble or water-insoluble polymer filler. *International Journal of Pharmaceutics* **2018**, *543* (1), 361.
- (231) Rajabi-Siahboomi, A. R.; Bowtell, R. W.; Mansfield, P.; Davies, M. C.; Melia, C. D. Structure and Behavior in Hydrophilic Matrix Sustained Release Dosage Forms: 4. Studies of Water Mobility and Diffusion Coefficients in the Gel Layer of HPMC Tablets Using NMR Imaging. *Pharmaceutical Research* **1996**, *13* (3), 376.
- (232) Tiwari, S.; Rajabi-Siahboomi, A. Modulation of drug release from hydrophilic matrices. *Pharmaceutical Technology Europe* **2008**, *20* (9).
- (233) Tonglairoum, P.; Brannigan, R. P.; Opanasopit, P.; Khutoryanskiy, V. V. Maleimide-bearing nanogels as novel mucoadhesive materials for drug delivery. *Journal of Materials Chemistry B* **2016**, *4* (40), 6581.
- (234) Ishwar Chauhan, S. R. K. N.; Publication, U. S. P. A., Ed. United States, 2009, DOI:<https://patents.google.com/patent/US20090280173A1/en>.
- (235) Cilurzo, F.; Gennari, C. G. M.; Selmin, F.; Epstein, J. B.; Gaeta, G. M.; Colella, G.; Minghetti, P. A new mucoadhesive dosage form for the management of oral lichen planus: Formulation study and clinical study. *European Journal of Pharmaceutics and Biopharmaceutics* **2010**, *76* (3), 437.
- (236) Yong Ni, B. P., Krishnaswamy Yeleswaram, Susan Erickson-Viitanen, William V Williams; Incyte Corporation: United States, 2023, DOI:[https://patents.google.com/patent/US11576865B2/en?q=\(Ruxolitinib+Sustained+Release+Dosage+Forms\)&oq=Ruxolitinib+Sustained+Release+Dosage+Forms](https://patents.google.com/patent/US11576865B2/en?q=(Ruxolitinib+Sustained+Release+Dosage+Forms)&oq=Ruxolitinib+Sustained+Release+Dosage+Forms).
- (237) Kapoor, D.; Maheshwari, R.; Verma, K.; Sharma, S.; Ghode, P.; Tekade, R. K. In *Drug Delivery Systems*; Tekade, R. K., Ed.; Academic Press, 2020, DOI:<https://doi.org/10.1016/B978-0-12-814487-9.00014-4>.
- (238) Pearnchob, N.; Bodmeier, R. Coating of pellets with micronized ethylcellulose particles by a dry powder coating technique. *International Journal of Pharmaceutics* **2003**, *268* (1), 1.
- (239) Chourasia, M. K.; Jain, S. K. Polysaccharides for Colon Targeted Drug Delivery. *Drug Delivery* **2004**, *11* (2), 129.
- (240) Sa, B.; Mukherjee, S.; Roy, S. K. Effect of polymer concentration and solution pH on viscosity affecting integrity of a polysaccharide coat of compression coated tablets. *International Journal of Biological Macromolecules* **2019**, *125*, 922.

- (241) Chourasia, M.; Jain, S. Polysaccharides for colon targeted drug delivery. *Drug Delivery* **2004**, *11* (2), 129.
- (242) Chakravorty, A.; Chakraborty, M.; Sa, B. Factors influencing delayed release followed by rapid pulse release of drugs from compression coated tablets for colon targeting. *International Journal of Pharmacy and Pharmaceutical Sciences* **2016**, 330.
- (243) Millar, J. F. ENTERIC COATED PRODUCT. *US Patent* **1957**.
- (244) Li, H.; Hou, W.; Li, X. Interaction between xanthan gum and cationic cellulose JR400 in aqueous solution. *Carbohydrate Polymers* **2012**, *89* (1), 24.
- (245) Patel, J.; Maji, B.; Moorthy, N. H. N.; Maiti, S. Xanthan gum derivatives: Review of synthesis, properties and diverse applications. *RSC advances* **2020**, *10* (45), 27103.
- (246) Guan, Y.; Yu, C.; Zang, Z.; Wan, X.; Naem, A.; Zhang, R.; Zhu, W. Chitosan/xanthan gum-based (Hydroxypropyl methylcellulose-co-2-Acrylamido-2-methylpropane sulfonic acid) interpenetrating hydrogels for controlled release of amorphous solid dispersion of bioactive constituents of *Pueraria lobata*. *International Journal of Biological Macromolecules* **2023**, *224*, 380.
- (247) Al Khateb, K.; Ozhmukhametova, E. K.; Mussin, M. N.; Seilkhanov, S. K.; Rakhypbekov, T. K.; Lau, W. M.; Khutoryanskiy, V. V. In situ gelling systems based on Pluronic F127/Pluronic F68 formulations for ocular drug delivery. *International Journal of Pharmaceutics* **2016**, *502* (1), 70.
- (248) Shabaan, O.; Abbas, A.; Fetih, G.; Abdellah, N.; Ibrahim, E.; Nasr, A.; Badran, S.; Abdullah, S. Once daily in-situ forming versus twice-daily conventional metronidazole vaginal gels for treatment of bacterial vaginosis: a randomized controlled trial. *J Genit Syst Disord* **2015**, *4* (5).
- (249) Laffleur, F. Mucoadhesive therapeutic compositions: a patent review (2011-2014). *Expert Opinion on Therapeutic Patents* **2016**, *26* (3), 377.
- (250) Smart, J. D. The basics and underlying mechanisms of mucoadhesion. *Advanced Drug Delivery Reviews* **2005**, *57* (11), 1556.
- (251) Sogias, I. A.; Williams, A. C.; Khutoryanskiy, V. V. Why is Chitosan Mucoadhesive? *Biomacromolecules* **2008**, *9* (7), 1837.
- (252) Grabovac, V.; Guggi, D.; Bernkop-Schnürch, A. Comparison of the mucoadhesive properties of various polymers. *Advanced Drug Delivery Reviews* **2005**, *57* (11), 1713.
- (253) Albarkah, Y. A.; Green, R. J.; Khutoryanskiy, V. V. Probing the Mucoadhesive Interactions Between Porcine Gastric Mucin and Some Water-Soluble Polymers. *Macromolecular Bioscience* **2015**, *15* (11), 1546.
- (254) Lele, B.; Hoffman, A. Mucoadhesive drug carriers based on complexes of poly (acrylic acid) and PEGylated drugs having hydrolysable PEG–anhydride–drug linkages. *Journal of controlled release* **2000**, *69* (2), 237.
- (255) Ayca Yildiz Peköz, Y. Ö. E., Derya Arslan; Office, E. P., Ed., 2017, DOI:<https://patents.google.com/patent/EP3173067A1/en>.
- (256) Ways, T. M. M.; Filippov, S. K.; Maji, S.; Glassner, M.; Cegłowski, M.; Hoogenboom, R.; King, S.; Lau, W. M.; Khutoryanskiy, V. V. Mucus-penetrating nanoparticles based on chitosan grafted with various non-ionic polymers: Synthesis, structural characterisation and diffusion studies. *Journal of Colloid and Interface Science* **2022**, *626*, 251.
- (257) Buang, F.; Fu, M.; Chatzifragkou, A.; Amin, M. C. I. M.; Khutoryanskiy, V. V. Hydroxyethyl cellulose functionalised with maleimide groups as a new excipient with enhanced mucoadhesive properties. *International Journal of Pharmaceutics* **2023**, *642*, 123113.

- (258) Nosalova, G.; Fleskova, D.; Jurecek, L.; Sadlonova, V.; Ray, B. Herbal polysaccharides and cough reflex. *Respiratory Physiology & Neurobiology* **2013**, *187* (1), 47.
- (259) Cohen, H. A.; Hoshen, M.; Gur, S.; Bahir, A.; Laks, Y.; Blau, H. Efficacy and tolerability of a polysaccharide-resin-honey based cough syrup as compared to carbocysteine syrup for children with colds: a randomized, single-blinded, multicenter study. *World Journal of Pediatrics* **2017**, *13* (1), 27.
- (260) Chalumeau, M.; Duijvestijn, Y. C. M. Acetylcysteine and carbocysteine for acute upper and lower respiratory tract infections in paediatric patients without chronic broncho-pulmonary disease. *Cochrane Database of Systematic Reviews* **2013**, DOI:10.1002/14651858.CD003124.pub4 10.1002/14651858.CD003124.pub4(5).
- (261) Pierre Attali, D. C. France, 2011, DOI:<https://patents.google.com/patent/WO2011070125A1/en?q=WO+2011070125+A1>.
- (262) Sekiguchi, K.; Obi, N. Studies on Absorption of Eutectic Mixture. I. A Comparison of the Behavior of Eutectic Mixture of Sulfathiazole and that of Ordinary Sulfathiazole in Man. *Chemical and Pharmaceutical Bulletin* **1961**, *9* (11), 866.
- (263) Chiou, W. L.; Riegelman, S. Pharmaceutical Applications of Solid Dispersion Systems. *Journal of Pharmaceutical Sciences* **1971**, *60* (9), 1281.
- (264) Naser, Y. A.; Tekko, I. A.; Vora, L. K.; Peng, K.; Anjani, Q. K.; Greer, B.; Elliott, C.; McCarthy, H. O.; Donnelly, R. F. Hydrogel-forming microarray patches with solid dispersion reservoirs for transdermal long-acting microdepot delivery of a hydrophobic drug. *Journal of Controlled Release* **2023**, *356*, 416.
- (265) Shan, X.; Williams, A. C.; Khutoryanskiy, V. V. Polymer structure and property effects on solid dispersions with haloperidol: Poly(N-vinyl pyrrolidone) and poly(2-oxazolines) studies. *International Journal of Pharmaceutics* **2020**, *590*, 119884.
- (266) Ali, W.; Williams, A. C.; Rawlinson, C. F. Stoichiometrically governed molecular interactions in drug: Poloxamer solid dispersions. *International journal of pharmaceutics* **2010**, *391* (1-2), 162.
- (267) Nielsen, R. B.; Larsen, B. S.; Holm, R.; Pijpers, I.; Snoeys, J.; Nielsen, U. G.; Tho, I.; Nielsen, C. U. Increased bioavailability of a P-gp substrate: Co-release of etoposide and zosuquidar from amorphous solid dispersions. *International Journal of Pharmaceutics* **2023**, *642*, 123094.
- (268) Janssens, S.; Van den Mooter, G. Review: physical chemistry of solid dispersions. *Journal of Pharmacy and Pharmacology* **2010**, *61* (12), 1571.
- (269) Zhang, J.; Guo, M.; Luo, M.; Cai, T. Advances in the development of amorphous solid dispersions: The role of polymeric carriers. *Asian Journal of Pharmaceutical Sciences* **2023**, *18* (4), 100834.
- (270) Bhujbal, S. V.; Mitra, B.; Jain, U.; Gong, Y.; Agrawal, A.; Karki, S.; Taylor, L. S.; Kumar, S.; Zhou, Q. Pharmaceutical amorphous solid dispersion: A review of manufacturing strategies. *Acta Pharmaceutica Sinica B* **2021**, *11* (8), 2505.
- (271) Greenhalgh, D. J.; Williams, A. C.; Timmins, P.; York, P. Solubility parameters as predictors of miscibility in solid dispersions. *J Pharm Sci* **1999**, *88* (11), 1182.
- (272) Qian, F.; Huang, J.; Zhu, Q.; Haddadin, R.; Gawel, J.; Garmise, R.; Hussain, M. Is a distinctive single Tg a reliable indicator for the homogeneity of amorphous solid dispersion? *International Journal of Pharmaceutics* **2010**, *395* (1), 232.

- (273) Li, N.; Taylor, L. S. Nanoscale Infrared, Thermal, and Mechanical Characterization of Telaprevir–Polymer Miscibility in Amorphous Solid Dispersions Prepared by Solvent Evaporation. *Molecular Pharmaceutics* **2016**, *13* (3), 1123.
- (274) Vasanthavada, M.; Tong, W.-Q.; Joshi, Y.; Kislalioglu, M. S. Phase Behavior of Amorphous Molecular Dispersions I: Determination of the Degree and Mechanism of Solid Solubility. *Pharmaceutical Research* **2004**, *21* (9), 1598.
- (275) Yang, R.; Zhang, G. G. Z.; Zemlyanov, D. Y.; Purohit, H. S.; Taylor, L. S. Release Mechanisms of Amorphous Solid Dispersions: Role of Drug-Polymer Phase Separation and Morphology. *Journal of Pharmaceutical Sciences* **2023**, *112* (1), 304.
- (276) Craig, D. Q. M. The mechanisms of drug release from solid dispersions in water-soluble polymers. *International Journal of Pharmaceutics* **2002**, *231* (2), 131.
- (277) Frost, G. I. Recombinant human hyaluronidase (rHuPH20): an enabling platform for subcutaneous drug and fluid administration. *Expert opinion on drug delivery* **2007**, *4* (4), 427.
- (278) Lee, E. S.; Youn, Y. S. Albumin-based potential drugs: focus on half-life extension and nanoparticle preparation. *Journal of Pharmaceutical Investigation* **2016**, *46*, 305.
- (279) Shan, X.; Gong, X.; Li, J.; Wen, J.; Li, Y.; Zhang, Z. Current approaches of nanomedicines in the market and various stage of clinical translation. *Acta Pharmaceutica Sinica B* **2022**, *12* (7), 3028.
- (280) Reed, K. W.; Yalkowsky, S. H. Lysis of human red blood cells in the presence of various cosolvents. *PDA Journal of Pharmaceutical Science and Technology* **1985**, *39* (2), 64.
- (281) Strickley, R. G. Solubilizing Excipients in Oral and Injectable Formulations. *Pharmaceutical Research* **2004**, *21* (2), 201.
- (282) U.S. Food and Drug Administration, I. i. f. a. d. p., DOI:<https://www.fda.gov/drugs/drug-approvals-and-databases/inactive-ingredients-database-download>. Accessed 8 Oct 2021.
- (283) U.S. Food and Drug Administration (2020) Full prescribing information: Orencia®. . DOI:<https://dailymed.nlm.nih.gov/dailymed/drugInfo.cfm?setid=0836c6ac-ee37-5640-2fed-a3185a0b16eb>. Accessed 7 Oct 2021.
- (284) Abuchowski, A.; McCoy, J. R.; Palczuk, N. C.; van Es, T.; Davis, F. F. Effect of covalent attachment of polyethylene glycol on immunogenicity and circulating life of bovine liver catalase. *Journal of Biological Chemistry* **1977**, *252* (11), 3582.
- (285) Harris, J. M.; Chess, R. B. Effect of pegylation on pharmaceuticals. *Nature Reviews Drug Discovery* **2003**, *2* (3), 214.
- (286) Immordino, M. L.; Dosio, F.; Cattel, L. Stealth liposomes: review of the basic science, rationale, and clinical applications, existing and potential. *Int J Nanomedicine* **2006**, *1* (3), 297.
- (287) Kumar, L. D.; Clarke, A. R. Gene manipulation through the use of small interfering RNA (siRNA): from in vitro to in vivo applications. *Advanced drug delivery reviews* **2007**, *59* (2-3), 87.
- (288) Gao, Y.; Joshi, M.; Zhao, Z.; Mitragotri, S. PEGylated therapeutics in the clinic. *Bioengineering & Translational Medicine* **2024**, *9* (1), e10600.
- (289) Harris, J. M. Laboratory synthesis of polyethylene glycol derivatives. *Journal of Macromolecular Science-Reviews in Macromolecular Chemistry and Physics* **1985**, *25* (3), 325.
- (290) Kozlowski, A.; Harris, J. M. Improvements in protein PEGylation: pegylated interferons for treatment of hepatitis C. *Journal of Controlled Release* **2001**, *72* (1-3), 217.

- (291) Piedmonte, D. M.; Treuheit, M. J. Formulation of Neulasta® (pegfilgrastim). *Advanced Drug Delivery Reviews* **2008**, *60* (1), 50.
- (292) Monfardini, C.; Schiavon, O.; Caliceti, P.; Morpurgo, M.; Harris, J. M.; Veronese, F. M. A branched monomethoxypoly (ethylene glycol) for protein modification. *Bioconjugate chemistry* **1995**, *6* (1), 62.
- (293) Turecek, P. L.; Bossard, M. J.; Schoetens, F.; Ivens, I. A. PEGylation of biopharmaceuticals: a review of chemistry and nonclinical safety information of approved drugs. *Journal of pharmaceutical sciences* **2016**, *105* (2), 460.
- (294) Lal, R. A.; Hoffman, A. R. Long-acting growth hormone preparations in the treatment of children. *Pediatric endocrinology reviews: PER* **2018**, *16* (Suppl 1), 162.
- (295) Pasut, G.; Veronese, F. M. Polymer–drug conjugation, recent achievements and general strategies. *Progress in Polymer Science* **2007**, *32* (8), 933.
- (296) Turecek, P.; Bossard, M.; Graninger, M.; Gritsch, H.; Höllriegl, W.; Kaliwoda, M.; Matthiessen, P.; Mitterer, A.; Muchitsch, E.-M.; Purtscher, M. BAX 855, a PEGylated rFVIII product with prolonged half-life. *Hämostaseologie* **2012**, *32* (S 01), S29.
- (297) Kaldybekov, D. B.; Tonglairoum, P.; Opanasopit, P.; Khutoryanskiy, V. V. Mucoadhesive maleimide-functionalised liposomes for drug delivery to urinary bladder. *European Journal of Pharmaceutical Sciences* **2018**, *111*, 83.
- (298) Kandzija, N.; Khutoryanskiy, V. V. Delivery of Riboflavin-5'-Monophosphate into the cornea: can liposomes provide any enhancement effects? *Journal of Pharmaceutical Sciences* **2017**, *106* (10), 3041.
- (299) Pitto-Barry, A.; Barry, N. P. E. Pluronic® block-copolymers in medicine: from chemical and biological versatility to rationalisation and clinical advances. *Polymer Chemistry* **2014**, *5* (10), 3291.
- (300) Nakashima, K.; Bahadur, P. Aggregation of water-soluble block copolymers in aqueous solutions: Recent trends. *Advances in Colloid and Interface Science* **2006**, *123-126*, 75.
- (301) Alexandridis, P.; Holzwarth, J. F.; Hatton, T. A. Micellization of Poly(ethylene oxide)-Poly(propylene oxide)-Poly(ethylene oxide) Triblock Copolymers in Aqueous Solutions: Thermodynamics of Copolymer Association. *Macromolecules* **1994**, *27* (9), 2414.
- (302) Owen, S. C.; Chan, D. P. Y.; Shoichet, M. S. Polymeric micelle stability. *Nano Today* **2012**, *7* (1), 53.
- (303) Russo, G.; Rossella Delpiano, G.; Carucci, C.; Grosso, M.; Dessì, C.; Söderman, O.; Lindman, B.; Monduzzi, M.; Salis, A. Tuning Pluronic F127 phase transitions by adding physiological amounts of salts: A rheology, SAXS, and NMR investigation. *European Polymer Journal* **2024**, *204*, 112714.
- (304) Li, Y.; Tian, Y.; Jia, X.; Zhang, Z.; Sun, D.; Xie, H.; Zang, D.; Liu, T. Effect of pharmaceutical excipients on micellization of Pluronic and the application as drug carrier to reverse MDR. *Journal of Molecular Liquids* **2023**, *383*, 122182.
- (305) Patel, D.; Patel, D.; Ray, D.; Kuperkar, K.; Aswal, V. K.; Bahadur, P. Single and mixed Pluronic® micelles with solubilized hydrophobic additives: Underscoring the aqueous solution demeanor and micellar transition. *Journal of Molecular Liquids* **2021**, *343*, 117625.
- (306) An, B.; Zhang, W.; Han, J.; Wang, Y.; Ni, L. The Cloud Point Behavior and Liquid–Liquid Equilibrium of Poly (Ethylene Glycol)–Block-Poly (Propylene Glycol)–Block-Poly (Ethylene Glycol) with Five Salting-Out Salts (K₂SO₄, K₂CO₃, KCl, KNO₃, KBr) at 283.15 K. *Journal of Solution Chemistry* **2016**, *45*, 1811.

- (307) Ohashi, K.; Hashizaki, K.; Taguchi, H.; Saito, Y. Effects of Inorganic Salts on Micellization and Solubilization in an Aqueous Solution of Poly (ethylene oxide)/Poly (propylene oxide)/Poly (ethylene oxide) Triblock Copolymer. *Journal of dispersion science and technology* **2009**, *30* (5), 720.
- (308) Bodratti, A. M.; Wu, J.; Jahan, R.; Sarkar, B.; Tsianou, M.; Alexandridis, P. Mono- and divalent salts as modifiers of PEO-PPO-PEO block copolymer interactions with silica nanoparticles in aqueous dispersions. *Journal of Dispersion Science and Technology* **2015**, *36* (12), 1806.
- (309) Kumar, M. S.; Dash, S. Effect of salts on micellization and clouding behavior of Pluronic F108 in aqueous solution using Trypan blue dye. *Surfaces and Interfaces* **2018**, *12*, 1.
- (310) Danson, S.; Ferry, D.; Alakhov, V.; Margison, J.; Kerr, D.; Jowle, D.; Brampton, M.; Halbert, G.; Ranson, M. Phase I dose escalation and pharmacokinetic study of pluronic polymer-bound doxorubicin (SP1049C) in patients with advanced cancer. *Br J Cancer* **2004**, *90* (11), 2085.
- (311) Valle, J. W.; Armstrong, A.; Newman, C.; Alakhov, V.; Pietrzynski, G.; Brewer, J.; Campbell, S.; Corrie, P.; Rowinsky, E. K.; Ranson, M. A phase 2 study of SP1049C, doxorubicin in P-glycoprotein-targeting pluronics, in patients with advanced adenocarcinoma of the esophagus and gastroesophageal junction. *Invest New Drugs* **2011**, *29* (5), 1029.
- (312) Panarin, E. F.; Ushakov, S. N. Synthesis of polymer salts and amides of penicillins. *Pharmaceutical Chemistry Journal* **1968**, *2* (5), 260.
- (313) Maeda, H.; Wu, J.; Sawa, T.; Matsumura, Y.; Hori, K. Tumor vascular permeability and the EPR effect in macromolecular therapeutics: a review. *Journal of Controlled Release* **2000**, *65* (1), 271.
- (314) Conover, C. D.; Greenwald, R. B.; Pendri, A.; Gilbert, C. W.; Shum, K. L. Camptothecin delivery systems: enhanced efficacy and tumor accumulation of camptothecin following its conjugation to polyethylene glycol via a glycine linker. *Cancer Chemotherapy and Pharmacology* **1998**, *42* (5), 407.
- (315) Loftsson, T.; Friðriksdóttir, H.; Guðmundsdóttir, T. K. The effect of water-soluble polymers on aqueous solubility of drugs. *International Journal of Pharmaceutics* **1996**, *127* (2), 293.
- (316) Rao, K. M.; Kim, E.; Kim, H. J.; Uthappa, U. T.; Han, S. S. Hyaluronic acid-quercetin pendant drug conjugate for wound healing applications. *International Journal of Biological Macromolecules* **2023**, *240*, 124336.
- (317) Wang, Y.; Wu, C. Site-specific conjugation of polymers to proteins. *Biomacromolecules* **2018**, *19* (6), 1804.
- (318) Gauthier, M. A.; Klok, H.-A. Peptide/protein-polymer conjugates: synthetic strategies and design concepts. *Chemical Communications* **2008**, (23), 2591.
- (319) Thilakarathne, V.; Briand, V. A.; Zhou, Y.; Kasi, R. M.; Kumar, C. V. Protein Polymer Conjugates: Improving the Stability of Hemoglobin with Poly(acrylic acid). *Langmuir* **2011**, *27* (12), 7663.
- (320) Mees, M. A.; Hoogenboom, R. Full and partial hydrolysis of poly(2-oxazoline)s and the subsequent post-polymerization modification of the resulting polyethylenimine (co)polymers. *Polymer Chemistry* **2018**, *9* (40), 4968.
- (321) Sedlacek, O.; Janouskova, O.; Verbraeken, B.; Hoogenboom, R. Straightforward Route to Superhydrophilic Poly(2-oxazoline)s via Acylation of Well-Defined Polyethylenimine. *Biomacromolecules* **2019**, *20* (1), 222.

- (322) Kagiya, T.; Narisawa, S.; Maeda, T.; Fukui, K. Ring-opening polymerization of 2-substituted 2-oxazolines. *Journal of Polymer Science Part B: Polymer Letters* **1966**, *4* (7), 441.
- (323) Saegusa, T.; Kobayashi, S.; Yamada, A. Graft Copolymerization of 2-Methyl-2-oxazoline onto Chloromethylated Polystyrene and Hydrolysis of Graft Copolymer to a Chelating Resin of Poly(styrene-g-ethylenimine). *Macromolecules* **1975**, *8* (4), 390.
- (324) Lambermont-Thijs, H. M. L.; Heuts, J. P. A.; Hoepfener, S.; Hoogenboom, R.; Schubert, U. S. Selective partial hydrolysis of amphiphilic copoly(2-oxazoline)s as basis for temperature and pH responsive micelles. *Polymer Chemistry* **2011**, *2* (2), 313.
- (325) Kem, K. M. Kinetics of the hydrolysis of linear poly [(acylimino)-ethylenes]. *Journal of polymer science: polymer chemistry edition* **1979**, *17* (7), 1977.
- (326) Pinnapireddy, S. R.; Duse, L.; Strehlow, B.; Schäfer, J.; Bakowsky, U. Composite liposome-PEI/nucleic acid lipopolyplexes for safe and efficient gene delivery and gene knockdown. *Colloids and Surfaces B: Biointerfaces* **2017**, *158*, 93.
- (327) Bolto, B. A. Soluble polymers in water purification. *Progress in Polymer Science* **1995**, *20* (6), 987.
- (328) Jäger, M.; Schubert, S.; Ochrimenko, S.; Fischer, D.; Schubert, U. S. Branched and linear poly(ethylene imine)-based conjugates: synthetic modification, characterization, and application. *Chemical Society Reviews* **2012**, *41* (13), 4755.
- (329) Soradach, S.; Williams, A. C.; Khutoryanskiy, V. V. Physically cross-linked cryogels of linear polyethyleneimine: influence of cooling temperature and solvent composition. *Macromolecules* **2022**, *55* (21), 9537.
- (330) Boussif, O.; Lezoualc'h, F.; Zanta, M. A.; Mergny, M. D.; Scherman, D.; Demeneix, B.; Behr, J.-P. A versatile vector for gene and oligonucleotide transfer into cells in culture and in vivo: polyethylenimine. *Proceedings of the National Academy of Sciences* **1995**, *92* (16), 7297.
- (331) Pandey, A. P.; Sawant, K. K. Polyethylenimine: A versatile, multifunctional non-viral vector for nucleic acid delivery. *Materials Science and Engineering: C* **2016**, *68*, 904.
- (332) Elzes, M. R.; Mertens, I.; Sedlacek, O.; Verbraeken, B.; Doensen, A. C. A.; Mees, M. A.; Glassner, M.; Jana, S.; Paulusse, J. M. J.; Hoogenboom, R. Linear Poly(ethylenimine-propylenimine) Random Copolymers for Gene Delivery: From Polymer Synthesis to Efficient Transfection with High Serum Tolerance. *Biomacromolecules* **2022**, *23* (6), 2459.
- (333) Casper, J.; Schenk, S. H.; Parhizkar, E.; Detampel, P.; Dehshahri, A.; Huwyler, J. Polyethylenimine (PEI) in gene therapy: Current status and clinical applications. *Journal of Controlled Release* **2023**, *362*, 667.
- (334) Liu, X.; Yang, J. W.; Miller, A. D.; Nack, E. A.; Lynn, D. M. Charge-Shifting Cationic Polymers That Promote Self-Assembly and Self-Disassembly with DNA. *Macromolecules* **2005**, *38* (19), 7907.
- (335) Liu, X.; Yang, J. W.; Lynn, D. M. Addition of “Charge-Shifting” Side Chains to Linear Poly(ethyleneimine) Enhances Cell Transfection Efficiency. *Biomacromolecules* **2008**, *9* (7), 2063.
- (336) Limiti, E.; Mozetic, P.; Giannitelli, S. M.; Pinelli, F.; Han, X.; Del Rio, D.; Abbruzzese, F.; Basoli, F.; Rosanò, L.; Scialla, S. et al. Hyaluronic Acid–Polyethyleneimine Nanogels for Controlled Drug Delivery in Cancer Treatment. *ACS Applied Nano Materials* **2022**, *5* (4), 5544.
- (337) Luo, Z.; Dai, Y.; Gao, H. Development and application of hyaluronic acid in tumor targeting drug delivery. *Acta Pharmaceutica Sinica B* **2019**, *9* (6), 1099.

- (338) Yang, C.; Guo, Q.; Lu, Y.; Zhang, B.; Nie, G. Ultrasensitive “signal-on” electrochemiluminescence immunosensor for prostate-specific antigen detection based on novel nanoprobe and poly (indole-6-carboxylic acid)/flower-like Au nanocomposite. *Sensors and Actuators B: Chemical* **2020**, *303*, 127246.
- (339) Englert, C.; Trützscher, A.-K.; Raasch, M.; Bus, T.; Borchers, P.; Mosig, A. S.; Traeger, A.; Schubert, U. S. Crossing the blood-brain barrier: Glutathione-conjugated poly(ethylene imine) for gene delivery. *Journal of Controlled Release* **2016**, *241*, 1.
- (340) Englert, C.; Pröhl, M.; Czaplowska, J. A.; Fritzsche, C.; Preußger, E.; Schubert, U. S.; Traeger, A.; Gottschaldt, M. d-Fructose-Decorated Poly(ethylene imine) for Human Breast Cancer Cell Targeting. *Macromolecular Bioscience* **2017**, *17* (8), 1600502.
- (341) Sedlacek, O.; Monnery, B. D.; Hoogenboom, R. Synthesis of defined high molar mass poly(2-methyl-2-oxazoline). *Polymer Chemistry* **2019**, *10* (11), 1286.
- (342) Soradach, S.; Kengkwasingh, P.; Williams, A. C.; Khutoryanskiy, V. V. Synthesis and evaluation of poly (3-hydroxypropyl ethylene-imine) and its blends with chitosan forming novel elastic films for delivery of haloperidol. *Pharmaceutics* **2022**, *14* (12), 2671.

Chapter 2.

On the mucoadhesive properties of synthetic and natural polyampholytes

(QUAD system contribution of Manfei Fu: 70% of conception and design, 80% of data collection, 90% of data analysis and conclusions, and 90% of manuscript preparation).

Chapter 2. On the mucoadhesive properties of synthetic and natural polyampholytes

(QUAD system contribution of Manfei Fu: 70% of conception and design, 80% of data collection, 90% of data analysis and conclusions, and 90% of manuscript preparation).

Manfei Fu^a, Sergey K. Filippov^b, Adrian C. Williams^a, Vitaliy V. Khutoryanskiy^{*a}

a. School of Pharmacy, University of Reading, Whiteknights, Post Office Box 224, Reading RG6 6AD, United Kingdom

b. DWI-Leibniz Institute for Interactive Materials e. V., Forckenbeckstraße 50, 52074, Aachen, Germany

*Corresponding author.

E-mail address: v.khutoryanskiy@reading.ac.uk (V.V. Khutoryanskiy).

<https://doi.org/10.1016/j.jcis.2023.12.176>

Received 10 October 2023; Received in revised form 6 December 2023; Accepted 29 December 2023

Available online 5 January 2024

0021-9797/© 2024 The Author(s). Published by Elsevier Inc.

This is an open access article under the CC BY license (<http://creativecommons.org/licenses/by/4.0/>).

Abstract

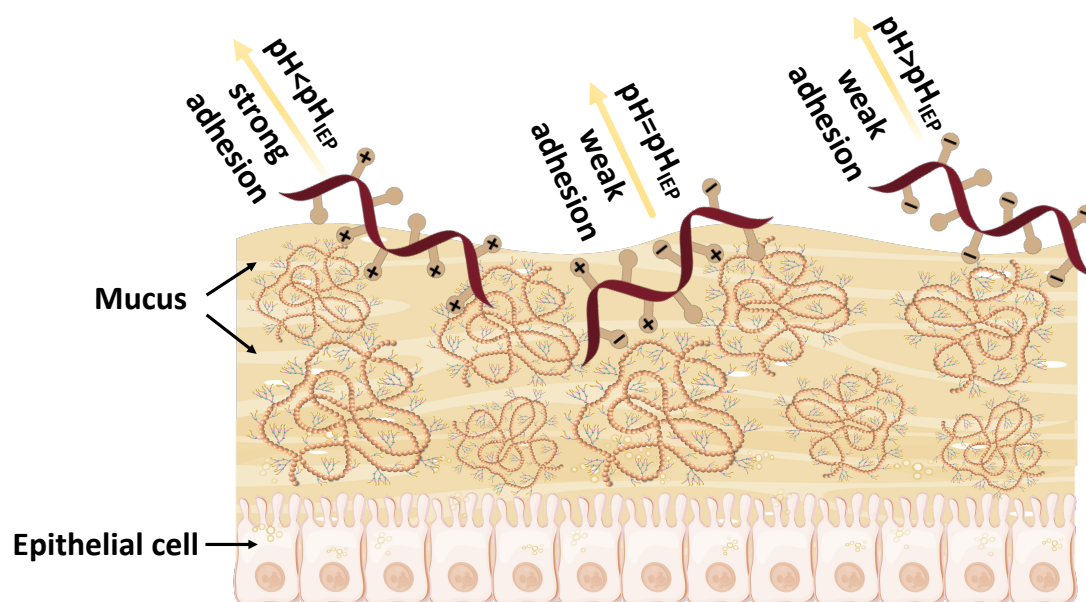
Hypothesis: The mucoadhesive characteristics of amphoteric polymers (also known as polyampholytes) can vary and are influenced by factors such as the solution's pH and its relative position against their isoelectric point (pH_{IEP}). Whilst the literature contains numerous reports on mucoadhesive properties of either cationic or anionic polymers, very little is known about these characteristics for polyampholytes.

Experiments: Here, two amphoteric polymers were synthesized by reaction of linear polyethylene imine (L-PEI) with succinic or phthalic anhydride and their mucoadhesive properties were compared to bovine serum albumin (BSA), selected as a natural polyampholyte. Interactions between these polymers and porcine gastric mucin were studied using turbidimetric titration and isothermal titration calorimetry across a wide range of pHs. Model tablets were designed, coated with these polymers and tested to evaluate their adhesion to porcine gastric mucosa at different pHs. Moreover, a retention study using fluorescein

isothiocyanate (FITC)-labelled polyampholytes deposited onto mucosal surfaces was also conducted.

Findings: All these studies indicated the importance of solution pH and its relative position against pH_{IEP} in the mucoadhesive properties of polyampholytes. Both synthetic and natural polyampholytes exhibited strong interactions with mucin and good mucoadhesive properties at $pH < pH_{IEP}$.

Keywords: mucoadhesion, polyampholytes, electrostatic interactions, mucin, proteins



2.1 Introduction

Mucoadhesion is defined as attractive interactions between materials of a dosage form and a mucosal surface^{250,343-345}. All water-soluble and weakly cross-linked hydrophilic polymers exhibit some mucoadhesive properties due to their interactions with mucin via hydrogen bonding or electrostatic effects or/and their ability to penetrate into the mucus gel to form an interpenetrating layer²⁵¹. Mucoadhesive polymers are commonly used in the design of dosage forms including tablets³⁴⁶, films³⁴⁷, patches³⁴⁸ and gels³⁴⁹ for transmucosal drug delivery. Mucoadhesion also plays important role in taste perception for some food formulations^{350,351} and in dental care³⁵².

Anionic polymers such as poly(acrylic acid), carboxymethylcellulose, alginate and pectin³⁵³ exhibit strong mucoadhesive properties due to the ability of their carboxylic groups to form hydrogen bonds with hydroxyl groups present in oligosaccharide fragments of mucins^{354,355}. Strong mucoadhesive properties of cationic polymers are usually due to the electrostatic attractive interactions with negatively charged carboxylic and sulphate groups

present in mucins. Non-ionic polymers typically exhibit poorer mucoadhesive properties compared to polyelectrolytes³⁵⁶ although their ability to adhere to mucosal tissues can be substantially enhanced by introducing functional groups capable of forming covalent bonds with mucins³⁵⁷.

Polyampholytes are macromolecules containing both anionic and cationic groups in their structure and can be synthetic or of natural origin. Polyampholytes have some unique physicochemical properties, including the existence of an isoelectric point (pH_{IEP}), which is defined as the pH at which the macromolecules have a net zero electrical charge³⁵⁸⁻³⁶⁰. At pHs below pH_{IEP} the macromolecules of polyampholytes carry an overall positive charge and at pHs above this point they become net negatively charged. Consequently, the behavior of polyampholytes is strongly dependent on solution pH. Proteins are natural polymers that have amphoteric properties due to the presence of both acidic (e.g. aspartic and glutamic acids) and basic (e.g. lysine and arginine) amino acid residues in their structure.

There are very few reports in the literature evaluating mucoadhesive properties of synthetic or natural polyampholytes. Some authors reported that mucoadhesive properties of gelatine, a denatured protein derived from collagen, are poor and comparable to non-ionic polymers³⁶¹. However, gelatine derivatised through its additional amination was shown to exhibit considerable mucoadhesive performance both in vitro and in vivo in rats³⁶². More recently, Nishio et al.³⁶³ reported strong mucoadhesive properties for polyampholyte hydrogels synthesised from acrylic acid and N,N-dimethylaminopropyl acrylamide. Adhesion of milk proteins to the oral mucosa was demonstrated by Withers et al.³⁶⁴ and was related to the drying sensation observed following consumption of protein rich dairy beverages. The current literature demonstrates that a detailed mechanistic understanding of the factors affecting the mucoadhesive properties of amphoteric polymers is lacking, which is especially important for proteins.

This study investigates the factors affecting the mucoadhesive properties of both synthetic and natural polyampholytes. Two polyampholytes were synthesized by reacting L-PEI with either succinic anhydride (SA) or phthalic anhydride (PA). Bovine serum albumin (BSA) was selected as a natural polyampholyte due to its easy availability, excellent solubility in water in a broad range of pHs, and good stability in solutions. The polyampholytes were fully characterized by proton nuclear magnetic resonance (¹H-NMR) and Fourier transformed infrared spectroscopies (FTIR), turbidity-pH measurements and electrophoretic mobility at various pHs. Turbidimetric titration and isothermal titration calorimetry (ITC) characterized the interactions of the polyampholytes with porcine gastric

mucin in solutions. Model mucoadhesive tablets, coated with polymers and the protein, were used to evaluate adhesion of the dosage form to porcine gastric mucosal surface. The retention of the polyampholytes in solutions on porcine gastric mucosal surfaces was evaluated by fluorescent labelling the polymers and using fluorescence microscopy-based flow-through assay. To the best of our knowledge, this is the first study to systematically evaluate the mucoadhesive properties of polyampholytes to elucidate the factors affecting their ability to adhere to mucosal surfaces.

2.2 Materials and methods

2.2.1 Materials

Poly(2-ethyl-2-oxazoline) (PEOZ, MW~50 kDa, \bar{D} =3-4), succinic anhydride, phthalic anhydride, dimethyl sulfoxide (DMSO), triethylamine (TEA), deuterium oxide (D₂O), deuterated methanol (MeOD-d₄), sodium fluorescein, fluorescein isothiocyanate (FITC), fluorescein isothiocyanate-dextran (FITC-dextran, average MW 10,000), bovine serum albumin (BSA) and mucin from porcine stomach (type II) (PGM) were obtained from Sigma-Aldrich (Gillingham, U.K.). Urea, hydrochloric acid (37%), sodium hydroxide, hydroxypropyl methylcellulose, microcrystalline cellulose, barium sulfate, magnesium stearate and phosphate-buffered saline (PBS) tablets were obtained from Fisher Scientific (Loughborough, U.K.). Dialysis membrane (MWCO 3.5 kDa) was purchased from Medicell Membranes Ltd. (U.K.). Fresh porcine gastric tissue was provided by P.C. Turner Abattoirs (Farnborough, UK). All other chemicals were of analytical grade and used without further purification.

2.2.2 Synthesis of succinylated L-PEI and phthaylated L-PEI

L-PEI was synthesized by acidic hydrolysis of poly(2-ethyl-2-oxazoline) (PEOZ) following the protocol of Shan et al.³⁶⁵ Succinic anhydride (0.50 eq, 1.16 g) or phthalic anhydride (1.00 eq, 3.47 g) were dissolved in 15.00 mL DMSO and then mixed with 45 mL of the L-PEI (1.00 g, 1.00 eq) solution in DMSO, before triethanolamine (1.50 eq, 3.25 mL) was added (SI). The mixture was stirred for 12 h at 40°C and then diluted with deionized water and dialyzed against deionized water for 72 h. All polymers were recovered by freeze-drying (1.88g (87.03 %) and 3.88g (86.80 %) yield for succinylated L-PEI and phthaylated L-PEI, respectively).

2.2.3 Characterization of succinylated L-PEI and phthaylated L-PEI

2.2.3.1 ¹H-nuclear magnetic resonance spectroscopy (¹H-NMR)

10mg succinylated L-PEI or phthaylated L-PEI was dissolved in 1 mL D₂O, whereas L-PEI was dissolved in 1 mL MeOD-d₄. Spectra were recorded as the average of 128 scans using a 400 MHz Bruker spectrometer. Further details can be found in SI.

2.2.3.2 Fourier transform infrared (FTIR) spectroscopy

Polymers were analysed between 4000–950 cm⁻¹ at a resolution of 4 cm⁻¹ as an average of 64 scans using a diamond sampling accessory. Data were recorded by a Nicolet iS5 spectrometer (Thermo Scientific, U.K.).

2.2.3.3 Turbidity measurements

The effects of pH on turbidity of succinylated L-PEI, phthaylated L-PEI and BSA solutions were studied using a JENWAY 7315 spectrophotometer (Bibby Scientific Ltd, UK) at 400 nm at different pHs. The pH was adjusted by adding 0.1 M NaOH or HCl. Every titration was repeated in triplicate and the turbidity values are reported as mean ± standard deviation.

2.2.3.4 Electrophoretic mobility measurements

The effects of pH on electrophoretic mobility of succinylated L-PEI, phthaylated L-PEI and BSA solutions were studied in folded DTS-1070 capillary cells by using a Malvern Zetasizer Nano-S (Malvern Instruments). All samples were dissolved in deionized water (1 mg/mL) and pH was adjusted by adding 0.1 M NaOH or HCl. All measurements were conducted at 25°C and repeated in triplicate; the values are reported as mean ± standard deviation.

2.2.4 Mucin interaction studies

All experiments were performed with 1 mg/mL polyampholyte aqueous solutions and mucin dispersions, freshly prepared prior to each experiment. Porcine gastric mucin (PGM) was dispersed in deionized water, sonicated for 15 min and centrifuged at 1000 rpm for 5 min. The pH of the supernatant was adjusted using 0.1 M NaOH or HCl. Mixtures of mucin dispersions with polymer solutions were prepared at a wide range of ratios before turbidity was measured at 400 nm using a JENWAY 7315 spectrophotometer (Bibby Scientific Ltd, UK). To verify the role of hydrogen bonding and hydrophobic effects on the mucoadhesive interactions³⁶⁶, in a separate set of experiments PGM dispersions and polymer solutions were

additionally prepared in 8 M urea, also at 1mg/mL. All measurements were repeated in triplicate, and values reported as mean \pm standard deviation.

2.2.5 Isothermal titration calorimetry (ITC)

Binding interactions between PGM and polymers³⁶⁷ were studied using a TA NANO ITC 2G Isothermal Titration Calorimeter (Calorimetry Science Corp., USA). In each titration experiment, 100 μ L of a polymer solution at a defined pH was loaded into the syringe and titrated into mucin dispersions with the same pH within a 950 μ L calorimeter sample cell. The control experiments of titrating polymer solutions or mucin into a buffer were conducted using solutions with the same pH value. Titrations were performed automatically with 5.05 μ L aliquots from the syringe injected into the sample cell every 300s. All ITC measurements were conducted at 25 °C. Titrations of mucin solution into a buffer were also performed as a negative control with buffer to buffer titrations used as a reference. The experimental change in enthalpy (ΔH) was obtained by integrating the raw data with results analysed using Origin Lab[®] version 9.0 and NanoAnalyze software. “One-set-of-sites” model was used for the fitting when applicable.³⁶⁸ $\Delta H_{\text{change}} = \Delta H_{\text{end}} - \Delta H_{\text{start}}$ was taken as a measure of enthalpy change during titration for non-sigmoidal processes. In light of mucin molecular weight uncertainty and rather broad synthesized polymer molecular weight, weight concentration was used for ITC data analysis instead of molar values. This feature makes the determination of a binding constant, and hence entropy change, ΔS , unreliable, and so we focus on the ΔH_{change} analysis.

2.2.6 *Ex vivo* gastric mucoadhesive studies

2.2.6.1 Mucoadhesive studies of tablets on porcine gastric mucosa

Blank tablets were prepared by compression of a blend of hydroxypropyl methylcellulose (40%), microcrystalline cellulose (40%), barium sulphate (19%) and magnesium stearate (1%) using a single punch tableting machine (RIVA G.B. Ltd, UK). The obtained tablets were coated with 2% (w/v) polymer aqueous solutions containing 5% (w/v) sodium fluorescein using a mini spray coater / drier (Caleva Process Solution Ltd, UK). The average tablet weight, thickness, diameter, hardness and coating efficiency were determined for 10 tablets in every batch (data in SI).

Mucoadhesion of the polymer coated tablets was determined using a tensile test with a TA.XT Plus Texture Analyser (Stable Micro Systems Ltd., Godalming, UK) with freshly excised porcine gastric mucosal tissue. Before each test, dissected gastric tissue (4.0 \times 4.0 cm²)

was mounted on a glass slide with the mucosal side upward and pre-rinsed with 2.5 mL of simulated gastric fluid (SGF), prepared by dissolving 2.0 g NaCl and 3.0 mL HCl in 1 L deionized water before adjusting pH with 0.1 M HCl or NaOH. The pH of each mucosal tissue was adjusted with 0.1 M NaOH or HCl and measured with a FiveEasy F20 pH meter (Mettler-Toledo GmbH, Switzerland). The tissue was placed in a temperature- and humidity-controlled chamber of a Stable Micro Systems texture analyser (Stable Micro Systems Ltd, UK) and equilibrated at $37.0\pm 0.1^\circ\text{C}$. The texture analyser was used in the ‘adhesive test’ mode with a pre-speed of 2.0 (mm/s) and test-speed of 2.0 mm/s. Each model tablet was attached to the probe by two-sided sticky tape and moved downward to the mucosal tissue surface with an applied force of 2N and remained in contact for 15s. The probe was subsequently withdrawn at 10.0 mm/s. Twenty tablets coated with each polymer were measured at each different pH and the work of adhesion was calculated from the area under the detachment curve; all values are reported as mean \pm standard deviation.

2.2.6.2 Retention studies on porcine gastric mucosa

The flow through method followed our previous report³⁶⁹. FITC and polymers at a weight ratio of 1:20 were dissolved in 30mL DMSO at 40°C and the mixture was stirred overnight. The resultant solution was diluted with deionized water and dialyzed against deionized water for 72 h. All FITC-labelled polymers were recovered by freeze-drying. Porcine gastric mucosal tissue ($1.5 \times 2.0 \text{ cm}^2$) was mounted on an inclined glass slide with the mucosal side upward and pre-rinsed with 1 mL freshly prepared solutions with different pHs, adjusted with 0.1 M NaOH or HCl. All experiments were conducted at $37.0\pm 0.1^\circ\text{C}$ in an incubator. Briefly, tissue background fluorescence intensity ($I_{\text{background}}$) was collected from each blank tissue. Then, 20 μL of FITC-succinylated L-PEI, FITC-phthaylated L-PEI, FITC-BSA or FITC-dextran (negative control) solution was dosed onto the mucosal surface and fluorescence images were recorded as initial fluorescence intensity (I_0). After 3 min of dosing, the mucosal surface was washed with solutions of different pH using a syringe pump (Harvard Apparatus model 981074, Holliston, MA, USA) at 0.43 mL/min. Fluorescence images of the mucosal tissue (I_t) were acquired periodically using a Leica MZ10F stereo-microscope (Leica Microsystems, Wetzlar, Germany) with the GFP filter-fitted Leica DFC3000G digital camera at $2.0\times$ magnification, 735 ms of exposure time, $2.0\times$ gain, $1.0\times$ gamma and pseudo color at 520 nm. The microscopy images from each time point were analysed using ImageJ software (Version 1.53t, 2022) and fluorescence intensity calculated according to Equation (1):

$$\text{Fluorescence intensity (\%)} = \frac{I_t - I_{\text{background}}}{I_0 - I_{\text{background}}} \times 100\% \quad (1)$$

where the 0 min point was set as 100%. Results are presented as the fluorescence intensity of the FITC-labelled polymers (after subtracting the background fluorescence from each wash image) at different wash-time points as a function of irrigation time (0-60 min). Triplicate experiments were performed for each polymer and values are reported as mean \pm standard deviation.

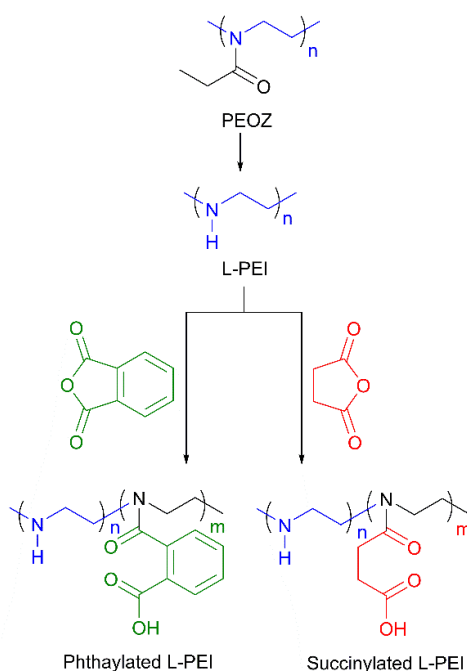
2.2.7 Statistical analysis

All experiments were conducted with a minimum of 3 replicates and data are presented as mean \pm standard deviations. GraphPad Prism software (version 9.5.1; GraphPad Software Inc., San Diego, CA, USA) was used to analyse data using a one-way analysis of variance (ANOVA) and two-tailed Student's t-tests where $p < 0.05$ was set as the statistical significance criterion.

2.3 Results and discussion

2.3.1 Synthesis and characterization of succinylated L-PEI and phthaylated L-PEI

Commercially available PEOZ (50 kDa) was fully hydrolysed to form L-PEI, which was subsequently reacted with succinic or phthalic anhydrides to synthesize succinylated L-PEI and phthaylated L-PEI (Scheme 2.3-1).



Scheme 2.3-1. Synthesis of succinylated and phthaylated L-PEI from PEOZ.

The resultant polymers were characterized using $^1\text{H-NMR}$ and FTIR spectroscopies. These results are presented and discussed in SI. The physicochemical properties of novel polyampholytes as well as BSA in solutions were evaluated using turbidity and electrophoretic mobility measurements at different pHs.

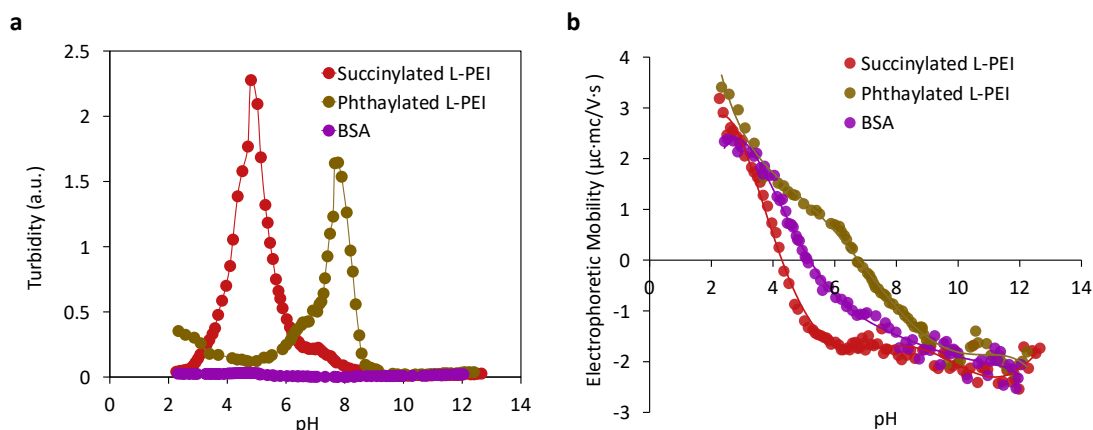


Figure 2.3-1. Effect of pH on solution turbidity (a) and electrophoretic mobility (b) of 1mg/mL succinylated L-PEI, phthaylated L-PEI and BSA aqueous solution.

It is well known that polyampholyte macromolecules undergo contraction and in some cases aggregation, when their solution pH is approaching $\text{pH}_{\text{IEP}}^{370}$. Enhanced aggregation usually manifests as onset of turbidity. This makes turbidimetric studies of their solutions at different pHs a suitable technique for determining their pH_{IEP} value. Figure 2.3-1 shows turbidity–pH and electrophoretic mobility–pH profiles for solutions of our novel synthetic polyampholytes and for BSA. Both succinylated and phthaylated L-PEI exhibit a very pronounced increase in solution turbidity with the maximal values at 4.85 ± 0.05 and 7.71 ± 0.08 , respectively. A further increase in solution pH results in substantial reduction of turbidity values. These turbidity – pH profiles are typical for solutions of polyampholytes, which undergo aggregation near $\text{pH}_{\text{IEP}}^{371}$. When $\text{pH} < \text{pH}_{\text{IEP}}$ or $\text{pH} > \text{pH}_{\text{IEP}}$, due to the presence of excess positively or negatively charged groups, the polymer is fully hydrated and water soluble. Aggregation of BSA when solution pH approaches pH_{IEP} was not observed; its solutions remain transparent across pH 2-12, potentially because it is insufficiently hydrophobic to aggregate. Therefore, it was not possible to determine pH_{IEP} of BSA using the turbidimetric technique.

Another useful method to determine pH_{IEP} for polyampholytes is to assess electrophoretic mobility at different solution pHs³⁷². These profiles are typical for amphoteric polymers and colloidal particles, where increases in solution pH results in a gradual transition

from positively charged values to negatively charged ones. The point on this profile, where electrophoretic mobility values cross zero corresponds to their pH_{IEP} .

The pH_{IEP} values determined using electrophoretic mobility measurements for succinylated L-PEI, phthaylated L-PEI and BSA were 4.30 ± 0.04 and 6.86 ± 0.16 and 5.09 ± 0.08 , respectively. The pH_{IEP} of BSA has been reported at 4.7-4.9³⁷³⁻³⁷⁵, which is broadly in agreement with the value determined in our work.

Table 2.3-1. Characteristics of polyampholytes

Polymer	^a DS	pH_{IEP} (Turbidity)	pH_{IEP} (Electrophoretic mobility)
Succinylated L-PEI	46%	pH 4.85 ± 0.05	pH 4.30 ± 0.04
Phthaylated L-PEI	86%	pH 7.71 ± 0.08	pH 6.86 ± 0.16
BSA	n.a.	-**	pH 5.09 ± 0.08

^a Degree of substitution; ** it was impossible to determine it using turbidimetric technique.

Table 2.3-1 summarises the pH_{IEP} values determined by the different methods. The IEP values from the two techniques are within a pH unit of each other with variance attributable to the different properties evaluated. For example, turbidity is detected only when relatively large aggregates are present, but the aggregation process may start at slightly different pH, and electrophoretic mobility is dependent on the conformation of macromolecules and shape of the aggregates. The hydrophobic group of phthaylated L-PEI, has weaker ionic content than succinylated L-PEI, and consequently displays a higher pH_{IEP} than the succinylated derivative. The substantial difference between the pH_{IEP} values of these three polyampholytes provided an opportunity to study their mucoadhesive interactions and properties over a broad range of pHs, below and above their pH_{IEP} .

2.3.2 Mucin interaction studies

The major role of mucus is protection and lubrication of epithelial cells^{376,377}. Mucins are glycoproteins with a high molecular weight (0.5-40 MDa)^{362,364} and are the major component of mucus. They bear a negative charge due to the presence of carboxylate groups and ester sulfates. Porcine gastric mucin (PGM) has good storage stability and relatively reproducible properties³⁷⁸. When dispersed in aqueous solutions it forms a colloidal system with polydisperse particles, whose size depend on pH. Fefelova et al.³⁷⁹ reported that when PGM is dispersed in deionised water (pH 6.8) it forms colloidal system with a bimodal size distribution, with mean particle sizes around 100 nm and 500 nm present. Under acidic

conditions (pH 2.0) PGM undergoes further aggregation and forms larger particles up to 3000 nm. Similar observations were also reported by Sogias et al.²⁵¹. Albarkah et al.²⁵³ additionally reported that the particle size and size distributions of PGM is strongly dependent on the use of sonication. Despite the polydispersity, pH- and sonication-dependent nature of the particles, PGM it is commonly used as a model system to study mucoadhesive interactions with polymers³⁸⁰⁻³⁸².

Turbidimetric titration is a very common and simple technique to study mucoadhesive interactions^{380,383,384}, which assesses aggregation of mucin particles when they bind to macromolecules of a mucoadhesive polymer. Here, turbidimetric titrations of PGM were conducted with solutions of polyampholytes at five or six different pHs, selected to represent conditions below, near and above pI_{IEP} of each polyampholyte. It should be noted that the ionic strength of solutions was not controlled in these experiments to mimic the physiological conditions better as it is known that this parameter varies throughout the GI tract.

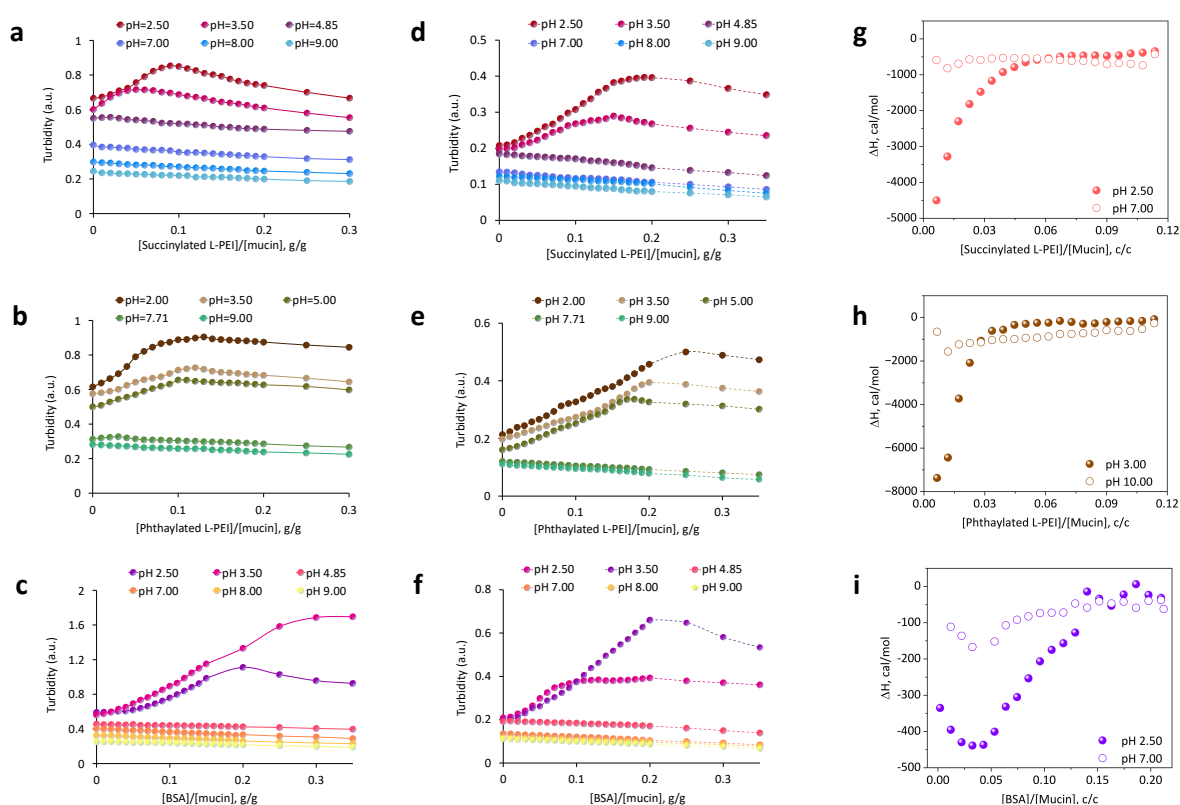


Figure 2.3-2. Turbidimetric titration curves of 1 mg/mL porcine gastric mucin with 1 mg/mL succinylated L-PEI (a), phthalylated L-PEI (b) and BSA (c) in aqueous solution; turbidimetric titration curves of 1 mg/mL porcine gastric mucin with 1 mg/mL succinylated L-PEI (d), phthalylated L-PEI (e) and BSA (f) in urea solution; effect of the pH on the interaction between polyampholytes and mucin using isothermal titration calorimetry: 1 mg/mL PGM was titrated with 1 mg/mL succinylated L-PEI at pH 2.50 and pH 7.00 (g), 1 mg/mL PGM was titrated with 1 mg/mL phthalylated L-PEI at pH 3.00 and pH 10.00 (h) and 1 mg/mL PGM was titrated with 1 mg/mL BSA at pH 2.50 and pH 7.00 (i). Mean average \pm standard deviation, n=3.

Figure 2.3-2a-c presents the results of these experiments. The initial turbidity values observed for PGM solutions were higher when solution pH was lower and this was consistent with the previous reports^{251,379} attributed to protonation of mucin's carboxylic groups and further aggregation of its particles. The titration of PGM with all three polyampholytes in solutions with $\text{pH} < \text{pH}_{\text{IEP}}$ clearly showed the presence of strong mucoadhesive interactions leading to increased solution turbidity and aggregation of mucin particles. The maximal turbidity values occur when the surface of the mucin particles is fully saturated with macromolecules of polyampholyte; these values are presented in Appendix VII (SI). The ratios of $[\text{polyampholyte}]/[\text{mucin}]$, at which the maximal turbidity values are observed are dependent on the nature of amphoteric polymers and solution pH.

It is interesting to note that when the solution pH was equal to or above pH_{IEP} of each polyampholyte, turbidity linearly decreased with addition of further portions of the polymer. This linear decrease is typically associated with simple dilution effects and indicates the absence of attractive interactions. Therefore, we can conclude that mucoadhesive interactions between polyampholyte and mucin are observed only at $\text{pHs} < \text{pH}_{\text{IEP}}$, where the macromolecules positively charged, and mucin remains negatively charged. This indicates that the nature of these interactions is primarily electrostatic. It is important to note that the interaction between a dosage form and a mucosal surface will be more complex than interactions between macromolecules of a polymer and mucin dispersions in solutions. This will be resulting in a deposition and adhesion of macromolecules on mucosal surface, their deeper penetration into the mucus gel and formation of an interpenetrating layer with mucin biomacromolecules.²⁵⁰

To further explore the nature of mucoadhesive interactions, additional turbidimetric titration experiments were conducted in solutions containing 8M urea (Figure 2.3-2d-f). Urea is known to disrupt hydrogen bonding and hydrophobic effects; it also has some mucolytic properties²⁵¹. The initial turbidity of mucin in urea solutions was around half of the values observed without any additive in aqueous solutions demonstrating the mucolytic properties of urea.

It is clearly seen from the titration curves that the presence of 8 M urea in solution does not prevent polyampholytes from interacting with mucin. However, there is a clear shift in $[\text{polyampholyte}]/[\text{mucin}]$ ratios at which maximal turbidity was detected, with higher values in the case of synthetic polyampholytes (Appendix VII, SI). This indicates that more macromolecules of synthetic polyampholytes are required to saturate the surface of mucin. Partially this is related to greater surface area of mucin, disrupted by mucolytic effect of urea

but may also be attributable to the involvement of hydrogen bonding and hydrophobic effects in the mucoadhesive interactions. In the case of BSA, the shift in the position of turbidity maximum on the titration curve is not observed at pH 2.0; however, at pH 3.5 saturation of mucin with BSA is seen at a lower [BSA]/[mucin] ratio. This could be related to the effects of urea on the conformation of BSA in contrast to minimal effects on the synthetic polyampholytes. Overall, the titration experiments conducted in the presence of 8M urea confirm that the primary nature of mucoadhesive interactions between polyampholytes and mucin is electrostatic attraction.

Isothermal titration calorimetry (ITC) is a powerful technique that can be used to study thermodynamics of specific interactions between compounds present in solutions.³⁸⁵⁻³⁸⁸ Previously, ITC has been reported in the studies of mucoadhesive interactions between mucins and chitosan^{389,390}, epigallocatechin³⁹¹ and poly(carboxylic acids)²⁵³. ITC data showed an exothermic interaction between polyampholytes and mucin at $\text{pH} < \text{pH}_{\text{IEP}}$. As enthalpy changes reflect the breakage and formation of bonds on the basis of their nature and strength, it can be used to assess the binding efficiency between species. The interaction between phthalylated L-PEI (Figure 2.3-2h) and mucin at pH 3.00 showed a strong binding effect with ΔH_{change} of -7.5 cal/mol and a high binding constant with a classical sigmoidal binding curve, whereas at pH=10.00 the data show weak non-specific interactions (ΔH_{change} of -1.5 cal/mol). Such difference confirms the previous findings from the turbidity experiments evidencing the role of electrostatic interactions between polymers and mucin. The profile of succinylated L-PEI interacting with mucins is similar to that of the phthalylated material but with a lower enthalpy change $\Delta H_{\text{change}} = -4.5$ cal/mol (Figure 2.3-2g). For BSA (Figure 2.3-2i), there is an initial dip in enthalpy change with low levels of mucin added, potentially reflecting changes in the BSA rather than interactions between the protein and the mucin. However, for succinylated L-PEI and BSA, at pH=2.50, both displayed stronger interactions with mucin than at pH=7.00 where only weak non-specific interactions were recorded. In summary, the ITC results confirmed the findings from the turbidimetric titrations that polymer : mucin interactions at $\text{pH} < \text{pH}_{\text{IEP}}$ are more pronounced than when $\text{pH} > \text{pH}_{\text{IEP}}$.

2.3.3 *Ex vivo* gastric mucoadhesion studies

Tensile testing is commonly used to quantify mucoadhesive properties of pharmaceutical formulations. In such tests, a pharmaceutical dosage form is usually attached to a mobile probe of a mechanical testing instrument, such as a texture analyser, and is then brought into contact with animal mucosal tissue. After a defined period of contact, the dosage

form is withdrawn from the mucosal tissue and a withdrawal force versus distance curve is recorded. This withdrawal curve is then used to calculate two mucoadhesion parameters, the peak force of detachment and the work of adhesion (calculated as the area under the curve). To conduct tensile tests, tablets were first formulated to ensure that they would not swell or rapidly disintegrate upon exposure to moisture. These tablets were subsequently spray-coated with polyampholytes mixed with sodium fluorescein.

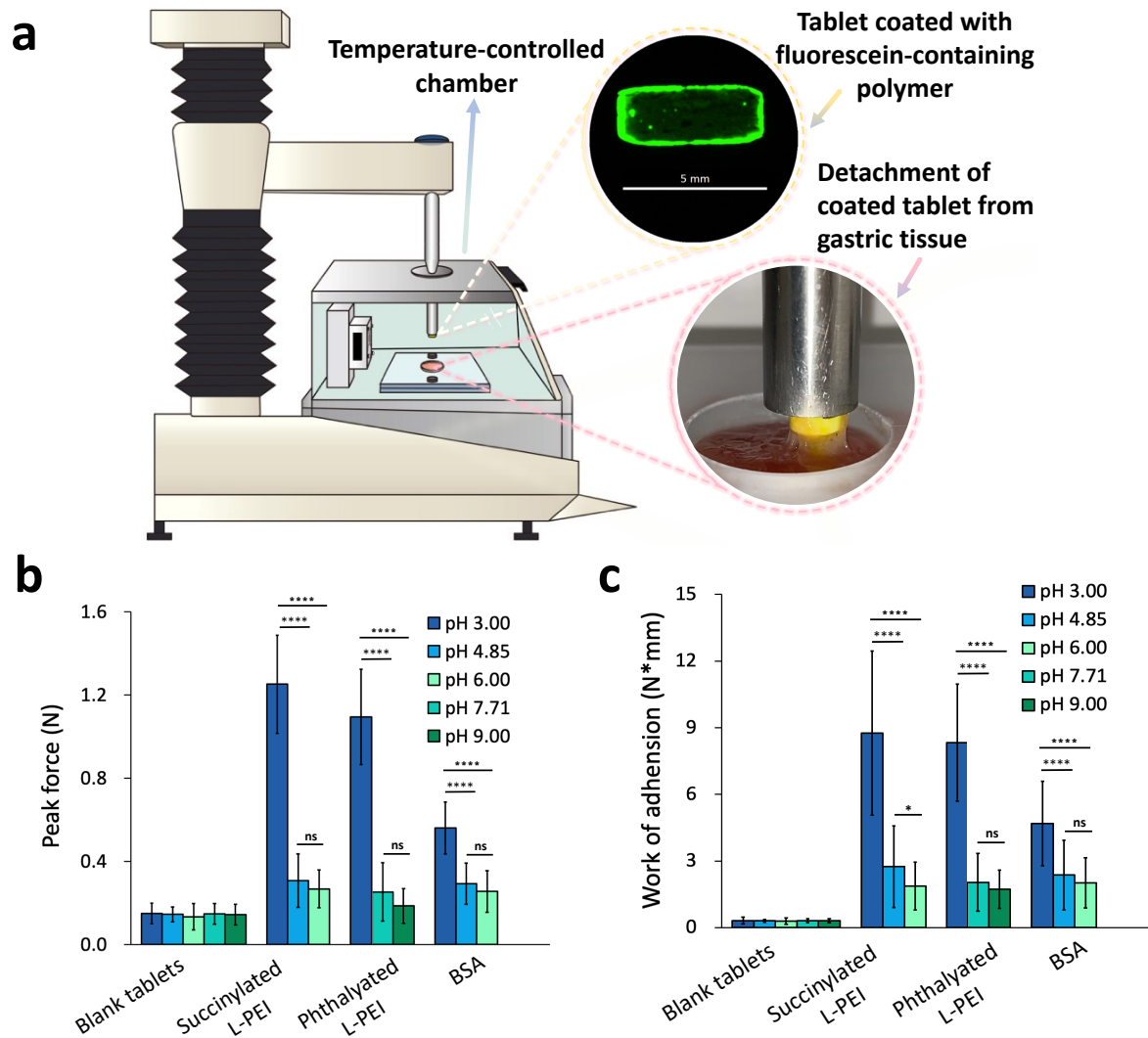


Figure 2.3-3. Illustration of tensile test methodology (a); effect of pH on peak force of detachment (b) and work of adhesion (c) of model tablets coated with succinylated L-PEI, phthalyated L-PEI and BSA on porcine gastric mucosa at $37 \pm 0.1^\circ\text{C}$. Mean \pm standard deviation, $n=20$. The statistically significant differences are represented as: **** $p < 0.0001$; ns: no significance.

The inclusion of sodium fluorescein allowed visualisation of the coating (Figure 3-3a) and the coating weight gain was 1.6%, 1.4% and 1.3%, for succinylated L-PEI, phthalyated L-PEI and BSA, respectively. Testing evaluated mucoadhesion of tablets coated with

succinylated L-PEI, phthalylated L-PEI and BSA, applied to porcine gastric mucosa and the peak force of detachment (Figure 3-3b) and the work of adhesion (Figure 3-3c) determined. The methodology for tensile testing followed that from the literature; Shitrit et al. attached tablets to the upper arm of the texture analyzer using double-sided adhesive tape.³⁹² A similar protocol was reported by Gyarmati et al. using double sided adhesive tape to adhere tablets to the probe.³⁸³ However, some groups prefer an alternative approach to fix tablets using cyanoacrylate adhesive, commonly referred to as “super glue”.³⁹³ Both strategies for fixing tablets have minimal effect on the test outcomes. In our study, the smaller size of model tablets (6mm in diameter) required faster speed, greater force and shorter contact time applied to the mucosal tissue surface. These parameters prevented tablets dropping from the probe of the texture analyzer, avoiding any potential interference with the results.

The pH of the mucosal tissues was varied in these experiments by adding small portions of 0.1 M NaOH or HCl directly on their surface, monitored with a pH meter. However, due to the irregularities of the mucosal surface, biological factors (e.g. enzymes, proteins) on the mucosal surface and limited sensitivity and range of typical pH meters, determination of pHs on mucosal surface is complex and tends to present as an average or aggregated value. Micro pH electrodes can be used to assess local pH of mucosal surfaces, but site-to-site variations still exist. Buffer solutions can be used to provide a constant pH in biological studies, supporting experimental reproducibility but may not fully capture the pH variations seen *in vivo*. The pHs of the solutions were again selected to where pH was either below, above or at pH_{IEP} of each polyampholyte. Blank tablets without polyampholyte coating were used as a negative control.

The blank tablets did not show any significant pH-dependent differences in their detachment characteristics (Figures 3-3b and c). In all cases, the polymer coated tablets showed stronger mucoadhesive properties than uncoated blank tablets. However, the tablets coated with polyampholytes exhibited strong adhesion dependence on the tissue pH. When the pH was below pH_{IEP} of each polyampholyte, the coated tablets exhibited significantly stronger mucoadhesive performance, both in terms of the peak force of detachment and the work of adhesion values ($p < 0.0001$). Under these conditions the polyampholyte is positively charged and so can interact with mucus predominantly electrostatically, resulting in strong mucoadhesion. However, other factors such as the effect of water transport and capillary forces may also play a considerable role in mucoadhesion^{394,395}. In contrast, a significant reduction in mucoadhesive properties was observed in experiments conducted at $pH \geq pH_{IEP}$. This can be attributed to a lack of electrostatic attraction between the dosage form and

mucosal tissue when the surface of tablets is either non-charged or negatively charged. The adhesion in this case can only be achieved either through weak hydrogen bonds or physical entanglements between the macromolecules of polyampholyte and mucins. There were no significant differences between adhesion at $\text{pH}=\text{pH}_{\text{IEP}}$ with adhesion when $\text{pH}>\text{pH}_{\text{IEP}}$.

The tablet adhesion studies show a strong correlation exists between the mucoadhesive properties of polyampholytes assessed in solutions (e.g. turbidimetry) and when applied in a solid state (as a tablet coating). In both cases, strong mucoadhesive properties were observed when pH was below the pH_{IEP} of the polyampholyte.

The above studies explored adhesion in essentially “static” systems which poorly reflect fluid dynamics encountered on clinical use. Previously, we have developed a fluorescence microscopy-based flow-through test that provides information on the retention mucoadhesive formulations on animal mucosal tissues^{5,369}.

The two synthetic polyampholytes and BSA were labelled fluorescently and prepared in solutions for flow through experiments. Retention of FITC-labelled succinylated L-PEI, phthaylated L-PEI and BSA was evaluated on porcine gastric mucosa washed with solutions of different pHs. FITC-labelled dextran was used as a negative control due to its poor mucoadhesive properties.

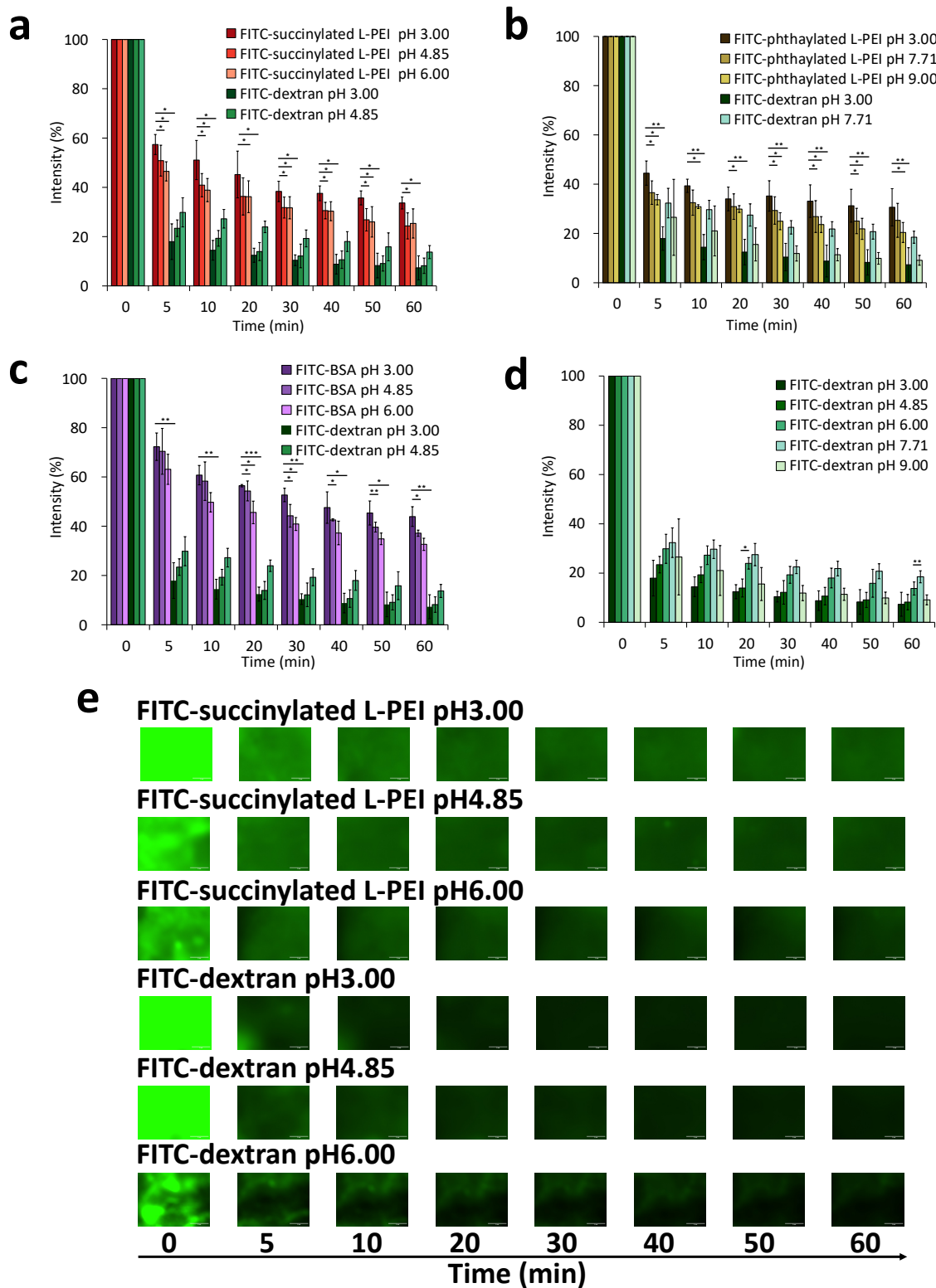


Figure 2.3-4. Effect of pH on mucosal retention of 1 mg/mL FITC-succinylated L-PEI (a), FITC-phthaylated L-PEI (b), FITC-BSA (c) and FITC-dextran (d) on porcine gastric mucosa washed with different volumes of SGF (0.43 mL/min) for 60 min and FITC-dextran as negative control at $37 \pm 0.1^\circ\text{C}$; exemplar fluorescence images (e) with retention of FITC labelled succinylated L-PEI and FITC-dextran after irrigation with different volumes of SGF under different pH at a flow rate of 0.43mL/min; FITC-dextran was used as negative control. Scale bars are 2 mm. Mean \pm standard deviation, n=3. The statistically significant differences are represented as: *** $p < 0.001$; ** $p < 0.01$; * $p < 0.05$; ns: no significance.

Fluorescence images (Figure 2.3-4e, Appendix V-VI) were analysed using Image J software and converted into numerical values (Figure 2.3-4a-d) taking fluorescence at time zero as 100% (with tissue background autofluorescence removed).

Throughout 60 min of washing with solutions at $\text{pH} < \text{pH}_{\text{IEP}}$, there was a statistically significant greater retention of all the polyampholytes compared to FITC-dextran. This is attributed to electrostatic attraction between the positively charged polyampholytes and negatively charged mucins.³⁹⁶ After 5 min washing, the retention of FITC-succinylated L-PEI, FITC-phthaylated L-PEI and FITC-BSA was 57.4%, 44.5% and 72.3%, respectively, whereas the retention of FITC-dextran was 17.9% (Appendix VIII, SI). Further, 33.6%, 30.6% and 43.9% of FITC-succinylated L-PEI, FITC-phthaylated L-PEI and FITC-BSA, respectively, remained on the tissue after 60 min washing. In contrast, FITC-dextran poorly interacted with the gastric mucosa and, resulting in only 7.3% of initial fluorescence remaining after 60 min washing through. It should be noted that it is feasible that this remaining fluorescence may derive from FITC-dextran penetrating into the gastric tissue rather than adhering to the surface. For our new synthetic polyampholytes, these results are in agreement with the peak force of detachment data (Figure 2.3-3b) with the succinylated material showing slightly greater peak force and retention values than the phthaylated derivative. This may be associated with the differences in the degrees of substitution (DS) of the synthetic polyampholytes (see SI). According to DS data, succinylated L-PEI (DS=46%) retains more cationic secondary amine groups than phthaylated L-PEI (DS=86%), leading to increased electrostatic interactions with carboxylate groups and ester sulfates within negatively charged mucins.

At $\text{pH} \geq \text{pH}_{\text{IEP}}$, polyampholytes illustrated significantly better retention compared to FITC-dextran. It could be explained by their polyelectrolyte nature and higher viscosity. However, FITC-BSA showed greater retention throughout the washing study than either FITC-succinylated L-PEI and FITC-phthaylated L-PEI. It is likely that the smaller molecular weight and compact conformation of BSA as a globular protein allows its greater penetration into the gastric mucosa which allows better retention.

It is interesting to note that retention of the negative control FITC-dextran over a wide range of pHs also was found to be pH-dependent with statistically significant differences between the wash-off profiles observed at pHs 4.85 and 6.00 when evaluated at 20 mins ($p < 0.05$) and at pH 6.00 and 7.71 after 60 min ($p < 0.01$). Dextran is a non-ionic polysaccharide and so does not carry a pH dependent charge. However, the gastric mucus itself is also affected by pH as gastric mucin undergoes a pH-dependent sol-gel transition,

existing in a gel state at acidic pHs, and in a “solution phase” at neutral pH³⁹⁷. Physiologically, at lower pH (e.g. pH~2 as in vivo), the gel phase mucin acts as a barrier to prevent diffusion of materials back to the tissue surface and indeed the high viscosity of the gastric mucus gel on the luminal side can prevent stomach HCl from reaching the mucosal tissue.³⁹⁸ At neutral pH, when the mucin is in a solution state, then FITC-dextran could penetrate into the mucus layer resulting in the highest retention at pH=7.71.

2.4 Conclusion

Polyampholytes have attracted lots of attention in the last decades due to their unique physicochemical properties. However, research exploring mucoadhesive properties and mechanisms of polyampholytes is limited. This is the first study that systematically explores the mucoadhesive properties of synthetic and natural polyampholytes. Two new polyampholytes were synthesised by reacting linear polyethylene imine with succinic or phthalic anhydrides. Bovine serum albumin was chosen as a representative of natural polyampholytes. These polyampholytes were used to study mucoadhesive interactions with mucin at different pHs. These materials were also evaluated as model dosage forms (coated tablets and solutions) in terms of their adhesion to and retention on porcine gastric mucosa at different pHs. It was established that pH of solution plays a major role in determining the extend of mucoadhesive interactions and ability of these materials to adhere to mucosal tissue. When the solution pH is below the pH_{IEP} of each polyampholyte, they exhibit strong attractive interactions with mucin and very good mucoadhesive ability towards mucosal tissues, driven predominantly by electrostatic forces with some contributions from chain entanglements and other weak attractions. When the solution pH is around or above the pH_{IEP} the polyampholytes exhibit modest mucoadhesive properties and is attributable to chain entanglement or penetration into the mucus layer. The use of three dissimilar polyampholytes, a broad range of pHs and experimental techniques to evaluate mucoadhesive properties in this study provides confidence that the relationship between solution pH, pH_{IEP} and mucoadhesive performance will be common for all amphoteric polymers. This information is important as it will allow predicting mucoadhesive performance of many amphoteric systems, including commonly used gelatin, many other proteins and also synthetic polymers.

2.5 References

- (343) Sau-Hung Spence, L.; Robinson, J. R. The contribution of anionic polymer structural features to mucoadhesion. *Journal of Controlled Release* **1987**, 5 (3), 223.

- (344) Haugstad, K. E.; Håti, A. G.; Nordgård, C. T.; Adl, P. S.; Maurstad, G.; Sletmoen, M.; Draget, K. I.; Dias, R. S.; Stokke, B. T. Direct Determination of Chitosan–Mucin Interactions Using a Single-Molecule Strategy: Comparison to Alginate–Mucin Interactions. *Polymers* **2015**, *7* (2), 161.
- (345) Gu, J.; Robinson, J.; Leung, S. Binding of acrylic polymers to mucin/epithelial surfaces: structure-property relationships. *Critical reviews in therapeutic drug carrier systems* **1988**, *5* (1), 21.
- (346) Javed, Q. U. A.; Syed, M. A.; Arshad, R.; Rahdar, A.; Irfan, M.; Raza, S. A.; Shahnaz, G.; Hanif, S.; Díez-Pascual, A. M. Evaluation and Optimization of Prolonged Release Mucoadhesive Tablets of Dexamethasone for Wound Healing: In Vitro–In Vivo Profiling in Healthy Volunteers. *Pharmaceutics* **2022**, *14* (4), 807.
- (347) Kristó, K.; Módra, S.; Hornok, V.; Süvegh, K.; Ludasi, K.; Aigner, Z.; Kelemen, A.; Sovány, T.; Pintye-Hódi, K.; Regdon, G. Investigation of Surface Properties and Free Volumes of Chitosan-Based Buccal Mucoadhesive Drug Delivery Films Containing Ascorbic Acid. *Pharmaceutics* **2022**, *14* (2), 345.
- (348) Banerjee, A.; Lee, J.; Mitragotri, S. Intestinal mucoadhesive devices for oral delivery of insulin. *Bioengineering & translational medicine* **2016**, *1* (3), 338.
- (349) Pagano, C.; Giovagnoli, S.; Perioli, L.; Tiralti, M. C.; Ricci, M. Development and characterization of mucoadhesive-thermoreponsive gels for the treatment of oral mucosa diseases. *European Journal of Pharmaceutical Sciences* **2020**, *142*, 105125.
- (350) Cook, S. L.; Methven, L.; Parker, J. K.; Khutoryanskiy, V. V. Polysaccharide food matrices for controlling the release, retention and perception of flavours. *Food Hydrocolloids* **2018**, *79*, 253.
- (351) Cook, S. L.; Woods, S.; Methven, L.; Parker, J. K.; Khutoryanskiy, V. V. Mucoadhesive polysaccharides modulate sodium retention, release and taste perception. *Food Chemistry* **2018**, *240*, 482.
- (352) Aspinall, S. R.; Parker, J. K.; Khutoryanskiy, V. V. Oral care product formulations, properties and challenges. *Colloids and Surfaces B: Biointerfaces* **2021**, *200*, 111567.
- (353) Chatterjee, B.; Amalina, N.; Sengupta, P.; Mandal, U. K. Mucoadhesive polymers and their mode of action: A recent update. *Journal of Applied Pharmaceutical Science* **2017**, *7* (5), 195.
- (354) Laffleur, F. Mucoadhesive polymers for buccal drug delivery. *Drug Development and Industrial Pharmacy* **2014**, *40* (5), 591.
- (355) Laffleur, F.; Netsomboon, K.; Bernkop-Schnürch, A.; Westmeier, D.; Stauber, R. H.; Docter, D. Comprehensive mucoadhesive study of anionic polymers and their derivate. *European Polymer Journal* **2017**, *93*, 314.
- (356) Khutoryanskiy, V. V. Advances in mucoadhesion and mucoadhesive polymers. *Macromolecular bioscience* **2011**, *11* (6), 748.
- (357) Brotherton, E. E.; Neal, T. J.; Kaldybekov, D. B.; Smallridge, M. J.; Khutoryanskiy, Vitaliy V.; Armes, S. P. Aldehyde-functional thermoresponsive diblock copolymer worm gels exhibit strong mucoadhesion. *Chemical Science* **2022**, *13* (23), 6888.
- (358) Bekturov, E. A.; Kudaibergenov, S. E.; Rafikov, S. R. SYNTHETIC POLYMERIC AMPHOLYTES IN SOLUTION. *Journal of Macromolecular Science, Part C* **1990**, *30* (2), 233.
- (359) Ciferri, A.; Kudaibergenov, S. Natural and Synthetic Polyampholytes, 1. *Macromolecular Rapid Communications* **2007**, *28* (20), 1953.

- (360) Kudaibergenov, S. E.; Ciferri, A. Natural and Synthetic Polyampholytes, 2. *Macromolecular Rapid Communications* **2007**, *28* (20), 1969.
- (361) Yang, X.; Robinson, J.; Academic Press: Sandiego, CA, USA, 1998.
- (362) Wang, J.; Tabata, Y.; Bi, D.; Morimoto, K. Evaluation of gastric mucoadhesive properties of aminated gelatin microspheres. *Journal of Controlled Release* **2001**, *73* (2), 223.
- (363) Nishio, F.; Hirata, I.; Nakamae, K.; Tsuga, K.; Kato, K. Mucoadhesion of polyamphoteric hydrogels synthesized from acrylic acid and N,N-dimethylaminopropyl acrylamide. *International Journal of Adhesion and Adhesives* **2021**, *104*, 102746.
- (364) Withers, C. A.; Cook, M. T.; Methven, L.; Gosney, M. A.; Khutoryanskiy, V. V. Investigation of milk proteins binding to the oral mucosa. *Food & Function* **2013**, *4* (11), 1668.
- (365) Shan, X.; Williams, A. C.; Khutoryanskiy, V. V. Polymer structure and property effects on solid dispersions with haloperidol: Poly(N-vinyl pyrrolidone) and poly(2-oxazolines) studies. *Int J Pharm* **2020**, *590*, 119884.
- (366) Philippova, O. E.; Volkov, E. V.; Sitnikova, N. L.; Khokhlov, A. R.; Desbrieres, J.; Rinaudo, M. Two Types of Hydrophobic Aggregates in Aqueous Solutions of Chitosan and Its Hydrophobic Derivative. *Biomacromolecules* **2001**, *2* (2), 483.
- (367) Freire, E.; Mayorga, O. L.; Straume, M. Isothermal titration calorimetry. *Analytical chemistry* **1990**, *62* (18), 950A.
- (368) Indyk, L.; Fisher, H. F. In *Methods in Enzymology*; Academic Press, 1998; Vol. 295.
- (369) Moiseev, R. V.; Kaldybekov, D. B.; Filippov, S. K.; Radulescu, A.; Khutoryanskiy, V. V. Maleimide-decorated PEGylated mucoadhesive liposomes for ocular drug delivery. *Langmuir* **2022**, *38* (45), 13870.
- (370) Kudaibergenov, S. E.; Nuraje, N. Intra- and Interpolyelectrolyte Complexes of Polyampholytes. *Polymers* **2018**, *10* (10), 1146.
- (371) Zhao, J.; Burke, N. A.; Stöver, H. D. Preparation and study of multi-responsive polyampholyte copolymers of N-(3-aminopropyl) methacrylamide hydrochloride and acrylic acid. *RSC advances* **2016**, *6* (47), 41522.
- (372) Bhattacharjee, S. DLS and zeta potential – What they are and what they are not? *Journal of Controlled Release* **2016**, *235*, 337.
- (373) de la Casa, E. J.; Guadix, A.; Ibáñez, R.; Guadix, E. M. Influence of pH and salt concentration on the cross-flow microfiltration of BSA through a ceramic membrane. *Biochemical engineering journal* **2007**, *33* (2), 110.
- (374) Łapińska, U.; Saar, K. L.; Yates, E. V.; Herling, T. W.; Müller, T.; Challa, P. K.; Dobson, C. M.; Knowles, T. P. Gradient-free determination of isoelectric points of proteins on chip. *Physical Chemistry Chemical Physics* **2017**, *19* (34), 23060.
- (375) Elgersma, A. V.; Zsom, R. L.; Norde, W.; Lyklema, J. The adsorption of bovine serum albumin on positively and negatively charged polystyrene latices. *Journal of Colloid and Interface Science* **1990**, *138* (1), 145.
- (376) Peppas, N. A.; Sahlin, J. J. Hydrogels as mucoadhesive and bioadhesive materials: a review. *Biomaterials* **1996**, *17* (16), 1553.
- (377) Allen, A.; Bell, A.; Mantle, M.; Pearson, J. P. In *Mucus in Health and Disease—II*; Chantler, E. N.; Elder, J. B.; Elstein, M., Eds.; Springer US: Boston, MA, 1982, DOI:10.1007/978-1-4615-9254-9_15 10.1007/978-1-4615-9254-9_15.
- (378) Kočevár-Nared, J.; Kristl, J.; Šmid-Korbar, J. Comparative rheological investigation of crude gastric mucin and natural gastric mucus. *Biomaterials* **1997**, *18* (9), 677.

- (379) Fefelova, N. A.; Nurkeeva, Z. S.; Mun, G. A.; Khutoryanskiy, V. V. Mucoadhesive interactions of amphiphilic cationic copolymers based on [2-(methacryloyloxy)ethyl]trimethylammonium chloride. *International Journal of Pharmaceutics* **2007**, *339* (1), 25.
- (380) Szilágyi, B. Á.; Mammadova, A.; Gyarmati, B.; Szilágyi, A. Mucoadhesive interactions between synthetic polyaspartamides and porcine gastric mucin on the colloid size scale. *Colloids and Surfaces B: Biointerfaces* **2020**, *194*, 111219.
- (381) Rossi, S.; Ferrari, F.; Bonferoni, M. C.; Caramella, C. Characterization of chitosan hydrochloride–mucin interaction by means of viscosimetric and turbidimetric measurements. *European journal of pharmaceutical sciences* **2000**, *10* (4), 251.
- (382) Menchicchi, B.; Fuenzalida, J.; Hensel, A.; Swamy, M.; David, L.; Rochas, C.; Goycoolea, F. Biophysical analysis of the molecular interactions between polysaccharides and mucin. *Biomacromolecules* **2015**, *16* (3), 924.
- (383) Gyarmati, B.; Stankovits, G.; Szilágyi, B. Á.; Galata, D. L.; Gordon, P.; Szilágyi, A. A robust mucin-containing poly(vinyl alcohol) hydrogel model for the in vitro characterization of mucoadhesion of solid dosage forms. *Colloids and Surfaces B: Biointerfaces* **2022**, *213*, 112406.
- (384) Haji, F.; Kim, D. S.; Tam, K. C. Tannic acid-coated cellulose nanocrystals with enhanced mucoadhesive properties for aquaculture. *Carbohydrate Polymers* **2023**, *312*, 120835.
- (385) Filippov, S. K.; Khusnutdinov, R. R.; Inham, W.; Liu, C.; Nikitin, D. O.; Semina, I. I.; Garvey, C. J.; Nasibullin, S. F.; Khutoryanskiy, V. V.; Zhang, H. Hybrid nanoparticles for haloperidol encapsulation: Quid est optimum? *Polymers* **2021**, *13* (23), 4189.
- (386) Khalili, H.; Brocchini, S.; Khaw, P. T.; Filippov, S. K. Comparative thermodynamic analysis in solution of a next generation antibody mimetic to VEGF. *RSC advances* **2018**, *8* (62), 35787.
- (387) Zhang, X.; Chytil, P.; Etrych, T. s.; Liu, W.; Rodrigues, L.; Winter, G.; Filippov, S. K.; Papadakis, C. M. Binding of HSA to Macromolecular p HPMA Based Nanoparticles for Drug Delivery: An Investigation Using Fluorescence Methods. *Langmuir* **2018**, *34* (27), 7998.
- (388) Filippov, S. K.; Papagiannopoulos, A.; Riabtseva, A.; Pispas, S. Adsorption of lysozyme on pH-responsive PnBA-b-PAA polymeric nanoparticles: studies by stopped-flow SAXS and ITC. *Colloid and Polymer Science* **2018**, *296*, 1183.
- (389) Menchicchi, B.; Fuenzalida, J.; Bobbili, K. B.; Hensel, A.; Swamy, M. J.; Goycoolea, F. Structure of chitosan determines its interactions with mucin. *Biomacromolecules* **2014**, *15* (10), 3550.
- (390) Meng-Lund, E.; Muff-Westergaard, C.; Sander, C.; Madelung, P.; Jacobsen, J. A mechanistic based approach for enhancing buccal mucoadhesion of chitosan. *International journal of pharmaceutics* **2014**, *461* (1-2), 280.
- (391) Zhao, Y.; Chen, L.; Yakubov, G.; Aminiafshar, T.; Han, L.; Lian, G. Experimental and theoretical studies on the binding of epigallocatechin gallate to purified porcine gastric mucin. *The journal of physical chemistry B* **2012**, *116* (43), 13010.
- (392) Shitrit, Y.; Bianco-Peled, H. Acrylated chitosan for mucoadhesive drug delivery systems. *International Journal of Pharmaceutics* **2017**, *517* (1), 247.
- (393) Bernkop-Schnürch, A.; Guggi, D.; Pinter, Y. Thiolated chitosans: development and in vitro evaluation of a mucoadhesive, permeation enhancing oral drug delivery system. *Journal of Controlled Release* **2004**, *94* (1), 177.

- (394) Pham, Q. D.; Nöjd, S.; Edman, M.; Lindell, K.; Topgaard, D.; Wahlgren, M. Mucoadhesion: mucin-polymer molecular interactions. *International Journal of Pharmaceutics* **2021**, *610*, 121245.
- (395) Ivarsson, D.; Wahlgren, M. Comparison of in vitro methods of measuring mucoadhesion: Ellipsometry, tensile strength and rheological measurements. *Colloids and Surfaces B: Biointerfaces* **2012**, *92*, 353.
- (396) Khutoryanskiy, V. V. Advances in Mucoadhesion and Mucoadhesive Polymers. *Macromol. Biosci.* **2011**, *11*, 748.
- (397) Celli, J.; Gregor, B.; Turner, B.; Afdhal, N. H.; Bansil, R.; Erramilli, S. Viscoelastic properties and dynamics of porcine gastric mucin. *Biomacromolecules* **2005**, *6* (3), 1329.

Author Contributions

MF: investigation, methodology, writing-original draft preparation; SKF: investigation; ACW: supervision, writing-review and editing; VVK: conceptualisation, supervision, resources, writing-review and editing. All authors have read and agreed to the published version of the manuscript.

Conflicts of interest

There are no conflicts to declare.

Acknowledgements

VVK acknowledges the financial support provided by the Royal Society for his Industry Fellowship (IF/R2/222031). VVK is also grateful to Prof Sarkyt E. Kudaibergenov from the Institute of Polymer Materials and Technologies (Kazakhstan) for useful discussions and the encouragement to study mucoadhesive properties of amphoteric polymers. The authors gratefully acknowledge Technical Services staff within Chemical Analysis Facility at the University of Reading for technical support & assistance in this work. The authors acknowledge Prof Rebecca Green for providing access to her isothermal titration calorimetry instrument.

2.6 Supporting Information

On the mucoadhesive properties of synthetic and natural polyampholytes

Manfei Fu^a, Sergej Filippov^b, Adrian C. Williams^a, Vitaliy V. Khutoryanskiy^{*a}

- School of Pharmacy, University of Reading, Whiteknights, Post Office Box 224, Reading RG6 6AD, United Kingdom
- Pharmaceutical Science Laboratory, Faculty of Science and Engineering, Åbo Akademi University, 20520 Turku, Finland

Experiment section

Synthesis of linear poly (ethyleneimine) (L-PEI)

L-PEI was synthesized by acidic hydrolysis of poly(2-ethyl-2-oxazoline) (PEOZ) following the protocol of Shan et al²⁶⁵. Briefly, PEOZ (5.00 g) was dissolved in 50 mL 37 wt% HCl followed by adding 50 mL deionized water and heated for 15 h at 100°C. Then the L-PEI solution was diluted in cold deionized water. Cool NaOH aqueous solution (4 M) was added dropwise to the L-PEI solution until the L-PEI precipitated at pH 10-11³²¹. The precipitate was washed with deionized water until neutral pH and dried over vacuum oven to obtain dried L-PEI (1.9 g, 89 %).

¹H-Nuclear magnetic resonance spectroscopy (¹H-NMR)

10mg succinylated L-PEI or phthaylated L-PEI was dissolved in 1 mL D₂O, whereas dried L-PEI dissolved in 1 mL methanol-d₄. The samples were transferred to NMR tube and analysed by a Bruker spectrometer operating at 400 MHz. All chemical shifts are given in ppm. PEOZ, ¹H NMR (400 MHz, MeOD) δ 3.56 (d, J = 30.0 Hz, 4H), 2.44 (ddd, J = 21.3, 13.5, 7.1 Hz, 2H), 1.12 (q, J = 7.5 Hz, 3H); L-PEI, ¹H NMR (400 MHz, MeOD) δ 2.76 (d, J = 15.5 Hz, 1H); PEI-SA, ¹H NMR (400 MHz, D₂O) δ 3.99 – 2.64 (m, 4H), 2.64 – 2.20 (m, 1H); PEI-PA, ¹H NMR (400 MHz, D₂O) δ 8.01 – 6.79 (m, 1H), 4.38 – 2.02 (m, 2H).

MestReNova software was used for spectral analysis. The degree of substitution (DS) of succinylated L-PEI and phthaylated L-PEI was calculated using peak integration, according to Equation (1) and Equation (2), separately:

$$\%DS = \frac{\int \text{Signal } c / n_c}{\int \text{Signal } a+b / n_{a+b}} \times 100 \quad (1)$$

$$\%DS = \frac{\int \text{Signal } d,e,f,g / n_{d,e,f,g}}{\int \text{Signal } a+b / n_{a+b}} \times 100 \quad (2)$$

where signal a is assigned to $-\text{CH}_2\text{CH}_2$ on the main backbone of unreacted L-PEI, signal b is associated with $-\text{CH}_2\text{CH}_2$ on the main backbone of amide group, signal c is contributed to side chain of succinic anhydride, signal d, e, f, g are contributed to side chain of phthalic anhydride, n_a is the number of protons in $-\text{CH}_2\text{CH}_2$ on the main backbone of unreacted L-PEI, n_b is number of protons in $-\text{CH}_2\text{CH}_2$ on the main backbone of amide group, n_c is number of $-\text{CH}_2\text{CH}_2$ on the side chain of succinic anhydride, n_d, e, f, g are the number of $-\text{CH}$ on the side chain of phthalic anhydride.

Turbidity measurements

All samples were dissolved in deionized water (1 mg/mL) and measured at 400 nm at different pH values. The pH was adjusted by adding 0.1 M NaOH or HCl. Every titration was repeated in triplicate and the turbidity values are reported as mean \pm standard deviation.

Electrophoretic mobility measurements

All samples were dissolved in deionized water (1 mg/mL) and pH was adjusted by adding 0.1 M NaOH or HCl. All measurements were conducted at 25°C and repeated in triplicate, the values are reported as mean \pm standard deviation.

Isothermal titration calorimetry (ITC)

100 μL polymer solution was loaded into the syringe and titrated into mucin dispersions loaded in 950 μL calorimeter sample cell. The reference cell was filled with a buffer at different pH values. Titrations were performed automatically, where 5.05 μL portions from the syringe were injected automatically into the sample cell every 300 s. All ITC measurements were conducted at 25 °C. The results were analysed using Origin Lab® version 9.0 software.

Preparation of polymer coated tablets

Blank tablets are composed of hydroxypropyl methylcellulose (HPMC) (40%), microcrystalline cellulose (MCC) (40%), barium sulphate (19%) and magnesium stearate (1%). All ingredients except for magnesium stearate were blended using tumble mixer (Glen Creston Ltd, UK) for 10 mins, subsequently magnesium stearate as lubricant was added and mixed for an additional 2 min. The mixtures were compressed by using a single punch tableting machine (RIVA G.B. Ltd, UK) with compression force set at 12. The speed of tableting machine is 40 tablets/min. The obtained blank tablets were coated with 2% polymer solutions and 5% sodium fluorescein was added to these solutions using mini spray coated

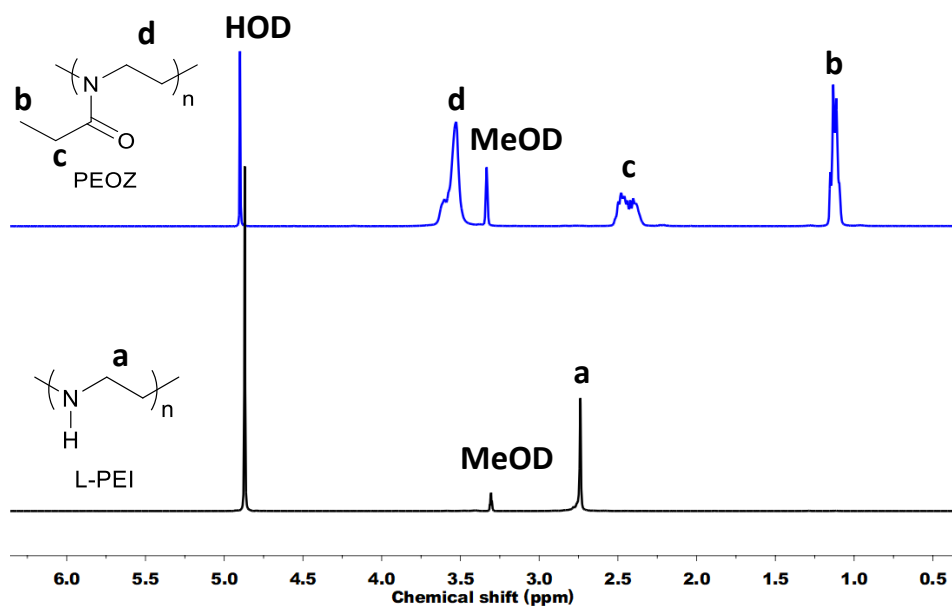
/ drier 2 machine (Caleva process solution Ltd, UK). All spray conditions were maintained as agitator power 65-70%, fan power 70-75%, pump power 100% and temperature at 42-44°C. The weight of blank tablets is 65.5 ± 0.6 mg, the size is 0.6*0.2 mm, the hardness is 40.3 ± 1.7 N.

Preparation of polymer-FITC solutions

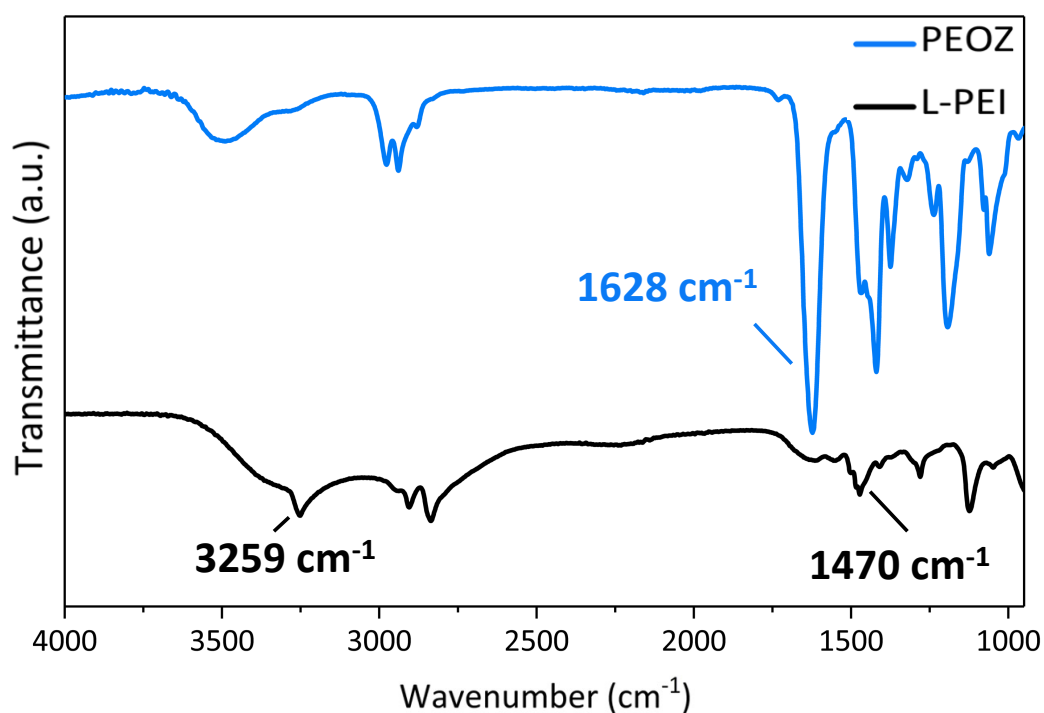
Succinylated L-PEI, phthalylated L-PEI and BSA were labelled with FITC, according to³⁶⁴. Polymer solutions were prepared in 0.1 M carbonate buffer (pH 9) (2 mg/mL), while FITC dissolved in DMSO (1 mg/mL). Adding FITC DMSO solution to polymer solutions reached a volume ratio of polymer to FITC 20:1. The resulting polymer-FITC solutions were incubated a light off container with stirring overnight at room temperature. The polymer-FITC solutions were dialyzed against 2.5 L of 0.01 M phosphate buffered saline (PBS) (MWCO 3.5KDa) at pH 7.4 for 72 h. All obtained mixtures were recovered by freeze-drying.

Characterization of L-PEI

Firstly, L-PEI was obtained via acidic hydrolysis of commercial PEOZ³²⁰. The full conversion was confirmed by ¹H-NMR (Appendix I) and FTIR spectra (Appendix II). The main backbone signal d of PEOZ and both signals b and c of its side chains was eliminated. And signal a was assigned to the backbone of L-PEI. The complete hydrolysis to L-PEI was confirmed by FTIR through the disappearance of the amide carbonyl vibration at 1628 cm^{-1} and the presence of new strong band at 1470 cm^{-1} and 3259 cm^{-1} was associated with the N-H vibration of L-PEI³⁴². Then obtained L-PEI was re-acylated via nucleophilic addition reaction and elimination reaction with succinic anhydride and phthalic anhydride in DMSO solution using TEA as a base.



Appendix I. ¹H-NMR spectra of PEOZ and L-PEI recorded in methanol-d₄.

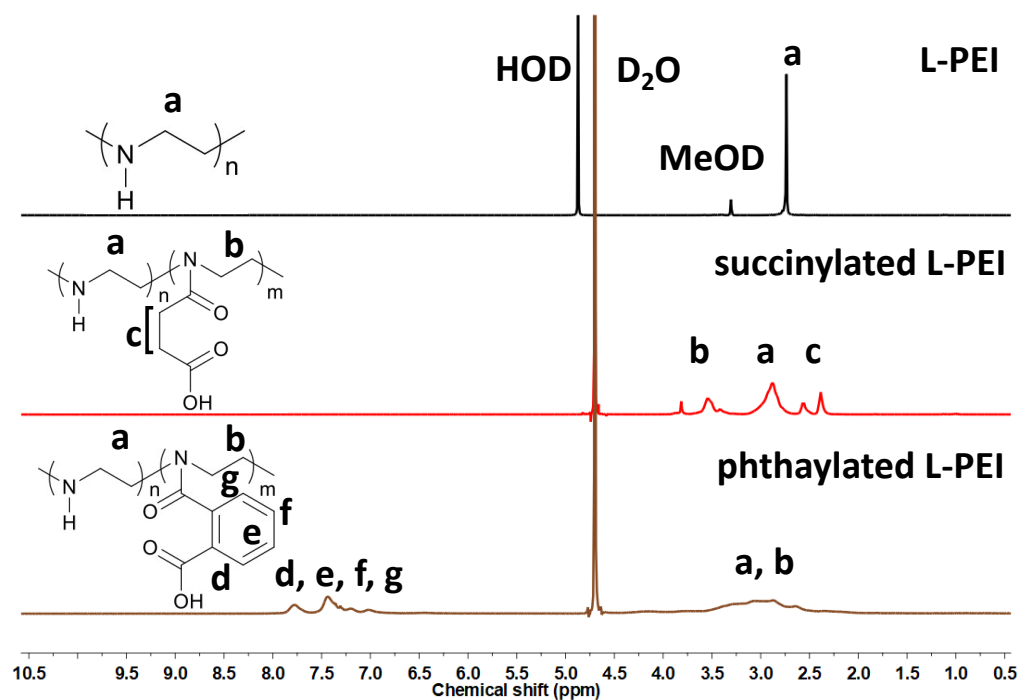


Appendix II. FTIR spectra of PEOZ and L-PEI.

Characterization of succinylated L-PEI and phthaylated L-PEI

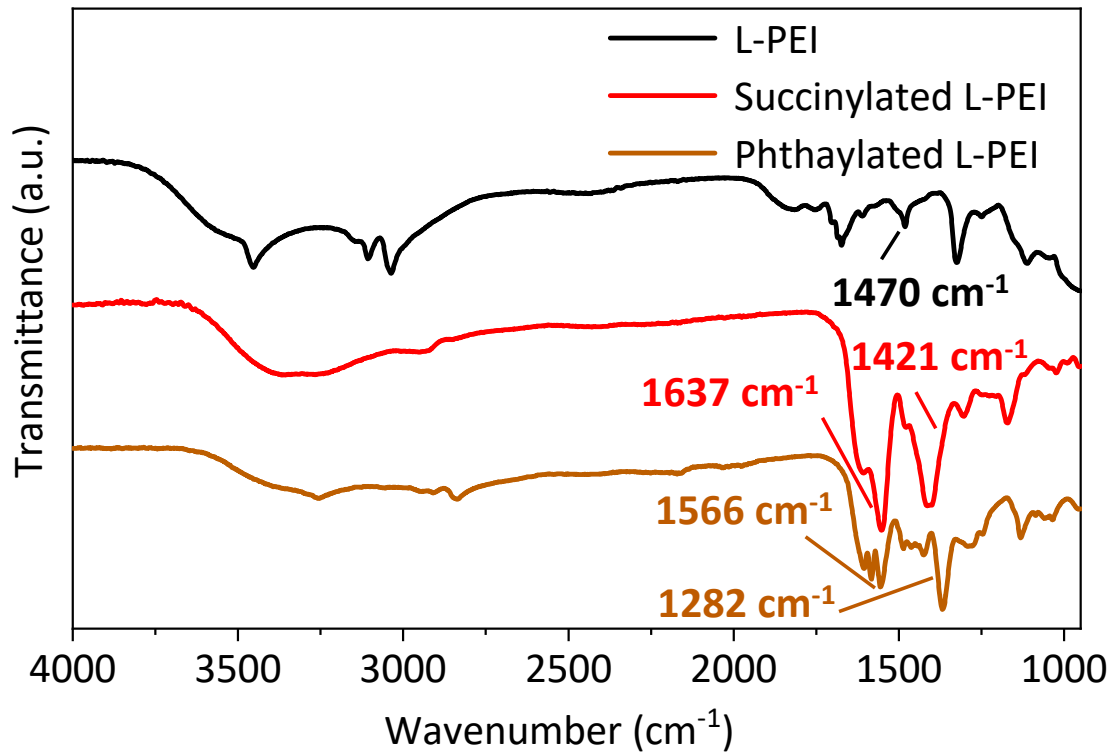
As shown in Appendix III, the backbone of L-PEI repeating units appeared at 2.75 ppm (signal a), while reacted L-PEI units shifted to 2.90-3.30 ppm (signal b) upon acylation with different anhydride as new formed amide group. And 3.40 ppm (signal c) was assigned to the side chain of succinylated L-PEI. 6.75-7.75 ppm (signal d, e, f, g) derived from the side chain

of phthaylated L-PEI. The degree of substitution (DS) of succinylated L-PEI and phthaylated L-PEI was determined by comparing the area under the signal from side group to the area under the signal of main backbone. The result confirmed that the DS of succinylated L-PEI and phthaylated L-PEI was 46% and 86%, respectively.

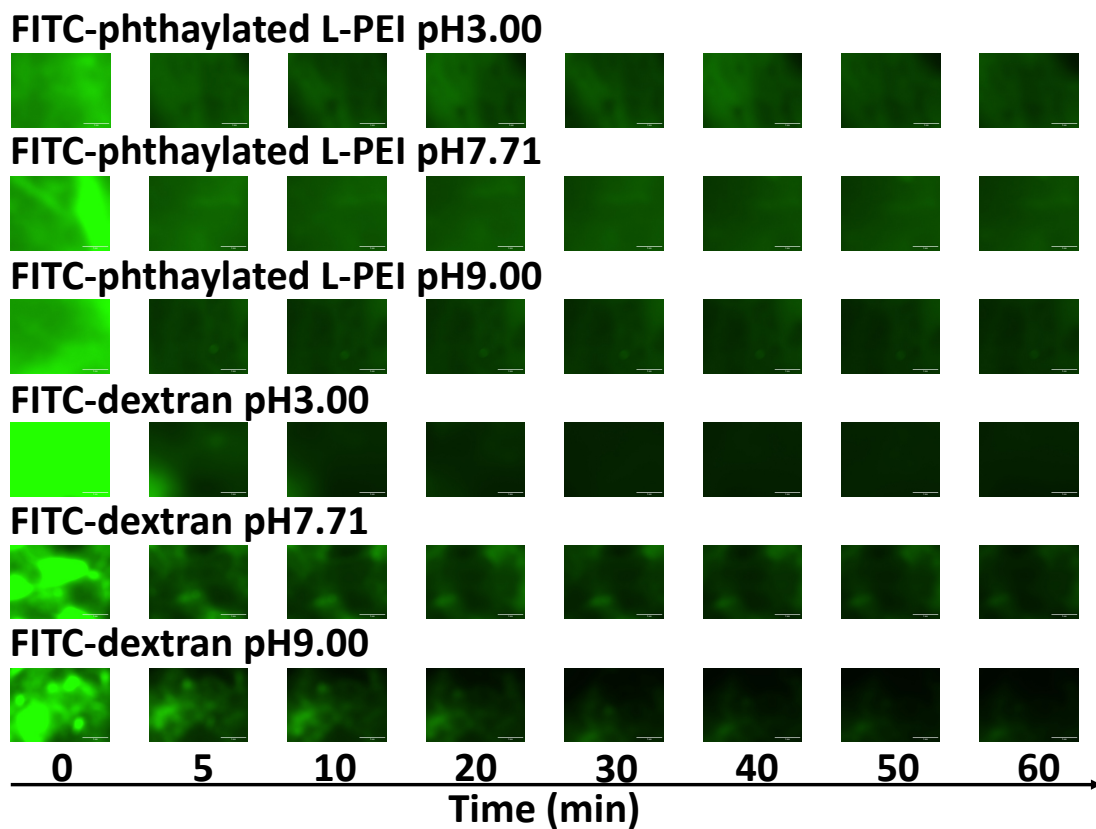


Appendix III. $^1\text{H-NMR}$ spectra of L-PEI recorded in methanol- d_4 ; succinylated L-PEI and phthaylated L-PEI recorded in D_2O .

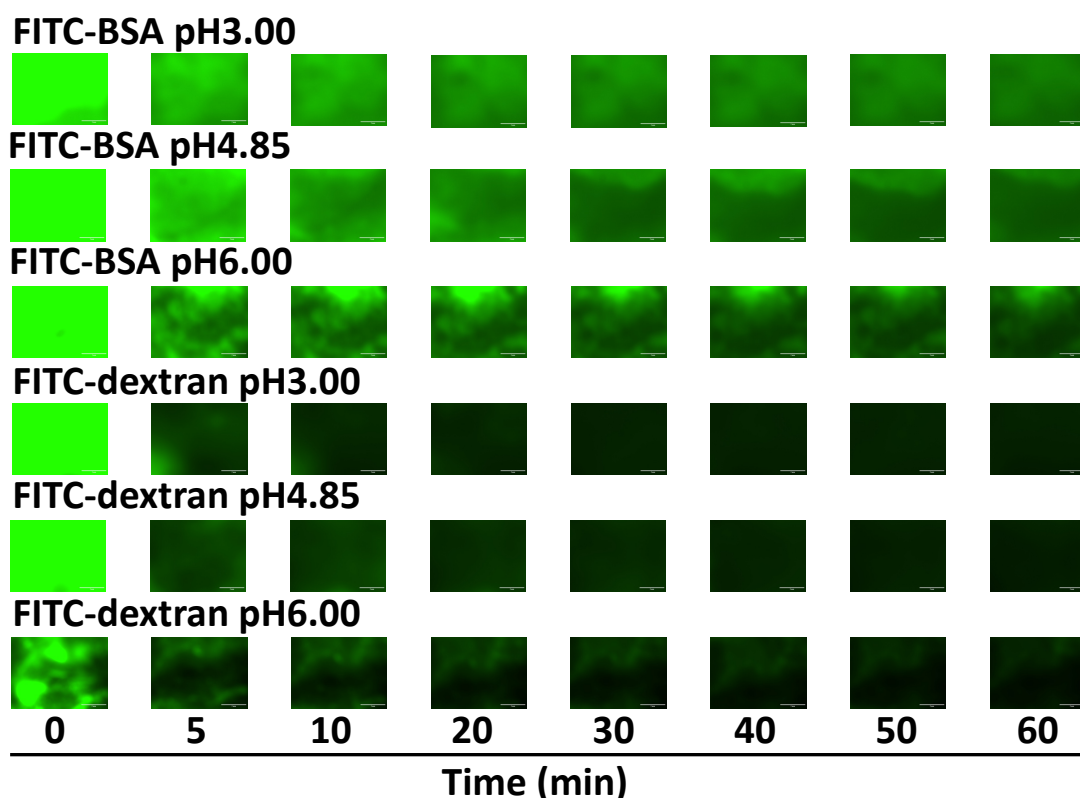
Further confirmation was conducted by FTIR (Appendix IV). In detail, the FTIR spectra displayed the presence of a new band at 1637 cm^{-1} , which was assigned to the formation of amide group and the loss of band at 1470 cm^{-1} , corresponding to the N-H vibration of L-PEI. The 1566 cm^{-1} feature was attributed to C=C stretching of the benzyl ring of phthaylated L-PEI, 1421 cm^{-1} was associated with CH bending of succinylated L-PEI, and 1282 cm^{-1} was from CN stretching.



Appendix IV. FTIR spectra of L-PEI, succinylated L-PEI and phthaylated L-PEI.



Appendix V. Representative fluorescence images showing retention of FITC labelled phthaylated L-PEI after irrigation with different volumes of SGF under different pH at a flow rate of 0.43mL/min, FITC-dextran as negative control. Scale bar = 2 mm.



Appendix VI. Representative fluorescence images showing retention of FITC labelled BSA after irrigation with different volumes of SGF under different pH at a flow rate of 0.43mL/min, FITC-dextran as negative control. Scale bar = 2 mm.

Appendix VII. Ratio of polymers to mucin for turbidimetric titration curve (g/g)

	Succinylated L-PEI		Phthalyated L-PEI		BSA	
	^a aqueous solution	^b urea solution	^a aqueous solution	^b urea solution	^a aqueous solution	^b urea solution
pH 2.00	/	/	0.13	0.25	/	/
pH 2.50	0.09	0.19	/	/	0.20	0.20
pH 3.50	0.05	0.15	0.12	0.20	0.35	0.20

^a turbidimetric titration curve of 1 mg/mL porcine gastric mucin with 1 mg/mL of polymers was determined in aqueous solution; ^b turbidimetric titration curve of 1 mg/mL porcine gastric mucin with 1 mg/mL of polymers was determined in 8M urea solution.

Appendix VIII. Retention study of FITC-labelled polyampholytes under different pHs at 5 min and 60 min.

	FITC-succinylated L-PEI		FITC-phthaylated L-PEI		FITC-BSA		FITC-dextran	
	5 min	60 min	5 min	60 min	5 min	60 min	5 min	60 min
pH<pI	^a 57.4%	^a 33.6%	^a 44.5%	^a 30.6%	^a 72.3%	^a 43.9%	^a 17.9%	^a 7.3%
pH=pI	^b 50.8%	^b 24.4%	^c 36.6%	^c 25.3%	^b 70.4%	^b 37.2%	^b 23.4% / ^c 32.3%	^b 8.2% / ^c 18.5%
pH>pI	^d 46.5%	^d 25.3%	^e 33.7%	^e 20.4%	^d 63.1%	^d 32.6%	^d 29.9% / ^e 26.6%	^d 13.7% / ^e 9.1%

a pH=3.00; b pH=4.85; c pH= 7.71; d pH=6.00; e pH=9.

Reference

- (265) Shan, X.; Williams, A. C.; Khutoryanskiy, V. V. Polymer structure and property effects on solid dispersions with haloperidol: Poly(N-vinyl pyrrolidone) and poly(2-oxazolines) studies. *International Journal of Pharmaceutics* **2020**, *590*, 119884.
- (320) Mees, M. A.; Hoogenboom, R. Full and partial hydrolysis of poly(2-oxazoline)s and the subsequent post-polymerization modification of the resulting polyethylenimine (co)polymers. *Polymer Chemistry* **2018**, *9* (40), 4968.
- (321) Sedlacek, O.; Janouskova, O.; Verbraeken, B.; Hoogenboom, R. Straightforward Route to Superhydrophilic Poly(2-oxazoline)s via Acylation of Well-Defined Polyethylenimine. *Biomacromolecules* **2019**, *20* (1), 222.
- (342) Soradech, S.; Kengkwasingh, P.; Williams, A. C.; Khutoryanskiy, V. V. Synthesis and evaluation of poly (3-hydroxypropyl ethylene-imine) and its blends with chitosan forming novel elastic films for delivery of haloperidol. *Pharmaceutics* **2022**, *14* (12), 2671.
- (364) Withers, C. A.; Cook, M. T.; Methven, L.; Gosney, M. A.; Khutoryanskiy, V. V. Investigation of milk proteins binding to the oral mucosa. *Food & Function* **2013**, *4* (11), 1668.

Chapter 3.

Exploring Mucoadhesive and Toxicological Characteristics Following Modification of Linear Polyethyleneimine with Various Anhydrides

(QUAD system contribution of Manfei Fu: 60% of conception and design, 70% of data collection, 80% of data analysis and conclusions, and 70% of manuscript preparation).

Chapter 3. Exploring Mucoadhesive and Toxicological Characteristics Following Modification of Linear Polyethyleneimine with Various Anhydrides

(QUAD system contribution of Manfei Fu: 60% of conception and design, 70% of data collection, 80% of data analysis and conclusions, and 70% of manuscript preparation).

Manfei Fu^a, Roman V. Moiseev^{a,b}, Silvia Amadesi^a, Adrian C. Williams^a, Vitaliy V. Khutoryanskiy^{*a,b}

^a School of Pharmacy, University of Reading, Whiteknights, Post Office Box 224, Reading RG6 6AD, United Kingdom

^b Physicochemical, Ex Vivo and Invertebrate Tests and Analysis Centre (PEVITAC, www.pevitac.co.uk), University of Reading, Whiteknights, Reading, RG6 6DX, UK

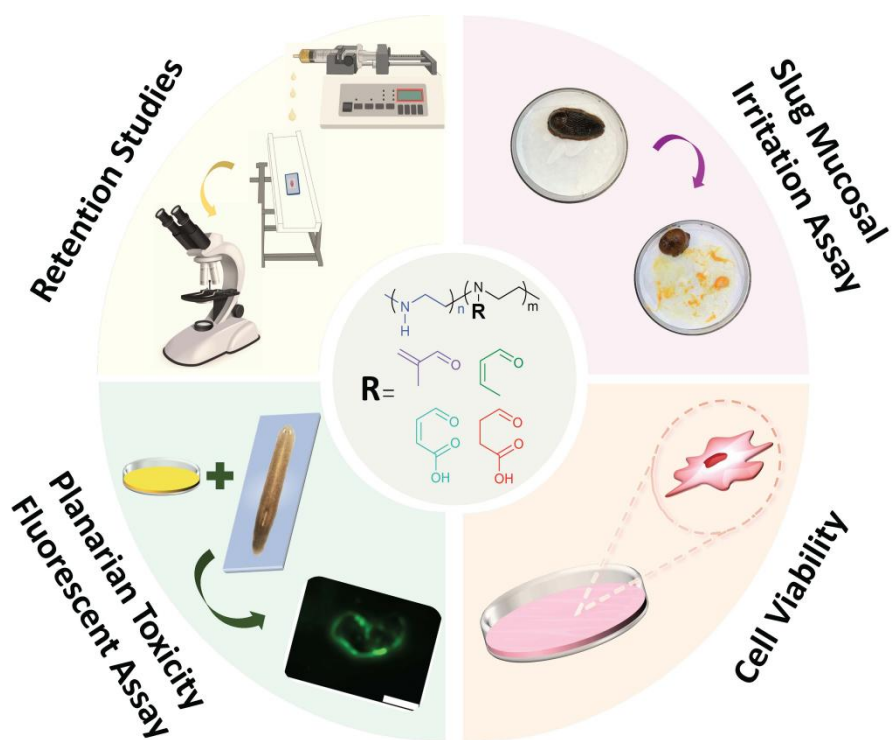
*Correspondence author: v.khutoryanskiy@reading.ac.uk

Reading School of Pharmacy, University of Reading, Whiteknights, PO Box 224, Reading RG6 6AD, United Kingdom

Abstract

Linear polyethyleneimine (L-PEI) has numerous applications, such as in pharmaceutical formulations, gene delivery, and water treatment. However, due to the presence of secondary amine groups, L-PEI shows relatively high toxicity and low biocompatibility. Here, various organic anhydrides were used to modify L-PEI to reduce its toxicity and enhance functionality. We selected methacrylic anhydride, crotonic anhydride, maleic anhydride and succinic anhydride to modify L-PEI. A fluorescence flow through method determined the mucoadhesive properties of the polymers to bovine palpebral conjunctiva. Methacrylated- and crotonylated L-PEI showed strong mucoadhesive properties at pH 7.4, due to covalent bonding with mucin thiol groups. In contrast, maleylated- and succinylated L-PEI were poorly-mucoadhesive as the pH was above their isoelectric point, resulting in electrostatic repulsion between the polymers and mucin. The toxicity of these polymers was evaluated using *in vivo* assays with planaria and the 3-(4,5-dimethylthiazol-2-yl)-2,5-diphenyl-2H-tetrazolium bromide (MTT) cell viability assay in human alveolar epithelial cells. Moreover, irritancy of polymers was assessed using a slug mucosa irritation assay. The results demonstrated that anhydride modification mitigated the adverse toxicity effects seen for the parent L-PEI.

KEYWORDS: mucoadhesion, planaria, slug, toxicity studies, linear PEI, anhydride



3.1 Introduction

Mucus is a biological barrier covering epithelial cells of the respiratory system, reproductive system and gastrointestinal tract³⁹⁹ to protect the underlying membranes⁴⁰⁰. Mucin is a primary component of mucus⁴⁰¹ and comprises a glycoprotein backbone and primarily O-linked glycan structures arranged in a bottle brush-like conformation.⁴⁰² Mucoadhesive polymers are commonly classified as anionic-, cationic-, amphoteric or neutral polymers; chitosan, xanthan gum and proteins are examples of charged polymers and exhibit relatively strong mucoadhesive properties⁴⁰³. Electrostatic interactions are usually predominantly responsible for mucoadhesion whilst hydrogen bonding and hydrophobic effects can also contribute²⁵¹. Mucoadhesion has been extensively used in drug delivery to enhance the retention time of formulations, employing chitosan⁴⁰⁴, xanthan gum⁴⁰⁵ and weakly crosslinked poly(acrylic acid)⁴⁰⁶.

Linear poly(ethylenimine) (L-PEI) has been explored for various applications⁴⁰⁷, such as gene delivery⁴⁰⁸⁻⁴¹⁰, water purification³²⁷, to produce functional inorganic minerals⁴¹¹ and in PEI-conjugates⁴¹²⁻⁴¹⁴. Due to the presence of cationic secondary amine groups within L-PEI, which can interact with negatively charged mucin, L-PEI has also gained some attention for mucoadhesive applications in nasal⁵ and buccal drug delivery³⁴².

Despite the numerous studies employing L-PEI as a gene delivery vector or as a pharmaceutical excipient, it is cytotoxic⁴¹⁵, predominantly attributed to electrostatic interactions with cell membranes and the extracellular matrix.³²⁸ Additionally, different structures, molecular weights, and macromolecular flexibility have been correlated with toxicity and delivery efficiency of L-PEI.⁴¹⁶

In this study, a series of amphoteric and cationic polymers were synthesized by modifying L-PEI with methacrylic anhydride, crotonic anhydride, maleic anhydride and succinic anhydride. These new polymers were fully characterized by ¹H-NMR and FTIR spectroscopies. A fluorescence flow through *ex vivo* method was used to assess retention of these polymers on bovine palpebral conjunctiva. The toxicity of the polymers was evaluated *in vivo* using the model planaria assay⁴¹⁷ and slug mucosal irritation test⁴¹⁸, and an *in vitro* 3-(4,5-dimethylthiazol-2-yl)-2,5-diphenyl-2H-tetrazolium bromide (MTT) cell viability assay in human alveolar epithelial cells.

3.2 Materials and methods

3.2.1 Materials

Poly(2-ethyl-2-oxazoline) (PEOZ, MW~50 kDa, PDI 3-4), succinic anhydride, maleic anhydride, methacrylic anhydride, crotonic anhydride, dimethyl sulfoxide (DMSO), triethylamine (TEA), deuterium oxide (D₂O), deuterium methanol (MeOD-d₄), fluorescein isothiocyanate (FITC), fluorescein isothiocyanate-dextran (FITC-dextran, average Mw 10 kDa), gelatin, branched polyethyleneimine (b-PEI, average MW 25 kDa), fluorescein sodium salt, benzalkonium chloride (BAC), fetal bovine serum (FBS), Dulbecco's phosphate buffered saline (DPBS), nutrient mixture F-12 ham, Hanks' Balanced Salt Solution (HBSS), trypsin-EDTA solution (EDTA), 6-diamidino-2-phenylindole (DAPI), thiazolyl blue tetrazolium bromide (MTT), formaldehyde solution 4% buffered (pH 6.9), penicillin/streptomycin and propidium iodide (PI) were obtained from Sigma-Aldrich (Gillingham, U.K.). Urea, hydrochloric acid (37%), sodium hydroxide, magnesium sulfate, magnesium chloride, potassium chloride, phosphate-buffered saline (PBS) tablets, sodium bicarbonate, sodium chloride and calcium chloride dihydrate were obtained from Fisher Scientific (Loughborough, U.K.). Dialysis membrane (MWCO 3.5 kDa) was purchased from Medicell Membranes Ltd. (U.K.). All other chemicals were of analytical grade and used without further purification.

3.2.2 Synthesis of linear polyethyleneimine (L-PEI)

L-PEI was synthesized by acidic hydrolysis of PEOZ following the protocol of Shan et al.³⁶⁵. Briefly, PEOZ (5.0 g) was dissolved in 50 mL 37 wt % HCl before 50 mL deionized water was added and heated overnight at 100 °C. Then, the L-PEI solution was diluted in cold deionized water. Cool NaOH aqueous solution (4 M) was added dropwise to the L-PEI solution until the L-PEI precipitated at pH 10-11³²¹. The precipitate was washed with deionized water until neutral pH and dried in a vacuum oven to obtain L-PEI yielding 1.90 g (89 %).

3.2.3 Synthesis of methacrylated L-PEI, crotonylated L-PEI, maleylated L-PEI and succinylated L-PEI

Either methacrylic anhydride (1.5 eq, 5.4 g), or crotonic anhydride (1.5 eq, 5.4 g), or maleic anhydride (1.5 eq, 3.4 g) or succinic anhydride (1.5 eq, 3.5 g) were dissolved in 15 mL dimethyl sulfoxide (DMSO) and then mixed with 45 mL of L-PEI (1 eq, 1.0 g) in DMSO, before triethanolamine (1.5 eq, 3.3 mL) was added. The mixture was stirred overnight at 40 °C. The obtained polymer solution was diluted with deionized water and dialyzed against deionized water (MWCO 3.5 kDa) for 72 h. All polymers were recovered by freeze-drying. The following product yields were recorded for methacrylated L-PEI, crotonylated L-PEI,

maleylated L-PE and succinylated L-PEI: 2.23 g (86%), 2.31 g (91%), 2.60 g (79%) and 2.08 g (89%), respectively.

3.2.4 Characterization of methacrylated L-PEI, crotonylated L-PEI, maleylated L-PEI and succinylated L-PEI

3.2.4.1 ¹H-nuclear magnetic resonance spectroscopy (¹H-NMR)

10 mg methacrylated-, crotonylated-, maleylated- or succinylated L-PEI was dissolved in 1 mL D₂O, whereas L-PEI was dissolved in 1 mL methanol-d₄. The samples were transferred to an NMR tube and analyzed by a Bruker spectrometer operating at 400 MHz. All chemical shifts are given in ppm. MestReNova software (version 9.1.0) was used for spectral analysis. The degree of substitution (DS) of methacrylated L-PEI, crotonylated L-PEI, maleylated L-PEI and succinylated L-PEI was calculated using peak integration, according to Equations (1-4) respectively:

$$\%DS = \frac{\int I_d / n_d}{\int I_{a+b} / n_{a+b}} \times 100 \quad (1)$$

$$\%DS = \frac{\int I_e / n_e}{\int I_{a+b} / n_{a+b}} \times 100 \quad (2)$$

$$\%DS = \frac{\int I_{h+i} / n_{h+i}}{\int I_{a+b} / n_{a+b}} \times 100 \quad (3)$$

$$\%DS = \frac{\int I_j / n_j}{\int I_{a+b} / n_{a+b}} \times 100 \quad (4)$$

where I_a is an integral of the signal assigned to the -CH₂CH₂- on the backbone of unreacted L-PEI, I_b is associated with -CH₂- adjacent with the substituted nitrogen, I_d from the methacrylated L-PEI spectrum is attributed to methyl group of methacrylic anhydride, I_e of crotonylated L-PEI spectrum is attributed to methyl group of crotonic anhydride, I_h and I_i of maleylated L-PEI spectrum is attributed to methyne group of maleic anhydride, I_j of succinylated L-PEI spectrum is attributed to methenyl group of succinic anhydride.

3.2.4.2 Fourier transform infrared (FTIR) spectroscopy

Polymers were analyzed from 4000–950 cm⁻¹ at a resolution of 4 cm⁻¹ taking 64 scans using a diamond sampling accessory. Data were recorded by a Nicolet iS5 spectrometer (Thermo Scientific, U.K.) and plotted using OriginLab® version 9.0 software.

3.2.4.3 Turbidity measurements

The effects of pH on solution turbidity of the modified L-PEIs were studied using a JENWAY 7315 spectrophotometer (Bibby Scientific Ltd, UK). All samples were dissolved in deionized water (1 mg/mL) and turbidity recorded at 400 nm as pH was varied by adding

0.1 M NaOH or HCl. Each titration was repeated in triplicate and the turbidity values are reported as mean \pm standard deviation.

3.2.4.4 Electrophoretic mobility measurements

The effects of pH on electrophoretic mobility of the polymers were studied using a Malvern Zetasizer Nano-S (Malvern Instruments, UK). All samples were dissolved in deionized water (1 mg/mL) and pH was adjusted by adding 0.1 M NaOH or HCl. Measurements were conducted at 25 °C and repeated in triplicate; reported values are the mean \pm standard deviation.

3.2.5 *Ex Vivo* mucoadhesion studies

3.2.5.1 Preparation of simulated tear fluid

Simulated tear fluid (STF) was prepared according to the protocol previously described by Moiseev et al.⁴¹⁹ Briefly, 6.7 g NaCl, 2.0 g NaHCO₃ and 0.8 g CaCl₂·2H₂O were dissolved in 1L of deionized water and then adjusted to pH 7.40.⁴²⁰ STF was kept at 37 °C throughout experimentation.

3.2.5.2 Preparation of fluorescently labelled polymers

Methacrylated-, crotonylated-, maleylated- and succinylated L-PEI were labelled with FITC, according to our previously reported protocol.³⁶⁴ Polymer solutions (2 mg/mL) were prepared in 0.1 M carbonate buffer (pH 9), while FITC was dissolved in DMSO (1 mg/mL). The FITC solution was added to the polymer solutions at 1:20 v/v (FITC : polymer) and then incubated in a light proof container with overnight stirring at room temperature. The polymer-FITC solutions were dialyzed against 2.5 L of 0.01 M phosphate buffered saline (PBS) using a cellulose membrane with MWCO 3.5 kDa at pH 7.4 for 72 h and then recovered by freeze-drying. Successful labelling of these polymers was confirmed using a fluorescence spectrophotometer (CARY Eclipse, US). The resultant polymers were dissolved in deionized water at 1 mg/mL. The excitation wavelength was 490 nm and the emission wavelength range was 500-600 nm at room temperature (25 \pm 3°C). The emission and excitation slit widths were set at 5 nm, the emission voltage was 500 mV and the scan speed was 600 nm/min. Data were recorded and plotted using OriginLab[®] version 9.0 software.

3.2.5.3 Retention studies on ocular tissues

Retention of FITC labelled polymers on bovine palpebral conjunctiva was studied with FITC-dextran used as a negative control, following a modified protocol we previously

reported^{369,421}. Bovine palpebral conjunctiva was dissected with a scalpel avoiding contact with surfaces. The ocular tissue (4 × 2 cm²) was mounted on a glass slide, with the mucosal side upward, and pre-rinsed with 1 mL freshly prepared STF. Briefly, background fluorescence of the tissue ($I_{\text{background}}$) was determined. Then, 40 μL of 1 mg/mL FITC-methacrylated L-PEI, FITC-crotonylated L-PEI, FITC-maleylated L-PEI, FITC-succinylated L-PEI or FITC-dextran solution in STF was applied onto the mucosal surface and fluorescence images recorded to give initial fluorescence intensities (I_0). After 3 min of dosing, the mucosal tissue was washed with STF using a syringe pump (Harvard Apparatus model 981074, Holliston, MA, US) at 0.1 mL/min, exceeding the normal human tear rate (1-2 μL/min)⁴²¹. All experiments were conducted at 34.5°C in an incubator⁴²². Fluorescence images of the mucosal tissue (I_t) were acquired periodically using a Leica MZ10F stereomicroscope (Leica Microsystems, Wetzlar, Germany) with the GFP filter-fitted Leica DFC3000G digital camera at 3.2× magnification, 80 ms of exposure time, 2.0× gain, 1.0× gamma and pseudo color at 520 nm. The acquired microscopy images from each time point were analyzed using ImageJ software (Version 1.53t, 2022) and fluorescence intensity calculated according to Equation (5):

$$\text{Fluorescence intensity (\%)} = \frac{I_t - I_{\text{background}}}{I_0 - I_{\text{background}}} \times 100\% \quad (5)$$

where the zero-time point was set as 100%.

The results are presented as fluorescence intensity as a function of the time of irrigation (0-30 min) after subtracting the background fluorescence from each image. Measurements were repeated in triplicate and all values are reported as mean ± standard deviation.

3.2.6 Slug mucosal irritation assay

Arion lusitanicus slugs were collected locally (Reading, United Kingdom), housed in plastic containers at room temperature and fed lettuce and carrots. The slug mucosal irritation test (SMIT) was conducted for methacrylated-, crotonylated-, maleylated- and succinylated L-PEI according to a previously published protocol.⁴¹⁸ To conduct experiments, slugs weighing 6-14 g, without macroscopic injuries and with clear tubercles and foot surfaces, were selected and housed separately in 1.5 L glass beakers. 20 mL of PBS solution at pH 7.40 was used to soak a paper towel sheet in the base of each beaker and covered with cling film perforated with a needle allowing air exchange. Slugs were maintained without food for 48 hours at room temperature prior to experiments. On the day of the experiment, slugs were individually weighed and then placed in a 90 mm plastic Petri dish lined with Whatman™

filter paper soaked in 2 mL of 1.0 mg/mL of each polymer solution in PBS or 1% benzalkonium chloride (BAC) in PBS solution as a positive control or PBS solution alone as the negative control. Immediately following the 60-minute contact period, the slugs were removed from the Petri dishes, rinsed with 10 mL of PBS solution, wiped gently with a paper towel, and re-weighed. The amount of mucus produced (MP%) by each slug in response to the contact with the chemicals was calculated by:

$$MP\% = \frac{m_b - m_a}{m_a} \times 100\% \quad (6)$$

where m_b and m_a are slug weights before and after exposure to test solutions, respectively. Tests used 5 slugs per solution with data presented as the mean \pm standard deviation.

3.2.7 Toxicology

3.2.7.1 Acute toxicity assay

Schmidtea mediterranea planaria were bred from a colony generously donated by Dr Jordi Solana (Oxford Brookes University). Planaria were maintained in artificial pond water (APW) at $25 \pm 3^\circ\text{C}$ in the dark, feeding calf liver twice per week. APW was prepared with 3.2 mL 5 M NaCl, 10 mL 1 M $\text{CaCl}_2 \cdot 6\text{H}_2\text{O}$, 10 mL 1 M MgSO_4 , 1 mL 1 M MgCl_2 , 1 mL 1 M KCl and 1.008 g NaHCO_3 in 10 L Milli-Q water and adjusted pH to 7-8 by adding 5 M HCl. The APW was changed every 3-4 days.

The planaria toxicity assay was modified from the method of Buang et al.²⁵⁷ Methacrylated L-PEI, crotonylated L-PEI, maleylated L-PEI, succinylated L-PEI and branched PEI (b-PEI) were dissolved at 1 mg/mL in APW. Individual planaria were placed in 12-well culture plate and treated with 4 mL of each polymer solutions, or b-PEI (used as a positive control) or APW alone (used as a negative control). Planaria were treated for 1, 24 and 48 hours. The number of live animals (with detectable movement) and dead animals (without detectable movement) was recorded. Five biological replicates were obtained for each of the treatment and for each time point.

3.2.7.2 Planarian toxicity fluorescent assay

The toxicity fluorescent assay was slightly modified from Shah et al.⁴¹⁷ Planaria that remained viable following the acute toxicity assay were washed with APW for 1 minute, exposed to 0.1% (w/v) sodium fluorescein solution in APW for 1 min, and then washed with APW for 1 minute to remove excess sodium fluorescein. Planaria were then placed on a microscope glass slide and immobilized with a few drops of 12 % (w/v) gelatin solution and

placed on ice. Fluorescence images were collected using a Leica MZ10F stereomicroscope (Leica Microsystems, UK) fitted with a DFC3000G digital camera set at 970 ms exposure time, 2.0× magnification, 5.1× gain, 0.7× gamma and pseudo color at 520 nm. The images were analyzed using ImageJ software (Version 1.53t, 2022). Five replicates with different worms were taken for each treatment and fluorescence intensity values are reported as mean ± standard deviation.

3.2.7.3 Cell viability

3.2.7.3.1 Cell culture and treatment

A549 cells were kindly provided by Prof Darius Widera (University of Reading, School of Pharmacy, Reading, United Kingdom). Cells were cultured in Ham's F-12 Nutrient Mixture (F-12) supplemented with 10 % Fetal bovine serum (FBS) and 100 U/mL penicillin and 100 µg/mL streptomycin. For the treatments, the synthesized polymers and b-PEI were dissolved in Ham's F-12 Nutrient Mixture (F-12) supplemented with 1% FBS and 100 U/mL penicillin and 100 µg/mL streptomycin at 1 mg/mL or 0.5 mg/mL and filter-sterilized with a 0.22 µm filter.

Cells were grown at 37 °C in a suitable incubator in a humidified atmosphere of 5 % CO₂, and routinely subcultured when reaching 70-80% confluency using 0.25 % (w/v) trypsin-0.53 mM EDTA solution and reseeded at a subcultivation ratio of 1:5. The medium was renewed 1 to 2 times per week.

3.2.7.3.2 MTT assay

Cell viability was assessed using the 3-(4,5-dimethylthiazol-2-yl)-2,5-diphenyltetrazolium bromide (MTT) assay, modified from Liu et al.⁴²³ A549 cells were seeded in a 96-well plate at 5,000 cells/well 24 h before the experiment. Cells were then treated with 0.5 mg/mL or 1.0 mg/mL methacrylated-, crotonylated-, maleylated-, succinylated L-PEI dissolved in complete medium 1% FBS for 24 h. Cells treated with complete medium 1 % FBS were used as a negative control and designated as 100 % cell viability. 0.5 mg/mL of the toxic b-PEI was used as a positive control. After 24 h, test reagents were removed, cells were washed with Hanks' Balanced Salt Solution (HBSS) and incubated with 25 µL MTT solution (5 mg/mL in HBSS) at 37 °C for 3 h to allow MTT reduction. The reaction was terminated by adding 275 µL DMSO per well. Absorbance values at 570 nm were determined with a microplate reader by SpectraMax®i3x imaging cytometer Softmax Pro 7.2 (Molecular devices, US), using 630 nm as the reference wavelength. The results are

given as cell viability (%) relative to the negative control (1% FBS) and were calculated using the following equation:

$$\text{Cell viability (\%)} = \frac{\text{Abs}_{\text{treatment}} - \text{Abs}_{\text{blank}}}{\text{Abs}_{\text{ve}} - \text{Abs}_{\text{blank}}} \times 100 \quad (7)$$

where Abs is absorbance and Abs_{ve} is negative control (= complete medium 1% FBS). All values are reported as mean ± standard deviation of a total of 6 biological replicates.

3.2.7.4 Measurement of cell death

Cell death was evaluated using 6-diamidino-2-phenylindole (DAPI) and propidium iodide (PI) staining⁴²⁴. A549 cells (adenocarcinomic human alveolar basal epithelial cells) were plated in 12 well plates (5×10⁴ cells / well) 24 h before the experiment.

Cells were then treated with aqueous solutions of methacrylated L-PEI or crotonylated L-PEI (0.5 mg/mL or 1.0 mg/mL) or with complete medium 1% FBS (negative control) or with aqueous solutions of b-PEI (0.5 mg/mL) used as a positive control known to cause cell apoptosis). After 24 h treatment, cell monolayers were washed twice with 0.75 mL Dulbecco's Phosphate-Buffered Saline (DPBS) and incubated with 0.75 mL DAPI (100 μM) and PI (35 μg/mL) for 10 minutes. Cells were then washed for 30 mins at 10 min intervals with 0.75 mL DPBS under light-shielded conditions. Cells were fixed in 0.75 mL of 4 % formaldehyde solution in the dark for 10 min at room temperature. Cells were then washed once with DPBS and observed using an Invitrogen™ EVOS™ FL Digital Inverted Fluorescence Microscope, under a 40× objective, with DAPI (360 nm excitation, 447 nm emission) and RFP (530 nm excitation, 593 nm emission) light cubes to visualize DAPI and PI staining, respectively. Fluorescence images were taken for each well using the Images the EVOS® FL Cell Imaging System Software. The cell permeable DAPI stained all cells (N_{DAPI}), whereas PI (N_{PI}), normally an impermeant fluorescent dye, stained dead cell with impaired plasma membrane permeability. Cell mortality (%) was calculated using the following equation:

$$\text{Cell mortality (\%)} = \frac{N_{\text{DAPI}} - N_{\text{PI}}}{N_{\text{DAPI}}} \times 100 \quad (8)$$

All values are reported as mean ± standard deviation for the total of nine biological replicates.

3.2.8 Statistical analysis

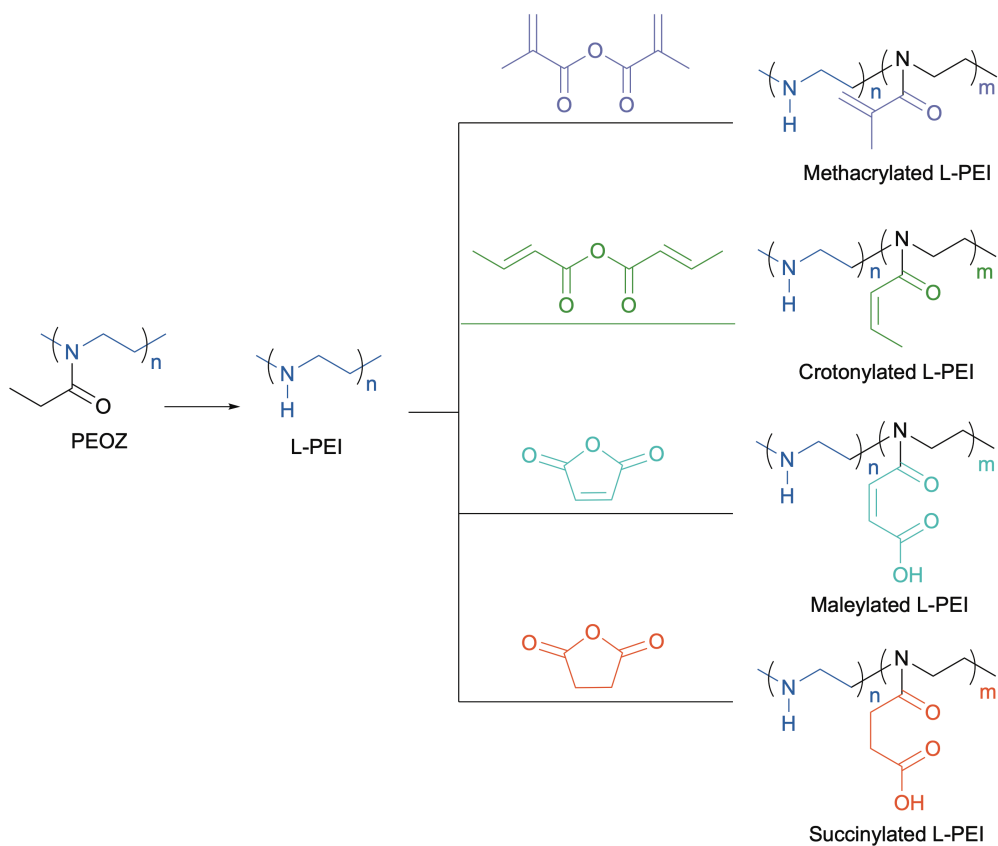
Student's t-test and one-way analysis of variance (ANOVA) were used to calculate p values, where p < 0.05 was set as the statistical significance criterion. The SMIT data were evaluated for significance using one-way analysis of variance (ANOVA) followed by a

Bonferroni's post hoc test using GraphPad Prism software (version 8.0.2; GraphPad Software Inc., San Diego, CA, USA) where $p < 0.05$ was set as the statistical significance criterion.

3.3 Results and discussion

3.3.1 Synthesis and characterization of methacrylated L-PEI, crotonylated L-PEI, maleylated L-PEI and succinylated L-PEI

Shan et al.³⁶⁵ previously reported a methodology to synthesize poly(2-oxazolines) from commercially available poly(2-ethyl-2-oxazoline) (PEOZ). Here, a similar strategy was used to synthesize methacrylated L-PEI, crotonylated L-PEI, maleylated L-PEI and succinylated L-PEI from commercially available PEOZ (50 kDa). Firstly, L-PEI was prepared via acidic hydrolysis of PEOZ³²⁰ (Scheme 3.3-1) with full conversion confirmed by ¹H NMR (Appendix IX) and FTIR spectroscopy (Appendix X). The main backbone signal of PEOZ and signals at 3.56, 1.12 and 2.44 ppm from its side chains disappeared from the NMR spectrum but a signal typical for the L-PEI backbone was recorded at 2.75 ppm. Hydrolysis of PEOZ to form L-PEI was also confirmed by FTIR through the loss of the PEOZ amide carbonyl group at 1628 cm⁻¹ and the presence of new strong bands at 1470 cm⁻¹ and 3259 cm⁻¹ consistent with the N-H bend of L-PEI³⁴². The obtained L-PEI was re-acylated via reaction with methacrylic anhydride, crotonic anhydride, maleic anhydride and succinic anhydride in DMSO, with addition of triethylamine as a base. The resultant polymers were also characterized by ¹H NMR and FTIR spectroscopies.



Scheme 3.3-1. L-PEI was obtained by acidic hydrolysis of PEOZ and subsequently modified with methacrylic anhydride, crotonic anhydride, maleic anhydride and succinic anhydride, respectively.

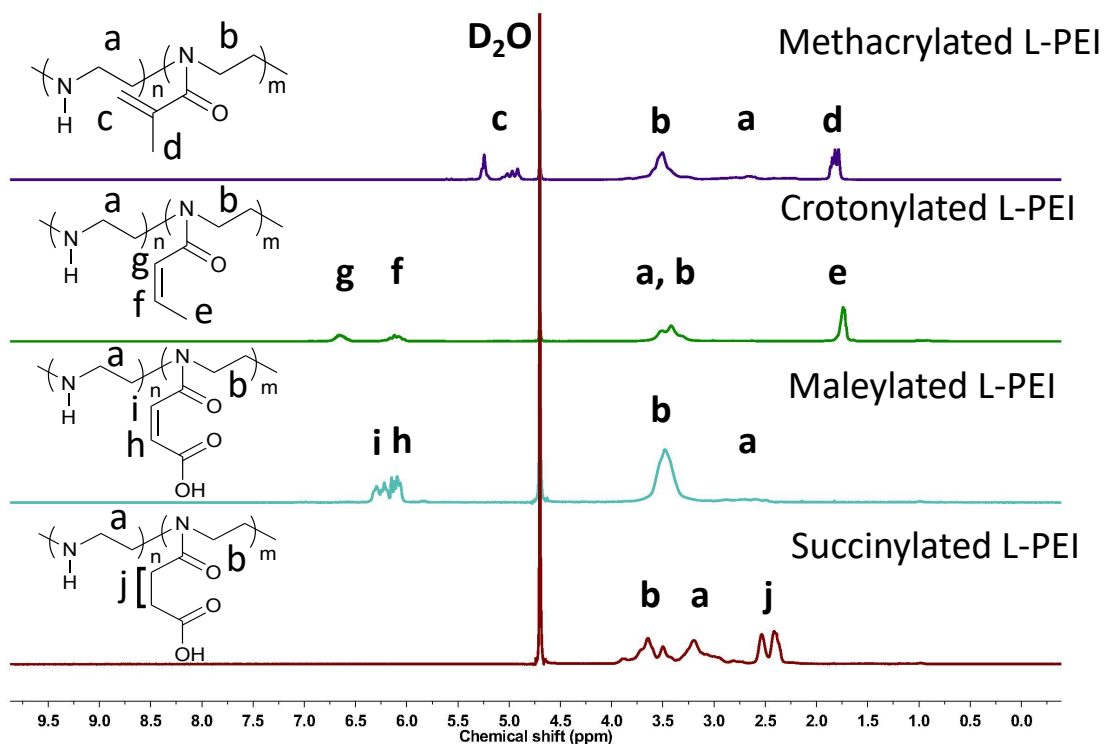


Figure 3.3-1. ^1H NMR spectra of methacrylated L-PEI, crotonylated L-PEI, maleylated L-PEI and succinylated L-PEI recorded in D_2O .

As shown in Figure 3.3-1, the backbone $-\text{CH}_2-\text{CH}_2-$ of L-PEI repeating units appeared at 2.75-3.50 ppm (signal a), which shifted to 2.90-3.75 ppm (signal b) upon acylation with the different anhydrides as new amide groups formed. For methacrylated L-PEI, signal d at 1.89 ppm and signal c at 5.08 ppm were assigned to the $-\text{CH}_2-$ and $-\text{CH}_3$ in the side group, respectively. For crotonylated L-PEI, signal e at 1.68 ppm, signal f at 6.05 ppm and signal g at 6.63 ppm are attributed to the $-\text{CH}-$, $-\text{CH}_2-$ and $-\text{CH}_3$ in the side group, respectively. For maleylated L-PEI, signal h and signal i at 6.01-6.37 ppm were assigned to $-\text{CH}_2-$ in the side group. For succinylated L-PEI signal j at 2.28-2.63 ppm, corresponded to the $-\text{CH}_2-$ in the side group. The degrees of substitution (DS) of methacrylated L-PEI, crotonylated L-PEI, maleylated L-PEI and succinylated L-PEI were 83%, 93 %, 80 % and 89 %, as calculated using Equations (1)-(4), respectively.

Further confirmation of successful synthesis was provided by FTIR spectroscopy (Appendix XI and Appendix XV). In particular, the FTIR spectra of the anhydride modified polymers display a new stretching mode at 1611 cm^{-1} (maleylated), 1631 cm^{-1} (succinylated), 1644 cm^{-1} (methacrylated) and 1657 cm^{-1} (crotonylated), which was attributed to the formation of an amide group. The peaks at 1563 cm^{-1} and 1606 cm^{-1} were assigned to $\text{C}=\text{C}$ stretching vibrations of maleic anhydride and crotonic anhydride residues, respectively. Additionally, a new feature at 1718 cm^{-1} was assigned to the $=\text{C}-\text{H}$ stretch of the methacrylic anhydride residue following its modification of L-PEI. Further, new peaks from maleylated L-PEI and succinylated L-PEI at 1706 cm^{-1} and 1709 cm^{-1} , respectively, were attributed to the $\text{C}=\text{O}$ stretch of the carboxylic acid groups in the side chain. The bands at 3356 cm^{-1} and 3363 cm^{-1} , correspond to the carboxyl group ($\text{O}-\text{H}$ stretch) of succinylated L-PEI and maleylated L-PEI, respectively.

The effects of pH on turbidity and electrophoretic mobility of the anhydride modified polymers in solutions were studied, with results summarized in Figure 3.3-2.

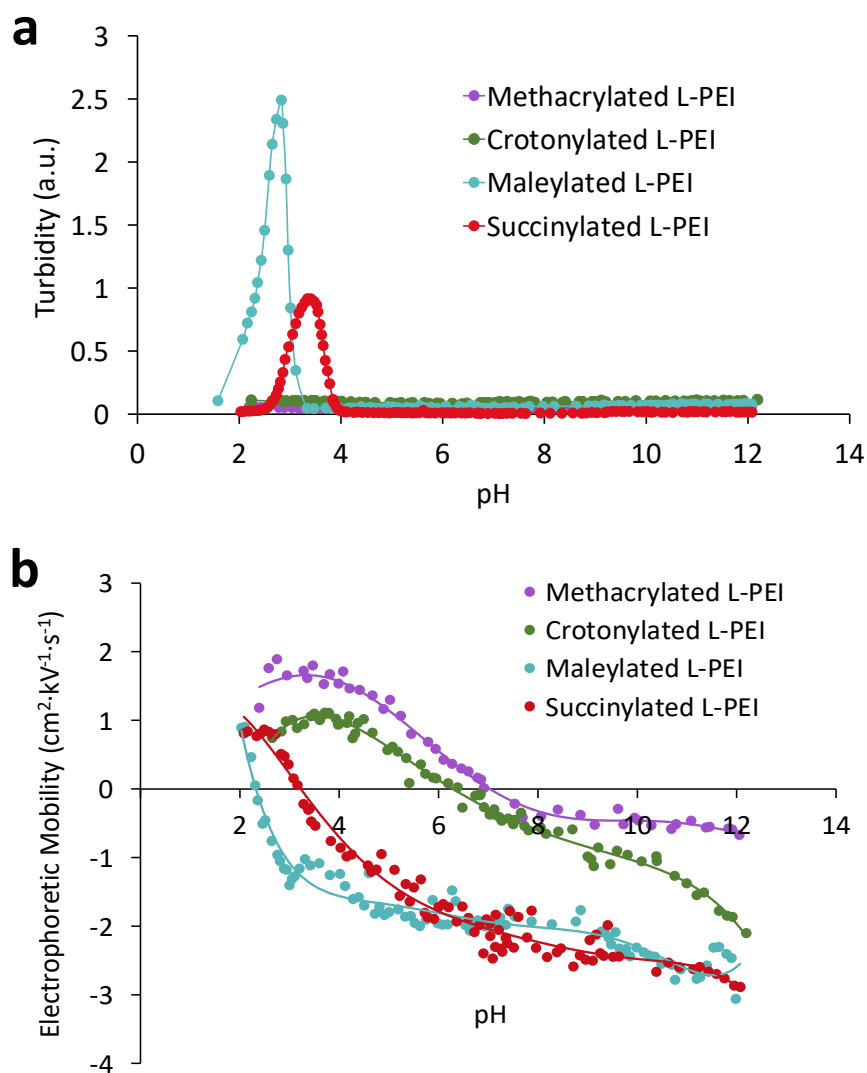


Figure 3.3-2. Effect of pH on solution turbidity (a) and electrophoretic mobility (b) of 1 mg/mL methacrylated L-PEI, crotonylated L-PEI, maleylated L-PEI and succinylated L-PEI aqueous solutions.

Turbidity - pH and electrophoretic mobility - pH profiles for the maleylated and succinylated L-PEI are typical for polyampholytes, showing minimum aqueous solubility or net charge when $\text{pH} = \text{pH}_{\text{IEP}}$ (isoelectric point).³⁶⁰ A reduction or increase in pH of polymer aqueous solutions (1 mg/mL) was achieved by addition of small portions of 0.1 M NaOH or HCl. The turbidimetric technique gave pH_{IEP} for maleylated L-PEI of 2.81 ± 0.07 , and for succinylated L-PEI 3.41 ± 0.08 . The solutions remained transparent until the pH approached the pH_{IEP} with a further pH rise resulting in a dramatic increase in turbidity, reaching the maximum turbidity at $\text{pH} = \text{pH}_{\text{IEP}}$. Subsequent addition of 0.1 M NaOH led the solution to become transparent again. When $\text{pH} < \text{pH}_{\text{IEP}}$ or $\text{pH} > \text{pH}_{\text{IEP}}$ the polymers provide excess positively or negatively charged groups and so are water soluble whereas when $\text{pH} = \text{pH}_{\text{IEP}}$ the polymer carries a net neutral charge and loses its aqueous solubility. The unsaturated maleic acid residue present in maleylated L-PEI may have stronger electron-withdrawing

ability which facilitates dissociation of the carboxyl group; this in turn may be a reason for a lower pH_{IEP} compared to the value recorded in the case of saturated succinylated L-PEI. Since methacrylated L-PEI and crotonylated L-PEI are not polyampholytes, they do not exhibit pH-dependent aqueous solubility behavior (i.e. they do not display the presence of the isoelectric point).

Electrophoretic mobility measurements are also suitable to determine the isoelectric point in polyampholytes^{425,426}. The electrophoretic mobility measurements gave pH_{IEP} of 2.30 ± 0.07 for maleylated L-PEI and of 3.16 ± 0.09 for succinylated L-PEI, which was slightly different from the pH_{IEP} values determined using turbidity-pH measurements. This could be attributed to the different principles of the measurements; the turbidity-pH measurements are based on aggregation of polymers at pH_{IEP} , whereas the EM-pH measurements record the migration of particles to an oppositely charged electrode in an electric field. Although crotonylated L-PEI and methacrylated L-PEI are not polyampholytes, they still show charge reversion at pHs 6.51 ± 0.14 and 7.05 ± 0.15 , respectively which may be explained by the presence of counter-ions surrounding each macromolecular coil or particles, and changes in their net charge. The DS of methacrylated L-PEI (83%) was lower than the DS value for crotonylated L-PEI (93%), resulting in more -NH- groups present in the methacrylated derivative. More -NH- groups available for protonation will result in greater pH_{IEP} values.

3.3.2 *Ex Vivo* mucoadhesion studies of methacrylated L-PEI, crotonylated L-PEI, maleylated L-PEI and succinylated L-PEI

Mucoadhesive properties of the synthesized polymers were investigated using a fluorescence flow through method³⁵⁶. Ocular mucosa was selected to evaluate mucoadhesive properties of new polymers as there is a strong need to develop new formulations with enhanced retention ability on these mucosal surfaces. The conjunctiva and cornea are the major barriers in ocular drug delivery.⁴²⁷ Ramsay et al.⁴²⁷ demonstrated that the cornea provides a near 10-fold greater barrier to drug permeation than the conjunctiva. Similarly, rabbit cornea was impermeable to FITC-dextran (Mw 20 kDa), whereas it was able to permeate through the conjunctiva.⁴²⁸ Moreover, the conjunctiva has been reported to have permeability towards hydrophilic drugs than the cornea⁴²⁹. The conjunctiva is a thin transparent membrane and covers the posterior surface of the upper and lower lids (palpebral conjunctiva) and the region from the upper and lower fornix over the sclera up to the cornea

(bulbar conjunctiva).⁴³⁰ This layer contains goblet cells which are responsible for secreting mucins^{431,432}, and so may be a significant site for mucoadhesion to the ocular surface.⁴³³

Firstly, methacrylated L-PEI, crotonylated L-PEI, maleylated L-PEI and succinylated L-PEI were successfully labelled with FITC (Appendix XII). Retention of FITC-labelled compounds was evaluated on bovine palpebral conjunctiva washed with simulated tear fluid (STF) at pH=7.4, with FITC-labelled dextran used as a negative control due to its well-documented poor mucoadhesive properties. The exemplar fluorescence images are shown in Appendix VI. All images were analyzed using Image J software (Figure 3.3-3).

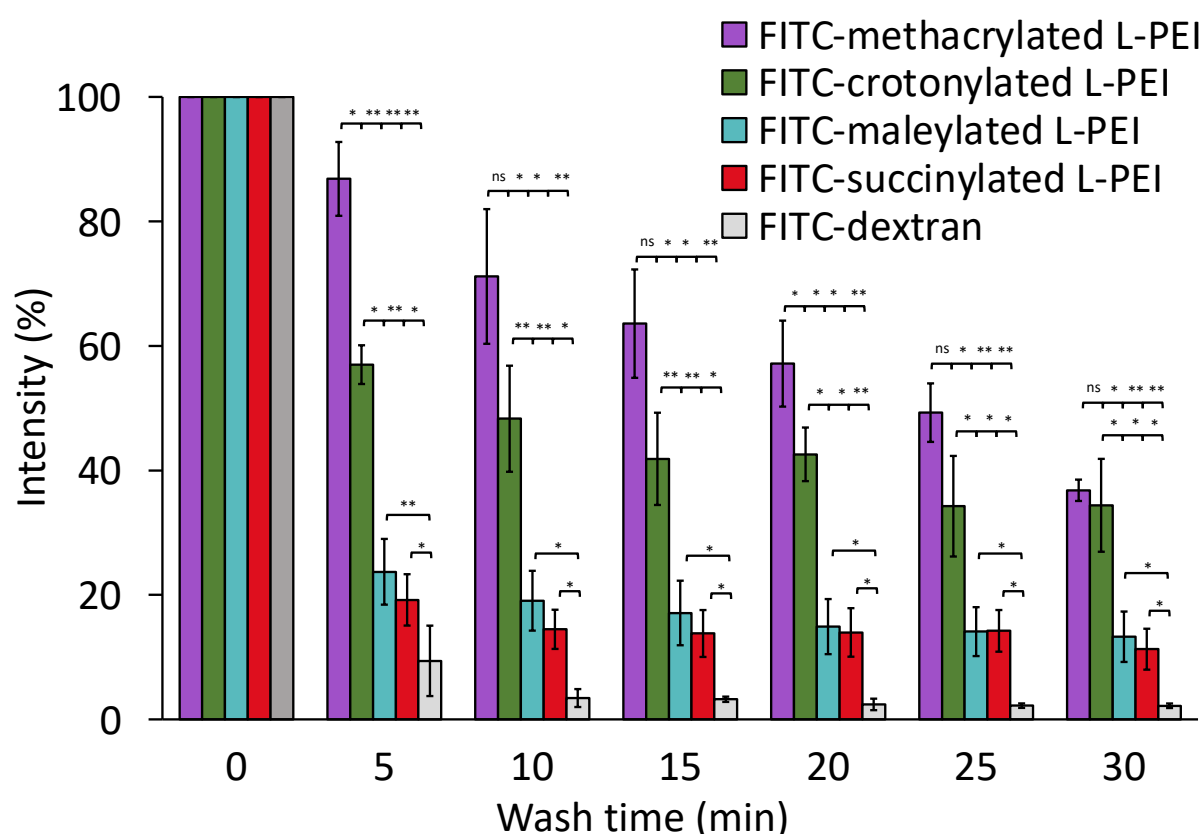


Figure 3.3-3. Retention of FITC-methacrylated L-PEI, FITC-crotonylated L-PEI, FITC-maleylated L-PEI, FITC-succinylated L-PEI and FITC-dextran on bovine palpebral conjunctiva when washed with STF (0.1 mL/min) for 30 min at 34.5±0.1°C. Mean ± standard deviation, n=3. The statistically significant differences are represented as: ** p < 0.01; * p < 0.05; ns – no significance.

Throughout 30 min of washing with STF, there was a statistically significant greater retention of all the studied L-PEI derivatives compared to the non-adhesive FITC-dextran. After 5 min washing, retention of FITC-methacrylated L-PEI, FITC-crotonylated L-PEI, FITC-maleylated L-PEI and FITC succinylated L-PEI was 87%, 57%, 24% and 18%, respectively, while the retention of FITC-dextran was 9%. The order of relative retention was maintained throughout the washout period, with 37%, 34%, 13% and 11% of FITC-

methacrylated L-PEI, FITC-crotonylated L-PEI, FITC-maleylated L-PEI and FITC succinylated L-PEI, remaining on the tissue after 30 min washing. Although poorly mucoadhesive, 2% of FITC-dextran fluorescence remained after 30 min washing but this could be attributed to its penetration into the bovine conjunctiva tissue rather than adhesion to the surface.

The strong adhesion of FITC-methacrylated L-PEI and crotonylated L-PEI can be attributed to the presence of unsaturated C=C within these polymers, which could form covalent bonds with thiol groups present on mucosal surfaces.⁴³⁴ The contribution of the amine groups within these polymers to adhesion will be minimal at pH to 7.4, since their macromolecules will be either non-charged or negatively charged. The methacrylated L-PEI displayed greater retention values than the crotonylated derivative possibly due to better tendency of methacryloyl groups to form covalent bonds with thiols compared to crotonyl groups, related to the steric hindrance of the methyl group.⁴³⁵

As described above, the pI_{IEP} of maleylated L-PEI and succinylated L-PEI, measured via the turbidimetric technique, was below pH 7.4 and so both these polymers carry a net negative charge throughout this retention study. As both the polyampholytes and mucin carry a net negative charge, electrostatic interactions with mucosal surface are unlikely. Other mucoadhesive mechanisms may operate such as interdiffusion when polymers are in intimate contact with the mucus layer.^{250,436} It is likely that the polyampholytes penetrated into the bovine palpebral conjunctiva tissue, synergized with diffusion of soluble mucins from the tissue, as has been previously reported.⁴³⁷ FITC-maleylated L-PEI showed greater retention than FITC-succinylated L-PEI, perhaps due to the presence of the C=C bond, capable of forming covalent bonds with thiol groups in mucin and which is absent in the succinylated polymer. It is also evident that all polymers were retained to a greater extent than the FITC-dextran; again, it is likely that our linear and flexible polymers diffuse into the mucus layer more readily than dextran.

3.3.3 Slug mucosal irritation test

A slug mucosal irritation test was developed by Adriaens et al.^{438,439}, measuring slug mucus production (MP%) to evaluate the irritation potential of pharmaceutical compositions on mucosal surfaces. Here, a modified version of the test previously developed within our research group was used to assess irritation of methacrylated-, crotonylated-, maleylated- and succinylated L-PEI^{440,441} with PBS as a negative control and 1% benzalkonium chloride (BAC) and b-PEI as two positive controls.

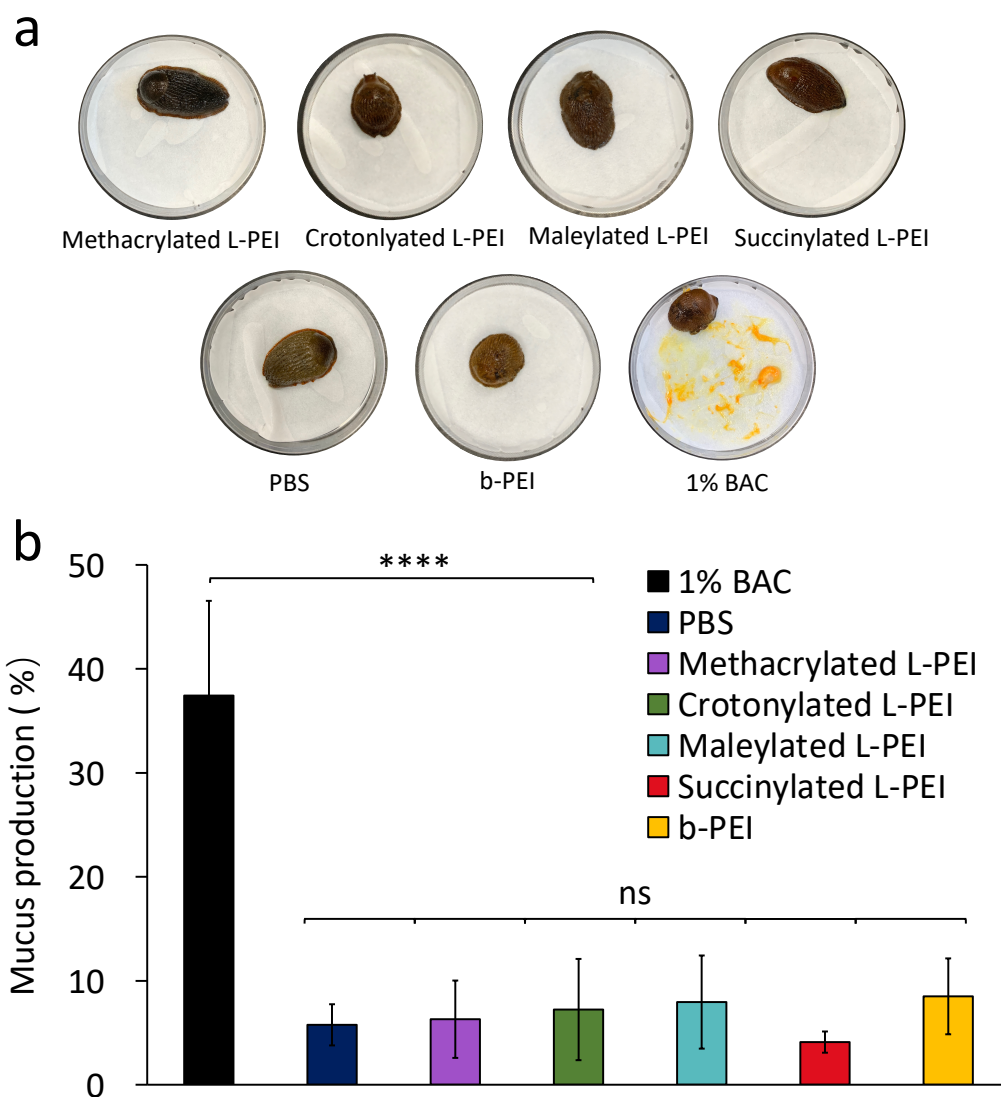


Figure 3.3-4. Exemplar images of slugs following 60 min of exposure to controls and test solutions using a slug mucosal irritation test (a); and mucus production in contact with 1% BAC in PBS, PBS, methacrylated L-PEI, crotonylated L-PEI, maleylated L-PEI, succinylated L-PEI and branched PEI (b). Data is given as mean \pm standard deviation ($n = 5$). Statistically significant differences were represented as: **** – $p < 0.0001$; ns – no significance.

Figure 3.3-4 gives exemplary images of slugs after 60 min of exposure to 1% BAC in PBS solution (positive control), PBS solution (negative control), 1.0 mg/mL methacrylated L-PEI, crotonylated L-PEI, maleylated L-PEI, succinylated L-PEI and b-PEI solutions, along with mucus production values. A significant irritation response was evident in slugs exposed to 1% BAC, reaching 37 ± 9 % mucus production. It should be noted that these positive control results have significant variability due to the slugs' increased activity and movement to minimize contact with the irritant but our data are in accord with prior reports.^{419,441} As expected, exposure to the negative control (PBS) generated 6 ± 2 % of mucus production,

consistent with previous reports by Adriaens et al.^{438,439} and by Khutoryanskaya et al⁴⁴⁰. Mucus production following exposure to our mucoadhesive polymers was not statistically different from the amount of mucus produced in control slugs, treated with PBS (mucus production: methacrylated L-PEI (6±4%), crotonylated L-PEI (7±5%), maleylated L-PEI (8±4%), succinylated L-PEI (4±1%), and b-PEI solutions (8± 4%)). These results suggest that the novel polymers are not strong irritants though it should be noted that b-PEI solutions also did not show significant mucosal irritation in slugs whereas it has well documented toxic properties in various cell culture assays⁴⁴²⁻⁴⁴⁴.

3.3.4 Toxicological tests in live planaria

Planaria are aquatic flatworms that have been recently proposed by our research group as an *in vivo* model for screening irritancy potential of formulations.⁴¹⁷ In this study, the potential toxicity of the novel polymers was evaluated using two *in vivo* assays in planaria.^{257,417} In the acute toxicity assay, live planaria were exposed to 1 mg/mL polymer solutions for up to 48 h. Under these conditions, all planaria survived throughout exposure, similar to worms that were exposed to PBS and artificial pond water, used as two negative controls. Planaria exposed to b-PEI at one tenth the above concentration (0.1 mg/mL) only survived for up to 1 h, before partially disintegrating at 24 h and 48 h (Appendix XIV). It should be noted that this test cannot be performed using L-PEI due to its tendency to form gels.³²⁹ The toxic nature of b-PEI is well documented in cell cultures⁴⁴⁴⁻⁴⁴⁶, and so was expected to have toxic effects on planaria. The results of this study indicate that chemical modification of L-PEI with anhydrides results in polymeric derivatives that reduce toxicity of the parent material.

The effects of the new polymers on the integrity of planaria epithelial membranes were explored using a fluorescence assay; Shah et al. demonstrated that sodium fluorescein can penetrate into planaria when its outer membrane is damaged following contact with irritant chemicals.⁴¹⁷

Planaria initially exposed to polymer solutions for 1, 24 or 48 hours, and subsequently exposed to solutions of sodium fluorescein, showed fluorescence levels similar to the negative controls or artificial pond water (Figure 3.3-5).

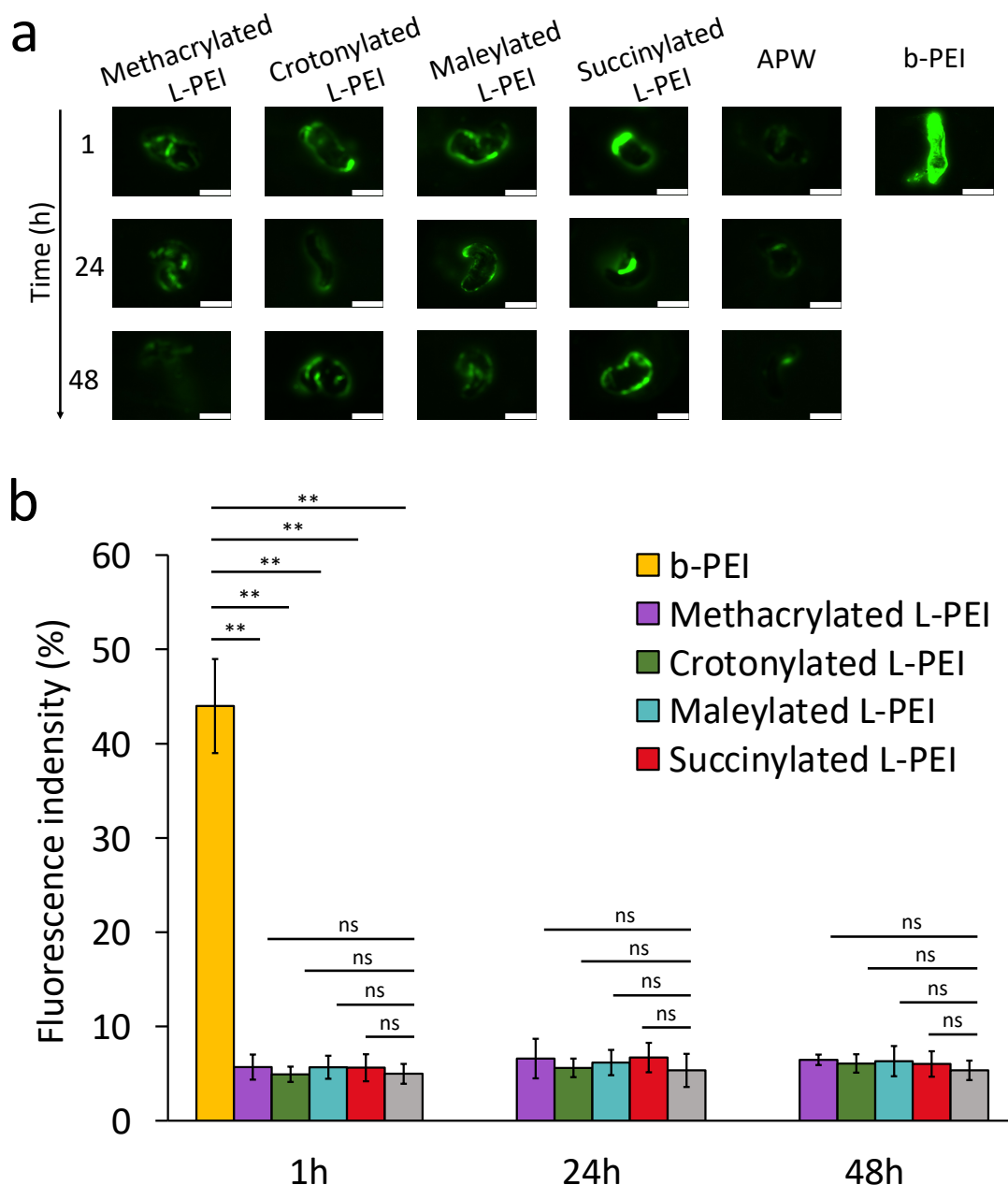


Figure 3.3-5. (a) Exemplar fluorescent images of individual planaria exposed to 1 mg/mL methacrylated-, crotonylated-, maleylated- and succinylated L-PEI with APW used as a negative control and 0.1 mg/mL b-PEI as a positive control. Note that fluorescent images could not be obtained after 24 h and 48 h exposure to b-PEI as these conditions resulted in partial disintegration of the worms. Scale bar is 2 mm. (b) Mean fluorescence intensity values of planaria exposed to 1 mg/mL methacrylated-, crotonylated-, maleylated- and succinylated L-PEI with APW as negative control and 0.1 mg/mL b-PEI as positive control, calculated from the analysis of images. Mean \pm standard deviation, $n=5$. The statistically significant differences are represented as: ** $p < 0.01$; ns: no significance.

These results indicate that the synthesized polymers do not adversely affect the planarian membrane and were equivalent to the results following exposure to artificial pond water. However, there was a statistically significant increase in fluorescence intensity when planaria were exposed to the strongly irritant 0.1mg/mL b-PEI, used at a tenth of the strength of our

new materials. Though 0.1 mg/mL b-PEI was non-irritant to slugs, it showed toxicity to planaria which may be explained by the ability of slugs to secrete a mucus layer that acts as a barrier to b-PEI, or simply due to differences in the resilience of the slug membrane compared to the more fragile and simpler planaria membrane.

The toxicity of the newly-synthesized polymers was also investigated in human A459 epithelial cells using the MTT assay to measure cell viability. A549 cells have been tested in a variety of applications, as they model the alveolar Type II pulmonary epithelium and in manufacturing constructs for use in clinical trials. A549 cells are adenocarcinoma human alveolar basal epithelial cells, which have been extensively applied in toxicology, drug therapy and pharmacological studies.^{447,448}

Figure 3.3-6 shows that all the new polymers at both concentrations (0.5 mg/mL or 1.0 mg/mL) tested for 24 hours, did not alter the viability of the A549 cells when compared to complete medium 1% FBS as negative control. On the contrary, the toxic b-PEI^{449,450} (used as a positive control) significantly reduced the cell viability by 86 %.

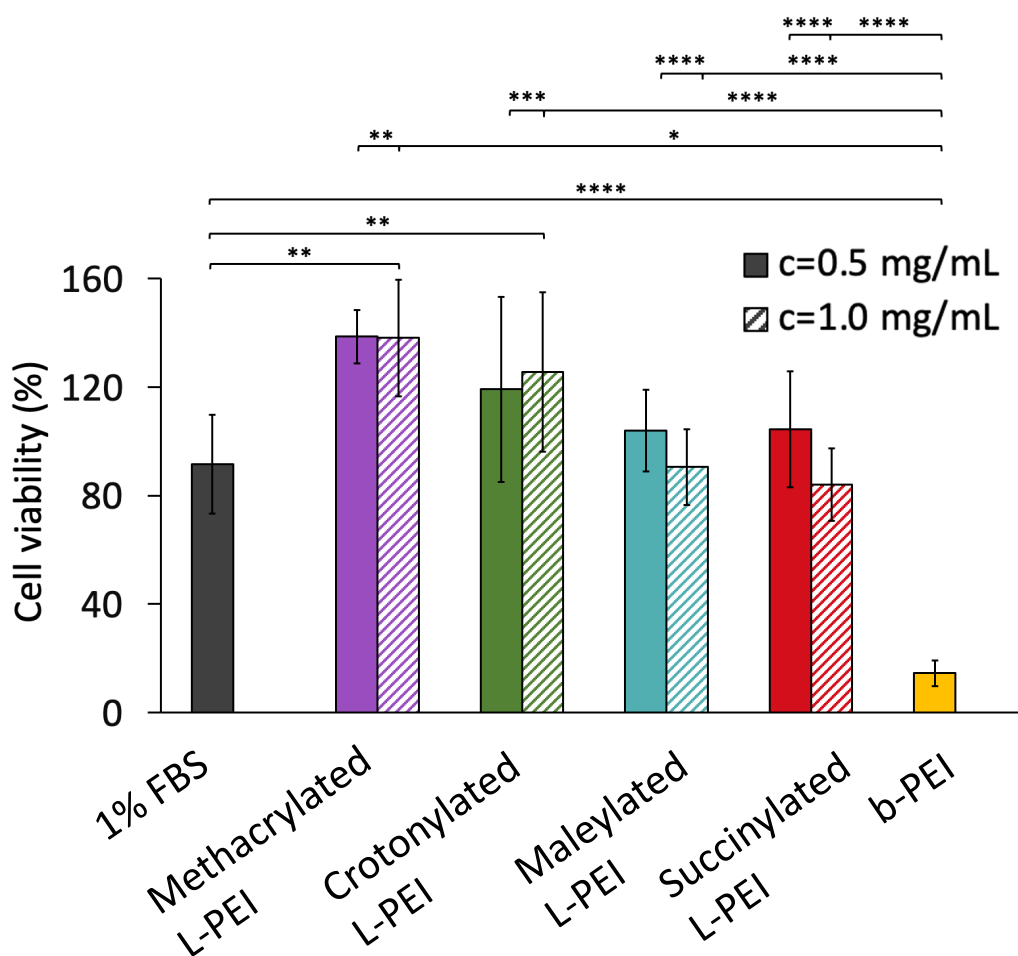


Figure 3.3-6. Viability of A549 cells determined after treatment with solutions of methacrylated L-PEI, crotonylated L-PEI, maleylated L-PEI and succinylated L-PEI for 24 h using MTT assay. Cells treated with

complete medium 1% FBS were used as a negative control and cells exposed to 0.5 mg/mL b-PEI were used as a positive control. Data are expressed as % of external control, cells untreated, left in complete medium 10% FBS. Values are shown as means \pm SD (n = 6 replicated per treatment). Statistically significant differences are represented as: * p < 0.05; ** p < 0.01; ns: *** p < 0.001; **** p < 0.0001.

Interestingly, viable cell numbers increased when treated with methacrylated L-PEI by 47 % at both concentration and with crotonylated L-PEI treatment increased 28 % (at 0.5 mg/mL) and 34 % (at 1.0 mg/mL) compared to complete medium 1 % FBS (control). It is feasible that these polymers promote cell growth and proliferation, as reported previously for a methacrylic anhydride-modified gelatin hydrogel.⁴⁵¹

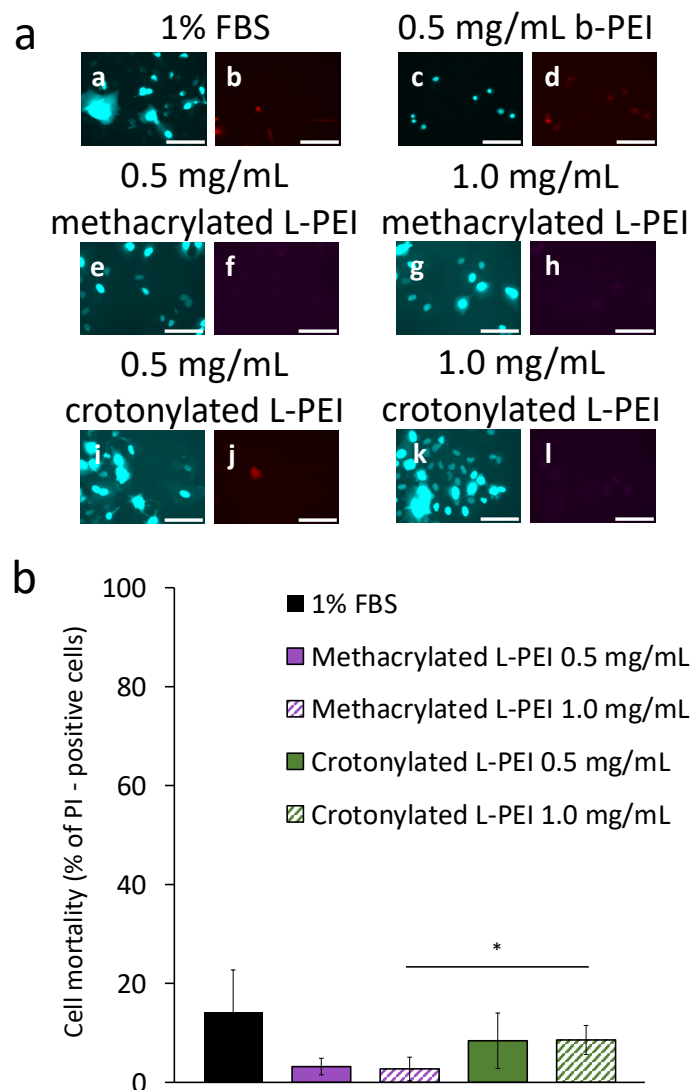


Figure 3.3-7. Mortality of A549 cells evaluated after treatment with methacrylated L-PEI and crotonylated L-PEI at 0.5 mg/mL and 1.0 mg/mL for 24 h, with untreated cells in 1% FBS as the negative control (a); representative DAPI (left) and PI (right) staining images of methacrylated L-PEI and crotonylated L-PEI at 0.5 mg/mL and 1.0 mg/mL with cells cultured in 1% FBS as a negative control and cells exposed in 0.5 mg/mL b-PEI as a positive control, scale bar is 100 nm (b). Cell mortality % is expressed as values are expressed as means \pm SD (n = 3). Statistically significant differences are represented as: * p < 0.05.

To further confirm the safety of our polymers, we assessed the plasma membrane integrity following 24 hours treatment, using the normally impermeant fluorescent DNA-binding dye PI⁴²⁴ to stain the DNA of dead cells⁴⁵², used in tandem with the nucleic acid stain DAPI, used to determine both cell numbers and thus proliferation. Also in this case, complete medium 1% FBS and 0.5 mg/mL b-PEI were used as negative and positive control, respectively.

Figure 3.3-7 illustrates cell mortality following their treatment with polymer solutions. Cell mortality from methacrylated L-PEI at 0.5 mg/mL and 1.0 mg/mL was 3.2 % and 2.7 %, respectively, while mortality from crotonylated L-PEI at 0.5 mg/mL and 1.0 mg/mL was 8.4 % and 8.6 %; both values are below that of cells cultured in 1% FBS (14.2%) whilst mortality following b-PEI treatment was 100 % (n=6). These results confirm the earlier findings that the new polymers show no adverse effects on cell viability and indeed suggest that they may have some protective effects against cell death.

3.4 Conclusion

In this work, cationic and amphoteric mucoadhesive polymers were synthesized by modification of L-PEI with methacrylic anhydride, crotonic anhydride, maleic anhydride and succinic anhydride. The mucoadhesive properties and mechanisms of action at physiological pH (7.4) were explored using a fluorescence flow through method on bovine palpebral conjunctiva tissue. Methacrylated L-PEI and crotonylated L-PEI showed greater mucoadhesion than the two amphoteric polymers due to their ability to form covalent bonds with thiols present on mucosal surfaces. Due to the toxicity of L-PEI limiting its pharmaceutical uses, the toxicological effects of our modified L-PEI materials were assessed. Irritation studies conducted on slugs showed no evidence that the new materials were irritant to a mucosal membrane. The rapid and low cost planaria assay similarly demonstrated no significant damage to membranes at the concentrations employed. The MTT assay and DAPI/PI staining of A549 cell also demonstrated that the polymers had no appreciable toxicity in a human cell line. This work thus provides a series of anhydride modified L-PEIs with improved biocompatibility and mucoadhesive properties that operate via a range of mechanisms from covalent bonding with mucins to electrostatic interactions or inter-diffusion. The toxicological evaluation of b-PEI using slug mucosal irritation assay, planaria-based assays and cell culture assay indicate that our new assays using planaria are more sensitive in detecting toxicity of compounds compared to the use of slugs.

3.5 References

- (398) Bhaskar, K. R.; Garik, P.; Turner, B. S.; Bradley, J. D.; Bansil, R.; Stanley, H. E.; LaMont, J. T. Viscous fingering of HCl through gastric mucin. *Nature* **1992**, *360* (6403), 458.
- (399) Bej, R.; Haag, R. Mucus-Inspired Dynamic Hydrogels: Synthesis and Future Perspectives. *Journal of the American Chemical Society* **2022**, *144* (44), 20137.
- (400) Wagner, C. E.; Krupkin, M.; Smith-Dupont, K. B.; Wu, C. M.; Bustos, N. A.; Witten, J.; Ribbeck, K. Comparison of Physicochemical Properties of Native Mucus and Reconstituted Mucin Gels. *Biomacromolecules* **2023**, *24* (2), 628.
- (401) Deleray, A. C.; Kramer, J. R. Biomimetic Glycosylated Polythreonines by N-Carboxyanhydride Polymerization. *Biomacromolecules* **2022**, *23* (3), 1453.
- (402) Allen, A.; PAIN, R. H.; ROBSON, T. R. Model for the structure of the gastric mucous gel. *Nature* **1976**, *264* (5581), 88.
- (403) Nouri, A.; Jelkmann, M.; Khoee, S.; Bernkop-Schnürch, A. Diaminated Starch: A Competitor of Chitosan with Highly Mucoadhesive Properties due to Increased Local Cationic Charge Density. *Biomacromolecules* **2020**, *21* (2), 999.
- (404) Wibel, R.; Braun, D. E.; Hämmerle, L.; Jörgensen, A. M.; Knoll, P.; Salvenmoser, W.; Steinbring, C.; Bernkop-Schnürch, A. In Vitro Investigation of Thiolated Chitosan Derivatives as Mucoadhesive Coating Materials for Solid Lipid Nanoparticles. *Biomacromolecules* **2021**, *22* (9), 3980.
- (405) Cazorla-Luna, R.; Notario-Pérez, F.; Martín-Illana, A.; Bedoya, L.-M.; Tamayo, A.; Rubio, J.; Ruiz-Caro, R.; Veiga, M.-D. Development and In Vitro/Ex Vivo Characterization of Vaginal Mucoadhesive Bilayer Films Based on Ethylcellulose and Biopolymers for Vaginal Sustained Release of Tenofovir. *Biomacromolecules* **2020**, *21* (6), 2309.
- (406) Yahagi, R.; Machida, Y.; Onishi, H.; Machida, Y. Mucoadhesive suppositories of ramosetron hydrochloride utilizing Carbopol®. *International Journal of Pharmaceutics* **2000**, *193* (2), 205.
- (407) Lambermont-Thijs, H. M. L.; van der Woerd, F. S.; Baumgaertel, A.; Bonami, L.; Du Prez, F. E.; Schubert, U. S.; Hoogenboom, R. Linear Poly(ethylene imine)s by Acidic Hydrolysis of Poly(2-oxazoline): Kinetic Screening, Thermal Properties, and Temperature-Induced Solubility Transitions. *Macromolecules* **2010**, *43* (2), 927.
- (408) Wightman, L.; Kircheis, R.; Rössler, V.; Carotta, S.; Ruzicka, R.; Kurs, M.; Wagner, E. Different behavior of branched and linear polyethylenimine for gene delivery in vitro and in vivo. *The Journal of Gene Medicine* **2001**, *3* (4), 362.
- (409) Goula, D.; Remy, J. S.; Erbacher, P.; Wasowicz, M.; Levi, G.; Abdallah, B.; Demeneix, B. A. Size, diffusibility and transfection performance of linear PEI/DNA complexes in the mouse central nervous system. *Gene Therapy* **1998**, *5* (5), 712.
- (410) Perevyazko, I. Y.; Bauer, M.; Pavlov, G. M.; Hoepfner, S.; Schubert, S.; Fischer, D.; Schubert, U. S. Polyelectrolyte Complexes of DNA and Linear PEI: Formation, Composition and Properties. *Langmuir* **2012**, *28* (46), 16167.
- (411) Madejová, J.; Barlog, M.; Slaný, M.; Bashir, S.; Scholtzová, E.; Tunega, D.; Jankovič, L. Advanced materials based on montmorillonite modified with poly(ethylenimine) and poly(2-methyl-2-oxazoline): Experimental and DFT study. *Colloids and Surfaces A: Physicochemical and Engineering Aspects* **2023**, *659*, 130784.

- (412) Akiyama, Y.; Harada, A.; Nagasaki, Y.; Kataoka, K. Synthesis of Poly(ethylene glycol)-block-poly(ethylenimine) Possessing an Acetal Group at the PEG End. *Macromolecules* **2000**, *33* (16), 5841.
- (413) Yang, T.; Hussain, A.; Bai, S.; Khalil, I. A.; Harashima, H.; Ahsan, F. Positively charged polyethylenimines enhance nasal absorption of the negatively charged drug, low molecular weight heparin. *Journal of Controlled Release* **2006**, *115* (3), 289.
- (414) Dai, Y.; Zhang, X.; Zhuo, R. Polymeric micelles stabilized by polyethylenimine–copper (C₂H₅N–Cu) coordination for sustained drug release. *RSC advances* **2016**, *6* (27), 22964.
- (415) Moghimi, S. M.; Symonds, P.; Murray, J. C.; Hunter, A. C.; Debska, G.; Szewczyk, A. A two-stage poly (ethylenimine)-mediated cytotoxicity: implications for gene transfer/therapy. *Molecular therapy* **2005**, *11* (6), 990.
- (416) Mintzer, M. A.; Simanek, E. E. Nonviral Vectors for Gene Delivery. *Chemical Reviews* **2009**, *109* (2), 259.
- (417) Shah, S. I.; Williams, A. C.; Lau, W. M.; Khutoryanskiy, V. V. Planarian toxicity fluorescent assay: A rapid and cheap pre-screening tool for potential skin irritants. *Toxicology in Vitro* **2020**, *69*, 105004.
- (418) Khutoryanskaya, O. V.; Morrison, P. W. J.; Seilkhanov, S. K.; Mussin, M. N.; Ozhmukhametova, E. K.; Rakhypbekov, T. K.; Khutoryanskiy, V. V. Hydrogen-Bonded Complexes and Blends of Poly(acrylic acid) and Methylcellulose: Nanoparticles and Mucoadhesive Films for Ocular Delivery of Riboflavin. *Macromolecular Bioscience* **2014**, *14* (2), 225.
- (419) Moiseev, R. V.; Steele, F.; Khutoryanskiy, V. V. Polyaphron Formulations Stabilised with Different Water-Soluble Polymers for Ocular Drug Delivery. *Pharmaceutics* **2022**, *14* (5), 926.
- (420) Van Haeringen, N. J. Clinical biochemistry of tears. *Survey of ophthalmology* **1981**, *26* (2), 84.
- (421) Cave, R. A.; Cook, J. P.; Connon, C. J.; Khutoryanskiy, V. V. A flow system for the on-line quantitative measurement of the retention of dosage forms on biological surfaces using spectroscopy and image analysis. *International Journal of Pharmaceutics* **2012**, *428* (1), 96.
- (422) Kessel, L.; Johnson, L.; Arvidsson, H.; Larsen, M. The relationship between body and ambient temperature and corneal temperature. *Investigative ophthalmology & visual science* **2010**, *51* (12), 6593.
- (423) Liu, Y.; Peterson, D. A.; Kimura, H.; Schubert, D. Mechanism of cellular 3-(4, 5-dimethylthiazol-2-yl)-2, 5-diphenyltetrazolium bromide (MTT) reduction. *Journal of neurochemistry* **1997**, *69* (2), 581.
- (424) Cummings, B. S.; Schnellmann, R. G. Measurement of Cell Death in Mammalian Cells. *Current Protocols in Pharmacology* **2004**, *25* (1), 12.8.1.
- (425) Jachimska, B.; Wasilewska, M.; Adamczyk, Z. Characterization of Globular Protein Solutions by Dynamic Light Scattering, Electrophoretic Mobility, and Viscosity Measurements. *Langmuir* **2008**, *24* (13), 6866.
- (426) Graur, D. The evolution of electrophoretic mobility of proteins. *Journal of Theoretical Biology* **1986**, *118* (4), 443.
- (427) Ramsay, E.; del Amo, E. M.; Toropainen, E.; Tengvall-Unadike, U.; Ranta, V.-P.; Urtti, A.; Ruponen, M. Corneal and conjunctival drug permeability: Systematic comparison and pharmacokinetic impact in the eye. *European Journal of Pharmaceutical Sciences* **2018**, *119*, 83.

- (428) Huang, A. J.; Tseng, S. C.; Kenyon, K. R. Paracellular permeability of corneal and conjunctival epithelia. *Investigative Ophthalmology & Visual Science* **1989**, *30* (4), 684.
- (429) Zambito, Y.; Di Colo, G. Polysaccharides as excipients for ocular topical formulations. *Biomaterials Applications for Nanomedicine* **2011**, 253.
- (430) Moiseev, R. V.; Morrison, P. W. J.; Steele, F.; Khutoryanskiy, V. V. Penetration Enhancers in Ocular Drug Delivery. *Pharmaceutics* **2019**, *11* (7), 321.
- (431) Silva, B.; São Braz, B.; Delgado, E.; Gonçalves, L. Colloidal nanosystems with mucoadhesive properties designed for ocular topical delivery. *International Journal of Pharmaceutics* **2021**, *606*, 120873.
- (432) Ludwig, A. The use of mucoadhesive polymers in ocular drug delivery. *Advanced Drug Delivery Reviews* **2005**, *57* (11), 1595.
- (433) Greaves, J. L.; Wilson, C. G. Treatment of diseases of the eye with mucoadhesive delivery systems. *Advanced Drug Delivery Reviews* **1993**, *11* (3), 349.
- (434) Shatabayeva, E. O.; Kaldybekov, D. B.; Ulmanova, L.; Zhaisanbayeva, B. A.; Mun, E. A.; Kenessova, Z. A.; Kudaibergenov, S. E.; Khutoryanskiy, V. V. Enhancing Mucoadhesive Properties of Gelatin through Chemical Modification with Unsaturated Anhydrides. *Biomacromolecules* **2024**, DOI:10.1021/acs.biomac.3c01183 10.1021/acs.biomac.3c01183.
- (435) Hill, C. A. S.; Cetin, N. S. Surface activation of wood for graft polymerisation. *International Journal of Adhesion and Adhesives* **2000**, *20* (1), 71.
- (436) Voiutskii, S. S. Autohesion and adhesion of high polymers. **1963**.
- (437) Hodges, R. R.; Dartt, D. A. Tear film mucins: front line defenders of the ocular surface; comparison with airway and gastrointestinal tract mucins. *Experimental eye research* **2013**, *117*, 62.
- (438) Adriaens, E.; Remon, J. P. Gastropods as an evaluation tool for screening the irritating potency of absorption enhancers and drugs. *Pharmaceutical research* **1999**, *16*, 1240.
- (439) Adriaens, E.; Dierckens, K.; Bauters, T. G.; Nelis, H. J.; Van Goethem, F.; Vanparys, P.; Remon, J. P. The mucosal toxicity of different benzalkonium chloride analogues evaluated with an alternative test using slugs. *Pharmaceutical research* **2001**, *18*, 937.
- (440) Khutoryanskaya, O. V.; Morrison, P. W.; Seilkhanov, S. K.; Mussin, M. N.; Ozhmukhametova, E. K.; Rakhypbekov, T. K.; Khutoryanskiy, V. V. Hydrogen-Bonded Complexes and Blends of Poly (acrylic acid) and Methylcellulose: Nanoparticles and Mucoadhesive Films for Ocular Delivery of Riboflavin. *Macromolecular bioscience* **2014**, *14* (2), 225.
- (441) Kaldybekov, D. B.; Filippov, S. K.; Radulescu, A.; Khutoryanskiy, V. V. Maleimide-functionalised PLGA-PEG nanoparticles as mucoadhesive carriers for intravesical drug delivery. *European journal of pharmaceutics and biopharmaceutics* **2019**, *143*, 24.
- (442) Aravindan, L.; Bicknell, K. A.; Brooks, G.; Khutoryanskiy, V. V.; Williams, A. C. Effect of acyl chain length on transfection efficiency and toxicity of polyethylenimine. *International Journal of Pharmaceutics* **2009**, *378* (1), 201.
- (443) Fischer, D.; Li, Y.; Ahlemeyer, B.; Krieglstein, J.; Kissel, T. In vitro cytotoxicity testing of polycations: influence of polymer structure on cell viability and hemolysis. *Biomaterials* **2003**, *24* (7), 1121.
- (444) Monnery, B. D.; Wright, M.; Cavill, R.; Hoogenboom, R.; Shaunak, S.; Steinke, J. H. G.; Thanou, M. Cytotoxicity of polycations: Relationship of molecular weight and the hydrolytic theory of the mechanism of toxicity. *International Journal of Pharmaceutics* **2017**, *521* (1), 249.

- (445) Kafil, V.; Omid, Y. Cytotoxic impacts of linear and branched polyethylenimine nanostructures in A431 cells. *Bioimpacts* **2011**, *1* (1), 23.
- (446) Venault, A.; Huang, Y. C.; Lo, J. W.; Chou, C. J.; Chinnathambi, A.; Higuchi, A.; Chen, W. S.; Chen, W. Y.; Chang, Y. Tunable PEGylation of branch-type PEI/DNA polyplexes with a compromise of low cytotoxicity and high transgene expression: in vitro and in vivo gene delivery. *Journal of Materials Chemistry B* **2017**, *5* (24), 4732.
- (447) Shi, Q.; Tang, J.; Liu, X.; Liu, R. Ultraviolet-induced photodegradation elevated the toxicity of polystyrene nanoplastics on human lung epithelial A549 cells. *Environmental Science: Nano* **2021**, *8* (9), 2660.
- (448) Chang, Y.; Yang, S.-T.; Liu, J.-H.; Dong, E.; Wang, Y.; Cao, A.; Liu, Y.; Wang, H. In vitro toxicity evaluation of graphene oxide on A549 cells. *Toxicology Letters* **2011**, *200* (3), 201.
- (449) Kim, Y. H.; Park, J. H.; Lee, M.; Kim, Y.-H.; Park, T. G.; Kim, S. W. Polyethylenimine with acid-labile linkages as a biodegradable gene carrier. *Journal of Controlled Release* **2005**, *103* (1), 209.
- (450) Lv, H.; Zhang, S.; Wang, B.; Cui, S.; Yan, J. Toxicity of cationic lipids and cationic polymers in gene delivery. *Journal of Controlled Release* **2006**, *114* (1), 100.
- (451) Liu, C.; Zeng, H.; Chen, Z.; Ge, Z.; Wang, B.; Liu, B.; Fan, Z. Sprayable methacrylic anhydride-modified gelatin hydrogel combined with bionic neutrophils nanoparticles for scar-free wound healing of diabetes mellitus. *International Journal of Biological Macromolecules* **2022**, *202*, 418.
- (452) Shi, L.; Günther, S.; Hübschmann, T.; Wick, L. Y.; Harms, H.; Müller, S. Limits of propidium iodide as a cell viability indicator for environmental bacteria. *Cytometry Part A* **2007**, *71A* (8), 592.
- (453) Ranke, J.; Mölter, K.; Stock, F.; Bottin-Weber, U.; Poczobutt, J.; Hoffmann, J.; Ondruschka, B.; Filser, J.; Jastorff, B. Biological Effects of Imidazolium Ionic Liquids with Varying Chain Lengths in Acute *Vibrio Fischeri* and Wst-1 Cell Viability Assays. *Ecotoxicology and environmental safety* **2004**, *58*, 396.

Author Contributions

MF: investigation, methodology, writing-original draft preparation; RVM: investigation; SA: investigation, supervision; ACW: supervision, writing-review and editing; VVK: conceptualization, supervision, resources, writing-review and editing. All authors have read and agreed to the published version of the manuscript.

Conflicts of interest

There are no conflicts to declare.

Acknowledgement

The authors gratefully acknowledge Technical Services staff within the Chemical Analysis Facility at the University of Reading for technical support & assistance in this work. VVK acknowledges the financial support provided by the Royal Society for his Industry Fellowship (IF/R2/222031). VVK and RVM acknowledge the University of Reading Early

Stage Research Commercialization Investment Fund for supporting the establishment of the Physicochemical, Ex Vivo and Invertebrate Tests and Analysis Centre (PEVITAC).

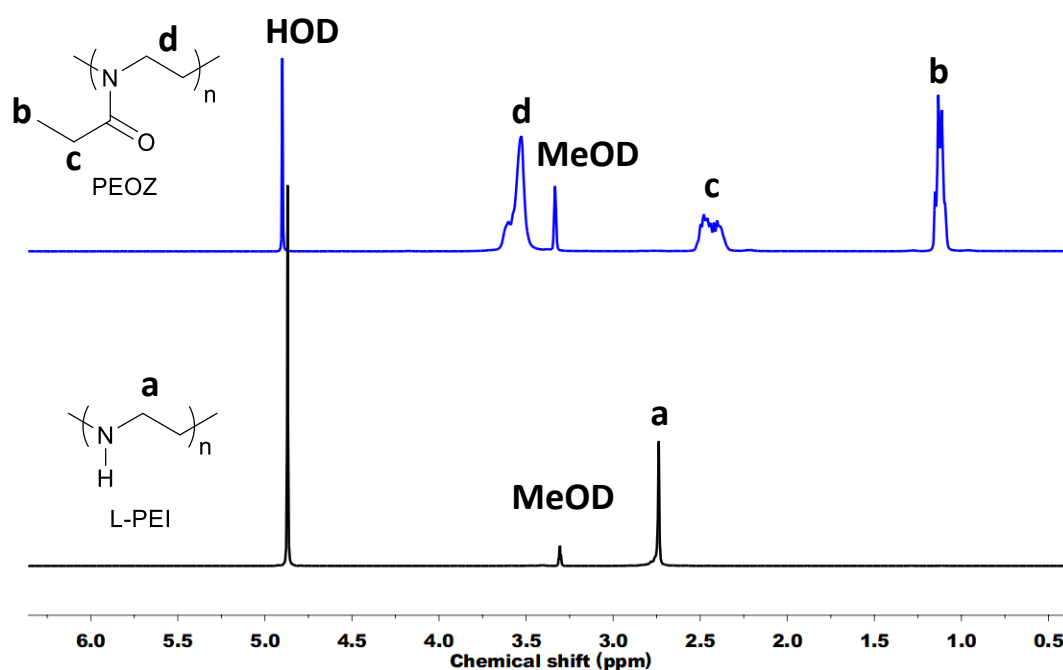
3.6 Supporting Information

Exploring Mucoadhesive and Toxicological Characteristics Following Modification of Linear Polyethyleneimine with Various Anhydrides

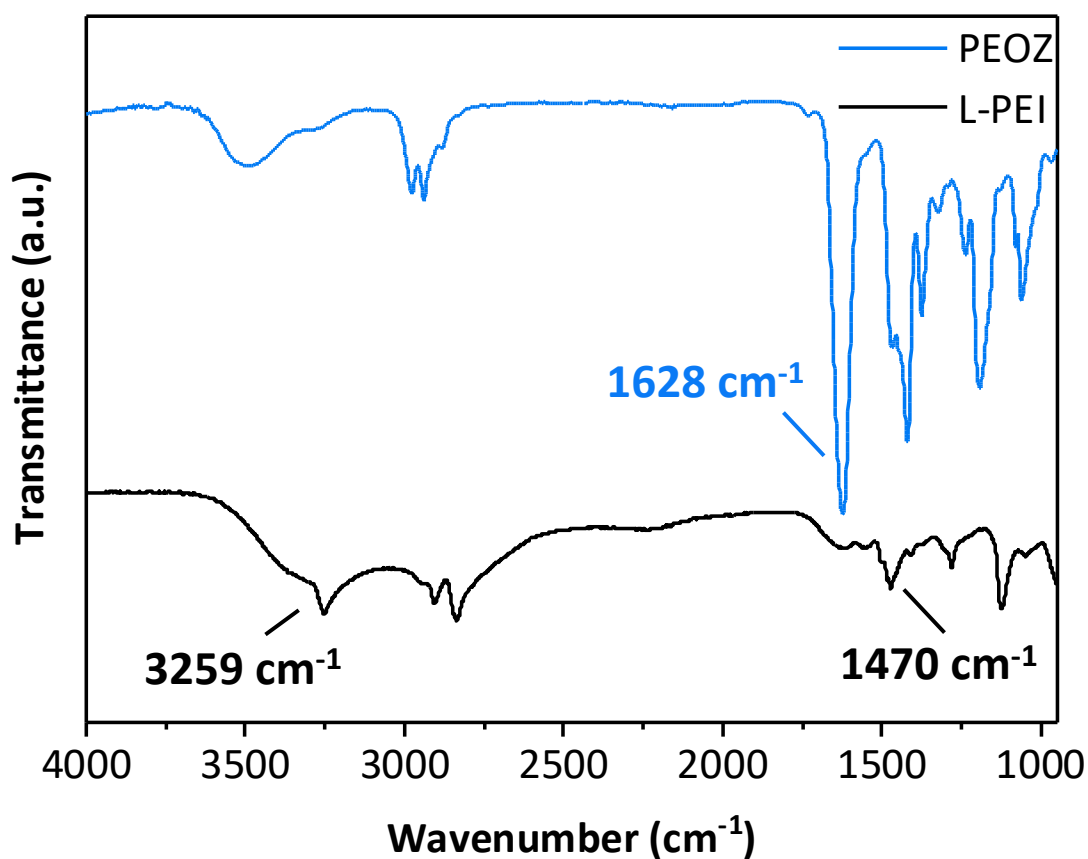
Manfei Fu^a, Roman V. Moiseev^{a,b}, Silvia Amadesi^a, Adrian C. Williams^a, Vitaliy V. Khutoryanskiy^{a*,b}

^a School of Pharmacy, University of Reading, Whiteknights, Post Office Box 224, Reading RG6 6AD, United Kingdom

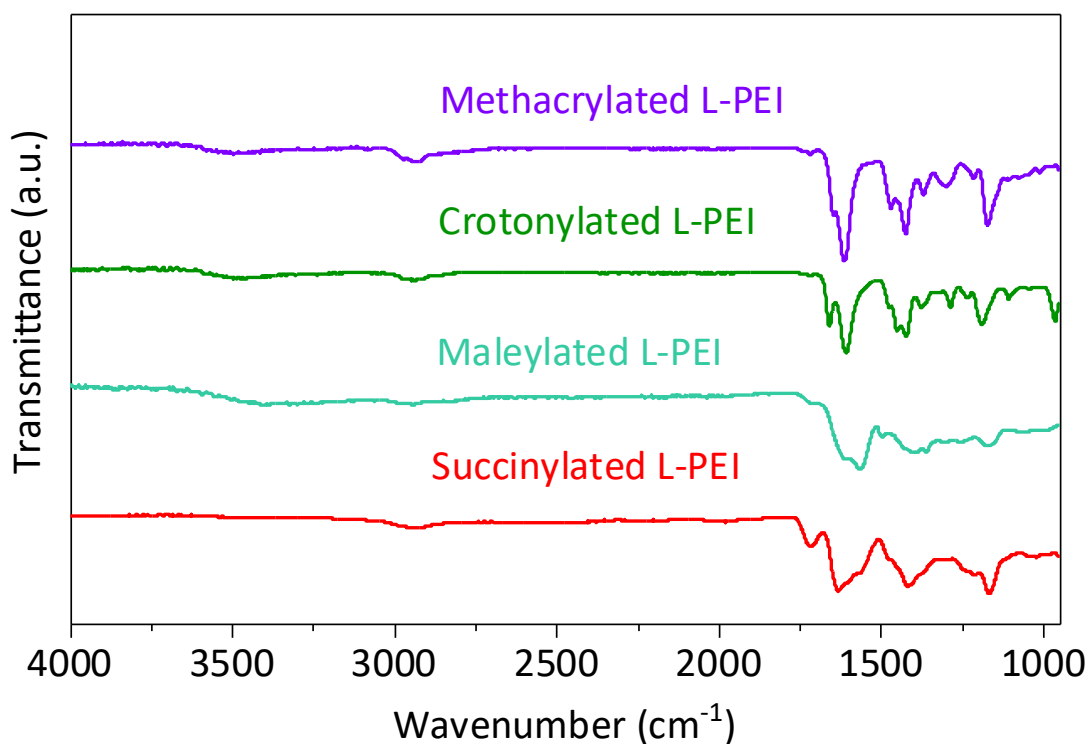
^b Physicochemical, Ex Vivo and Invertebrates Tests and Analysis Centre (PEVITAC), University of Reading, Whiteknights, Reading, RG6 6DX, UK



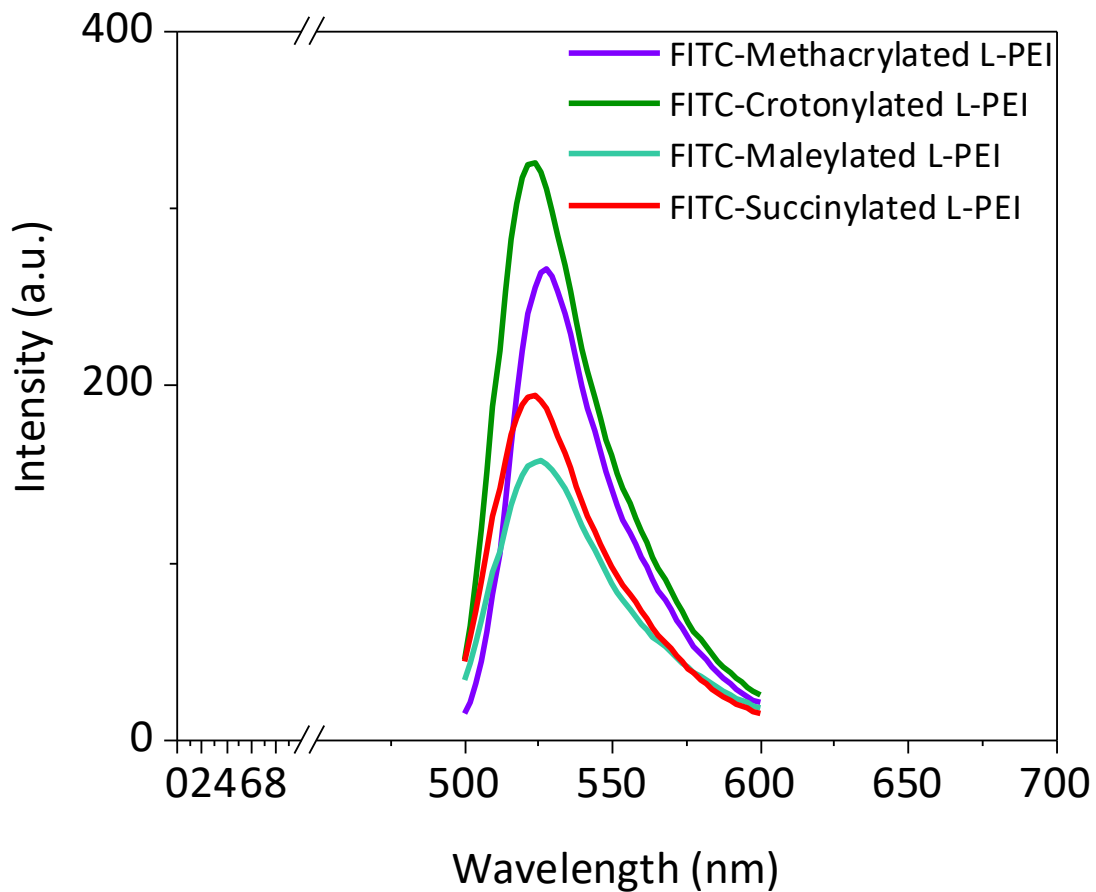
Appendix IX. ¹H-NMR spectra of PEOZ and L-PEI recorded in methanol-d₄.



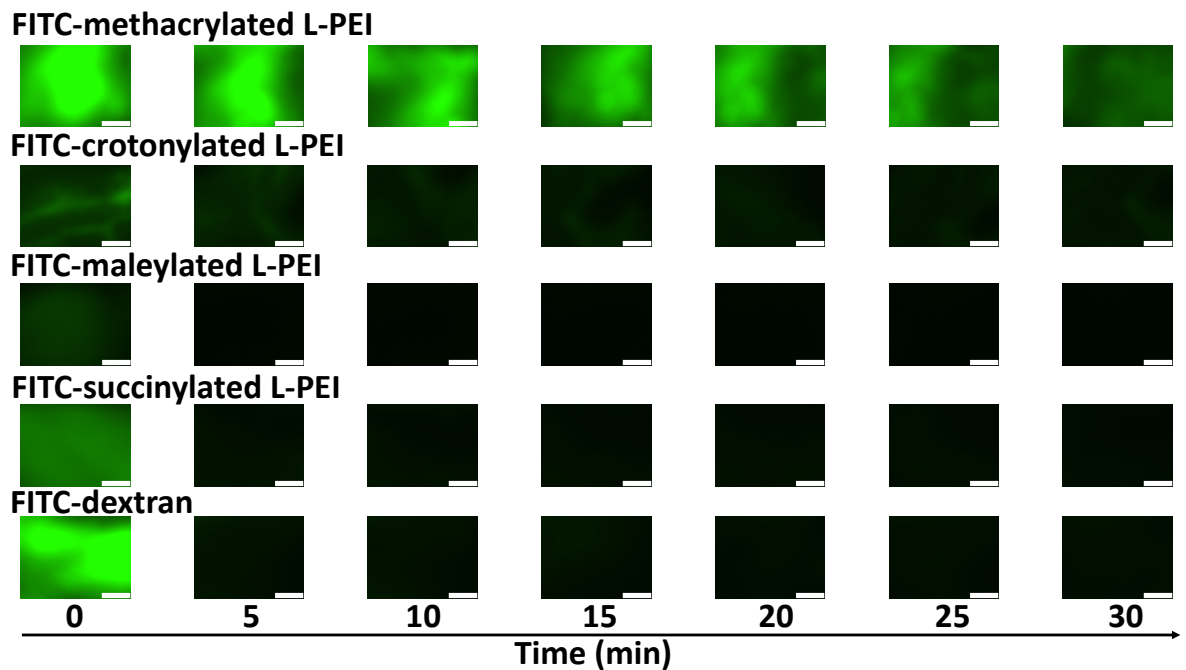
Appendix X. FTIR spectra of PEOZ and L-PEI.



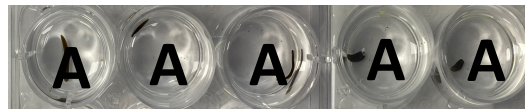
Appendix XI. FTIR spectra of methacrylated L-PEI, crotonylated L-PEI, maleylated L-PEI and succinylated L-PEI.



Appendix XII. Fluorescence spectra of FITC labelled methacrylated L-PEI, crotonylated L-PEI, maleylated L-PEI and succinylated L-PEI at 1mg/mL.



Appendix XIII. Exemplar images of *ex vivo* bovine palpebral conjunctiva with applied FITC-dextran, FITC-methacrylated L-PEI, FITC-crotonylated L-PEI, FITC-maleylated L-PEI and FITC-succinylated L-PEI. Scale bars are 1 mm.

Methacrylated L-PEI**Succinylated L-PEI****Crotonylated L-PEI****APW****Maleylated L-PEI****b-PEI**

Appendix XIV. Acute toxicity assay was conducted after 48h exposure of planaria to 1 mg/mL methacrylated L-PEI, crotonylated L-PEI, maleylated L-PEI, succinylated L-PEI, APW and 24h exposure of planaria to 0.1 mg/mL b-PEI. 'A' denotes live planaria whereas 'D' denotes dead planaria.

Appendix XV. FTIR absorption bands from methacrylated L-PEI, crotonylated L-PEI, maleylated L-PEI and succinylated L-PEI.

FTIR Absorption band of polymers (cm ⁻¹)				Assignment
Methacrylated L-PEI	Crotonylated L-PEI	Maleylated L-PEI	Succinylated L-PEI	
3495	3458	3466	3470	N-H stretch
/	/	3363	3356	O-H stretch
2938	2938	2927	2915	C-H stretch
1718	/	/	/	=C-H Stretch
1644	1657	1706, 1611	1709, 1631	C=O stretch
/	1606	1563	/	C=C stretch
1422	1420	1403	1416	C-H bend
1297	1285	1287	1299	C-N stretch
1171	1188	1173	1175	C-O stretch
974	962	988	988	C-H bend

Chapter 4. Concluding remarks and future work

Chapter 4. Concluding remarks and future work

4.1 General discussion and conclusion

Polymers containing -OH, -COOH, -NH₂ that form hydrogen bonds with water molecules are classed as water-soluble polymers. For the last few decades, the applications of water-soluble polymers in pharmaceutical formulations, cosmetics, foods, industrial water treatment, oral care and fuel cells have been extensively explored. The properties and applications of exemplar water-soluble polymers in pharmaceutical formulation were reported by Kadajji and Betageri¹⁰. However, comprehensive descriptions of water-soluble polymers on the basis of their structures and functional pharmaceutically applications are rare. Here, pharmaceutical applications of common water-soluble polymers which are characterized as cationic, anionic, amphoteric and non-ionic polymers on the basis of their structures are extensively discussed in the introduction chapter.

Owing to the abundant mucosal surface area and high blood flow rate, mucoadhesive drug delivery systems enable bypassing first pass effect and avoidance of drug degradation in GI tract compared to oral drug formulations, resulting in improved bioavailability, prolonged residence time and rapid absorption. Linear poly(ethylenimine) (L-PEI) as a water-soluble polymer has been applied in several fields, such as gene delivery⁴⁰⁸⁻⁴¹⁰, water purification³²⁷, to produce functional inorganic minerals⁴¹¹ and in PEI-conjugates⁴¹²⁻⁴¹⁴. Because of the presence of cationic secondary amine groups within L-PEI, which can interact with negatively charged mucin, L-PEI has also gained some attention for mucoadhesive applications in nasal⁵ and buccal drug delivery³⁴². However, the abundant content of amine groups within L-PEI lead to relatively high toxicity and low biocompatibility, predominantly attributed to electrostatic interactions with cell membranes and the extracellular matrix.³²⁸ Thereby, various organic anhydrides were introduced to modify L-PEI to improve its mucoadhesive properties and reduce its toxicity. The obtained polymers carried ionic groups as polyampholytes and cationic polyelectrolytes.

Due to a lack of reports in the literature demonstrating the mucoadhesive properties of polyampholytes, the factors affecting the mucoadhesive properties of both synthetic and natural polyampholytes were investigated. In this work, two synthetic polyampholytes, succinylated L-PEI and phthaylated L-PEI, were prepared with bovine serum albumin (BSA) selected as a natural polyampholyte. The interactions between the polyampholytes and porcine gastric mucin were studied by the turbidimetric technique and isothermal titration calorimetry (ITC) demonstrating polyampholytes interact with mucin at $\text{pH} < \text{pH}_{\text{IEP}}$ and were

more pronounced than when $\text{pH} \geq \text{pH}_{\text{IEP}}$, where electrostatic interaction played a significant role. *Ex vivo* gastric mucoadhesive studies supported this finding via tensile testing and fluorescence flow through method. In summary, both synthetic and natural polyampholytes showed superior mucoadhesive ability and interactions with mucin at $\text{pH} < \text{pH}_{\text{IEP}}$.

Methacrylic anhydride, crotonic anhydride, maleic anhydride and succinic anhydride were then selected to modify L-PEI to enhance its mucoadhesive properties and reduce its toxicity. The mucoadhesive properties and mechanisms of action were evaluated at physiological pH (7.4). The toxicity studies used *in vivo* assays with planaria and *in vitro* MTT assay. Moreover, the irritancy of the polymers was assessed via a slug mucosa irritation assay *in vivo*. In summary, the cationic polyelectrolytes methacrylated L-PEI and crotonylated L-PEI showed greater mucoadhesion than the two polyampholytes (maleylated- and succinylated L-PEI) due to their ability to form covalent bonds with thiols present on mucosal surfaces. And all prepared polymers mitigated the adverse toxicity effects seen for the parent L-PEI.

The physicochemical properties of obtained polyampholytes (succinylated- (DS=46% and 89%, respectively), maleylated- and phthaylated L-PEI) and cationic polyelectrolytes (methacrylated- and crotonylated L-PEI) in solutions were evaluated using turbidity and electrophoretic mobility measurements at different pHs. The behavior of polyampholytes is strongly dependent on solution pH; succinylated-, maleylated- and phthaylated L-PEI showed maximum turbidity at their isoelectric point (pH_{IEP}) and a decrease of turbidity values when pHs were away from their pH_{IEP} . This was explained since when $\text{pH} < \text{pH}_{\text{IEP}}$ or $\text{pH} > \text{pH}_{\text{IEP}}$, the existence of excess positively or negatively charged groups lead to full hydration of the polyampholytes. While methacrylated L-PEI and crotonylated L-PEI are not polyampholytes, they do not exhibit pH-dependent aqueous solubility behavior (i.e. they do not display the presence of an isoelectric point).

Table 4.1-1. pH_{IEP} values of succinylated L-PEI, maleylated L-PEI and phthaylated L-PEI determined by turbidimetric technique and electrophoretic mobility measurement.

Polymer	DS	pH_{IEP} (Turbidity)	pH_{IEP} (Electrophoretic mobility)
Succinylated L-PEI	46%	pH 4.85±0.05	pH 4.30±0.04
	89%	pH 3.41±0.08	pH 3.16±0.09
Phthaylated L-PEI	86%	pH 7.71±0.08	pH 6.86±0.16
Maleylated L-PEI	80%	pH 2.81±0.07	pH 2.30±0.07

The isoelectric points determined from two different techniques are within a pH unit of each other with variance attributable to the different properties evaluated (Table 4.1-1). For example, turbidity is detected only when relatively large aggregates are present, but the aggregation process may start at an earlier pH, and electrophoretic mobility is dependent on the conformation of macromolecules and shape of the aggregates. The pH_{IEP} of succinylated L-PEI (DS=46%) is higher than succinylated L-PEI (DS=89%) that is attributed to availability of -NH groups for protonation. When the degree of substitution of succinylated L-PEI is 46%, more of the -NH groups are prone to be protonated leading to greater pH_{IEP} values. Similar profiles were observed in electrophoretic mobility measurement of methacrylated L-PEI and crotonylated L-PEI. Though they are not polyampholytes, they display charge reversion behavior at pHs 6.51 ± 0.14 and 7.05 ± 0.15 , respectively, which could be induced by the existence of counter-ions surrounding each macromolecular coil or particle, and changes in their net charge. The DS of methacrylated L-PEI (83%) was lower than crotonylated L-PEI (93%), resulting in fewer -NH- groups within crotonylated L-PEI to participate in protonation. Though succinylated- (DS=89%), maleylated- and phthaylated L-PEI have similar DS, they possess different pH_{IEP} , which is attributed to the different structures of their pendant chains. The unsaturated maleic acid residue present in maleylated L-PEI may have stronger electron-withdrawing ability which facilitates dissociation of the carboxyl group; this in turn may be a reason for a lower pH_{IEP} compared to the value recorded in the case of saturated succinylated L-PEI. Further, phthaylated L-PEI contains aromatic rings while succinylated L-PEI and maleylated L-PEI contain alkyl groups; the hydrophobic group of phthaylated L-PEI has weaker ionic content, leading to a higher pH_{IEP} than the succinylated and maleylated derivatives.

Both succinylated L-PEI and phthaylated L-PEI displayed superior mucoadhesive properties at $pH < pH_{IEP}$ and succinylated L-PEI showed slightly greater peak force and retention values than phthaylated L-PEI. This could be explained by the differences in DS since succinylated L-PEI (DS=46%) possesses more cationic secondary amine groups than phthaylated L-PEI (DS=86%), resulting in more pronounced electrostatic interactions with carboxylate groups and ester sulfates within negatively charged mucins. However, a considerable decrease in mucoadhesive properties was assessed in experiments conducted at $pH \geq pH_{IEP}$, due to the absence of electrostatic interaction between non-charged or negatively charged polyampholytes and negatively charged mucin. Though protonation of the amine groups plays a significant role in electrostatic interaction, the structure of polyampholytes may also affect mucoadhesive properties. We assume succinylated L-PEI

may have slightly greater mucoadhesive properties than phthaylated L-PEI at the same degree of substitution, because steric effects of the aromatic rings within phthaylated polymers may hamper the interaction between negatively charged mucin and positively charge polymers.

The investigation of mucoadhesive properties for maleylated L-PEI and succinylated L-PEI (DS=89%) demonstrated that the relationship between solution pH, pH_{IEP} and mucoadhesive performance is generally applicable for all polyampholytes. The retention studies illustrated that 37%, 34%, 13% and 11% of FITC-methacrylated L-PEI, FITC-crotonylated L-PEI, FITC-maleylated L-PEI and FITC succinylated L-PEI, remained on the tissue after 30 min washing at $pH=7.4$. The poor mucoadhesive activity of FITC-maleylated L-PEI and FITC succinylated L-PEI are due to the pH of the buffer solution being above their pH_{IEP} , therefore these polyampholytes carry a net negative charge throughout the retention study leading to electrostatic repulsion between polyampholytes and mucosal surface. During the irrigation period, the C=C bond within FITC-maleylated L-PEI is susceptible to form covalent bonds with thiol groups in mucin, leading to greater retention than FITC-succinylated L-PEI where the C=C bond is absent. Herein, it could be inferred that maleylated L-PEI may show greater mucoadhesive properties than succinylated L-PEI at $pH < pH_{IEP}$.

Moreover, the conformation of covalent bonds between C=C bond within methacrylated L-PEI and crotonylated L-PEI and thiol group within tissue mucosa appear to be predominantly responsible for mucoadhesive properties at $pH=7.4$.⁴³⁴ Since methacrylated L-PEI and crotonylated L-PEI are non-charged or negatively charged, the amine group within the polyelectrolytes exert minimal contribution for adhesion at $pH=7.4$. The methacrylated L-PEI exhibited greater retention values than the crotonylated derivative; this may be associated with the stronger tendency of methacryloyl groups to form covalent bonds with thiols compared to crotonyl groups, related to the steric hindrance of the methyl group.⁴³⁵

From the results, all prepared polymers were showed greater retention ability than FITC-dextran, which suggested that interdiffusion^{250,436}, water transportation and capillary forces^{394,395} may have synergetic effects for mucoadhesion when polymers are in intimately contact with the mucus layer.

Different structures, molecular weights, and macromolecular flexibility have been related to toxicity and delivery efficiency of L-PEI.⁴¹⁶ Because of the similarity of pendant chains within resultant polymers, the toxicity of methacrylated L-PEI, crotonylated L-PEI, maleylated L-PEI and succinylated L-PEI were explored via the slug mucosal irritation assay, planaria-based assays and cell culture assay. These results suggested that the obtained L-PEI polymeric derivates alleviated the adverse toxicity effects seen for the parent L-PEI, which

may be due to the high degree of substitution of the organic anhydride modification leading to a reduction of amine groups within L-PEI to interact with cell membranes and the extracellular matrix³²⁸ and short alkyl chains may have minor adverse effect on toxicity⁴⁵³. It is notable that cell viability following methacrylated L-PEI and crotonylated L-PEI treatments were higher than complete medium 1% FBS (control) and other L-PEI polymeric derivatives which promote cell growth and proliferation, and demonstrated that methacrylated L-PEI and crotonylated L-PEI have superior cell compatibility and some protective effects against cell death.

In summary, amphoteric and cationic polyelectrolytes were prepared to enhance mucoadhesive properties and reduce toxicity of L-PEI by introducing succinic anhydride, phthalic anhydride, methacrylic anhydride, crotonic anhydride and maleic anhydride. Succinylated L-PEI and phthalylated L-PEI exhibited pronounced mucoadhesive properties at $\text{pH} < \text{pH}_{\text{IEP}}$ due to the electrostatic interactions between the positively charged polyampholytes and negatively charged mucin, while methacrylated L-PEI and crotonylated L-PEI displayed superior mucoadhesive properties on the basis of a different mechanism and the formation of covalent bonds between C=C moieties within methacrylated L-PEI and crotonylated L-PEI and thiol group at the mucosal surface. Also, these studies suggested hydrogen bonding, hydrophobic effects, interdiffusion^{250,436}, water transportation and capillary forces^{394,395} may have synergetic effects for mucoadhesion. The relationship between solution pH, pH_{IEP} and mucoadhesive performance was clarified to predict mucoadhesive performance of polyampholytes. Toxicological characterizations demonstrated that the *in vivo* planaria assay is a more sensitive and rapid pre-screening tool for assessing toxicity of compounds compared to the slug mucosal irritation assay, which provides encouragement for using the readily assessable planaria model as an early pre-testing tool to inform consequent sophisticated toxicological assessments. The MTT assay and DAPI/PI staining of A549 cell indicated that anhydrides modification of L-PEI mitigated its appreciable toxicity and so expands the application scope of L-PEI in pharmaceutical formulations.

4.2 Future work

Viscosity measurements essentially monitor conformational transitions in solutions of polyampholytes upon changes in pH. The viscosity of succinylated L-PEI, phthalylated L-PEI and maleylated L-PEI could be conducted in future studies. Generally, minimal viscosity of polyampholytes is expected close to their pH_{IEP} . At $\text{pHs} < \text{pH}_{\text{IEP}}$, the carboxylic groups of

polyampholytes are protonated and not charged whereas amino groups are protonated and positively charged. This leads to electrostatic repulsion between positively charged groups, unfolding of the macromolecules and an increase in viscosity. At $\text{pH} = \text{pH}_{\text{IEP}}$, the number of positively charged groups in the macromolecules is equal to the number of negatively charged groups and the net charge is zero. Under these conditions the macromolecules acquire their most compact conformation and viscosity of their solutions is minimal since viscosity is inversely proportional to polymer density. At $\text{pHs} > \text{pH}_{\text{IEP}}$, the amino groups are fully deprotonated and not charged whereas carboxylic groups are deprotonated and negatively charged. This again increases electrostatic repulsion between negatively charged groups and is expected to increase solution viscosity.

Turbidimetric titration is a common and straightforward technique to investigate mucoadhesive interactions^{380,383,384}, and determines aggregation of mucin particles when they bind to macromolecules of a mucoadhesive polymer. The studies reported here demonstrated increased solution turbidity and aggregation of mucin particles at $\text{pH} < \text{pH}_{\text{IEP}}$ and the maximal turbidity values were measured when the surface of mucin particles was fully saturated with macromolecules of the polyampholytes. Dynamic light scattering (DLS) measurements are a simple and reproducible tool that could be performed to confirm the results of the turbidimetric titrations. DLS results reflect the interaction between mucin and polyampholytes. The ratio of [polyampholyte] / [mucin] giving maximum particle sizes are expected broadly align with the ratio of [polyampholyte] / [mucin] at maximal turbidity values. However, it is also feasible that the ratio of [polyampholyte] / [mucin] at maximum size values could differ to the ratio of [polyampholyte] / [mucin] at maximal turbidity values, since DLS measures R_{H} (hydrodynamic radius) and only provide an indicative size of a colloid³⁷², which is influenced by particles hydration. At $\text{pH} \geq \text{pH}_{\text{IEP}}$, the size is expected to remain at their initial values (or potentially lower) due to the simple dilution effects.

The determination of mucoadhesive properties for maleylated L-PEI on tissue mucosa over a wide range of pHs could be conducted. This would provide an opportunity to explore the effects of molecular structure for succinylated L-PEI, phthaylated L-PEI and maleylated L-PEI. Maleylated L-PEI is expected to exhibit more pronounced mucoadhesive properties than succinylated L-PEI and phthaylated L-PEI, due to the synergistic effects of electrostatic interaction and the formation of covalent bonds.

The effect of different DS (46% and 89%) on mucoadhesive properties of succinylated L-PEI at a wide range of pHs could also be investigated using the fluorescence microscopy-based flow-through assay. Succinylated L-PEI at DS=46% is expected to display greater

mucoadhesive properties than succinylated L-PEI at DS=89%, since succinylated L-PEI (DS=46%) possesses more cationic secondary amine groups than succinylated L-PEI (DS=89%), leading to stronger electrostatic interactions with carboxylate groups and ester sulfates within the negatively charged mucins.

In vivo studies could be conducted to compare with *ex vivo* mucoadhesion studies, and explore if the polymers have the similar mucoadhesive performance in an *ex vivo* assay due to the physiological conditions of the GI tract or ocular tissue is more complicated. Deposition and adhesion of polymers on mucosal surface is expected due to penetration of the polymers into the mucus gel and consequent formation of an interpenetrating layer with mucin biomacromolecules.²⁵⁰

Since methacrylated L-PEI and crotonylated L-PEI are water-soluble and show superior mucoadhesive properties in bovine palpebral conjunctiva, they possess great potential being employed in ocular delivery system (e.g. eye drops, artificial tears). A suitable pharmaceutical formulation of methacrylated L-PEI and crotonylated L-PEI could be designed and *in vivo* mucoadhesive studies conducted to evaluate their mucoadhesive properties.

4.3 Reference

- (5) Shan, X.; Aspinall, S.; Kaldybekov, D. B.; Buang, F.; Williams, A. C.; Khutoryanskiy, V. V. Synthesis and Evaluation of Methacrylated Poly(2-ethyl-2-oxazoline) as a Mucoadhesive Polymer for Nasal Drug Delivery. *ACS Applied Polymer Materials* **2021**, *3* (11), 5882.
- (10) Kadajji, V. G.; Betageri, G. V. Water Soluble Polymers for Pharmaceutical Applications. *Polymers* **2011**, *3* (4), 1972.
- (250) Smart, J. D. The basics and underlying mechanisms of mucoadhesion. *Advanced Drug Delivery Reviews* **2005**, *57* (11), 1556.
- (327) Bolto, B. A. Soluble polymers in water purification. *Progress in Polymer Science* **1995**, *20* (6), 987.
- (328) Jäger, M.; Schubert, S.; Ochrimenko, S.; Fischer, D.; Schubert, U. S. Branched and linear poly(ethylene imine)-based conjugates: synthetic modification, characterization, and application. *Chemical Society Reviews* **2012**, *41* (13), 4755.
- (342) Soradach, S.; Kengkwasingh, P.; Williams, A. C.; Khutoryanskiy, V. V. Synthesis and evaluation of poly (3-hydroxypropyl ethylene-imine) and its blends with chitosan forming novel elastic films for delivery of haloperidol. *Pharmaceutics* **2022**, *14* (12), 2671.
- (372) Bhattacharjee, S. DLS and zeta potential – What they are and what they are not? *Journal of Controlled Release* **2016**, *235*, 337.
- (380) Szilágyi, B. Á.; Mammadova, A.; Gyarmati, B.; Szilágyi, A. Mucoadhesive interactions between synthetic polyaspartamides and porcine gastric mucin on the colloid size scale. *Colloids and Surfaces B: Biointerfaces* **2020**, *194*, 111219.
- (383) Gyarmati, B.; Stankovits, G.; Szilágyi, B. Á.; Galata, D. L.; Gordon, P.; Szilágyi, A. A robust mucin-containing poly(vinyl alcohol) hydrogel model for the *in vitro* characterization of

- mucoadhesion of solid dosage forms. *Colloids and Surfaces B: Biointerfaces* **2022**, *213*, 112406.
- (384) Haji, F.; Kim, D. S.; Tam, K. C. Tannic acid-coated cellulose nanocrystals with enhanced mucoadhesive properties for aquaculture. *Carbohydrate Polymers* **2023**, *312*, 120835.
- (394) Pham, Q. D.; Nöjd, S.; Edman, M.; Lindell, K.; Topgaard, D.; Wahlgren, M. Mucoadhesion: mucin-polymer molecular interactions. *International Journal of Pharmaceutics* **2021**, *610*, 121245.
- (395) Ivarsson, D.; Wahlgren, M. Comparison of in vitro methods of measuring mucoadhesion: Ellipsometry, tensile strength and rheological measurements. *Colloids and Surfaces B: Biointerfaces* **2012**, *92*, 353.
- (408) Wightman, L.; Kircheis, R.; Rössler, V.; Carotta, S.; Ruzicka, R.; Kursá, M.; Wagner, E. Different behavior of branched and linear polyethylenimine for gene delivery in vitro and in vivo. *The Journal of Gene Medicine* **2001**, *3* (4), 362.
- (409) Goula, D.; Remy, J. S.; Erbacher, P.; Wasowicz, M.; Levi, G.; Abdallah, B.; Demeneix, B. A. Size, diffusibility and transfection performance of linear PEI/DNA complexes in the mouse central nervous system. *Gene Therapy* **1998**, *5* (5), 712.
- (410) Perevyazko, I. Y.; Bauer, M.; Pavlov, G. M.; Hoepfner, S.; Schubert, S.; Fischer, D.; Schubert, U. S. Polyelectrolyte Complexes of DNA and Linear PEI: Formation, Composition and Properties. *Langmuir* **2012**, *28* (46), 16167.
- (411) Madejová, J.; Barlog, M.; Slaný, M.; Bashir, S.; Scholtzová, E.; Tunega, D.; Jankovič, Ľ. Advanced materials based on montmorillonite modified with poly(ethylenimine) and poly(2-methyl-2-oxazoline): Experimental and DFT study. *Colloids and Surfaces A: Physicochemical and Engineering Aspects* **2023**, *659*, 130784.
- (412) Akiyama, Y.; Harada, A.; Nagasaki, Y.; Kataoka, K. Synthesis of Poly(ethylene glycol)-block-poly(ethylenimine) Possessing an Acetal Group at the PEG End. *Macromolecules* **2000**, *33* (16), 5841.
- (413) Yang, T.; Hussain, A.; Bai, S.; Khalil, I. A.; Harashima, H.; Ahsan, F. Positively charged polyethylenimines enhance nasal absorption of the negatively charged drug, low molecular weight heparin. *Journal of Controlled Release* **2006**, *115* (3), 289.
- (414) Dai, Y.; Zhang, X.; Zhuo, R. Polymeric micelles stabilized by polyethylenimine–copper (C 2 H 5 N–Cu) coordination for sustained drug release. *RSC advances* **2016**, *6* (27), 22964.
- (416) Mintzer, M. A.; Simanek, E. E. Nonviral Vectors for Gene Delivery. *Chemical Reviews* **2009**, *109* (2), 259.
- (434) Shatabayeva, E. O.; Kaldybekov, D. B.; Ulmanova, L.; Zhaisanbayeva, B. A.; Mun, E. A.; Kenessova, Z. A.; Kudaibergenov, S. E.; Khutoryanskiy, V. V. Enhancing Mucoadhesive Properties of Gelatin through Chemical Modification with Unsaturated Anhydrides. *Biomacromolecules* **2024**, DOI:10.1021/acs.biomac.3c01183 10.1021/acs.biomac.3c01183.
- (435) Hill, C. A. S.; Cetin, N. S. Surface activation of wood for graft polymerisation. *International Journal of Adhesion and Adhesives* **2000**, *20* (1), 71.
- (436) Voiutskii, S. S. Autohesion and adhesion of high polymers. **1963**.
- (453) Ranke, J.; Mölter, K.; Stock, F.; Bottin-Weber, U.; Poczobutt, J.; Hoffmann, J.; Ondruschka, B.; Filser, J.; Jastorff, B. Biological Effects of Imidazolium Ionic Liquids with Varying Chain Lengths in Acute *Vibrio Fischeri* and Wst-1 Cell Viability Assays. *Ecotoxicology and environmental safety* **2004**, *58*, 396.